

frontiers

RESEARCH TOPICS

ION CHANNEL SCREENING: ADVANCES IN TECHNOLOGIES AND ANALYSIS

Hosted by
Ralf F. Kettenhofen, Dermott W.
O'Callaghan, Juha Kammonen,
Marzia Martina and Geoff A. Mealing



frontiers in
PHARMACOLOGY



frontiers

FRONTIERS COPYRIGHT STATEMENT

© Copyright 2007-2012
Frontiers Media SA.
All rights reserved.

All content included on this site, such as text, graphics, logos, button icons, images, video/audio clips, downloads, data compilations and software, is the property of or is licensed to Frontiers Media SA ("Frontiers") or its licensees and/or subcontractors. The copyright in the text of individual articles is the property of their respective authors, subject to a license granted to Frontiers.

The compilation of articles constituting this e-book, as well as all content on this site is the exclusive property of Frontiers. Images and graphics not forming part of user-contributed materials may not be downloaded or copied without permission.

Articles and other user-contributed materials may be downloaded and reproduced subject to any copyright or other notices. No financial payment or reward may be given for any such reproduction except to the author(s) of the article concerned.

As author or other contributor you grant permission to others to reproduce your articles, including any graphics and third-party materials supplied by you, in accordance with the Conditions for Website Use and subject to any copyright notices which you include in connection with your articles and materials.

All copyright, and all rights therein, are protected by national and international copyright laws.

The above represents a summary only. For the full conditions see the Conditions for Authors and the Conditions for Website Use.

Cover image provided by Ibbl sarl, Lausanne CH

ISSN 1664-8714

ISBN 978-2-88919-035-5

DOI 10.3389/978-2-88919-035-5

ABOUT FRONTIERS

Frontiers is more than just an open-access publisher of scholarly articles: it is a pioneering approach to the world of academia, radically improving the way scholarly research is managed. The grand vision of Frontiers is a world where all people have an equal opportunity to seek, share and generate knowledge. Frontiers provides immediate and permanent online open access to all its publications, but this alone is not enough to realize our grand goals.

FRONTIERS JOURNAL SERIES

The Frontiers Journal Series is a multi-tier and interdisciplinary set of open-access, online journals, promising a paradigm shift from the current review, selection and dissemination processes in academic publishing.

All Frontiers journals are driven by researchers for researchers; therefore, they constitute a service to the scholarly community. At the same time, the Frontiers Journal Series operates on a revolutionary invention, the tiered publishing system, initially addressing specific communities of scholars, and gradually climbing up to broader public understanding, thus serving the interests of the lay society, too.

DEDICATION TO QUALITY

Each Frontiers article is a landmark of the highest quality, thanks to genuinely collaborative interactions between authors and review editors, who include some of the world's best academicians. Research must be certified by peers before entering a stream of knowledge that may eventually reach the public - and shape society; therefore, Frontiers only applies the most rigorous and unbiased reviews.

Frontiers revolutionizes research publishing by freely delivering the most outstanding research, evaluated with no bias from both the academic and social point of view.

By applying the most advanced information technologies, Frontiers is catapulting scholarly publishing into a new generation.

WHAT ARE FRONTIERS RESEARCH TOPICS?

Frontiers Research Topics are very popular trademarks of the Frontiers Journals Series: they are collections of at least ten articles, all centered on a particular subject. With their unique mix of varied contributions from Original Research to Review Articles, Frontiers Research Topics unify the most influential researchers, the latest key findings and historical advances in a hot research area!

Find out more on how to host your own Frontiers Research Topic or contribute to one as an author by contacting the Frontiers Editorial Office: researchtopics@frontiersin.org

ION CHANNEL SCREENING: ADVANCES IN TECHNOLOGIES AND ANALYSIS

Hosted By

Ralf F. Kettenhofen, Axiogenesis AG, Germany

Dermott W. O'Callaghan, 74 Consulting, United Kingdom

Juha Kammonen, Pfizer, United Kingdom

Marzia Martina, National Research Council of Canada, Canada

Geoff A. Mealing, National Research Council of Canada, Canada

Ion channel research has increased tremendously in the past 35 years since the first publication of the patch clamp technique by Neher and Sakmann in 1976. This is documented by the rising number of publications listed in Pubmed (<http://www.ncbi.nlm.nih.gov/pubmed>) including the keyword 'ion channel' from just 186 hits in 1976 to almost 180,000 hits today.

Ion channels attract this great interest due to their pivotal role in the control of fundamental physiological processes in a plethora of different tissues. Moreover, their importance in a wide range of inherited and drug-induced pathologies spanning all major therapeutic areas makes them attractive targets for pharmacological drug screening and potential risk factors when assessing drug safety (Ashcroft, 2006; Clare, 2010; Dunlop 2008; Milligan 2009).

Several methods and technologies have been developed to meet the analytical needs for studying ion channels. These approaches have addressed ion channel function directly as well as in the context of the cell and tissue. Scaling of these technologies has allowed ion channel analysis to be carried out on high throughput and high content assay systems.

In this Research Topic we want to provide an up-to-date collection of the latest developments and improvements in ion channel screening; defining the cutting edge and indicating further developments required in the future.

References:

- Clare JJ. Targeting ion channels for drug discovery. *Discov Med.* 2010 Mar;9(46):253–60.
- Ashcroft FM. From molecule to malady. *Nature* 440:440–7, 2006.
- Dunlop J, Bowlby M, Peri R, Vasilyev D, Arias R. High-throughput electrophysiology: an emerging paradigm for ion-channel screening and physiology. *Nat Rev Drug Discov.* 2008 Apr;7(4):358–68.
- Milligan CJ, Li J, Sukumar P, Majeed Y, Dallas ML, English A, Emery P, Porter KE, Smith AM, McFadzean I, Beccano-Kelly D, Bahnasi Y, Cheong A, Naylor J, Zeng F, Liu X, Gamper N, Jiang LH, Pearson HA, Peers C, Robertson B, Beech DJ. Robotic multiwell planar patch-clamp for native and primary mammalian cells. *Nat Protoc.* 2009;4(2):244–55.

Table of Contents

- 05 *Ion channel screening: advances in technologies and analysis***
Marzia Martina
- 07 *State-of-the-Art Automated Patch Clamp Devices: Heat Activation, Action Potential, and High Throughput in Ion Channel Screening***
Sonja Stoelzle, Alison Obergrussberger, Andrea Brüggemann, Claudia Haarmann, Michael George, Ralf Kottenhofen and Niel Fertig
- 18 *Neurons on a chip – toward high throughput network and pharmacology investigations***
John Michael Nagarah
- 20 *From Understanding Cellular Function to Novel Drug Discovery: The Role of Planar Patch-Clamp Array Chip Technology***
Christophe Py, Marzia Martina, Gerardo A. Diaz-Quijada, Collin C. Luk, Dolores Martinez, Mike W. Denhoff, Anne Charrier Tanya Comas, Robert Monette, Anthony Krantis, Naweel I. Syed and Geoffrey A.R. Mealing
- 36 *The Importance of Being Profiled: Improving Drug Candidate Safety and Efficacy Using Ion Channel Profiling***
Gregory J. Kaczorowski, Maria L. Garcia, Jacob Bode, Stephen D. Hess and Umesh A. Patel
- 47 *Automated Electrophysiology Makes the Pace for Cardiac Ion Channel Safety Screening***
Clemens Möller and Harry Witchel
- 54 *Toward a New Gold Standard for Early Safety: Automated Temperature-controlled hERG Test on the PatchLiner®***
Liudmilla Polonchuk
- 61 *Screening Action Potentials: the Power of Light***
Lars Kaestner and Peter Lipp
- 66 *Targeting GIRK Channels for the Development of New Therapeutic Agents***
Kenneth B. Walsh
- 74 *Finding inward rectifier channel inhibitors: why and how***
Marcel A.G. van der Heyden

76 *Discovery, Characterization, and Structure-Activity Relationships of an Inhibitor of Inward Rectifier Potassium (Kir) Channels with Preference for Kir2.3, Kir3.X, and Kir7.1*

Rene Raphemot, Daniel F. Loneragan, Thuy T. Nguyen, Thomas Utley, L. Michelle Lewis, Rashin Kadakia, C. David Weaver, Rocco Gogliotti, Corey Hopkins, Craig W. Lindsley and Jerod S. Denton

94 *Voltage- and Temperature-Dependent Allosteric Modulation of $\alpha 7$ Nicotinic Receptors by PNU120596*

Fabrizio Sitzia, Jon T. Brown, Andrew D. Randall and John Dunlop



Ion channel screening: advances in technologies and analysis

Marzia Martina*

Synaptic Therapies and Devices Group, Institute for Biological Sciences, National Research Council of Canada, Ottawa, ON, Canada

*Correspondence: marzia.martina@nrc-cnrc.gc.ca

This issue provides a comprehensive picture of the most recent technological advances in the field of ion channel screening. Ion channels are proteins that form pores in cell membranes. They are involved in the control of many fundamental physiological processes in various tissues and alterations in their functions give rise to pathological conditions. Ion channels were discovered in the membrane of electrically excitable cells such as neurons, cardiomyocytes, and skeletal muscle fibers and, for decades, drugs modulating cell excitability have been targeted by the pharmaceutical industry. Ion channels also play many roles in non-excitable tissues. Approximately 13% of marketed drugs act on ion channels (Clare, 2010) and new ion channel screening technologies continue to be developed to discover new drugs.

Patch-clamp is the gold standard technique to record ion channel activity (Hamill et al., 1981). The costs associated with this technique, however, are high as a result of the need for top-quality equipment (e.g., anti-vibrating table, micromanipulator, microscope with IR-CCD camera), highly trained personnel, and low throughput. Over the years, there have been attempts to build devices to increase throughput, notably with automated electrophysiology systems. Such systems have revolutionized ion channel drug discovery by enabling the screening of numerous compounds on many types of ion channels and cellular models. These systems have also been important for safety pharmacology testing of many types of ion channels. These methods, however, need improvements with respect to throughput, quality of the electrophysiological recordings and the physiological cellular models used for drugs and safety testing.

In this issue, Stoelzle et al. (2011) review the development of new automated patch-clamp (APC) systems capable of recording 96 cells in parallel and offering 5,000 data points per day, providing a high throughput per experiment. The development of other important features such as temperature control, the ability to record action potentials, and the testing of drugs on more relevant physiological models improve the quality of results. These APC systems, however, can only be used with suspended cell lines transfected with the ion channels to be studied, thereby not allowing for the study of the processes involved in synaptic communication. Synaptic communication is critical to information processing within neuronal networks – the disruption of which is at the basis of many neurodegenerative diseases – so better understanding of the mechanisms underlying synaptic function requires interrogation of pre- and post-synaptic activity by monitoring/manipulating trans-membrane potential or currents from connected neurons.

Accordingly, there is a need for devices that will be simple to use and lead to higher throughput while providing high quality recordings for both the screening of native neuronal ion channels and the study of neuronal networks. Py et al. (2011) describe a new planar patch-clamp chip in which pipettes are replaced by

apertures on a planar surface suitable for neuronal culture. Using synaptically connected snail neurons cultures on these chips, high quality recordings were obtained in both current- and voltage-clamp. If successfully translated to mammalian neurons, this new technology will provide an important tool for developing and testing drugs on more relevant physiological disease models (see also Nagarah, 2011).

The development of new technologies has increased the number of drugs that can be identified, synthesized, characterized, screened, and tested for therapeutic efficacy and safety. However, the process of drug discovery is long and expensive. Pharmaceuticals spend \$50 billion annually in R&D and the average cost to bring a new drug to the market is estimated at \$1.8 billion (Paul et al., 2010). Most compounds fail in clinical trials, requiring development of new strategies, and methodologies. Kaczorowski et al. (2011) suggest that the profiling of putative lead compounds to identify off-target activities joined with medicinal chemistry research to minimize such activities could save valuable time and money during the pre-clinical lead optimization phase.

Since ion channels control conduction of electrical activity in the heart, it is crucial to discern if off-target activities of drug candidates include cardiac ion channels. Möller and Witchel (2011) review the most recent methods to screen drug candidates in major cardiac ion channels. These methods include APC using heterologous expression systems and automated action potential recordings from stem-cell derived cardiomyocyte. Polonchuk (2012) evaluates the use of a fully APC system with integrated temperature control – the PatchLiner (Nanion Technologies GmbH, Munich, Germany) – with an ether-à-go-go related gene K^+ channels assay, in an effort to set a new standard in ion channel research for drug safety testing. For their part, Kaestner and Lipp (2011) describe the advantages of screening cardiac action potentials for drug safety using optical devices to reduce mechanic manipulation of the cells.

Despite the efforts from public and private research to discover new compounds, development of treatment options for many human diseases remains frustratingly slow. It is therefore crucial to continue to seek new therapeutic targets. G protein-coupled inward rectifier K^+ (GIRK) channels are expressed in the brain, heart and skeletal muscle, and endocrine tissue. GIRK channels are activated via G protein-coupled receptors and regulate the electrical activity of neurons, cardiomyocytes, and β -pancreatic cells, making them an important target for new drug discovery for treatment of neuropathic pain, drug addiction, and cardiac arrhythmias (atrial fibrillation). Walsh (2011) describes the development of a screening assay which uses pituitary and cardiac cell lines expressing GIRK channels combined with patch-clamp and imaging techniques to expand on the limited pharmacology of these channels. Raphemot et al. (2011) describe the use of a thallium (see Van der Heyden, 2012 for commentary) flux-based fluorescence assay to screen a

Kir1.1 inhibitor library for antagonists of GIRK. Their finding of a new compound, VU573, could be useful to investigate the function and pharmacology of these channels.

Given the importance of identifying new therapeutic targets, the work of Sitzia et al. (2011) on $\alpha 7$ nicotinic receptors – involved in schizophrenia and other diseases involving cognitive impairment as well as in neuroprotection – and their finding of the role played

by temperature variations in the modulation of these receptors is an appropriate way of concluding this overview of recent advances in ion channel screening.

The huge developments in the field of ion channel screening technologies described in this issue clearly indicate that the future is pointed toward the screening of drugs in more physiological relevant cellular models and networks.

REFERENCES

- Clare, J. J. (2010). Targeting ion channels for drug discovery. *Discov. Med.* 9, 253–260.
- Hamill, O. P., Marty, A., Neher, E., Sakmann, B., and Sigworth, F. J. (1981). Improved patch-clamp techniques for high-resolution current recording from cells and cell-free membrane patches. *Pflügers Arch.* 391, 85–100.
- Kaczorowski, G. J., Garcia, M. L., Bode, J., Hess, S. D., and Patel, U. A. (2011). The importance of being profiled: improving drug candidate safety and efficacy using ion channel profiling. *Front. Pharmacol.* 2:78. doi: 10.3389/fphar.2011.00078
- Kaestner, L., and Lipp, P. (2011). Screening action potentials: the power of light. *Front. Pharmacol.* 2:42. doi: 10.3389/fphar.2011.00042
- Möller, C., and Witchel, H. (2011). Automated electrophysiology makes the pace for cardiac ion channel safety screening. *Front. Pharmacol.* 2:73. doi: 10.3389/fphar.2011.00073
- Nagarah, J. M. (2011). Neurons on a chip – toward high throughput network and pharmacology investigations. *Front. Pharmacol.* 2:74. doi: 10.3389/fphar.2011.00074
- Paul, S. M., Mytelka, D. S., Dunwiddie, C. T., Persinger, C. C., Munos, B. H., Lindborg, S. R., and Schacht, A. L. (2010). How to improve R&D productivity: the pharmaceutical industry's grand challenge. *Nat. Rev. Drug Discov.* 9, 203–214.
- Polonchuk, L. (2012). Toward a new gold standard for early safety: automated temperature-controlled hERG test on the PatchLiner®. *Front. Pharmacol.* 2:3. doi: 10.3389/fphar.2012.00003
- Py, C., Martina, M., Diaz-Quijada, G. A., Luk, C. C., Martinez, D., Denhoff, M. D., Charrier, A., Comas, T., Monette, R., Krantis, A., Syed, N. I., and Mealing, G. A. R. (2011). From understanding cellular function to novel drug discovery: the role of planar patch-clamp array chip technology. *Front. Pharmacol.* 2:51. doi: 10.3389/fphar.2011.00051
- Raphemot, R., Lonergan, D. F., Nguyen, T. T., Utley, T., Lewis, L. L., Kadakia, R., Weaver, C. D., Gogliotti, R., Hopkins, C., Lindsley, C. W., and Denton, J. S. (2011). Discovery, characterization, and structure-activity relationships of an inhibitor of inward rectifier potassium (Kir) channels with preference for Kir2.3, Kir3.X, and Kir7.1. *Front. Pharmacol.* 2:75. doi: 10.3389/fphar.2011.00075
- Sitzia, F., Brown, J. T., Randall, A. D., and Dunlop, J. (2011). Voltage- and temperature-dependent allosteric modulation of $\alpha 7$ nicotinic receptors by PNU120596. *Front. Pharmacol.* 2:81. doi: 10.3389/fphar.2011.00081
- Stoelzle, S., Obergrussberger, A., Brüggemann, A., Haarmann, C., George, M., Kettenhofen, R., and Fertig, N. (2011). State-of-the-art automated patch clamp devices: heat activation, action potentials, and high throughput in ion channel screening. *Front. Pharmacol.* 2:76. doi: 10.3389/fphar.2011.00076
- Van der Heyden, M. A. G. (2012). Finding inward rectifier channel inhibitors: why and how? *Front. Pharmacol.* 2:95. doi: 10.3389/fphar.2011.00095
- Walsh, K. B. (2011). Targeting GIRK channels for the development of new therapeutic agents. *Front. Pharmacol.* 2:64. doi: 10.3389/fphar.2011.00064

Received: 16 April 2012; accepted: 17 April 2012; published online: 07 May 2012.

Citation: Martina M (2012) Ion channel screening: advances in technologies and analysis. *Front. Pharmacol.* 3:86. doi: 10.3389/fphar.2012.00086

This article was submitted to *Frontiers in Pharmacology of Ion Channels and Channelopathies*, a specialty of *Frontiers in Pharmacology*.

Copyright © 2012 Martina. This is an open-access article distributed under the terms of the Creative Commons Attribution Non Commercial License, which permits non-commercial use, distribution, and reproduction in other forums, provided the original authors and source are credited.



State-of-the-art automated patch clamp devices: heat activation, action potentials, and high throughput in ion channel screening

Sonja Stoelzle^{1*}, Alison Obergrussberger¹, Andrea Brüggemann¹, Claudia Haarmann¹, Michael George¹, Ralf Kettenhofen² and Niels Fertig¹

¹ Nanion Technologies GmbH, Munich, Germany

² Axiogenesis AG, Cologne, Germany

Edited by:

Juha Kammonen, Pfizer, UK

Reviewed by:

Christian Wahl-Schott,
Ludwig-Maximilian University,
Germany

Michel Vivaudou, Institut de Biologie
Structurale, France

Lishuang Cao, Pfizer, UK

*Correspondence:

Sonja Stoelzle, Nanion Technologies
GmbH, Gabrielenstrasse 9, 80636
Munich, Germany.
e-mail: sonja@nanion.de

Ion channels are essential in a wide range of cellular functions and their malfunction underlies many disease states making them important targets in drug discovery. The availability of standardized cell lines expressing ion channels of interest lead to the development of diverse automated patch clamp (APC) systems with high-throughput capabilities. These systems are now available for drug screening, but there are limitations in the application range. However, further development of existing devices and introduction of new systems widen the range of possible experiments and increase throughput. The addition of well controlled and fast solution exchange, temperature control and the availability of the current clamp mode are required to analyze standard cell lines and excitable cells such as stem cell-derived cardiomyocytes in a more physiologically relevant environment. Here we describe two systems with different areas of applications that meet the needs of drug discovery researchers and basic researchers alike. The here utilized medium throughput APC device is a planar patch clamp system capable of recording up to eight cells simultaneously. Features such as temperature control and recordings in the current clamp mode are described here. Standard cell lines and excitable cells such as stem cell-derived cardiomyocytes have been used in the voltage clamp and current clamp modes with the view to finding new drug candidates and safety testing methods in a more physiologically relevant environment. The high-throughput system used here is a planar patch clamp screening platform capable of recording from 96 cells in parallel and offers a throughput of 5000 data points per day. Full dose response curves can be acquired from individual cells reducing the cost per data point. The data provided reveals the suitability and relevance of both APC platforms for drug discovery, ion channel research, and safety testing.

Keywords: automated patch clamp, electrophysiology, temperature control, TRPV3, hERG, nAChR, current clamp, ion channels

INTRODUCTION

Ion channels are pore-forming proteins that catalyze the passive transport of ions through biological membranes. Given the importance of ion channels in many physiological processes, it is no surprise that they are a major therapeutic target (Hille, 1992; Ashcroft, 2000). To date over 13% of currently known drugs have been shown to act primarily on ion channels, a multi-billion dollar industry (Clare, 2010).

Patch clamp electrophysiology remains the gold standard for studying ion channels since it was first described in the 1970s (Neher and Sakmann, 1976). However, conventional patch clamp is notoriously low throughput and technically demanding. Thus, automation of the patch clamp technique increases throughput and ease of use (Farre et al., 2009), bringing patch clamp to a wider audience.

Over the last decade, several automated patch clamp (APC) devices became available and are now commonplace in many laboratories (for recent reviews see Dunlop et al., 2008; Farre et al.,

2008). These devices provide information rich data whilst increasing throughput, which is essential for both drug discovery and safety testing. Such APC devices are not limited to the pharmaceutical industry. Universities and research institutions have also started to implement the use of higher throughput APC devices in their laboratories (Milligan et al., 2009; Balansa et al., 2010). National screening centers and high-throughput core facilities are appearing worldwide, combining increased throughput, sophistication, and high quality.

However, the providers of APC devices are pushing the boundaries by continually improving existing platforms and creating new and innovative devices, which have higher throughput and new features. Such features are introduced in this paper.

MATERIALS AND METHODS

SYSTEM COMPONENTS

The medium throughput patch clamp device used here was a Patchliner System (Nanion Technologies, Germany). It includes

four (Patchliner Quattro) or eight (Patchliner Octo) amplifier channels (EPC-10 Quadro amplifiers, HEKA Elektronik, Germany), PatchControlHT software, integrated with PatchMaster (HEKA Elektronik, Germany), for acquisition of data, and online analysis of the recorded data. The data analysis software for visualization of traces and results of data analysis is IGOR Pro-based (WaveMetrics, USA). The data output and compound information is compatible with most database formats. A graphical user interface is used to program and execute up to 48 unattended recordings, approximately 500 data points per day can be generated. User intervention is possible at any time during an experiment. The software offers a detailed user control in combination with versatile experimental possibilities. In comparison to other available APC devices the Patchliner is equipped with temperature control, continuous waste removal allowing an unlimited number of compound additions, and the ability to perform current clamp recordings.

The high-throughput system utilized here was the SyncroPatch 96 (Nanion Technologies, Germany), a screening platform capable of recording from 96 cells in parallel. Full dose response curves can be acquired from individual cells with giga-ohm ($G\Omega$) seals, generation of up to 5000 data points per day is possible. The platform has built-in amplifiers (Triton+, Tecella LLC, USA), its own dedicated software (PatchControl96, Nanion Technologies, Germany), and a data analysis package. Temperature control or current clamp are not integrated features. Data output and compound information is compatible with most database formats.

For both systems, planar borosilicate-glass patch clamp chips are used (Farre et al., 2009).

CELL CULTURE FOR PLANAR PATCH CLAMP

For planar patch clamp, a wide range of different cell suspensions can be used (Bruggemann et al., 2008; Li et al., 2008; Milligan et al., 2009). Cell suspensions for APC devices utilizing planar patch clamp chips should be homogeneous (Milligan et al., 2009), since the cell capture is blind. The cells are ideally single. Cell clusters, cell fragments, or debris in the suspension decrease the cell capture rate and, thus, the overall success rate.

Standard cell lines

The confluency of the cells should be in the range of 50–80%. For culturing cells for use on the Patchliner and SyncroPatch 96, T75 flasks are typically used. For harvesting the cells for patch clamp experiments, no significant difference in percentage of giga-ohm seals could be found for using Trypsin, accutase, or phosphate-buffered saline ethylenediaminetetraacetic acid (PBS–EDTA) for lifting the cells.

Cell lines used in this paper:

hERG stably expressed in HEK cells (Millipore, USA).
 hTRPV3 stably expressed in HEK cells (Millipore, USA).
 hNa_v1.5 stably expressed in HEK cells (Millipore, USA).
 P2X_{2/3} receptors stably expressed in 1321N1 cells (Evotec, Germany).
 HEK cells stably expressing homomeric human nAChR $\alpha 7$ subunits (Galantos Pharma GmbH, Germany).

GABA_A subunits $\alpha 1\beta 2\gamma 2$ stably expressed in HEK cells (source anonymous).

Harvesting protocol for cell lines. Amounts are listed for a T75 flask exemplarily:

- Wash twice with 10 ml PBS (without Ca²⁺ and Mg²⁺).
- Add 2 ml of detacher (PBS–EDTA 2 mM, Trypsin/EDTA, Accutase etc.).
- Incubate approximately 3 min in a humidified incubator at 37°C and 95% O₂/5% CO₂.
- Check the detachment of cells using a microscope. Move the plate or flask gently to detach all cells from the bottom (do not hit the flask, tap gently if necessary).
- Add 10 ml of cell culture medium (room temperature, RT), according to the cells used.
- Pipette the cells gently up and down with a 10-ml pipette.
- After pipetting five times, look at the cells under a microscope. If the cells are single (80–90%), no further pipetting is needed.
- If cells still form clusters, gently pipette cells another 10 times. Repeat this step until cells are single (80–90%).
- Centrifuge the cells (2 min, 100 g).
- Discard the supernatant.
- Resuspend the cells in external recording solution resulting in a cell density of approximately 1×10^6 cells/ml.
- A visual control of the cell suspension under the microscope should reveal single, round cells with smooth membrane edges and few cell clusters.
- Transfer cells to the cell hotel of the Patchliner where cells are continuously pipetted up and down to maintain single cells and viability.

Stem cell-derived cardiomyocytes

Differentiation of genetically modified mouse embryonic stem cells (mESC) and the antibiotic selection of the mESC-derived cardiomyocytes have been described previously in detail (Kolossov et al., 2006).

Vials of at least one or five million viable mESC-derived cardiomyocytes (Cor.At cells, Lonza, Walkersville, USA, catalog numbers XCAC-1010 or XCAC-1050, respectively) obtained directly from the manufacturer (Axiogenesis, Cologne, Germany) were thawed as described in the distributors technical manual (<https://www.lonza.com/go/literature/>). For long-term storage, the cells are frozen as single cell suspensions in liquid nitrogen or –150°C freezers. When cultured overnight at an appropriate cell density, the thawed cardiomyocytes form spontaneously and synchronously contracting monolayers.

Cells were seeded at a density of 10^5 viable cells/cm² culture area in one T25 cell culture flask with 5 ml Cor.At Complete Culture Medium when a vial with one million viable mESC-derived cardiomyocytes was used. Two T75 cell culture flasks each with 10 ml Cor.At Complete Culture Medium were used when a vial containing five million mESC-derived cardiomyocytes was taken.

iCell cardiomyocytes (Cellular Dynamics International, Madison, WI, USA) were plated on T25 culture flasks coated with 0.1% gelatin as per manufacturers' instructions. A vial

containing $> 1.5 \times 10^6$ platable cells (catalog number CMC-100-110-001) was plated on one T25 flask, a vial containing $> 7.5 \times 10^6$ platable cells (catalog number CMC-100-110-005) was plated on five T25 flasks. For each 1×10^6 viable cells, 9 ml cold iCell Cardiomyocytes Plating Media (4°C) was used. After 24 h the media was exchanged for iCell Cardiomyocytes Maintenance Media.

Harvesting protocol for mouse stem cell-derived Cor.At cardiomyocytes. Amounts are listed for a T75 flask exemplarily:

- Cells must be cultured for at least 2–4 days before patch clamp experiments are performed.
- Wash twice with 10 ml 4°C cold PBS (without $\text{Ca}^{2+}/\text{Mg}^{2+}$)/EDTA (2 mM).
- Incubate at 4°C for 15 min.
- Remove PBS/EDTA.
- Add 5 ml pre-warmed (RT) Trypsin 0.05%/EDTA 0.02% in PBS solution.
- Incubate 4–5 min in a humidified incubator at 37°C and 95% $\text{O}_2/5\%$ CO_2 .
- Check the detachment of cells under a microscope. Move the plate or flask gently to detach all cells from the bottom (do not hit the flask).
- Add 10 ml of Cor.At Complete Culture Medium (RT).
- Centrifuge the cells (2 min, 100 g).
- Discard the supernatant.
- Add external recording solution resulting in a cell density of approximately 1×10^6 – 5×10^7 /ml. Carefully resuspend the cells by gentle pipetting (two times max.).
- A visual control of the cell suspension under the microscope should reveal single, round cells with smooth membrane edges and no cell clusters.
- Transfer cells to the cell hotel of the Patchliner where cells are continuously pipetted up and down to maintain single cells and viability.

Harvesting protocol for human iPS cell-derived iCell cardiomyocytes. Amounts are listed for a T25 flask exemplarily:

- Cells should be cultured for at least 2–4 days before patch clamp experiments are performed.
- Wash twice with 5 ml 4°C cold PBS (without $\text{Ca}^{2+}/\text{Mg}^{2+}$)/EDTA (2 mM).
- Add 5 ml 4°C cold PBS (without $\text{Ca}^{2+}/\text{Mg}^{2+}$)/EDTA (2 mM).
- Incubate at 4°C for 15 min.
- Remove PBS/EDTA.
- Add 2 ml Trypsin 0.05%/EDTA 0.02% in PBS solution.
- Rock the dish from side to side to ensure an even distribution of Trypsin.
- Immediately remove the Trypsin (before cells start to detach). Despite removing the liquid, there is still enough Trypsin on the surface to detach the cells.
- Incubate the flask for 3–8 min at 37°C and 95% $\text{O}_2/5\%$ CO_2 . Check the detachment of cells under a microscope after 3 min. Move the plate or flask gently to detach all cells from the bottom (do not hit the flask, tap gently if required). If cells are not detached return the flask to the incubator.

- Once cells start to detach, add 1 ml media and 1 ml external recording solution. Carefully resuspend the cells by gentle pipetting (two times max.).
- Transfer cells to the cell hotel of the Patchliner where cells are continuously pipetted up and down to maintain single cells and viability.

Patch clamp solutions. Internal solution: 50 mM KCl, 10 mM NaCl, 60 mM KF, 20 mM EGTA, 10 mM HEPES/KOH, pH 7.2 (for Figures 1, 2, 5, 6, and 8) or 50 mM CsCl, 10 mM NaCl, 60 mM

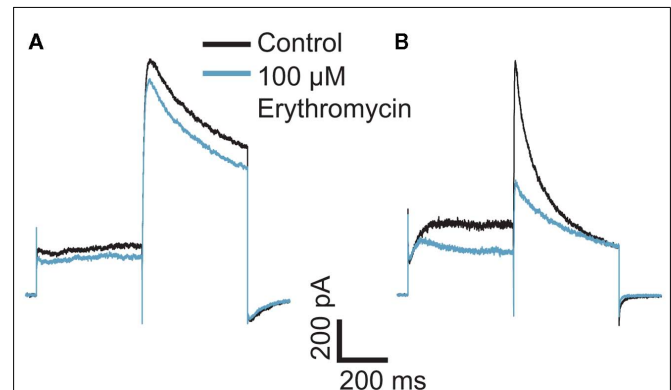


FIGURE 1 | Effect of erythromycin on hERG-mediated currents at (A) room temperature and (B) 35°C. The graphs are shown on the same scale. Hundred micromolar erythromycin significantly blocked hERG currents at 35°C but had little effect on hERG currents at RT, $n = 1$ each.

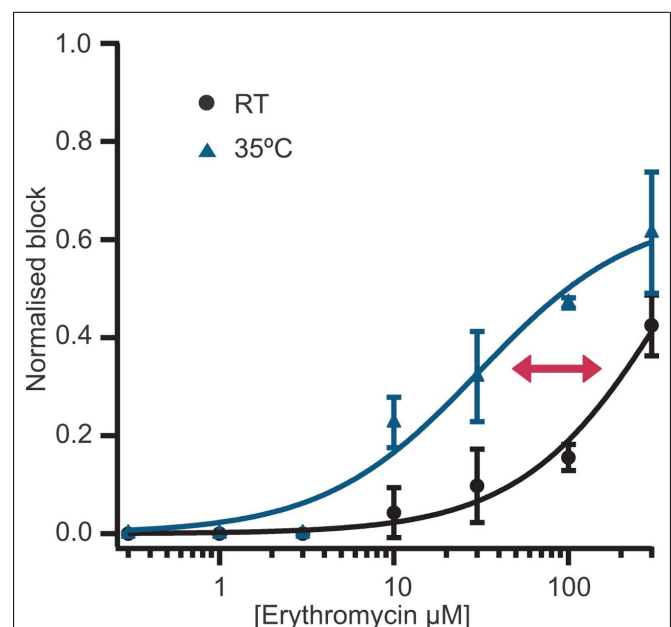
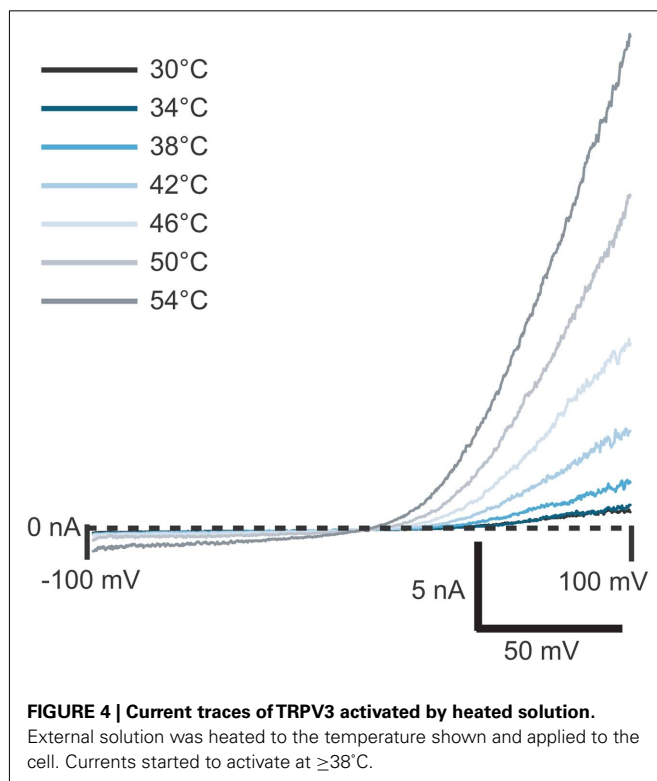
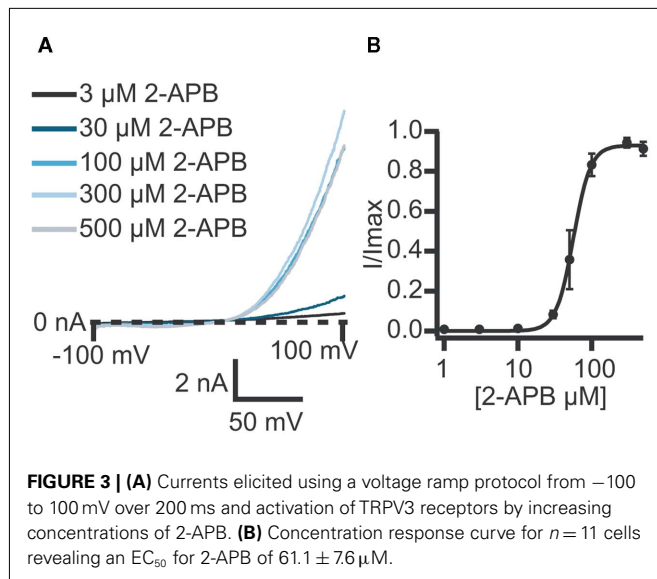


FIGURE 2 | Concentration response curves for erythromycin at room temperature ($n = 12$) and at 35°C ($n = 18$). Erythromycin is approximately 10-fold more potent at 35°C compared with room temperature. An overlay of the concentration response curves at room temperature and 35°C clearly shows the shift in potency.



CsF, 20 mM EGTA, 10 mM HEPES/CsOH (for **Figures 3, 4, 9, and 10**). External solution (except for recordings shown in **Figure 9B**): 140 mM NaCl, 4 mM KCl, 1 mM MgCl_2 , 2 mM CaCl_2 , 5 mM D-Glucose monohydrate, 10 mM HEPES/NaOH pH 7.4 . External solution for nicotinic $\alpha 7$ channel recordings (**Figure 9B**): 80 mM NaCl, 3 mM KCl, 45 mM CaCl_2 , 10 mM HEPES (Na^+ salt)/HCl, pH 7.4 . Solutions for action potential (AP) recording in the conventional patch clamp rig (**Figure 5G**) were 130 mM KAs, 15 mM KCl, 5.5 mM MgCl_2 , 5 mM Na_2ATP , 5 mM K_2 phosphocreatine,

10 mM HEPES, pH 7.25 (internal) and 140 mM NaCl, 4 mM KCl, 2 mM CaCl_2 , 1 mM MgCl_2 , 10 mM glucose, 10 mM HEPES, pH 7.35 (external).

Electrophysiology. Whole cell patch clamp recordings were conducted as previously described (Farre et al., 2009; Stoelzle et al., 2011). Currents were elicited using voltage protocols in the voltage clamp mode. For hERG, a voltage step protocol from the holding potential (-80 mV) to $+40$ mV for 500 ms followed by a 500 -ms step to -40 mV, repeated every 20 s. Peak amplitude at -40 mV was used for analysis. For $\text{Na}_v 1.5$, currents were elicited using 10 ms voltage steps from -120 to 0 mV repeated every 1 s. For ligand-gated experiments, cells were held at a constant holding potential of -80 mV and solutions were exchanged within 100 ms to activate receptors and minimize ligand exposure time. For heat activation of TRPV3 channels, external solution was heated to the temperature indicated and applied to the cell. Alternatively, 2-APB at increasing concentrations at RT was used to activate TRPV3. A voltage ramp protocol from -100 to 100 mV over 200 ms was used to record TRPV3 currents. Current amplitude at 90 mV was used for analysis. APs were generated using a depolarizing pulse to the threshold at which an AP was elicited. Membrane potential was kept at -80 to -100 mV (cell dependent). The AP traces shown represent an average response of four recorded APs. The APs were normalized to the time point of the beginning of the upstroke. Equipment: NPC-16 Patchliner Octo (with temperature control option) and SyncroPatch 96 (Nanion Technologies GmbH, Germany). Patch clamp amplifier for the Patchliner: EPC-10 Quadro (HEKA Elektronik GmbH, Germany), patch clamp amplifier for the SyncroPatch 96: Triton + (Tecella, CA, USA), PatchControl HT and PatchControl 96 software (Nanion Technologies GmbH, Germany). Software for data acquisition (PatchMaster, HEKA Elektronik GmbH, Germany; PatchControl 96, Nanion Technologies GmbH, Germany) and analysis (IGOR Pro WaveMetrics Inc., OR, USA and SyncroPatch Data Analysis Package, Nanion Technologies GmbH, Germany). NPC-16 or NPC-96 chips (single-use, disposable; Nanion Technologies GmbH, Germany) were used.

APPLICATIONS AND NOVEL FEATURES

TEMPERATURE REGULATION

Experiments at physiological temperature

Compounds can display different properties or different potencies at physiological temperature (35°C) vs. RT. Therefore, it is a desirable option to be able to study ion channels at elevated temperature. To meet this need, several heating elements were introduced into the Patchliner. The surrounding of the planar patch clamp chip can be heated to maintain constant, physiological temperature. The solution, which is pipetted onto the cell, can also be heated separately. To prevent any degradation of compounds inside the pipette due to long heating phases, only the volume which is required (typically 40 – $100 \mu\text{l}$, depending on the application) is heated, directly before application to the chamber of the patch clamp chip. Heating of the solution, which is applied to the cell takes 23.4 ± 4 s (for temperatures between 30 and 70°C ; data not shown).

One compound, which has been shown to have an increase in potency at physiological temperature, is erythromycin.

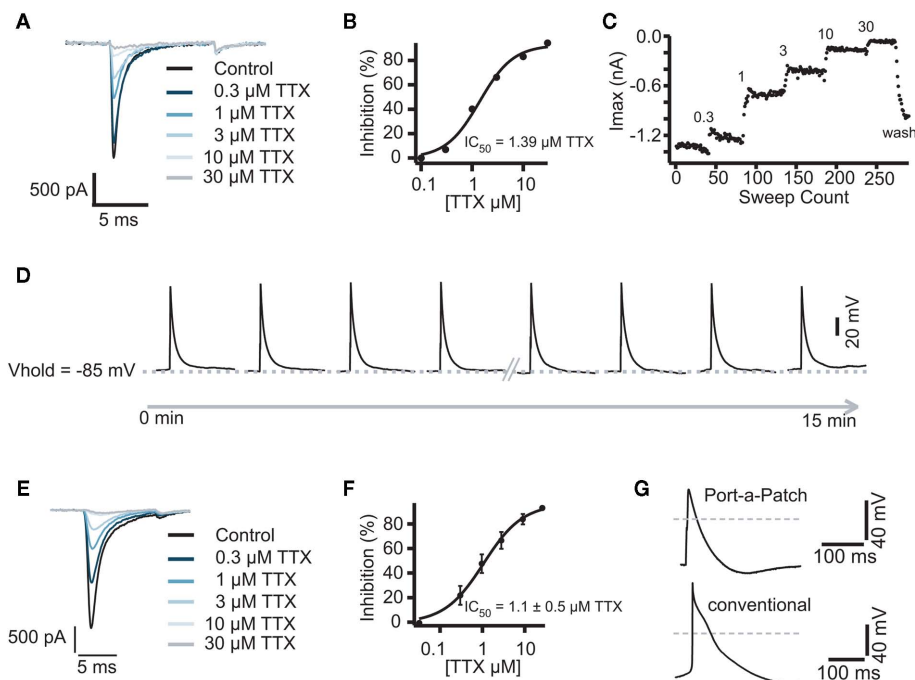


FIGURE 5 | (A) Representative traces of a Cor. At cardiomyocyte recorded in the voltage clamp mode and block by increasing concentrations of TTX. Raw data of Na^+ currents in control solution and in the presence of increasing TTX concentrations (0.3, 1, 3, 10, and 30 μM), elicited by 10 ms voltage steps to 0 mV from a holding potential of -80 mV , sweep interval 2 s. **(B)** Corresponding concentration response curve with a calculated IC_{50} of $1.3 \pm 0.4 \mu\text{M}$ ($n = 3$). **(C)** Corresponding time plot of the experiment showing the stability of the recording. Current amplitude was reduced step by step upon application of the increasing concentrations. A washout

of TTX was performed at the end of experiment. **(D)** Representative traces of highly reproducible APs as recorded in the current clamp mode. Sweep interval between each stimulus was 10 s. Traces were recorded over 15 min, the first and the last 4 APs are shown. The same experiment as shown in **(A)** was performed on the semi-automated patch clamp system Port-a-Patch **(E)**. The corresponding IC_{50} was calculated to be $1.1 \pm 0.5 \mu\text{M}$ ($n = 4$). **(F)**, **(G)** Comparison of an AP recorded with the Port-a-Patch (top trace) and using a conventional patch clamp rig (lower trace). Gray line indicates 0 mV.

Erythromycin is a macrolide antibiotic, which can cause QT prolongation and cardiac arrhythmia. Erythromycin has been shown to block hERG channels at physiological temperature with an IC_{50} of approximately $40 \mu\text{M}$ (Stanat et al., 2003). However, at RT erythromycin is much less potent. At a concentration of $100 \mu\text{M}$, erythromycin causes no significant block of hERG currents at RT but significantly blocks currents at physiological temperature (Guo et al., 2005).

Here we present data collected on a Patchliner Octo with temperature control at RT and at 35°C and the effect this has on the potency of erythromycin. Current responses of two individual cells to 500 ms voltage pulses to $+40 \text{ mV}$ and then -40 mV in the presence and absence of $100 \mu\text{M}$ erythromycin at RT and 35°C are shown in **Figure 1**. At RT (**Figure 1A**) $100 \mu\text{M}$ erythromycin caused little reduction in current amplitude (at -40 mV ; approx. 15%) compared with an almost 50% reduction in current amplitude at 35°C (**Figure 1B**). This is in good agreement with the literature (Guo et al., 2005).

Typically, single concentrations of erythromycin were applied to each cell. **Figure 2** shows averaged concentration response curves for erythromycin at RT and at 35°C overlaid. At higher concentrations ($300 \mu\text{M}$), erythromycin did block hERG currents at RT by approximately 40% and gave an IC_{50} of $427.5 \mu\text{M}$ calculated from the graph ($n = 12$). At $300 \mu\text{M}$, erythromycin blocked

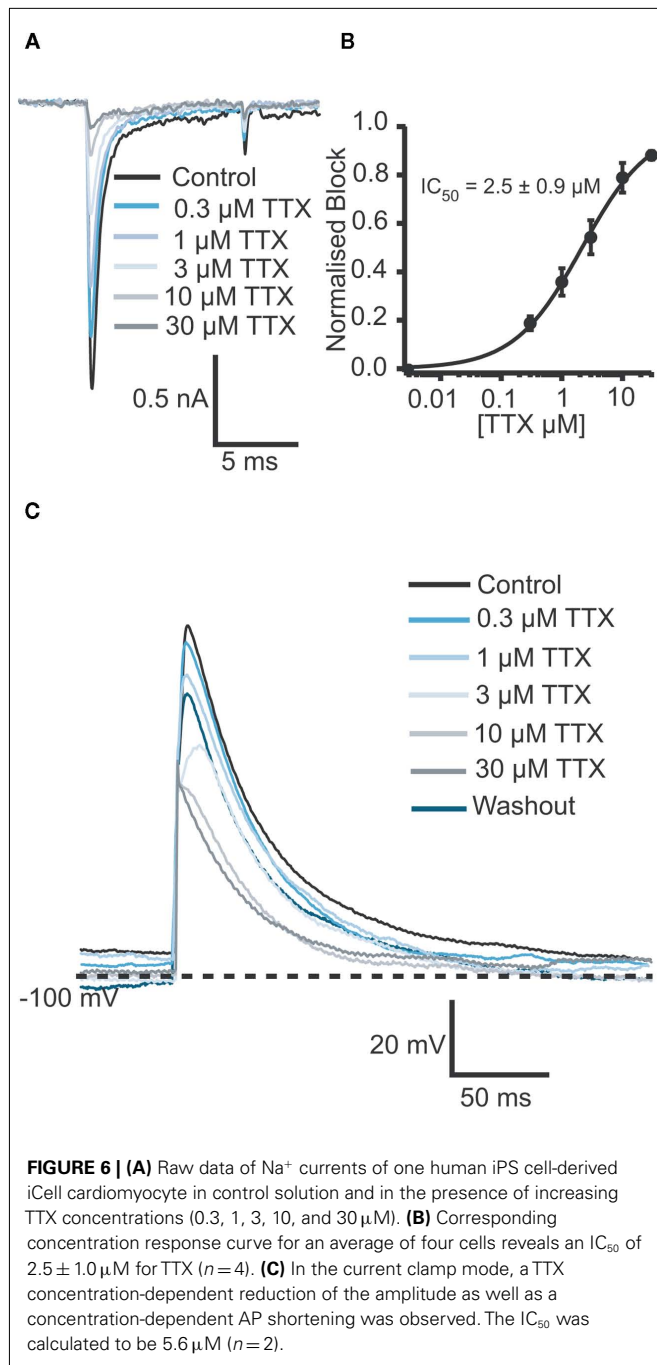
hERG currents at 35°C by 70% and the IC_{50} at this temperature was calculated to be $30.7 \mu\text{M}$ ($n = 18$). This is in excellent agreement with values reported in the literature (Stanat et al., 2003).

Table 1 shows success rates of reaching a giga-ohm seal and cell parameters for hERG stably expressed in HEK cells (Millipore, USA), $n = 35$.

Heat activation of TRPV3

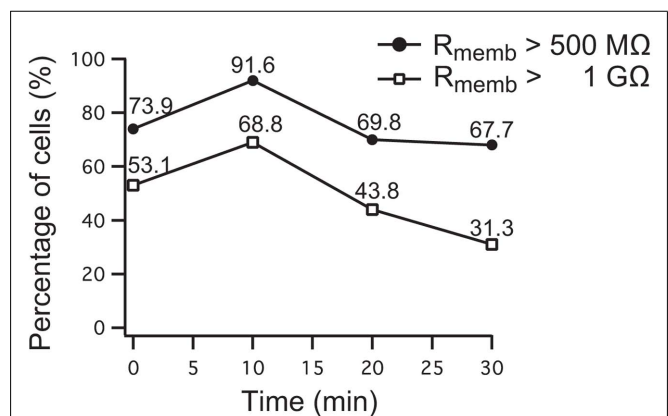
Transient receptor potential (TRP) channels are an important class of receptors found widely distributed throughout the mammalian central and peripheral nervous systems. They have been shown to be activated by many stimuli including temperature, mechanostimulation, divalent cations, and pH (for review see Clapham, 2003). TRP channels are receiving much attention as potential targets for the treatment of, for example, chronic pain, asthma, and diabetes insipidus (Clapham, 2003; Gudermann and Flockerzi, 2005).

We have used the Patchliner to study TRPV3 channels using either 2-APB or heat to activate the receptors. High quality data could be achieved with a high success rate for obtaining seals in the $\text{G}\Omega$ range ($> 80\%$). **Table 2** shows success rates and cell parameters for TRPV3 stably expressed in HEK cells (Millipore, USA) activated by either 2-APB or heat.



TRPV3 currents were activated by 2-APB in a concentration-dependent manner. **Figure 3** shows current traces of TRPV3 expressed in HEK cells and activation by 2-APB. The concentration response curve is also shown revealing an $EC_{50} = 61.1 \pm 7.6 \mu$ M ($n = 11$). This is in good agreement with values reported in the literature (Chung et al., 2004; Hu et al., 2009).

TRPV3 receptors can also be activated by temperature. **Figure 4** shows the activation of TRPV3 channels by increasing temperature. To do these experiments, external bath solution was heated in the robotic pipette and after the set temperature was reached,



the heated solution was applied to the cell at a speed of 10μ l/s. Outwardly rectifying currents started to activate at 38°C and increased in amplitude as temperature increased, up to 54°C , in good agreement with the literature (Peier et al., 2002; Smith et al., 2002; Xu et al., 2002).

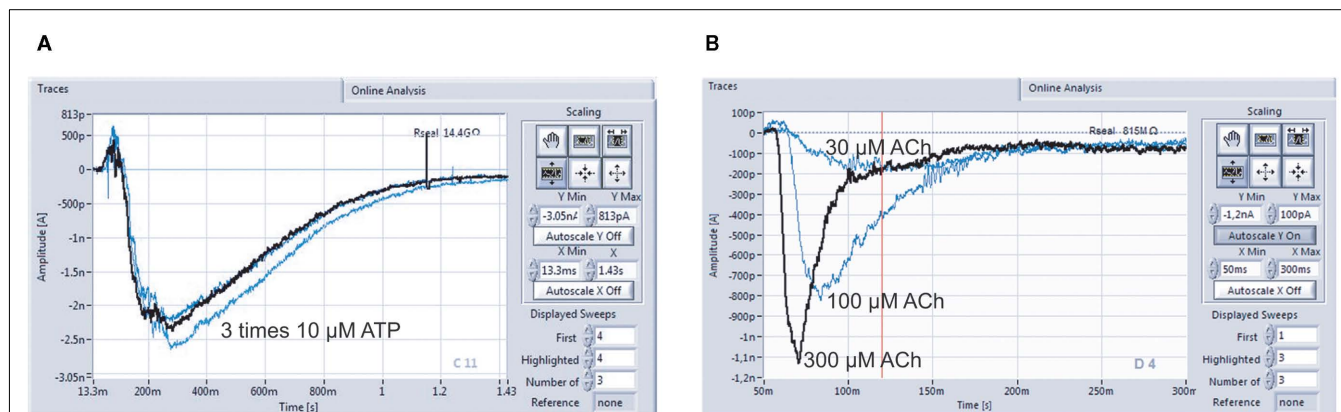


FIGURE 9 | Multiple compound additions can be performed, allowing the generation of full concentration response curves on individual cells. (A) P2X_{2/3} receptors expressed in a 1321N1 cell were repeatedly activated by 10 μM ATP (three times activation with

intermittent wash steps; data courtesy of Evotec AG). **(B)** Activation of nicotinic α7 receptors with 30, 100, and 300 μM ACh in one cell. Cells stably expressing human nAChRs were kindly provided by Galantox Pharma GmbH.

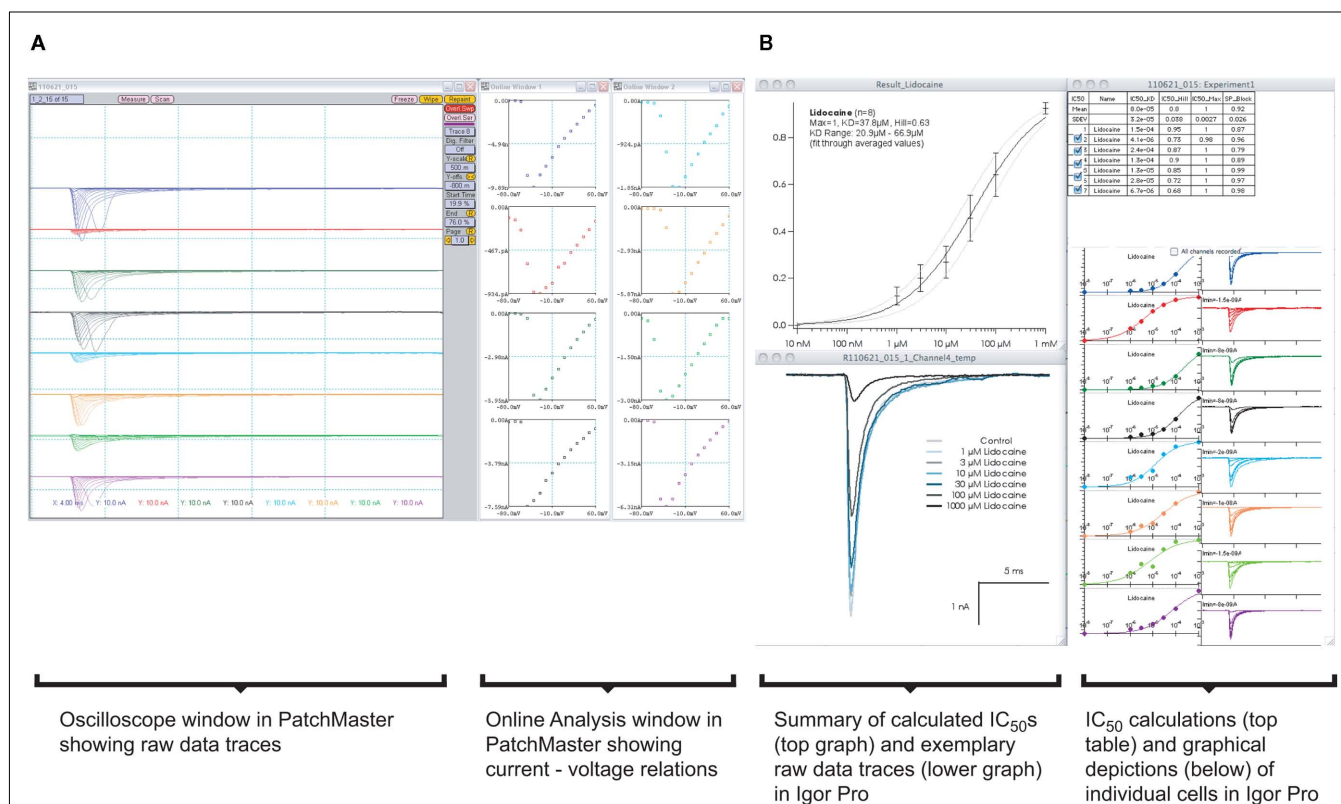


FIGURE 10 | (A) Graphical user interface for software used on a Patchliner system. PatchMaster raw data files from eight parallel recordings of Na_v1.5 expressing HEK cells. A screenshot of the oscilloscope with current traces and online analysis windows with corresponding current-voltage relations are

shown. Data are loaded into IGOR Pro **(B)** with aid of a macro. After a few mouse clicks, individual IC₅₀ values for a compound (here lidocaine) from each cell and the averaged data, including all relevant values and calculations, are displayed.

PARALLEL CURRENT CLAMP MEASUREMENTS

The Patchliner was used in combination with stem cell-derived cardiomyocytes, a standardized and pure cardiac myocyte model. This is a new opportunity because cardiac toxicity can now be

evaluated in a cell type which better represents the real physiological environment compared with a cell line overexpressing a particular ion channel. Patch clamp measurements with cardiac myocytes are sophisticated experiments that were, until now,

only possible using conventional patch clamp using freshly isolated cardiac myocytes from animals. Stem cell-derived cardiac myocytes are commercially available, a pure population and ready-to-use resulting in a quicker cell preparation time and better reproducibility of the assay.

The Patchliner was used for pharmacological experiments in both voltage clamp and current clamp modes so that the effects of cardiotoxic compounds could be directly investigated on both ion currents and APs. The eight-channel system Patchliner and the one-channel system Port-a-Patch (Farre et al., 2007) are the currently only APC devices which allow for both voltage and current clamp recordings. We used mouse stem cell-derived Cor.At cardiomyocytes and human iPS cell-derived iCell cardiomyocytes. The cells showed expression of Na^+ , Ca^{2+} , and K^+ channels in the voltage clamp mode after a minimum of 2 days of culturing (for Cor.At cells, see also Stoelzle et al., 2011). Cor.At cardiomyocytes which had been in culture for more than 4 days required a prolonged incubation with the digestion enzyme to obtain single cell suspensions. This in turn reduced the success rates to obtain giga-ohm seals, hence we used cells that were in culture for 2–4 days. We did not see a difference between those cells with regards to channel expression or success rate.

After optimization of the harvesting methods, the Cor.At and iCell cardiomyocytes had a high success rate when used on the Patchliner, which resulted in long lasting recordings both in voltage clamp and current clamp modes (Figures 5 and 6). A typical pharmacological experiment in the voltage clamp mode using multiple concentrations of a compound (in this case TTX) and washout to check reversibility was performed with a Patchliner (Figures 5A–C and 6) and also with the Port-a-Patch (Figures 5E,F). In the current clamp mode, APs were elicited by a short depolarizing pulse (1 ms current injection to the threshold at which an AP was elicited). The shape was not only comparable to the shape of APs recorded with the one-cell-at-a-time system Port-a-Patch and a conventional patch clamp rig (Figure 5G), but also stable over a long period of time (Figure 5D), confirming that the cells are suitable for analyzing compound effects on APs. Therefore the generation of a full concentration response curve on an individual cell can be generated easily due to the stability of the measurements (Figure 5D; see also Stoelzle et al., 2011). Pharmacological experiments on APs have been extensively studied on Cor.At cells, including a study on frequency dependent inhibition of Na^+ channels (Stoelzle et al., 2011). Figure 6C shows APs generated using iCell cardiomyocytes using a short depolarizing pulse (as described above) and the expected shortening of the AP duration and a slowing of velocity of the upstroke by increasing concentrations of TTX. The IC_{50} achieved in the current clamp mode [$\text{IC}_{50} = 5.6 \mu\text{M}$ ($n = 2$)] agrees well with the IC_{50} from voltage clamp [$2.5 \pm 0.9 \mu\text{M}$ ($n = 4$)]. Table 3 shows success rate and cell parameters for iCell cardiomyocytes ($n = 69$).

HIGH-THROUGHPUT AUTOMATED PATCH CLAMP

The SyncroPatch 96 (Figure 7) is a screening platform which generates high quality patch clamp data and provides accurate pharmacology because full dose response curves can be acquired from individual cells with giga-ohm seals. It is a well suited tool for secondary screening efforts and for safety testing either for dose

Table 1 | Success rate, cell parameters, and experiment duration for $n = 35$ HEK cells stably expressing hERG.

Success rate (%)	R_{memb} (G Ω)	Cm (pF)	Rs (M Ω)	Exp. duration (min)
65	2.4 ± 0.5	7.9 ± 1	7.0 ± 1	19 ± 2

Parameters of cells recorded at RT and 35°C were pooled since no difference was observed between those conditions. Given errors are standard errors of the mean. Sixty-five percent of the cells had a membrane resistance of $2.4 \pm 0.5 \text{ G}\Omega$; the seals were stable over $19 \pm 2 \text{ min}$.

Table 2 | Success rate, cell parameters, and experiment duration for $n = 87$ HEK cells stably expressing TRPV3.

Success rate (%)	R_{memb} (M Ω)	Cm (pF)	Rs (M Ω)	Exp. duration (min)
81	934 ± 191	18 ± 1	6.2 ± 0.4	39 ± 2

Given errors are standard errors of the mean. Eighty-one percent of the cells had a membrane resistance of $934 \pm 191 \text{ M}\Omega$, the seals were stable over $39 \pm 2 \text{ min}$.

Table 3 | Success rate, cell parameters, and experiment duration for $n = 69$ iCell cardiomyocytes.

Success rate (%)	R_{memb} (G Ω)	Cm (pF)	Rs (M Ω)	Exp. duration (min)
46	1.4 ± 0.3	12.9 ± 1	6.0 ± 0.6	18.2 ± 1

Given errors are standard errors of the mean. Forty-six percent of the cells had a membrane resistance of $1.4 \pm 0.3 \text{ G}\Omega$, the seals were stable over $18.2 \pm 1 \text{ min}$.

Table 4 | In total, 64 of the 96 cells reached a seal resistance of around 1.8 G Ω within the first 10 min after reaching the whole cell mode, 21 cells reached a resistance of around 783 M Ω .

Number of cells	R_{memb} (M Ω)	Number of cells stable for 20 min (%)	Number of cells stable for 30 min (%)
64	1865 ± 99	43.8	31.3
21	783 ± 29	69.8	67.7
11	152 ± 48	n.a.	n.a.

The remaining cells had a resistance of around 152 M Ω . 43.8% of the cells having a giga-ohm seal remained their seal for 20 min, 31.3% had the giga-ohm seal still after 30 min. 69.8% of the cells having around 783 M Ω as a seal resistance remained their seal for 20 min, 67.7% for 30 min. $N = 96$ cells, recorded on one NPC-96 patch clamp chip, given errors are standard errors of the mean.

response analysis or single-point screening. Table 4 shows success rates of representative experiments using $\text{Na}_v1.5$ overexpressing HEK cells on one patch clamp chip (NPC-96 patch clamp chip for 96 cells being recorded in parallel). Furthermore, the stability of cells over time is listed as well. Figure 8 shows a corresponding graphical depiction of the development of the seal stability over time.

Voltage clamp recordings are continuous during compound application and solution exchange time is in the order of 100 ms. This allows for screening of compound action on ligand- and voltage-gated ion channels. An APC device with fast solution exchange is a prerequisite for studying fast desensitizing channels such as nicotinic acetylcholine receptor (nAChR). Enhancers of nAChRs, such as galantamine, may have therapeutic benefit for Alzheimer's disease (Samochocki et al., 2003). It is, therefore, essential to be able to search for nAChR agonists and enhancers at a higher throughput.

Figure 9A shows a typical screenshot with recordings of a ligand-gated ion channel, P2X_{2/3}. P2X_{2/3} receptors in a 1321N1 cell were repeatedly activated by 10 μ M ATP, demonstrating the reliability of repetitive drug applications. nAChR $\alpha 7$ expressing HEK cells were activated by increasing concentrations of ACh (30, 100, 300 μ M; **Figure 9B**). Given the importance of this channel as a potential therapeutic target for conditions such as Alzheimer's disease, schizophrenia, and Parkinson's disease (for review see Colquhoun et al., 2003; Albuquerque et al., 2009), it is critical that researchers have tools to study them reliably.

The disposable planar borosilicate-glass substrate used for seal formation ensures high quality data and long lasting seals when using the Patchliner and SyncroPatch 96. In general, with a success rate for completed experiments of $51.7 \pm 10\%$ ($n = 567$), the SyncroPatch 96 has a data throughput of approximately 5000 data point per day. With a Patchliner Octo, having a success rate of around 80%, approximately 500 data points can be generated per day (Farre et al., 2009).

DATA ANALYSIS

Increasing the throughput in APC devices results in an increase in data generation and, thereby, necessitates the need for automated data analysis. **Figure 10A** shows a screenshot of one run on a Patchliner Octo, which records from eight cells at a time. Here, Na_v1.5 stably expressing HEK cells were used (Millipore, USA). The raw data are saved as PatchMaster (.dat) files and an additional Microsoft office excel spreadsheet is generated, which can be easily loaded in IGOR Pro (WaveMetrics, USA). We developed a macro which is implemented in IGOR Pro that enables the upload, graphical display of raw data traces and IC₅₀ calculation of individual cells or an average of all cells for each compound in summary (**Figure 10B**).

For the analysis of concentration response curves, the SyncroPatch 96 software provides an intuitive graphical user interface (**Figure 11**). The recording sites are color coded according to user defined success criteria (membrane resistance, access resistance, current amplitude etc.). The user can generate individual IC₅₀ values or an average IC₅₀ of the recorded cells. Current-voltage relationships, leak-subtraction, and time-dependence of recorded values can be displayed besides a repertoire of other calculations.

DISCUSSION AND OUTLOOK

The APC devices used here for data recordings are equipped for studying ion channels in various areas of research, drug discovery, and safety screening. The data quality and reproducibility of pharmacological experiments is consistent between the automated systems and a manual patch clamp rig or semi-automated patch clamp system like the Port-a-Patch as shown for current clamp

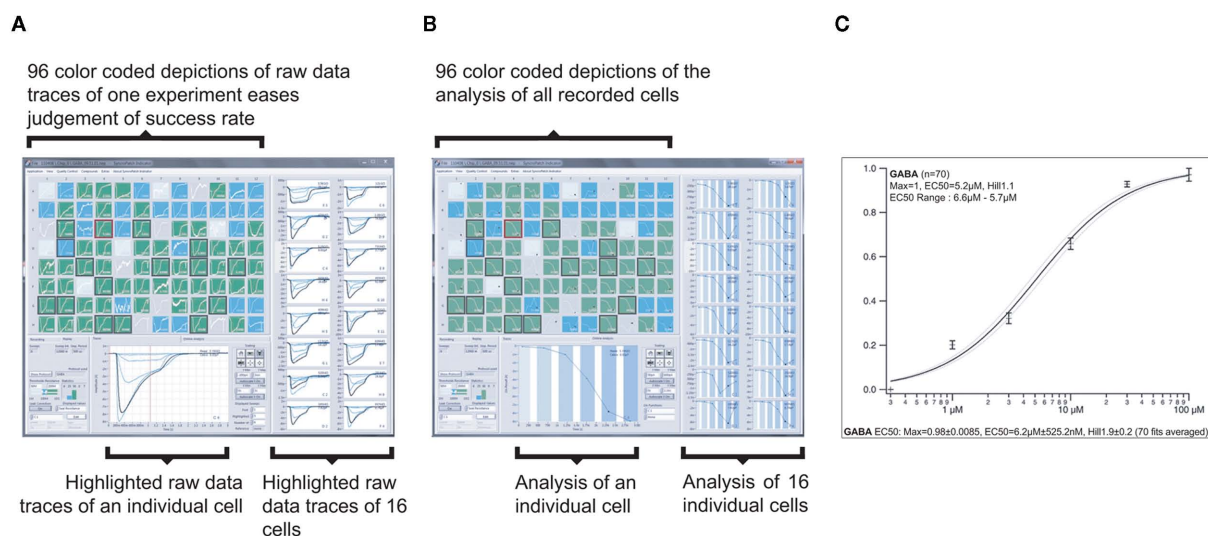


FIGURE 11 | Graphical user interface of the screening and data analysis software used on the SyncroPatch 96. (A) Screenshot of depiction of raw data of GABA_A subunits $\alpha 1\beta 2\gamma 2$ expressing HEK cells as recorded on one NPC-96 patch clamp chip. Ninety-six small color coded pictures as seen in the upper left part display all 96 parallel recordings. Depending on the seal resistance, pictures are green ($R_{\text{memb}} > 100 \text{ M}\Omega$), blue ($R_{\text{memb}} = 50\text{--}100 \text{ M}\Omega$), light blue or gray ($R_{\text{memb}} < 50 \text{ M}\Omega$ or no cell capture). One highlighted experiment is displayed below, 16 other selected experiments are displayed on the right. Traces show currents of individual cells which were activated by

six GABA concentrations (0.3, 1, 3, 10, 30, and 100 μ M). Intermittent wash steps with control solution were performed. **(B)** Screenshot showing the same experiment as in **(A)**, but displaying individual concentration response curves. For highlighted experiments (in lower part and right), note the different shades of blue overlaid on the curves, representing the six increasing concentrations of GABA. The white color represents the intermittent wash steps. **(C)** Averaged concentration response curve and related parameters of successful experiments (here 70 out of 96) of the same experiment.

recordings from pluripotent stem cell-derived cardiomyocytes. The overall instrument performance, success rates, longevity of recordings, and compatibility with various cell lines and assay types are fundamental for effective screening work in electrophysiology departments. Effective screening in the broader sense also means cost effectiveness, which is, of course, an essential qualification. The combination of an *in vitro* cardiac cell model with higher throughput patch clamp screening technology opens up a new way for cardiotoxicity prediction in a physiologically relevant cell system. The ability to perform current clamp recordings and a temperature-regulated cell environment are unique features of the Patchliner, currently not available on other higher throughput APC systems. Furthermore, the temperature control feature of the Patchliner can be used to record ion currents and APs at physiological temperatures and to activate temperature-regulated receptors such as the TRP family of receptors to discover specific inhibitors with a reduced side-effect profile. The data shown on TRP channels prove not only the versatility of the liquid handling that is needed to repeatedly activate the cell by perfusing heated solution, but also the exactness of heating and precisely timed exposure of the cell to the heated solution.

The Patchliner is compatible with many different cell lines, showing little discrepancy between the cell lines used (data described in this paper and Bruggemann et al., 2006; Farre et al., 2007, 2009). Interestingly, recordings of a variety of primary cells have also been described using the Patchliner (Milligan et al., 2009). Few, if any, other APC devices have been able to demonstrate such compatibility with primary cells.

REFERENCES

- Albuquerque, E. X., Pereira, E. F., Alkon-don, M., and Rogers, S. W. (2009). Mammalian nicotinic acetylcholine receptors: from structure to function. *Physiol. Rev.* 89, 73–120.
- Ashcroft, F. M. (2000). *Ion Channels and Disease: Channelopathies*, London: Academic Press.
- Balansa, W., Islam, R., Fontaine, F., Piggott, A. M., Zhang, H., Webb, T. I., Gilbert, D. F., Lynch, J. W., and Capon, R. J. (2010). Irciniactams: subunit-selective glycine receptor modulators from Australian sponges of the family Irciniidae. *Bioorg. Med. Chem.* 18, 2912–2919.
- Bruggemann, A., Farre, C., Haarmann, C., Haythornthwaite, A., Kreir, M., Stoelzle, S., George, M., and Fertig, N. (2008). Planar patch clamp: advances in electrophysiology. *Methods Mol. Biol.* 491, 165–176.
- Bruggemann, A., Stoelzle, S., George, M., Behrends, J. C., and Fertig, N. (2006). Microchip technology for automated and parallel patch-clamp recording. *Small* 2, 840–846.
- Chung, M. K., Lee, H., Mizuno, A., Suzuki, M., and Caterina, M. J. (2004). 2-Aminoethoxydiphenyl borate activates and sensitizes the heat-gated ion channel TRPV3. *J. Neurosci.* 24, 5177–5182.
- Clapham, D. E. (2003). TRP channels as cellular sensors. *Nature* 426, 517–524.
- Clare, J. J. (2010). Targeting ion channels for drug discovery. *Discov. Med.* 9, 253–260.
- Colquhoun, D., Unwin, N., Shelly, C., Hatton, C., and Sivilotti, L. (2003). “Nicotinic acetylcholine receptors,” in *Burger’s Medicinal Chemistry and Drug Discovery: Drug Discovery and Drug Development*, eds A. Burger and D. J. Abraham (New York: Wiley), 357–405.
- Dunlop, J., Bowlby, M., Peri, R., Tawa, G., Larocque, J., Soloveva, V., and Morin, J. (2008). Ion channel screening. *Comb. Chem. High Throughput Screen.* 11, 514–522.
- Farre, C., George, M., Bruggemann, A., and Fertig, N. (2008). Ion channel screening – automated patch clamp on the rise. *Drug Discov. Today Technol.* 5, e23–e25.
- Farre, C., Haythornthwaite, A., Haarmann, C., Stoelzle, S., Kreir, M., George, M., Bruggemann, A., and Fertig, N. (2009). Port-a-patch and patchliner: high fidelity electrophysiology for secondary screening and safety pharmacology. *Comb. Chem. High Throughput Screen.* 12, 24–37.
- Farre, C., Stoelzle, S., Haarmann, C., George, M., Bruggemann, A., and Fertig, N. (2007). Automated ion channel screening: patch clamping made easy. *Expert Opin. Ther. Targets* 11, 557–565.
- Gudermann, T., and Flockerzi, V. (2005). TRP channels as new pharmacological targets. *Naunyn Schmiedeberg Arch. Pharmacol.* 371, 241–244.
- Guo, J., Zhan, S., Lees-Miller, J. P., Teng, G., and Duff, H. J. (2005). Exaggerated block of hERG (KCNH2) and prolongation of action potential duration by erythromycin at temperatures between 37 degrees C and 42 degrees C. *Heart Rhythm* 2, 860–866.
- Hille, B. (1992). *Ionic Channels of Excitable Membranes*. Sunderland, MA: Sinauer Associates.
- Hu, H., Grandl, J., Bandell, M., Petrus, M., and Patapoutian, A. (2009). Two amino acid residues determine 2-APB sensitivity of the ion channels TRPV3 and TRPV4. *Proc. Natl. Acad. Sci. U.S.A.* 106, 1626–1631.
- Kolossov, E., Bostani, T., Roell, W., Breitenbach, M., Pillekamp, F., Nygren, J. M., Sasse, P., Rubenchik, O., Fries, J. W., Wenzel, D., Geisen, C., Xia, Y., Lu, Z., Duan, Y., Kettenhofen, R., Jovine, S., Bloch, W., Bohlen, H., Welz, A., Hescheler, J., Jacobsen, S. E., and Fleischmann, B. K. (2006). Engraftment of engineered ES cell-derived cardiomyocytes but not BM cells restores contractile function to the infarcted myocardium. *J. Exp. Med.* 203, 2315–2327.
- Li, J., Sukumar, P., Milligan, C. J., Kumar, B., Ma, Z. Y., Munsch, C. M., Jiang, L. H., Porter, K. E., and Beech, D. J. (2008). Interactions, functions, and independence of plasma membrane STIM1 and TRPC1 in vascular smooth muscle cells. *Circ. Res.* 103, e97–e104.
- Milligan, C. J., Li, J., Sukumar, P., Majeed, Y., Dallas, M. L., English, A., Emery, P., Porter, K. E., Smith, A. M., Mcfadzean, I., Beccano-Kelly, D., Bahnasi, Y., Cheong, A., Naylor, J., Zeng, F., Liu, X., Gamper, N., Jiang, L. H., Pearson, H. A., Peers, C., Robertson, B., and Beech, D. J. (2009). Robotic multiwell planar patch-clamp for native and primary mammalian cells. *Nat. Protoc.* 4, 244–255.

In both academic and pharmaceutical laboratories it is of advantage to be able to record ion channels in a more physiologically relevant environment, e.g., primary cell cultures, for drug discovery, biophysical and physiological analysis, and safety pharmacology using an APC system.

Fast external exchange, minimal compound exposure, and continuous current recording make the Patchliner and SyncroPatch 96 suited to ligand-gated ion channel measurements. Fast desensitizing receptors such as the nicotinic $\alpha 7$ receptor can be reliably recorded when taking advantage of the possibility to minimize the exposure time of the cell to the compound. The applied compound solution, e.g., containing the ligand can be replaced by a control solution after 200 ms. Volumes of the ligand containing or control solution and speed of application are set by the user to control speed of exchange and ligand exposure time. Settings can be adapted according to the receptor of interest to optimize reproducibility of current responses.

Providers of APC devices constantly strive to improve and extend the application range of these devices and features. As described in this manuscript, recordings in the current clamp mode and at physiological temperature are relevant features and will be of good use in the future in both academic and pharmaceutical research.

ACKNOWLEDGMENTS

We thank Davide Pau, Scottish Biomedical, UK for performing AP recordings on a conventional patch clamp rig and for letting us use his data.

- Neher, E., and Sakmann, B. (1976). Single-channel currents recorded from membrane of denervated frog muscle fibres. *Nature* 260, 799–802.
- Peier, A. M., Reeve, A. J., Andersson, D. A., Moqrich, A., Earley, T. J., Hergarden, A. C., Story, G. M., Colley, S., Hogenesch, J. B., McIntyre, P., Bevan, S., and Patapoutian, A. (2002). A heat-sensitive TRP channel expressed in keratinocytes. *Science* 296, 2046–2049.
- Samochocki, M., Höfle, A., Fehrenbacher, A., Jostock, R., Ludwig, J., Christner, C., Radina, M., Zerlin, M., Ullmer, C., Pereira, E. F. R., Lübbert, H., Albuquerque, E. X., and Maelicke, A. (2003). Galantamine is an allosterically potentiating ligand of neuronal nicotinic but not of muscarinic acetylcholine receptors. *J. Pharmacol. Exp. Ther.* 305, 1024–1036.
- Smith, G. D., Gunthorpe, M. J., Kelsell, R. E., Hayes, P. D., Reilly, P., Facer, P., Wright, J. E., Jerman, J. C., Walhin, J. P., Ooi, L., Egerton, J., Charles, K. J., Smart, D., Randall, A. D., Anand, P., and Davis, J. B. (2002). TRPV3 is a temperature-sensitive vanilloid receptor-like protein. *Nature* 418, 186–190.
- Stanat, S. J., Carlton, C. G., Crumb, W. J. Jr., Agrawal, K. C., and Clark, C. W. (2003). Characterization of the inhibitory effects of erythromycin and clarithromycin on the HERG potassium channel. *Mol. Cell. Biochem.* 254, 1–7.
- Stoelzle, S., Haythornthwaite, A., Kettenhofen, R., Kolossov, E., Bohlen, H., George, M., Bruggemann, A., and Fertig, N. (2011). Automated patch clamp on mESC-derived cardiomyocytes for cardiotoxicity prediction. *J. Biomol. Screen.*
- Xu, H., Ramsey, I. S., Kotecha, S. A., Moran, M. M., Chong, J. A., Lawson, D., Ge, P., Lilly, J., Silos-Santiago, I., Xie, Y., Distefano, P. S., Curtis, R., and Clapham, D. E. (2002). TRPV3 is a calcium-permeable temperature-sensitive cation channel. *Nature* 418, 181–186.
- Conflict of Interest Statement:** The authors declare that the research was conducted in the absence of any commercial or financial relationships that could be construed as a potential conflict of interest.
- Received: 01 August 2011; accepted: 07 November 2011; published online: 24 November 2011.
- Citation: Stoelzle S, Obergrussberger A, Bruggemann A, Haarmann C, George M, Kettenhofen R and Fertig N (2011) State-of-the-art automated patch clamp devices: heat activation, action potentials, and high throughput in ion channel screening. *Front. Pharmacol.* 2:76. doi: 10.3389/fphar.2011.00076
- This article was submitted to *Frontiers in Pharmacology of Ion Channels and Channelopathies*, a specialty of *Frontiers in Pharmacology*.
- Copyright © 2011 Stoelzle, Obergrussberger, Bruggemann, Haarmann, George, Kettenhofen and Fertig. This is an open-access article subject to a non-exclusive license between the authors and Frontiers Media SA, which permits use, distribution and reproduction in other forums, provided the original authors and source are credited and other Frontiers conditions are complied with.



Neurons on a chip – toward high throughput network and pharmacology investigations

John Michael Nagarah*

Broad Fellows Program, Division of Biology, California Institute of Technology, Pasadena, CA, USA

*Correspondence: jnagarah@caltech.edu

A commentary on

From understanding cellular function to novel drug discovery: the role of planar patch-clamp array chip technology

by Py, C., Martina, M., Diaz-Quijada, G. A., Luk, C. C., Martinez, D., Denhoff, M. W., Charrier, A., Comas, T., Monette, R., Krantis, A., Syed, N. I., and Mealing, G. A. R. (2011). *Front. Pharmacol.* 2:51. doi: 10.3389/fphar.2011.00051

The biophysical properties of single neurons and synaptic connections between populations of neurons enable the brain to form memories, make decisions, and perceive the surrounding environment. The ability of neurons to transmit signals is reliant on ion channel proteins embedded in the plasma membrane (Hodgkin and Huxley, 1952; Koch, 2005). Ion channel defects and neural network dysfunction are the basis of several neurological disorders (Ackerman and Clapham, 1997; Palop et al., 2006; Seeley et al., 2009). The development of new technologies, such as those mentioned within this issue, is fueled by the desire not only to understand the fundamental processes underlying neuronal signals, but also, to gain a better understanding of the causes, and thus potential treatments for neurological diseases.

Traditionally, ion channel protein activity in single cells has been monitored using the glass pipette patch-clamp technique (Hamill et al., 1981). Our detailed understanding of ion channel kinetics and pharmacological properties made possible by this technique is one of the reasons why so many drug targets include ion channels (Wang and Li, 2003). However, the patch-clamp technique has been limited by the number of cells from which it can simultaneously record. Recent advances in robotics have enabled measurements in brain slices from 12 simultaneous pipette patch-clamp electrodes, illustrating novel

electrophysiological principles that govern network behavior, though these experiments are still demanding on the user (Anastassiou et al., 2011). In contrast, multi-electrode arrays (MEAs) and silicon-based transistor arrays allow for extracellular recordings from hundreds and thousands of electrodes simultaneously (Pine, 1980; Hutzler et al., 2006). Despite the limited amount of biophysical information obtained from these experiments, the high throughput of MEAs has enabled their successful use in discovering novel network mechanisms (Hosoya et al., 2005) and in screening potential pharmaceutical compounds (Hill et al., 2010; Redon et al., 2010). As each technique presents its own strengths and weaknesses, combining the throughput of the MEA platform with the resolution and control of the patch-clamp would provide a unique hybrid that would be highly welcomed in many areas of neuroscience.

Recently, researchers have succeeded in replacing the glass pipette with a micro-machined orifice in a planar substrate. Through their ability to achieve an electrical resistance greater than 1 gigaohm between the cell membrane and pore, planar patch-clamp electrodes have enabled high quality electrophysiology recordings (Fertig et al., 2002; Nagarah et al., 2010). Automated patch-clamp (APC) systems have been used primarily for pharmaceutical screening against ion channels of interest expressed in cell lines. Only recently have APCs been used to investigate primary cells or physiologically more relevant cells derived from pluripotent stem cells (Milligan et al., 2009; Stoelzle et al., 2011). In this issue, Py et al. (2011) describe their success in integrating cultured neurons onto planar patch-clamp electrodes. A significant accomplishment of theirs is obtaining gigaohm seals between poly-L-lysine (PLL) coated apertures and cultured neurons. This is surprising consider-

ing the contamination susceptibility of patch-clamp electrodes, suggesting the sealing mechanism of suspended cells is different than that of cultured neurons. Their platform has allowed for intracellular recordings of neuronal activity from cultured neurons and synapse formation on the chip, demonstrated by dual planar and pipette measurements along with pharmacological characterization. Simultaneous recordings from synaptically connected neurons with dual planar electrodes have proven difficult so far, but nonetheless, they are able to record from multiple apertures simultaneously using an improved device fabrication scheme and microfluidic channels. The authors are also making advancements in chemical patterning methods to precisely localize neurons onto the planar orifices which will eliminate the need for manual placement.

While the bulk of recordings have been from snail neurons, the authors have recently integrated mammalian neurons onto their device, increasing the applicability of this platform to drug screening. High throughput pharmaceutical screening on patch-clamped neuronal cultures will enable the observation of a drug's effect on synaptic transmission as well as ion channel behavior. Additionally, the planar nature of the devices described here opens up the possibility of integrating with it other technologies. For example, a novel microfluidic culture system has allowed for investigations of the cell biology of synaptic functions with high spatial and temporal resolution (Taylor et al., 2010). Combining a similar system with planar patch-clamp electrodes would add electrophysiological control to cell biology experiments, and provide even more detail to synaptic dynamics investigations. Further development is still needed before such experiments are made possible, but Py et al.'s efforts will undoubtedly contribute to the growing list

of tools that neuroscientists use to provide insight in neural computation, the nature of neurological diseases, and the treatment of diseases.

REFERENCES

- Ackerman, M. J., and Clapham, D. E. (1997). Ion channels – basic science and clinical disease. *N. Engl. J. Med.* 336, 1575–1586.
- Anastassiou, C. A., Perin, R., Markram, H., and Koch, C. (2011). Ephaptic coupling of cortical neurons. *Nat. Neurosci.* 14, 217–223.
- Fertig, N., Klau, M., George, M., Blick, R. H., and Behrends, J. C. (2002). Activity of single ion channel proteins detected with a planar microstructure. *Appl. Phys. Lett.* 81, 4865–4867.
- Hamill, O. P., Marty, A., Neher, E., Sakmann, B., and Sigworth, F. J. (1981). Improved patch-clamp techniques for high-resolution current recording from cells and cell-free membrane patches. *Pflugers Arch.* 391, 85–100.
- Hill, A. J., Jones, N. A., Williams, C. M., Stephens, G. J., and Whalley, B. J. (2010). Development of multi-electrode array screening for anticonvulsants in acute rat brain slices. *J. Neurosci. Methods* 185, 246–256.
- Hodgkin, A. L., and Huxley, A. F. (1952). A quantitative description of membrane current and its application to conduction and excitation in nerve. *J. Physiol. (Lond.)* 117, 500.
- Hosoya, T., Baccus, S. A., and Meister, M. (2005). Dynamic predictive coding by the retina. *Nature* 436, 71–77.
- Hutzler, M., Lambacher, A., Eversmann, B., Jenkner, M., Thewes, R., and Fromherz, P. (2006). High-resolution multitransistor array recording of electrical field potentials in cultured brain slices. *J. Neurophysiol.* 96, 1638.
- Koch, C. (2005). *Biophysics of Computation: Information Processing in Single Neurons*. New York, NY: Oxford University Press.
- Milligan, C. J., Li, J., Sukumar, P., Majeed, Y., Dallas, M. L., English, A., Emery, P., Porter, K. E., Smith, A. M., and Mcfadzean, I. (2009). Robotic multi-well planar patch-clamp for native and primary mammalian cells. *Nat. Protoc.* 4, 244.
- Nagarah, J. M., Paek, E., Luo, Y., Wang, P., Hwang, G. S., and Heath, J. R. (2010). Batch fabrication of high performance planar patch clamp devices in quartz. *Adv. Mater.* 22, 4622–4627.
- Palop, J. J., Chin, J., and Mucke, L. (2006). A network dysfunction perspective on neurodegenerative diseases. *Nature* 443, 768.
- Pine, J. (1980). Recording action potentials from cultured neurons with extracellular microcircuit electrodes. *J. Neurosci. Methods* 2, 19–31.
- Py, C., Martina, M., Diaz-Quijada, G. A., Luk, C. C., Martinez, D., Denhoff, M. W., Charrier, A., Comas, T., Monette, R., Krantis, A., Syed, N. I., and Mealing, G. A. R. (2011). From understanding cellular function to novel drug discovery: the role of planar patch-clamp array chip technology. *Front. Pharmacol.* 2:51. doi: 10.3389/fphar.2011.00051
- Redon, N., Lanneau, C., Cervello, P., Biton, B., Daniel, B., Oury-Donat, F., and Avenet, P. (2010). “Importance of multielectrode array recordings in drug discovery,” in *Seventh International Meeting on Substrate-Integrated Microelectrode Arrays*, ed. A. Stett (BIOPRO Baden-Württemberg GmbH), Stuttgart, 167–168.
- Seeley, W. W., Crawford, R. K., Zhou, J., Miller, B. L., and Greicius, M. D. (2009). Neurodegenerative diseases target large-scale human brain networks. *Neuron* 62, 42–52.
- Stoelzle, S., Haythornthwaite, A., Kettenhofen, R., Kolossov, E., Bohlen, H., George, M., Brüggemann, A., and Fertig, N. (2011). Automated patch clamp on meSc-derived cardiomyocytes for cardiotoxicity prediction. *J. Biomol. Screen.* 16, 910–916.
- Taylor, A. M., Dieterich, D. C., Ito, H. T., Kim, S. A., and Schuman, E. M. (2010). Microfluidic local perfusion chambers for the visualization and manipulation of synapses. *Neuron* 66, 57–68.
- Wang, X., and Li, M. (2003). Automated electrophysiology: high throughput of art. *Assay Drug Dev. Technol.* 1, 695–708.

Received: 10 October 2011; accepted: 06 November 2011; published online: 23 November 2011.

Citation: Nagarah JM (2011) Neurons on a chip – toward high throughput network and pharmacology investigations. *Front. Pharmacol.* 2:74. doi: 10.3389/fphar.2011.00074

This article was submitted to *Frontiers in Pharmacology of Ion Channels and Channelopathies*, a specialty of *Frontiers in Pharmacology*.

Copyright © 2011 Nagarah. This is an open-access article subject to a non-exclusive license between the authors and Frontiers Media SA, which permits use, distribution and reproduction in other forums, provided the original authors and source are credited and other Frontiers conditions are complied with.



From understanding cellular function to novel drug discovery: the role of planar patch-clamp array chip technology

Christophe Py^{1*}, Marzia Martina², Gerardo A. Diaz-Quijada³, Collin C. Luk⁴, Dolores Martinez¹, Mike W. Denhoff¹, Anne Charrier⁵, Tanya Comas², Robert Monette², Anthony Krantis⁶, Naweel I. Syed⁴ and Geoffrey A. R. Mealing²

¹ Institute for Microstructural Sciences, National Research Council of Canada, Ottawa, ON, Canada

² Institute for Biological Sciences, National Research Council of Canada, Ottawa, ON, Canada

³ Steacie Institute for Molecular Sciences, National Research Council of Canada, Ottawa, ON, Canada

⁴ Hotchkiss Brain Institute, University of Calgary, Calgary, AB, Canada

⁵ Centre Interdisciplinaire de Nanoscience de Marseille, Centre National de la Recherche Scientifique, Marseille, France

⁶ Centre for Research in Biopharmaceuticals and Biotechnology, University of Ottawa, Ottawa, ON, Canada

Edited by:

Ralf Franz Kettenhofen, Axiogenesis AG, Germany

Reviewed by:

Niels Fertig, Nanion Technologies GmbH, Germany

John Michael Nagarah, California Institute of Technology, USA

*Correspondence:

Christophe Py, Institute for Microstructural Sciences, National Research Council of Canada, Canada, 1200 Montreal Road, Ottawa, ON, Canada K1A0R6.
e-mail: christophe.py@nrc.ca

All excitable cell functions rely upon ion channels that are embedded in their plasma membrane. Perturbations of ion channel structure or function result in pathologies ranging from cardiac dysfunction to neurodegenerative disorders. Consequently, to understand the functions of excitable cells and to remedy their pathophysiology, it is important to understand the ion channel functions under various experimental conditions – including exposure to novel drug targets. Glass pipette patch-clamp is the state of the art technique to monitor the intrinsic and synaptic properties of neurons. However, this technique is labor intensive and has low data throughput. Planar patch-clamp chips, integrated into automated systems, offer high throughputs but are limited to isolated cells from suspensions, thus limiting their use in modeling physiological function. These chips are therefore not most suitable for studies involving neuronal communication. Multielectrode arrays (MEAs), in contrast, have the ability to monitor network activity by measuring local field potentials from multiple extracellular sites, but specific ion channel activity is challenging to extract from these multiplexed signals. Here we describe a novel planar patch-clamp chip technology that enables the simultaneous high-resolution electrophysiological interrogation of individual neurons at multiple sites in synaptically connected neuronal networks, thereby combining the advantages of MEA and patch-clamp techniques. Each neuron can be probed through an aperture that connects to a dedicated subterranean microfluidic channel. Neurons growing in networks are aligned to the apertures by physisorbed or chemisorbed chemical cues. In this review, we describe the design and fabrication process of these chips, approaches to chemical patterning for cell placement, and present physiological data from cultured neuronal cells.

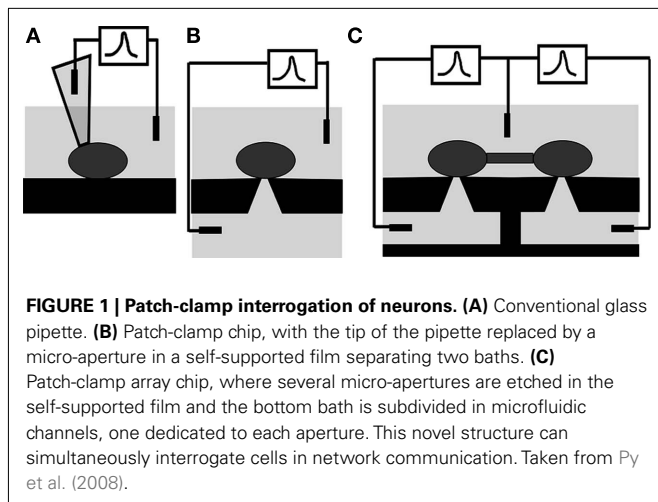
Keywords: patch-clamp whole-cell recordings, planar patch-clamp chip, giga-seal, synaptic transmission, cultured neuron pair, cell placement, chemical patterning

INTRODUCTION

Neuronal functions – ranging for resting membrane potential, action potential propagation, transmitter release, synaptic transmission to plasticity-rely upon a variety of proteins embedded in the plasma membrane called ion channels. A common harbinger of many neurodegenerative diseases is the disruption of neural network activity caused by the impairment of synaptic function (Palop et al., 2006; Seeley et al., 2009). *Per se*, most drugs designed to treat neuronal pathologies are targeted toward ion channels (Conte Camerino et al., 2007). The search for novel therapeutic targets and the need for reliably predictive assessments of potential therapeutics are driving the demand for improved screening technologies against ion channels in cells that are synaptically

connected (Stett et al., 2003a). Simple but physiologically relevant *in vitro* preparations, which are capable of modeling key aspects of brain function and are interfaced with a high-resolution functional interrogation system that permits high-throughput assessment at reasonable cost, need to be developed to address this demand.

The patch-clamp method developed by Nobel laureates Neher and Sakmann (1976) has proven to be the state of the art technique for high-resolution interrogation of electrophysiological activity. This technique consists in approaching a glass pipette, filled with a physiological saline solution and with a micron-sized tip aperture, to the surface of a cell and to isolate a “patch” of its membrane by forming a high resistance seal between the membrane and the perimeter of the aperture (cell-attached configuration; **Figure 1A**).



Using an amplifier connected to chlorate silver wires, one inserted in the glass pipette, the other in the culture bath, the activity of individual ion channels spanning the membrane patch can be recorded. The rupture of the membrane patch provides access to the intracellular space of the cell (whole-cell configuration), allowing the electrical access to ion channels populating the entire cell membrane. The patch-clamp approach is important as it allows direct visualization of microstates of single ion channel proteins, and how they are targeted by disease as well as drugs (Wang and Li, 2003). Most federal drug agencies mandate that patch-clamp data be provided for drugs that target ion channels. Additionally, any drug, regardless of its target, must be screened against certain ion channels to show that it does not perturb function of other organs/systems. The patch-clamp method has been refined and has led to techniques for high-resolution recording of current in excised membrane patches (inside-out and outside-out configurations; Hamill et al., 1981). Conventional patch-clamp requires highly qualified personnel and is labor intensive, making it slow and expensive, which limits its potential as a high-resolution interrogation tool for drug development assays.

Planar patch-clamp chips have been developed and refined over the last decade to specifically address the above limitation (Sigworth and Klemic, 2005; Behrends and Fertig, 2007). The tip of the pipette (Figure 1A) is replaced by a micron-sized aperture through a self-supported thin film (Figure 1B) separating an upper cell suspension chamber from an underlying “pipette” chamber. This chip is mounted in a two-chamber setup, the top one serving as the culture dish and the bottom one as the equivalent of the inside of the glass pipette. The cell is patched on the micrometer-sized aperture. The activity of the cell is measured through an amplifier connected to the recording electrode placed in the bottom chamber (subterranean microfluidic) and the reference electrode in the culture dish (Figure 1B).

This design makes the mechanized delivery of isolated cells in suspension to the aperture possible and, in combination with programmed seal detection and stimulation-recording routines, has led to the automation of patch-clamp. An alternative approach developed to increase the throughput of direct ion channel interrogation is the dual sharp electrode voltage-clamp system developed

to record currents from ion channels over-expressed in oocytes (Schnizler et al., 2003). This process is also amenable to automation by using robotically controlled electrodes and assay chambers (Wang and Li, 2003). Automated patch-clamp and dual electrode voltage-clamp systems have been commercialized by several companies (Dunlop et al., 2008) and are now used to complement fluorometric imaging plate reader assays (Molecular-Devices-Corp¹; Allenby et al., 2001) for high-throughput drug screening. These systems improve data throughput, a critical advantage for primary drug screening. However, the technique is predominantly used to study ion channels over-expressed in non-neuronal cell lines and is restricted to isolated cells lacking synaptic communication, resulting in models of questionable biological relevance mostly inadequate for secondary screening. Since the majority of drugs acting on ion channels target synaptic transmission, interrogation of individual cells at multiple sites in communicating networks has enormous potential for pharmaceutical assays.

Multielectrode arrays (MEAs) allow interrogation of activity in communicating networks of neurons using cell culture, brain slice, or *in vivo* preparations (Taketani and Baudry, 2006; Jones et al., 2011) by sensing extracellular field potentials from proximal cells. MEAs are powerful and readily available tools to monitor the activity of networks of neurons and their perturbations by diseases or drugs (MEA Meeting, 2010). Commercially available MEAs (AlphaMED²; Axion-Biosystems³; Ayanda⁴; Multi-Channel-Systems⁵) typically incorporate up to a few hundred electrodes, permitting recording of passive and stimulated electrophysiological activity from various sized windows within a neuronal network with varying spatial resolution (typically 30–100 μm). More recently, field-effect transistor array technology (Fromherz et al., 1991; Fromherz, 2003; Patolsky, 2007; Frey et al., 2009) has allowed the integration of up to 16,384 electrodes with sub-cellular spatial resolution (Lambacher et al., 2004), although this platform is not yet commercially available (Graham et al., 2011) and data analyses are daunting. Furthermore, progress in nanotechnology has allowed the development of lower impedance electrodes resulting in remarkable improvements in signal-to-noise ratios (Ben-Jacob and Hanein, 2008; Huys et al., 2008; Hai et al., 2010). Despite these advances, intracellular control, and notably voltage- and current-clamp, is not possible using MEA technology, and specific information pertaining to ion channel activity is challenging to extract from multiplexed signals.

The majority of drugs acting on ion channels targets synaptic transmission (Conte Camerino et al., 2007). Consequently, a tool which provides a high-resolution patch-clamp interrogation of individual cells at multiple sites in communicating networks has enormous potential for pharmaceutical assays to investigate *in vitro* models of disease, as well as neuronal physiology and synaptic plasticity. A planar patch-clamp array technology that combines key benefits of both conventional patch-clamp and MEAs on a chip has been proposed (Mealing et al.,

¹<http://www.moleculardevices.com/Products/Instruments/FLIPR-Systems.html>

²<http://www.med64.com/>

³<http://www.axionbiosystems.com/>

⁴<http://www.ayanda-biosys.com/>

⁵<http://www.multichannelsystems.com/>

2005a,b; Py et al., 2008). In this concept, individual neurons are probed through apertures that connect to dedicated subterranean microfluidic channels (**Figure 1C**), allowing the simultaneous high-resolution patch-clamp interrogation of individual cultured neurons at multiple sites in communicating networks. Cells are first aligned to these apertures by patterned chemical adhesion or guidance cues and can subsequently form synaptic connections. This patch-clamp array chip offers the opportunity to develop more physiologically relevant *in vitro* models, extract unique information on brain function and network communication from them, and better predict therapeutic efficacy, notably as it pertains to synaptic physiology.

Two novel designs have been developed: a single aperture chip fabricated on a silicon platform and a two apertures chip constructed by laminating a polyimide film on a silicone plastic substrate in which the two apertures are connected to independent subterranean microfluidic channels. Proof-of-concepts have been demonstrated using synaptically connected snail neurons cultured over both chips. Preliminary data using primary cortical neurons cultured directly on the chip surface suggest that interrogation of synaptically communicating mammalian neurons on a patch-clamp chip is possible. In this review we describe and discuss the design and fabrication of these chips (see Chips Fabrication) and the experiments conducted to demonstrate the validity of both designs (see Proof-of-Concept for Si and PI Chips). Parameters controlling the formation of a tight cell to aperture seal (giga-seal) are discussed. Cell placement and adhesion strategies, essential to develop cultured *in vitro* networks and eliminate the need for manual manipulation of cells are also described (see Cell Placement).

CHIPS FABRICATION

CHIP MATERIALS PLATFORMS

The first planar patch-clamp devices were fabricated in silicon (Hediger et al., 1999; Fertig et al., 2000; Schmidt et al., 2000); the material was also machined to mimic the tip of a micropipette (Lehnert et al., 2002; Stett et al., 2003b). Quartz or glass (Fertig et al., 2001, 2003), polydimethyl siloxane (PDMS or silicone; Klemic et al., 2002, 2005), and polyimide (Stett et al., 2003c) patch-clamp chips were subsequently designed to overcome the high capacitive coupling between the culture media and the measuring media resulting through the semiconductive silicon substrate. The convenient molding properties of PDMS inspired lateral-patch chips with integrated fluidic channels for the delivery of cell suspensions (Seo et al., 2004; Ionescu-Zanetti et al., 2005; Chen and Folch, 2006; Lau et al., 2006; Ong et al., 2007; Tang et al., 2010). Still, the advantages of silicon as a material are considerable. Silicon micromachining is well understood thanks to its pervasive use for microelectronics applications and its offshoot in Micro-Electro-Mechanical Systems (MEMS; Gad-el-Hak, 2001), so large quantities of chips can be produced with very high yield and critical process control. This is a significant advantage compared to competing technologies. Additionally, silicon is attractive for the integration of multiple functionalities, such as on-chip amplification (Kaul et al., 2004; Aziz et al., 2007), and which could extend to other co-located sensors using conventional MEMS technology. For these reasons, several groups have still chosen silicon as a

platform for patch-clamp chips in recent years (Pandey et al., 2004; Pantoja et al., 2004; Picollet et al., 2004; Matthews and Judy, 2006; Curtis et al., 2008; Sordel et al., 2010); likewise, we have developed a similar design consisting of a single aperture in a suspended silicon nitride/silicon dioxide film stack on silicon for single site recording. We refer to it as the silicon (Si) chip in this review.

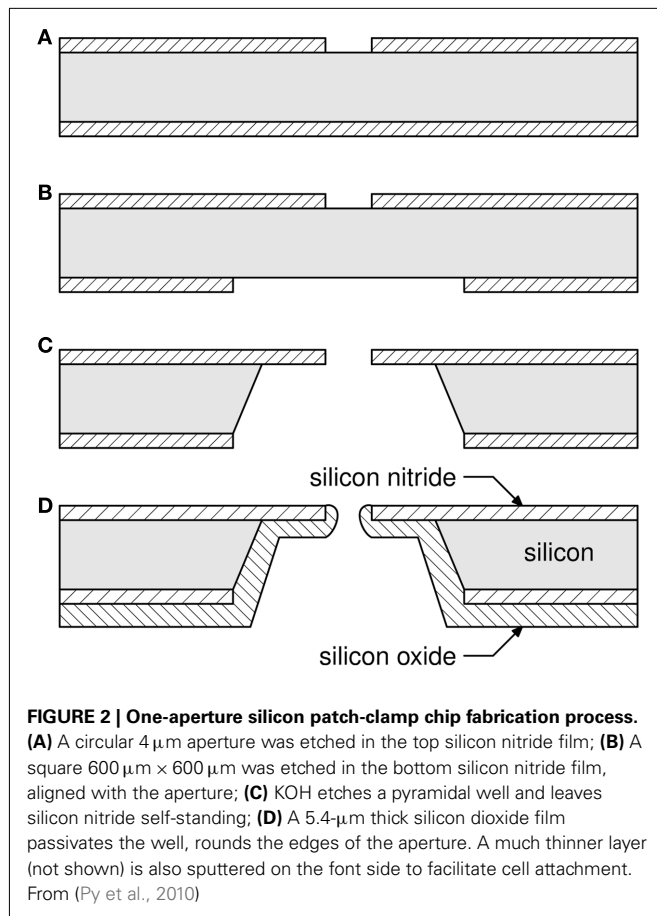
Unfortunately, the integration of multiple apertures on-chip, each with a dedicated subterranean microfluidic channel, proved problematic in silicon. For the film in which the micro-aperture is machined to be supported by the substrate, the microfluidic channels must be coupled to apertures on its underside. The micro-aperture is connected to the bottom “pipette” chamber through a well which in our process has a pyramid shape with a fixed angle determined by the anisotropic wet etch of silicon. The well could have straight walls if dug by deep reactive ion etching instead, but the pyramid shape is desirable as it lowers the access resistance of the chip. However, it also limits the capacity to integrate apertures to at least several hundred microns – more than the optimal distance between neurons in a cultured network. A favored fabrication method is therefore to transfer the thin film containing the apertures away from the wafer on which they are machined to the top of the microfluidic channels, which can thus be integrated much closer. As a proof of our concept, we chose to integrate a polyimide (PI) thin film on top of a PDMS microfluidic chip. The latter was chosen for its convenient and reliable method of fabrication by replication (Qin et al., 2010); the former because of its cytocompatibility (Stett et al., 2003c), high chemical and mechanical stability, and its low dielectric constant. Additionally, polyimide processing techniques are standard in the microelectronics industry; polyimide films have been laminated to fabricate microfluidic devices (Metz et al., 2001) and in particular perforated MEAs (Egert et al., 2005). In this review we refer to that second generation chip as the polyimide (PI) chip.

ONE-APERTURE SILICON CHIP

The fabrication process was previously described in detail (Py et al., 2010) and is adapted from (Schmidt et al., 2000); it is schematically represented in **Figure 2**. It is carried out on 150 mm double-side polished (100) silicon wafers at the Canadian Photonics Fabrication Centre⁶. The membrane separating the culture media from the measuring media must have a high dielectric rigidity, and the small dimension of the aperture requires the membrane to also be thin and mechanically strong enough so that it can be suspended. We chose a 1- μm thick silicon nitride film rather than silicon dioxide for its superior mechanical strength and inertness to the potassium hydroxide (KOH) solution used for bulk micromachining of silicon (step c). A low-pressure chemical vapor deposition (LPCVD) process was optimized for low stress coating of silicon nitride.

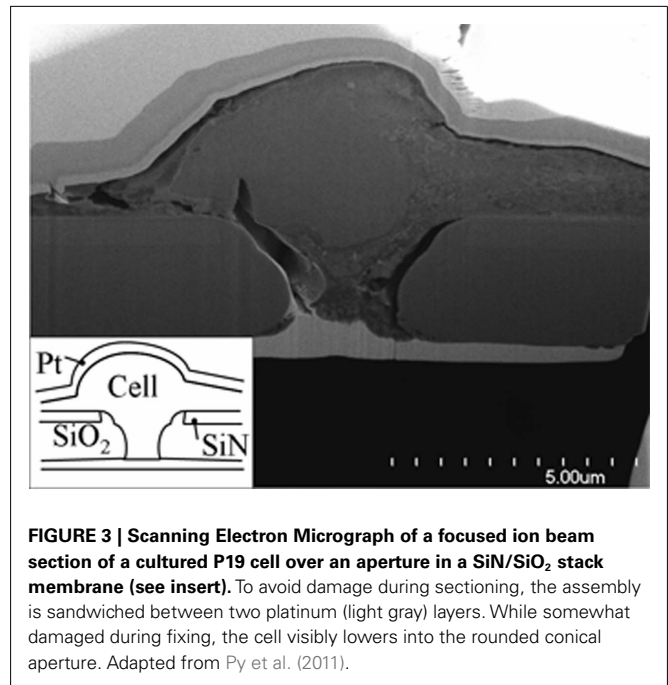
After deposition, 4 μm apertures were opened (step a) in the silicon nitride layer by lithography and reactive ion etching. A second lithography and etching step at the back of the wafer (step b) opened large windows in the silicon nitride along $\langle 100 \rangle$ Si crystallographic axes and centered with the apertures on the top side. The

⁶<http://cpfc-ccfdp.nrc-cnrc.gc.ca/>



silicon bulk was then anisotropically etched in a hot KOH solution (step c), resulting in an inverted truncated pyramid-shaped well and a 100 \times 100- μm^2 membrane in the silicon nitride film where the aperture had been patterned. The KOH etch left bare silicon walls in the well which were passivated by depositing a 5.4- μm thick low stress plasma-enhanced chemical vapor deposition silicon dioxide film (step d). The coating reduced the diameter of the aperture by 2 μm while rounding its edges. Finally, a 0.1- μm thick silicon dioxide film was deposited by the same method on the front side of the wafer. Surface functionalization was found to be more successful on that surface than on silicon nitride, which we hypothesize is due to a lower concentration of silanol groups on our silicon nitride surfaces. It is well known that the structure and therefore concentration of silanol groups in silicon nitride surfaces varies considerably and is difficult to control (Hamblin et al., 2007). The resulting surfaces were smooth, with a roughness measured by atomic force microscopy to be 6–8 Å over a 1- μm^2 area. There is mounting evidence that aperture size, morphology, and smoothness are important factors to obtain a high proportion of high quality cell to aperture seals (Sordel et al., 2006; Lehnert et al., 2007; Curtis et al., 2008; Chen et al., 2009; Nagarah et al., 2010). We have provided the first visual evidence of an intimate cell to aperture interaction (Py et al., 2011), see Figure 3.

Each 150 mm wafer produced about one hundred fifty 1 cm^2 chips, and a yield higher than 90% was routinely achieved in several batches. Wafers were easily diced into chips using grooves patterned in the well etching step.



Various fluidic interfaces have been developed to allow perfusion and cell culture (Li et al., 2006; Matthews and Judy, 2006; Morales et al., 2008; Alberti et al., 2010; Chen et al., 2011). Our chips were mounted in packages machined at low cost from Plexiglas G sheets. The packages consist of a 16 mm diameter, 6 mm deep culture chamber at the bottom of which the chip is glued in a square recess. Under the membrane of the chip, a 1.5-mm diameter hole connects the chip to subterranean fluidic conduits opened on each side of the chip to allow easy perfusion of the physiological saline solution or other chemicals. Packages were cleaned with isopropanol in an ultrasonic bath and 1.5 mm glass tubes were glued at each end of the subterranean fluidic circuit to be fitted with silicone tubing for perfusion. Two rings of Dow Corning RTV silicone 3140 glue were necessary to avoid leaks and minimize the shunt capacitance of the chip, nominally 17 pF. Our design achieves this comparatively low value thanks to the thick silicon dioxide back coating, rather than by limiting the contact surface on the cell culture side (Pantoja et al., 2004; Matthews and Judy, 2006), which somewhat restricts the interrogated biological model. It is, however, still higher than the typical 1–10 pF of a glass pipette (Hamill et al., 1981; Zhou and Kang, 2000). This disadvantage is compensated by the fact that the access resistance, at approximately 1.5 M Ω for a typical 150 mM Phosphate Buffered Saline (PBS) solution, is much lower than the typical 5–10 M Ω access resistance of a glass pipette. Packaged chips were sterilized in an air plasma cleaner for 15 min. The process also oxidizes all surfaces, facilitating fluidic loading. To avoid trapping bubbles, a pressure of 1 atm is typically applied in the subterranean fluidics while loading the physiological solutions.

TWO APERTURES POLYIMIDE CHIP

Figure 4A presents a micrograph of the chip: the top PI membrane (3 μm thick, transparent) contains two 3 μm round apertures spaced 50 μm apart and individually accessible through the

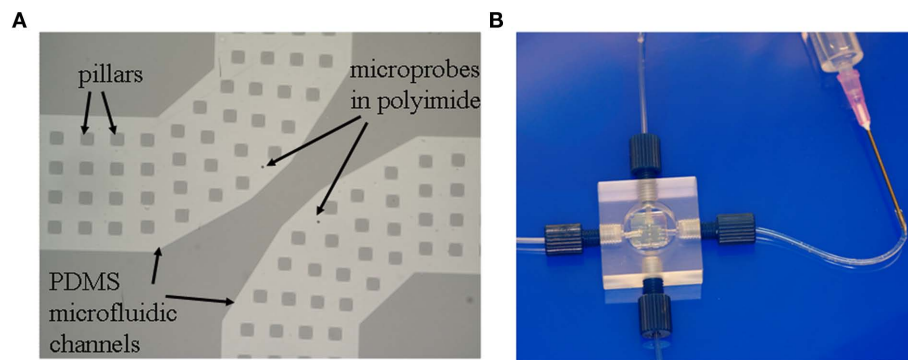


FIGURE 4 | Two-aperture transparent PI-PDMS chip. (A) Scanning electron micrograph showing the two apertures, each with a dedicated microfluidic channel for perfusion and measurement, seen through the transparent PI film in lighter gray. The channels are supported by many

square pillars part of the PDMS structure. (B) The chip is packaged in a Plexiglas enclosure with a top cell culture vial and a dedicated input and output for each aperture. **Figure 4A** adapted from Martinez et al. (2010).

bottom PDMS microchannels (each $200\ \mu\text{m}$ wide and $10\ \mu\text{m}$ deep, also transparent). Square pillars ($20\ \mu\text{m} \times 20\ \mu\text{m}$) are integrated in the microchannels as support for the thin PI film. Four via holes punched through the PDMS at the extremities of the microchannels allow perfusion of chemicals and electrophysiological probing in the underlying fluidics (not seen on the picture). The chip is packaged in a machined Plexiglas culture chamber with aligned inlets and outlets (**Figure 4B**), allowing easy perfusion of the physiological saline solution or other chemicals.

To minimize capacitance, the choice of a polymer membrane with a low dielectric constant is obviously advantageous. The shunt capacitance is also proportional to the section of the microfluidic channels and the inverse of the PI thickness. The access resistance is the resistance of the aperture plus that of the microfluidic channel. The former is directly proportional to the PI membrane thickness and the latter is inversely proportional to its section. Increasing the thickness of the PI film will thus decrease the shunt capacitance but increase the access resistance. The access resistance and shunt capacitance are however minimized independently by designing deep and narrow microfluidic channels, respectively. The dimensions described above result in $7.7\ \text{pF}$ shunt capacitance, similar to a glass pipette, and an access resistance of $1.6\ \text{M}\Omega$ for a $150\ \text{mM}$ PBS solution, in agreement with modeling and similar to the Si chip. These values make the microchip capable of high fidelity patch-clamp recording (Sigworth and Klemic, 2005).

Figure 5 presents a schematic of the polymer microchip fabrication, detailed in a previous publication (Martinez et al., 2010b). The two layers forming the chip, PDMS and PI, were processed independently starting from $2''$ Si wafers and bonded with alignment, producing nine $1\ \text{cm} \times 1\ \text{cm}$ chips. PDMS microchannels were fabricated by replica-molding from a SU8-on-Si master mold. Shrinking of the replicated PDMS during curing was found to be irreproducible, making wafer level assembly over several centimeters impossible. Multilayer soft-lithography techniques were developed a decade ago to fabricate microfluidic components (Unger et al., 2000). To reduce PDMS shrinking variations, we used a variation of that technique as depicted in **Figure 5**, steps 1a to 1d. A first thick PDMS slab was obtained by curing a Sylgard 184 resin mixture and curing it for 3 h cure at 120°C (step 1a). A

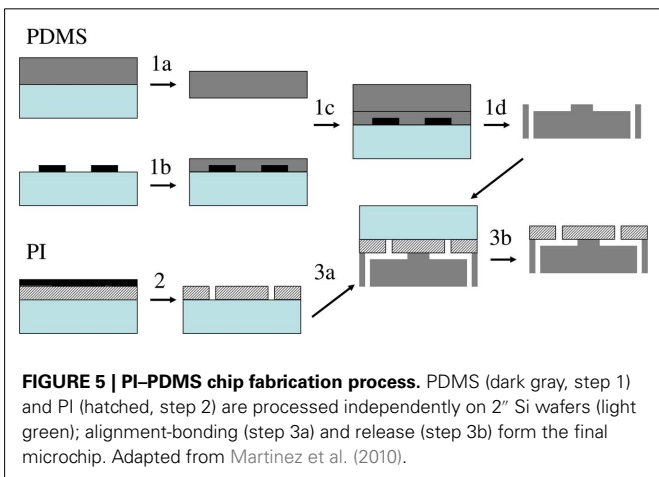


FIGURE 5 | PI-PDMS chip fabrication process. PDMS (dark gray, step 1) and PI (hatched, step 2) are processed independently on $2''$ Si wafers (light green); alignment-bonding (step 3a) and release (step 3b) form the final microchip. Adapted from Martinez et al. (2010).

second thinner layer was spin coated on the SU8-on-silicon master, producing a thin structure containing the microchannels. After a 5-min partial cure on a hot plate at 95°C (step 1b), thin and thick PDMS layers were covalently bonded following plasma treatment of both surfaces (step 1c). The resulting PDMS chip was peeled from the SU8-on-Si mold and fully cured. The thick PDMS slab acted as a support for the thin PDMS containing the microchannels, resulting in microstructures with minimized shrinking variations (to $6 \pm 4\ \mu\text{m}$ over $1\ \text{cm}$ compared to $138 \pm 13\ \mu\text{m}$ over $1\ \text{cm}$ without the thick pre-cured support), low enough to allow alignment-bonding to the upper PI layer at the wafer level. Fluidics access via holes were punched in the PDMS at both ends of both channels using a machined syringe needle (step 1d), producing $200\ \mu\text{m}$ diameter via holes.

A $3\text{-}\mu\text{m}$ thick PI film was spun on a Si wafer and cured in three stages up to 350°C , and an aluminum mask layer was evaporated on the PI film (step 2a). Apertures were defined by lithography in the aluminum mask, oxygen reactive ion etching transferred them to the PI, and the residual aluminum was removed in a metal etchant (step 2). To facilitate bonding, an adhesion promoter was spun on the PI layer, and the PDMS wafer was treated in air plasma. PI and PDMS wafers were aligned and bonded in a M9 flip-chip bonder

(step 3a). The assembly was heated at 65°C for 2 h and peeled from the Si substrate supporting the PI film (step 3b). Wafers were diced in nine 1 cm × 1 cm chips, which were then bonded to a lower glass support and glued to a machined Plexiglas package fitted with connectors for easy microchannel access (see **Figure 4B**). After 5 min sterilization in an air plasma cleaner, microfluidic channels were filled with the electrophysiological recording solution.

PROOF-OF-CONCEPT FOR SI AND PI CHIPS

CELL PREPARATION

Testing and validation of both generations of chips has been accomplished (Martinez et al., 2010b; Py et al., 2010; Martina et al., 2011) through a series of patch-clamp experiments conducted using a well characterized *Lymnaea* neuron model. The *Lymnaea stagnalis* preparation was selected because of the ease with which its well characterized neurons can be positioned and cultured. Due to the significantly smaller central nervous systems of *Lymnaea* and larger soma of their neurons, this simple model approach is more amenable to cellular analysis than its mammalian counterparts. Moreover, the innate propensity of individually isolated neurons to re-form proper synaptic connections with exquisite accuracy *in vitro* make it ideal to study the mechanisms underlying synaptic formation and transmission. The soma–soma model has been established, where identified pre- and post-synaptic neurons juxtaposed in culture re-form proper synaptic connections seen *in vivo* without requiring neuronal outgrowth (Feng et al., 1997; Hamakawa et al., 1999; Woodin et al., 1999, 2002). This circuit is known to form an excitatory cholinergic synapse between pre-synaptic respiratory neuron Visceral Dorsal 4 (VD4) and post-synaptic Left Pedal Dorsal 1 (LPeD1) neurons (Feng et al., 1997). The neurons have specifically characterized (from genes to molecules) both cholinergic and dopaminergic networks that mediate the neural control of breathing in this model, and these networks have been reconstructed in cell culture (Bell and Syed, 2009). Importantly, it has been demonstrated that the dopaminergic and cholinergic networks function in a manner similar to that of vertebrates. Therefore, understanding the fundamental principles behind synaptic communication in this model is relevant to understanding neurodegenerative and neurodevelopmental disorders – at a resolution unattainable in most vertebrate models. Moreover, fundamental mechanisms of neuronal communications revealed in this simple model are directly applicable to their vertebrate counterparts. Experiments using mammalian primary cortical neurons are also being performed in our laboratories. Preliminary current-clamp recordings obtained from a 14 days old primary cortical culture have been obtained with a Si chip (Martinez et al., 2010a). This result is encouraging and suggests that chip application to mammalian cells is a realistic objective that could be reliably achieved.

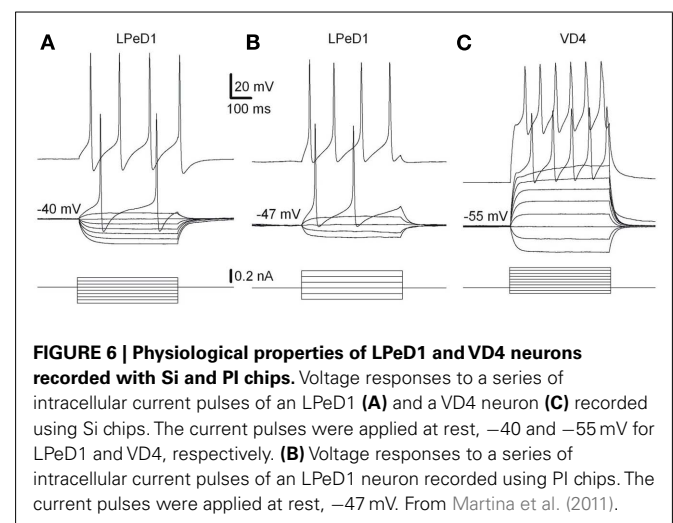
PATCH-CLAMP RECORDINGS FROM LYMNAEA NEURONS

Lymnaea neurons (VD4 and LPeD1) were manually positioned over the apertures of Si and PI chips and cultured at room temperature for a minimum of 2 h (Martinez et al., 2010b; Py et al., 2010) or 8–12 h to establish synaptic communication (Martina et al., 2011). The cells were found to be viable

and maintained their electrophysiological properties. Whole-cell recordings were obtained over prolonged periods of time. Most neurons were tested only once over a period of 20–40 min, but some neurons were re-tested several hours after the initial analysis and found to behave in similar fashion. High quality recordings in current- and voltage-clamp were achieved with both Si and PI chips (Martinez et al., 2010b; Py et al., 2010; Martina et al., 2011). Specifically, the first action potential recordings ever recorded from neurons cultured on a patch-clamp chip (**Figure 6**), voltage-clamp induction of whole-cell ion channel currents with exceptional fidelity (**Figure 8**) and post-synaptic recordings from neurons communicating through synaptic connections and evidence of synaptic plasticity (**Figures 7 and 8**), were all obtained.

In particular, the suitability of chips in obtaining meaningful physiological data and describing a network behavior have been achieved by recording from synaptically connected neurons cultured on the chips and manipulating the post-synaptic responses in the VD4–LPeD1 system. The *Lymnaea* model have been described to develop cholinergic excitatory synapses between VD4 and LPeD1 neurons (Woodin et al., 1999) and the addition of tubo-curarine (100 μM), a cholinergic receptor antagonist, to the bath solution blocked the excitatory post-synaptic potentials (EPSPs) in LPeD1 (**Figure 7C**), confirming that the synaptic transmission between the pair is cholinergic.

Synaptic plasticity is a fundamental process in learning and memory, and its impairment is associated with numerous neuro-pathologies. Our chips make it possible to reproduce *in vitro* the fundamental mechanism of synaptic transmission. This is pivotal in the testing and screening of drugs acting on ion channels involved in synaptic transmission and plasticity. Synaptically connected VD4 and LPeD1 neurons have also been reported to show a transient potentiation in synaptic transmission following tetanic stimulation of the pre-synaptic neuron (Luk et al., 2011). To verify the reproducibility of this event on chips, brief burst of action potentials in VD4 neuron were applied (8–15 action potentials at 5–10 Hz), generated by a continuous depolarizing current injection using a sharp electrode and responses were recorded from the post-synaptic LPeD1 neuron on-chip in both current- and



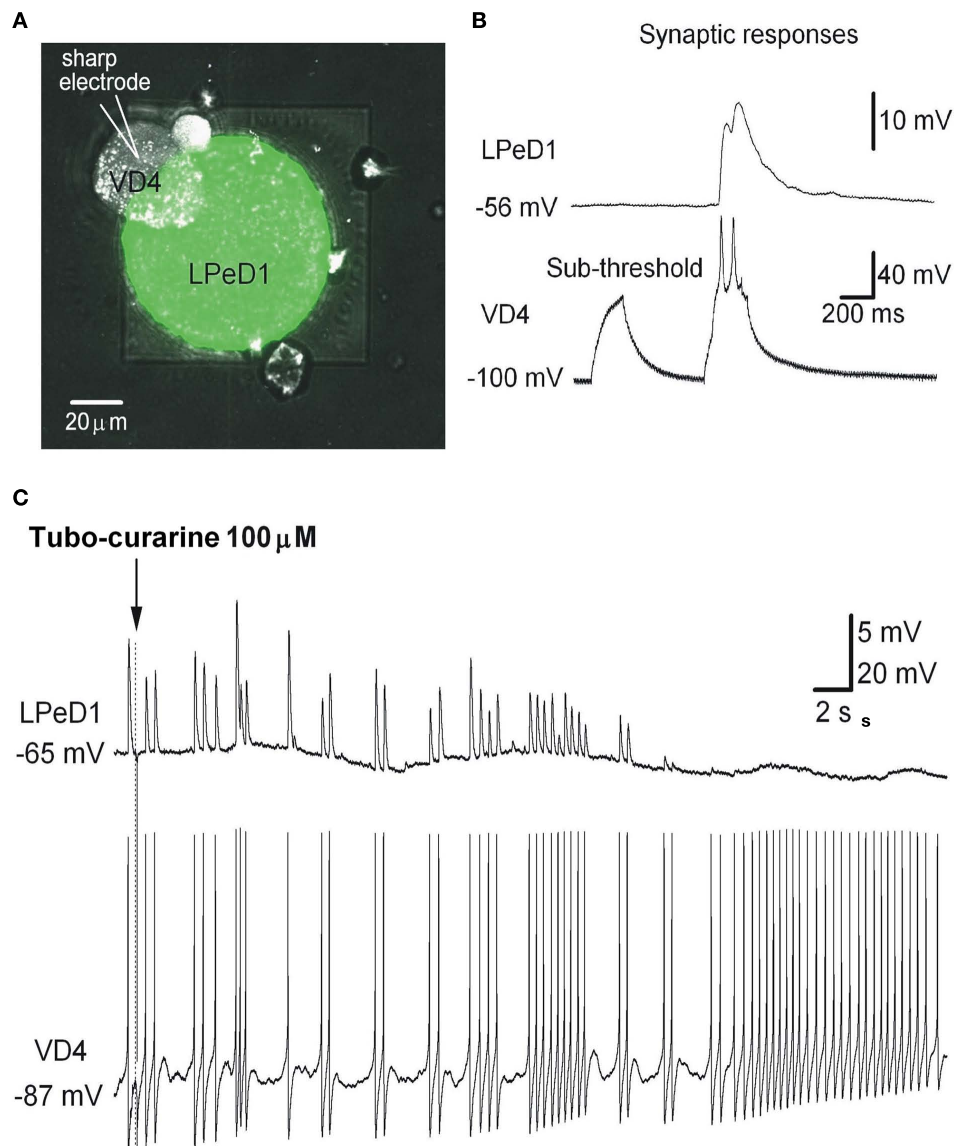


FIGURE 7 | Cultured LPeD1 and VD4 neurons forming a soma-soma synapse on a Si chip. (A) Superposition of reflected light and fluorescence confocal imaging of a Si chip with an LPeD1 neuron plated over the aperture and forming a soma-soma synapse with a VD4 neuron. Subterranean fluidics were filled with a recording solution containing a green dye. (B) Simultaneous whole-cell recordings in

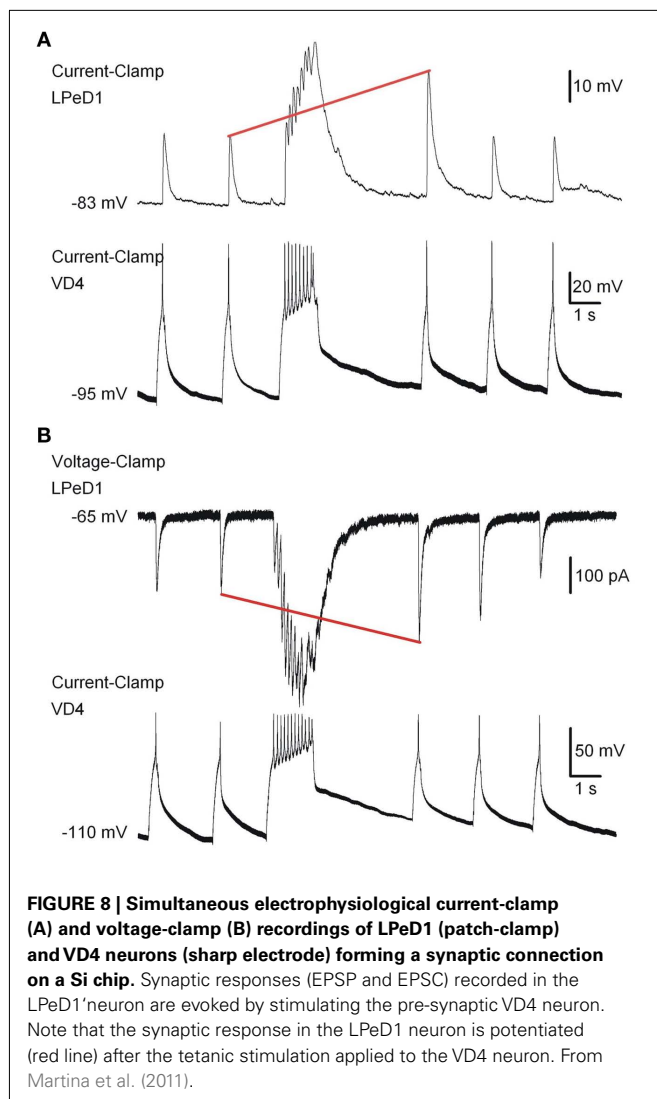
current-clamp mode of an LPeD1 (patch-clamp) and a VD4 neuron (sharp electrode). Sub-threshold stimulation of the pre-synaptic VD4 neuron does not evoke any response in the post-synaptic LPeD1 neuron, but above-threshold stimulation does. (C) Turbo-curarine is shown to suppress the responses evoked in the LPeD1 neuron while stimulating the VD4 neuron. From Martina et al. (2011).

voltage-clamp modes (Figures 8A,B, respectively). The amplitudes of EPSPs, evoked by single action potentials in the pre-synaptic cell, were transiently increased following burst stimulation (Figure 8A, red line), suggesting the induction of potentiation in the LPeD1 neuron. The same phenomenon was also examined in voltage-clamp mode, and excitatory post-synaptic currents (EPSCs) are shown in Figure 8B.

DOUBLE PATCH-CLAMP RECORDINGS

A current limitation of the Si chip design is its single recording aperture, which confined on-chip acquisition to post-synaptic

responses, relying on an external electrode for pre-synaptic stimulation and recording. PI chips were developed to overcome that limitation and enable simultaneous patch-clamp recordings from neuron pairs. Double simultaneous recordings have been described using PI chip and VD4-LPeD1 neurons (Figure 9). However, while each neuron was independently excitable, they did not propagate a synaptic response, suggesting that no synapse was present between the two neurons. Synapse formation requires interaction between specialized pre-synaptic and post-synaptic intracellular machinery. Cell-cell signaling (Scheiffele, 2003), intrinsic cell-cell interactions involving activity-dependent



mechanisms (Shatz, 1990; Katz and Shatz, 1996; Dan and Poo, 2004), and extrinsic molecules present in the extracellular milieu (Vicario-Abejo'n et al., 1998; Craig et al., 2006), are all critical for the establishment, maturation, and remodeling of synapses. The absence of functional synapses on PI chips may have been due to increased cytoplasmic dialysis resulting from the larger apertures on PI chips (see Giga-seal Formation and Success Rate of Recordings), particularly affecting the smaller VD4 neurons.

To observe VD4 and LPeD1 plated on the chips, cytoplasmic perfusion of these neurons was accomplished *via* the subterranean microfluidics of the PI chip with two different dyes (Figures 7A and 9). In both Si and PI chips, these neurons displayed no change in resistance following dye loading, indicating that microfluidic perfusion did not compromise seal integrity. Figure 9 shows a confocal 3-D reconstruction of a VD4/LPeD1 neuron pair (VD4 in red; LPeD1 in green) cultured on a PI chip. This capability could be advantageous to studies of signaling molecules where intracellular delivery of compounds or dyes is required.

It is noteworthy that in our *Lymnaea* neuron model, the synapses are formed between the soma which in turn sit on top

of the chip apertures, providing direct and controlled access to synaptic sites. The combination of these chips and cell model thus allows us to record and monitor synaptic currents without space clamp errors.

GIGA-SEAL FORMATION AND SUCCESS RATE OF RECORDINGS

In the glass pipette patch-clamp approach, the formation of a giga-seal ($>1 \text{ G}\Omega$) between the cell membrane and the patch pipette is critical and has been extensively studied (Sachs and Qin, 1993; Priel et al., 2007; Suchyna et al., 2009). Similarly, planar patch-clamp technology depends upon formation of a highly resistive seal between the cell membrane and the circumference of an on-chip aperture feature. Planar patch-clamp chips reported to date have used isolated cells in suspension, and rely on suction to draw cells to the aperture to form a giga-seal. Consequently, unlike conventional patch-clamp, planar patch-clamp technology has not been used to interrogate cultured cells, which precludes their use for the analysis of synaptic communication. Giga-seal formation with our chips occurs mostly spontaneously while neurons are establishing in culture and does not rely on suction (Ong et al., 2006). The quality of the giga-seal is directly linked to the success rate in chip recordings. In Table 1, the success rates for VD4 and LPeD1 neurons using Si and PI chips are summarized.

Several factors warrant consideration in giga-seal formation:

- (1) *Aperture geometry.* It has previously been reported that a rounded hourglass profile maximizes contact with the cell membrane and facilitates seal formation on planar patch-clamp chips (Sordel et al., 2006; Lehnert et al., 2007; Curtis et al., 2008; Chen et al., 2009), while an impressive 80% of giga-seals have been recently reported for a cell line with a conical profile (Nagarah et al., 2010). Si chips have circular $2 \mu\text{m}$ diameter rounded conical apertures (Figure 3) and meaningful cell connections were obtained in 58% of cases. By contrast, the PI chips have substantially square opening with $3 \mu\text{m}$ sides, and a 35% success rate was obtained. The square shape of the aperture may induce damage in the cell membrane, and the larger section makes the cells more vulnerable to dialysis. This hypothesis would also explain the lower success rate in recording from smaller VD4 neurons ($\sim 35 \mu\text{m}$ diameter) compared to LPeD1 ($50\text{--}100 \mu\text{m}$) in PI chips. This issue is being addressed by patterning circular $2 \mu\text{m}$ diameter apertures in recent PI chip designs. To delay the onset of dialysis, entry into the whole-cell configuration should be postponed (see below).
- (2) *Bath and subterranean channel ("pipette") solutions.* Giga-seal formation was dependent upon the use of microfluidic solution (μFS ; in mM: 50 KCl, 5 MgCl_2 , 5 EGTA, and 5 HEPES; pH 7.4; 130 mOsm), in the subterranean channel, and consistently occurred spontaneously. Indeed, absence of cell-attached or whole-cell configuration was observed when using conditioned medium (CM: isolated snail brains incubated in defined media for 3–4 days) in the subterranean microfluidics (Martina et al., 2011). We speculate that this phenomenon is related to microscale changes in osmotic pressure at the membrane patch, due to the ionic composition of the μFS (K^+ 50 mM), even though the bath (in mM: 51.3 NaCl, 1.7

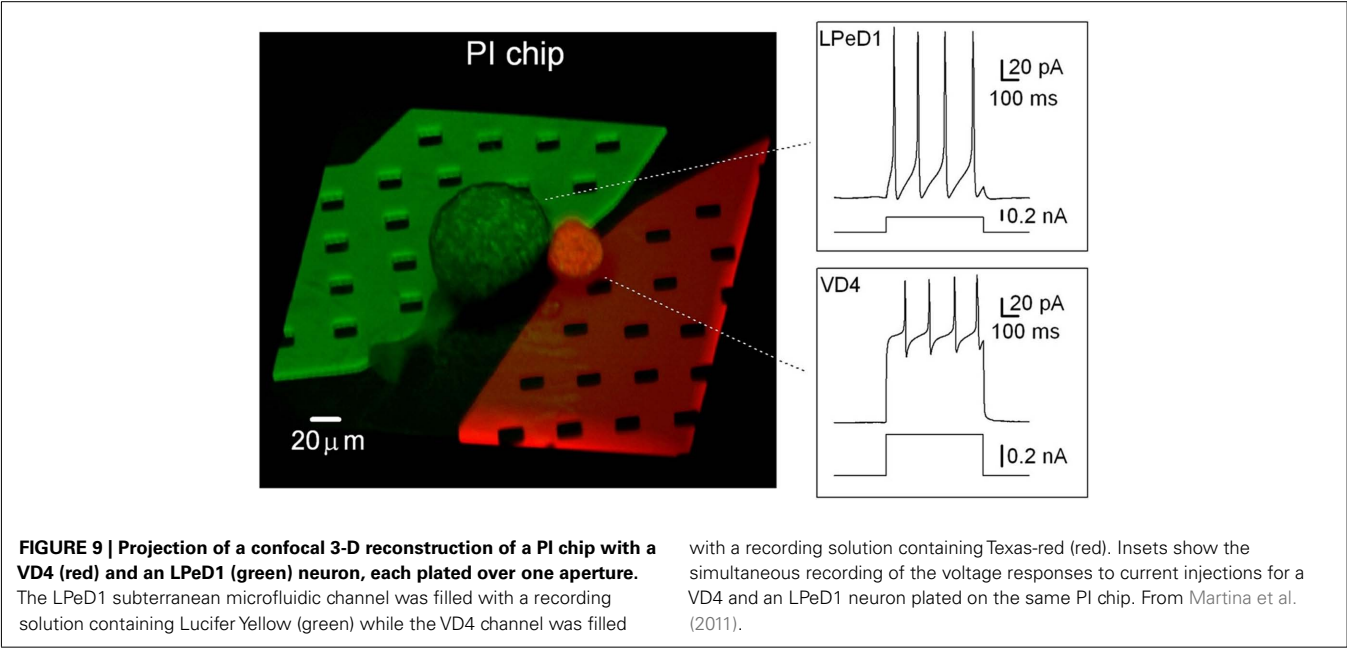


Table 1 | Summary of the experiments performed with Si and PI planar patch-clamp chips.

	Cell	<i>n</i>	C-A	C-A to W-C	Tot W-C	Tot success	Bad cells	Bad ephys
Si chip	LPeD1	58	9 (19%)	5 (56%)	28 (48%)	32 (55%)	14 (24%)	12 (21%)
	VD4	26	4 (15%)	2 (50%)	15 (58%)	17 (65%)	2 (8%)	7 (27%)
	Total	84	13 (18%)	7 (54%)	43 (51%)	49 (58%)	16 (19%)	19 (23%)
PI chip	LPeD1	63	7 (11%)	5 (71%)	25 (40%)	27 (43%)	0	36 (57%)
	VD4	51	1 (2%)	1 (100%)	13 (25%)	13 (25%)	5 (10%)	33 (65%)
	Total	114	8 (7%)	6 (75%)	38 (33%)	40 (35%)	5 (4%)	69 (60%)

C-A indicate cells in the cell-attached configuration, and C-A to W-C those cells that transitioned from there to the whole-cell mode. Tot W-C is the total number of cells in whole-cell mode, and Tot Success the total number of cells for which a meaningful cell connections could be obtained. Bad Cells indicate instances where cells were dead or had moved away from the aperture, Bad Ephys are chips from which no electrophysiological recording could be obtained. Modified from (Martina et al., 2011)

KCl, 4 CaCl₂, and 1.5 MgCl₂; buffered to pH 7.9 with HEPES) and subterranean channel solutions were iso-osmotic. This may also account for the frequently observed spontaneous entry into the whole-cell configuration. It would be advantageous to promote giga-seal formation early, and delay entry into the whole-cell configuration by culturing neurons with CM instead of μ FS in the fluidics, thereby allowing long-term cell-attached recording of ion channel activity.

(3) *Cell preparation.* Molluscan neurons are large, relatively robust and maintain their intrinsic and synaptic properties in cell culture (see Cell preparation). The next step in the development of this technology is the use of mammalian neurons. It is difficult to predict how mammalian cells will interact with the aperture features and surfaces on these chips. This is the subject of an ongoing study and encouraging preliminary results using primary cortical cultures from rats have, however, been reported (Martinez et al., 2010a). In addition the success rates were similar when snail neurons were cultured for 2–4 or 8–12 h suggesting that the time in culture does not affect successful whole-cell entry.

CELL PLACEMENT

The snail neurons used to validate our technology are large enough that they can be manually positioned on the aperture. This method however requires high technical skills, just like glass pipette patch-clamping, and many smaller cells will not be amenable to it. Current automated patch-clamp systems, working from suspensions, aspirate the cell in place (Fluxion⁷; Molecular-Devices⁸; Nanion⁹; Sophion¹⁰). Cultured neurons, however, offer a biological model that is substantially more relevant for experimentation, notably for network communication. However, since cultures are typically too sparse to rely on chance for a cell to be positioned on the aperture, specific strategies for positioning the cells are needed. While topographical features have been shown to restrict cells and guide the growth of processes (Faid et al., 2005; Merz and Fromherz, 2005; Sorkin et al., 2009), chemical patterning is by far the favored

⁷<http://fluxionbio.com/>
⁸<http://www.moleculardevices.com>
⁹<http://www.nanion.de/>
¹⁰<http://www.sophion.dk/>

method (Wheeler and Brewer, 2010). Chemical modification can be used not only to immobilize cells on the aperture, but also to promote the formation of a high quality cell to aperture seal. We have studied several strategies to position cells on the apertures, and report here the aligned stamping of polylysine on our apertures. We improve on that process by using standard lithography for alignment and replacing physisorption by chemisorption.

STAMPING

Micro-contact printing, or PDMS stamping, has been demonstrated to result in the transfer of chemicals with high spatial resolution (Kumar et al., 1994; Qin et al., 2010) and to result in cell placement (Wheeler et al., 1999; Wyart et al., 2002; Vogt et al., 2005; Charrier et al., 2006; Offenhausser et al., 2007). In order to induce placement of neurons on our chips, Poly-D-lysine (PDL) patterns were stamped (Charrier et al., 2010). PDL is a commonly used cell attachment factor (Branch et al., 1998; Chang et al., 2003; Li and Folch, 2005) and cultured cryopreserved rat cortical cells (QBM Cell Sciences, Ottawa, ON, Canada) adhere well to PDL.

PDMS stamps were designed with square features of sizes and spacings of 25, 50, and 100 μm to determine optimal conditions for placement (Charrier et al., 2010). Fabrication was done by replica-molding from a SU8-on-Si master mold, using the same polymer as for the microchannels in PI chips. To remove any remaining non-polymerized PDMS, stamps were washed in solvents by reflux following an established procedure (Voicu et al., 2007). Stamps were mounted on glass slides, washed in 70% ethanol, deionized (DI) water, and 10% Sodium Dodecyl Sulfate (SDS). Modification of the PDMS surface with SDS has been shown to enhance the transfer of polylysine to the substrate (Chang et al., 2003). Stamps were quickly rinsed in DI water, blow-dried with nitrogen, immersed for 30 min in a PDL saline solution (33 mg/mL PDL in standard PBS) then thoroughly blow-dried. Stamps (surface area approximately 0.5 cm^2) were applied to chips with a constant and homogeneous pressure of 500 g for 1 min and left another minute without pressure. The chips were finally sterilized 2 min in 70% ethanol, rinsed in DI water and dried.

Cryopreserved rat cortical cells were thawed in a 37°C water bath, resuspended in media and plated on stamped chips. Four hours post-plating, media was removed and replaced with 1 mL of serum-free Neurobasal Medium. Media changes were performed biweekly by replacing half of the media with fresh Neurobasal Medium. Cell cultures were maintained at 37°C in a 5% CO_2 humidified incubator for 14 days before imaging. The cells have a body diameter of 10–12 μm , and the size of the PDL-patterned areas will influence the number of neurons that will adhere and grow on individual squares. We found by fluorescence imaging studies that 100 μm PDL squares were covered with 10 ± 3 cells ($n = 25$), 50 μm squares had 3 ± 2 cells ($n = 60$), and 25 μm squares 1 ± 1 ($n = 60$, 50% vacant). In cases where the number of neurons per PDL area exceeded 12, large three dimensional aggregates formed, covering most of the patterned area. Based on these observations, we selected the 50 μm patterns to investigate further. Immunostaining was used to confirm the identity of neurons (MAP2-red) and astrocytes (GFAP-green) growing on the chips. Cultures were fixed, incubated overnight at 4°C in Mouse monoclonal Map2 antibody and goat anti-rabbit GFAP antibody, rinsed

in PBS, incubated in secondary antibodies Alexa Fluor 568 goat anti-mouse and Alexa Fluor 488 goat anti-rabbit for 1 h at room temperature, and samples inverted onto coverslips containing a drop of fluorescent mounting medium.

As seen in **Figure 10**, processes extended between small groups of neurons isolated on 50 μm squares to proximal populations of neurons on neighboring squares, such that 3 ± 1 extended from each neuronal subpopulation ($n = 25$). It can be seen that processes extend preferentially, though not exclusively, to immediate neighboring squares. Stamps with 50 μm squares patterns were then aligned to the apertures of a patch-clamp chip using a chip bonder and stamped with a force of 500 g applied for 60 s. **Figure 11** shows images of neurons growing on this region of the substrate after 14 days *in vitro*. The image is a superimposition of reflection and fluorescence images. A slight shift of the pattern occurred while stamping on the lower aperture region, probably due to deformation of the PDMS stamp while applying pressure. However, the upper aperture region is covered with cells and a neuron is growing directly over the aperture.

CHEMISORPTION AND LITHOGRAPHY

While **Figures 10** and **11** clearly demonstrate cell placement on patch-clamp chips, the stamping method is not commensurate with manufacturing. Soft PDMS stamps tend to collapse where protruding features, bearing the patterns to be printed, are separated by distances large in comparison with the height of the features. Furthermore, precise alignment of the stamp to the

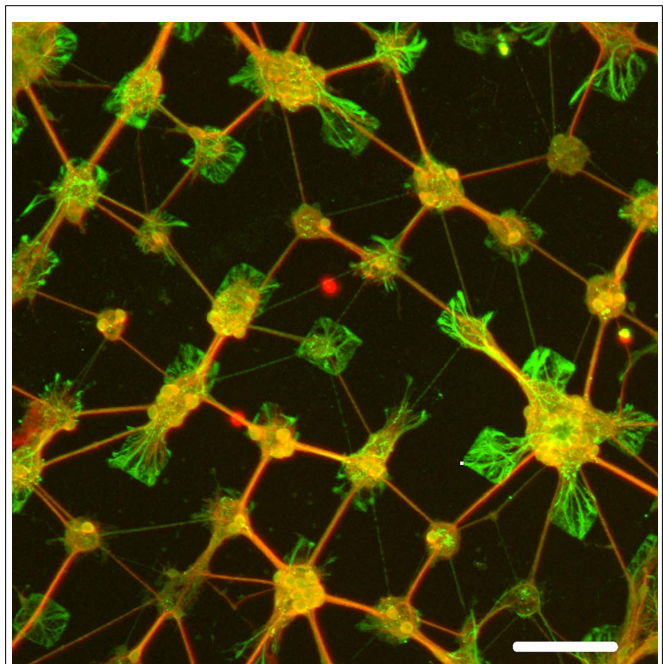


FIGURE 10 | Immunofluorescence staining of cultured brain cells on chips stamped with 50 μm PDL pattern spaced by 50 μm separation.

Neurons are stained red with MAP2, while astrocytes are stained green with GFAP. Note the processes that extend mostly immediately neighboring squares. Scale bar: 100 μm . From Charrier et al. (2010).

patch-clamp array chip is a low-yield process and complicated by distortions and defects in planarization. An alternate process based on standard lithography was developed, and derivatization of the SiO₂ surface of the Si chips was designed to provide a generalized chemical bonding attachment method rather than rely on physisorption, which may be too weak or unstable for some cell attachment factors (Diaz-Quijada et al., 2011).

The derivatization process is described in **Figure 12A**. Si chips were piranha cleaned [H₂SO₄:H₂O₂ (3:1)] and reacted with aminopropyltriethoxysilane (APTES) to obtain an amine-terminated surface. It was then reacted with buffered poly(methacrylic acid) in the presence *N*-(3-dimethylaminopropyl)-*N*'-ethylcarbodiimide hydrochloride (EDC) and *N*=hydroxysuccinimide (NHS), resulting in a carboxylic acid-terminated surface (Diaz-Quijada et al., 2007). The substrates were then washed, dried, activated in the presence of NHS and EDC before the immobilization of a cell adhesion promoter such as PDL. The carboxylic acid-terminated surfaces are highly versatile as they can be activated and made reactive toward a variety

of amine rich biomolecules (such as proteins) or cell adhesion promoters. Polymers and large biomolecules such as proteins can physisorb on surfaces, as it is the case for Bovine Serum Albumin (Zhao et al., 2007; Milligan et al., 2009; Ogi et al., 2009), due to ionic, dipole, and Van der Waals interactions between molecules and surfaces. Consequently, it is traditional to simply physisorb polylysine on surfaces such as SiO₂ or glass (Pleasure et al., 1981; Feldner et al., 1983). Such modifications are however not stable over time in environments of high ionic strength. A comparative study of physisorbed and chemisorbed PDL indicates that in the physisorbed case PDL not only smears out during washing with PBS buffer but also yields a lower surface density than in the chemically immobilized case. It is also important to note that physisorption is not a viable method for the modification of surfaces with small molecules. This is illustrated in our study (Diaz-Quijada et al., 2011) with short peptide sequences cyclo(RGDFK-PEG) peptide (PCI-3696-PI), which induces cell adhesion via a molecular recognition event (Ruoslahti and Pierchbacker, 1986), and cyclo(RADFK-PEG) (PCI-3954-PI), which differs by only one amino acid and does not induce cell adhesion. Cultured cells attach on chemisorbed PCI-3696-PI with high density, but are not viable on either physisorbed PCI-3696-PI or chemisorbed PCI-3954-PI.

As shown in **Figure 12B**, chemical patterning of PDL was accomplished by defining square openings in a photosensitive resin, derivatizing the surface as illustrated in **Figure 12A**, reacting the surface to PDL in the presence of EDC and NHS and finally dissolving the photoresist in acetone. Photolithography has been demonstrated as a potential technique for chemical patterning of surfaces (Lom et al., 1993; Butler et al., 2006; Falconnet et al., 2006). Our strategy for the chemical immobilization of cell adhesion promoters was modified and optimized to be compatible with common photoresists, which would swell or dissolve in polar organic solvents. The preparation of carboxylic acid surfaces was performed with poly(acrylic acid) instead of glutaric anhydride. This polymeric reagent has the advantage of not only producing a high concentration of carboxylic acid groups, but also allows the reaction with the amino terminated surfaces to be carried out in aqueous media in the presence of EDC and NHS. Efficient modification of the exposed regions of SiO₂ require clean surfaces, free from residual photoresist or any other substances that may mask the surface and prevent the reaction with silane reagents. Consequently, conventional photoresist adhesion promoters were avoided, all samples were over developed and then cleaned in an air plasma. To facilitate photoresist adhesion, wafers were instead dehydrated at 105°C prior to spin-coating (Madou, 1997); an alternative approach, which proved to have a higher success rate, was based on amino modification of the chips. Undesirable crosslinking effects were observed in the photoresist, resulting in difficulties with the photoresist dissolution step. The effect is likely due to the generation of hydroxyl and carboxylic acid groups in the photoresist which can react with each other to form ester groups in the presence of EDC and NHS. These groups are formed during the plasma cleaning performed immediately prior to silanization, which had to be kept to a minimum. In addition to the above key points, we observed that the reaction of APTES with the photoresist patterned SiO₂ surface had to be limited to 4 h in the gas phase to prevent swelling and detachment of the photoresist.

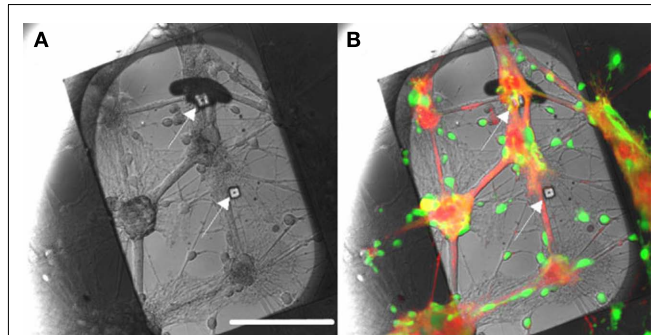


FIGURE 11 | Patch-clamp chip with two apertures (100 μm apart), stamped with 50 μm PDL squares. Note that subterranean microfluidic channels are not visible here. The stamp was aligned with the apertures using an aligner-bonder and stamped with a 500-g force for 1 min. After 14 days *in vitro*, cells bodies were labeled with Calcein-AM (green) and membranes with WGA conjugate (red). **(A)** Reflection image: apertures are indicated by arrows. **(B)** Superimposition of the images obtained in reflection mode and fluorescence. A neuron is positioned over the upper aperture. Scale bar: 100 μm. From Charrier et al. (2010).

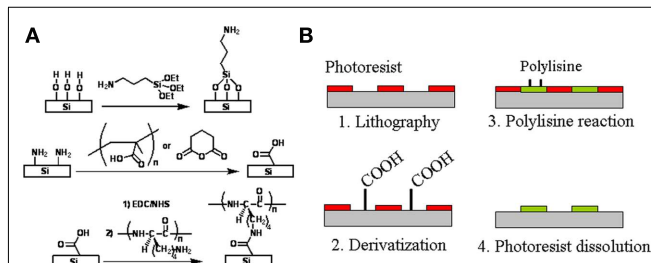


FIGURE 12 | Chemical patterning of polylysine squares. **(A)** Surface derivatization to successively obtain amino- and carboxylic acid-terminated surfaces on which a polylysine peptide is chemically bonded. **(B)** Chemical patterning is obtained by lithographically defining openings in a photoresist, derivatizing the surface, reacting it to polylysine in the presence of EDC and NHS and dissolving the photoresist. Adapted from Diaz-Quijada et al. (2011).

To illustrate the concept with our chemical strategy, blank Si chips were photolithographically patterned with 100 μm squares with a pitch of 200 or 400 μm . Alexafluor 555 modified PDL was chemically immobilized on the patterned surface in the presence of NHS and EDC. Fluorescent imaging of the chemically patterned surface is presented in **Figure 13**. Cryopreserved rat cortical neurons were cultured as described in 4.1 for 14–19 days on a wafer patterned with unlabeled PDL. Staining of the cells with Calcein (green) for cell viability and RH-237 (red) for cell membranes allow the visualization of the patterned cells along with their processes.

CONCLUSION

A silicon patch-clamp chip with an optimized aperture shape to facilitate the formation of seals has been designed, fabricated, and successfully tested (Py et al., 2010). It is fabricated on 6" wafers in a commercial-grade prototyping foundry with near-perfect yield, and is highly manufacturable. A novel polyimide-silicone (PI-PDMS) hybrid chip (Martinez et al., 2010b) which may simultaneously monitor several neurons engaged in network communication at the resolution of the patch-clamp technique (Mealing et al., 2005a,b), has also been reduced to practice (Martina et al., 2011). While their shunt capacitance are still somewhat higher than what is attainable with glass pipettes (Hamill et al., 1981), the access resistance of those two patch-clamp chips is very low and the quality of traces they can record is high (**Figure 6**).

Fifty-eight percentage of meaningful cell to aperture connections were observed with Si chips and 35% with PI chips. These success rates are lower than the best values reported for cells from suspensions (Milligan et al., 2009; Nagarath et al., 2010), but high enough to validate this technology. The optimization of the

aperture size and shape, and the perfusion of different solutions in the subterranean channels to control giga-seals and whole-cell entry are the parameters at play in the formation of seals, and must be optimized in further studies to bring up the success rates. The capacity of both Si and PI chips to allow cytoplasmic perfusion via subterranean microfluidics without disruption of recording has been shown; it could be used in disease models or pharmaceutical studies alike in order to modify the fate of individual cells within a functioning network. The ability to keep the cells in the whole-cell mode for several hours affords the possibility of studying long-term effects and as such is of value to secondary drug screening. While the challenges of applying this technology to mammalian cells should not be underestimated, preliminary whole-cell patch-clamp recordings from rat cortical cultures (Martinez et al., 2010a) suggest that this is an achievable goal well worth pursuing. It is also important to recognize the potential for application of multiple-aperture patch-clamp array chips to other biological disciplines where high-resolution assessment of cell-to-cell communication is required, including cardiology (Witchel, 2010).

The simultaneous recording of the activity of multiple cultured cells requires chemical patterning to promote their placement on the apertures. A proof-of-concept method that effectively brings cells over the apertures has been reported (Charrier et al., 2010) and the polypeptide stamping technique has been refined for a manufacturable process that provides stable chemical bonds (Diaz-Quijada et al., 2011). While the polylysine attachment factor we used in our experiments provides satisfactory placement when simply physisorbed, short peptide sequences such as RGD and RAD would not adhere. We also suggest that cell placement allows the synthesis of organized networks where processes are controlled between immediate neighbors. Organized network with neurons

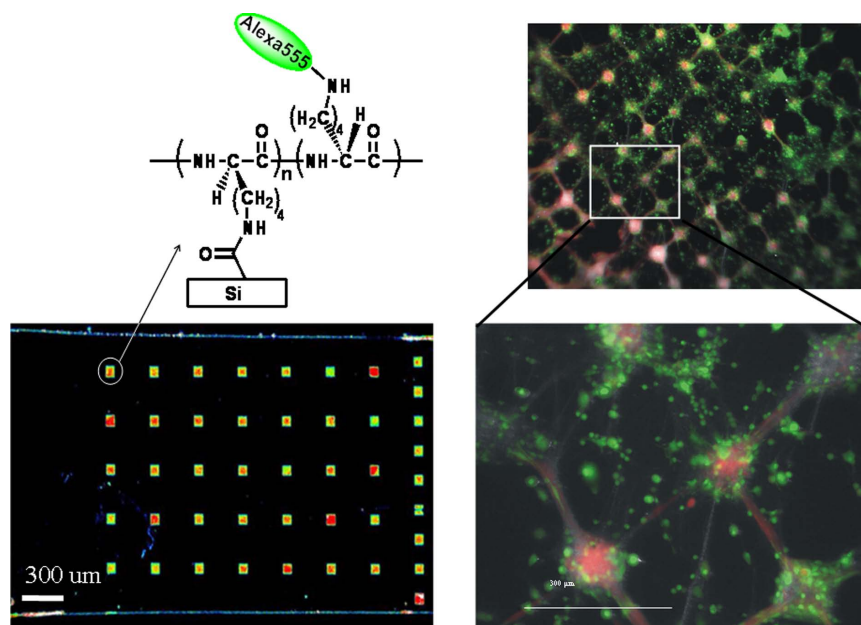


FIGURE 13 | Proof-of-concept demonstration of chemical patterning of fluorescently labeled polylysine (left) using conventional photolithography, followed by culture of cryopreserved rat cortical neurons (right). Cells were visualized by staining with Calcein (viability) and RH-237 (membrane) dyes. Adapted from Diaz-Quijada et al. (2011).

aligned on apertures will facilitate the analysis and modeling of brain connectivity, which determines functionality in neuronal circuits (Honey et al., 2010).

Many of the patch-clamp chip developments reported to date make it possible, or actually demonstrate, the integration of multiple patches on-chip (see part 2 for references). The application of those multiple patches on-chip are either to conduct parallel measurements that increase throughput in drug screening [Molecular-Devices (see footnote 8); Nanion¹¹; Sophion (see footnote 10); Kiss et al., 2003; Bruggemann et al., 2006], or to obtain population recordings [Fluxion (see footnote 7); Ionescu-Zanetti et al., 2005]. However, to our knowledge, only one other team has reported an attempt to monitor the activity of networks with the patch-clamp method (Alberti et al., 2010). We have reported the first application of a planar patch-clamp technology to examine neuronal synaptic communication. Positioning pre- and post-synaptic *Lymnaea* neurons in close proximity allowed functional synapses to establish in culture on the chip substrate. Data acquired with the Si and PI chips from neurons organized in this elementary network were used to describe network properties and demonstrate the suitability of our chip designs for synaptically connected neurons. Action potentials were evoked in LPeD1 and VD4 neurons. Functionality and nature of these VD4/LPeD1 neuron synapses were demonstrated by direct recordings and pharmacologically testing post-synaptic responses from LPeD1 on-chip. Importantly, a transient increase in the amplitude of spontaneous

events (synaptic potentiation) following a short burst of action potentials in the pre-synaptic cell was recorded on-chip.

The polyimide-silicone chip is readily scalable to multiple recording sites. Practical limitations imposed by the subterranean microfluidic channels, such as space and chip-to-world interfacing, would require a different design to expand beyond eight apertures. However, for many assessment studies it is of greater importance to be able to patch-clamp several connected neurons than it is to monitor extracellular field potentials from hundreds or thousands of neurons. Simultaneous pre- and post-synaptic recordings on a patch-clamp chip have tremendous value as a model to investigate synaptic function and for use as an assay to advance drug development. Furthermore, fundamental aspects of complex network activity, resulting in specific functions such as the acquisition of memory, can be reduced to modeling and studying interactions between just three neurons (Lukowiak and Syed, 1999; Milo et al., 2002; Song et al., 2005). This makes the application of multiple-aperture patch-clamp array chips to cultures of communicating neurons an important and promising technology to advance functional assay development.

ACKNOWLEDGMENTS

The authors wish to thank Alexei Bogdanov, Simon Wingar, Juan Caballero, and the CPFC team for fabrication of the Si chips, Hue Tran and Allan Horner for packaging, Jeff Fraser for SEM imaging, Mark Malloy, Raluca Movileanu, and Christy Maynard for chip functionalization, and Walli Zaidi for the preparation of cultured neurons. This work was supported in part by a CIHR grant to NIS. Collin Luk is supported by AIHS and NSERC studentship awards.

¹¹<http://www.nanion.de/products/syncropatch-96.html>.

REFERENCES

- Alberti, M., Snakenborg, D., Lopacinska, J. M., Dufva, M., and Kutter, J. P. (2010). Characterization of a patch-clamp microchannel array towards neuronal networks analysis. *Nanofluid.* 9, 963–972.
- Allenby, G., Dodgson, K., Harper, P., Kassam, A., Leam, M., Dale, I., and Sullivan, E. (2001). Automated high throughput screening of fluorescent imaging plate reader (FLIPR) assays using assay platform™ integrated with activity base for ‘on the fly’ compound reconfirmation. *J. Assoc. Lab. Autom.* 6, 48–50.
- Aziz, J. N. Y., Genov, R., Bardakjian, B. L., Derchansky, M., and Carlen, P. L. (2007). Brain-silicon interface for high-resolution in-vitro neural recording. *IEEE Trans. Biomed. Circuits Syst.* 1, 56–62.
- Behrends, J. C., and Fertig, N. (2007). “Planar patch-clamp,” in *Patch-Clamp Analysis: Advanced Techniques*, Chapt. 14, 2nd Edn. ed. W. Walz (Secaucus, NJ: Springer Protocols), 411–433.
- Bell, H. J., and Syed, N. I. (2009). Hypoxia-induced modulation of the respiratory CPG. *Front. Biosci.* 14, 3825–3835.
- Ben-Jacob, E., and Hanein, Y. (2008). Carbon nanotube micro-electrodes for neuronal interfacing. *J. Mater. Chem.* 18, 5181–5186.
- Branch, D., Corey, J., Weyhenmeyer, J., Brewer, G., and Wheeler, B. (1998). Microstamp patterns of biomolecules for high-resolution neuronal networks. *Med. Biol. Eng. Comput.* 36, 135–141.
- Bruggemann, A., Stolzle, S., George, M., Behrends, J. C., and Fertig, N. (2006). Microchip technology for automated and parallel patch-clamp recording. *Small* 2, 840–846.
- Butler, R. T., Ferrell, N. J., and Hansford, D. J. (2006). Spatial and geometrical control of silicification using a patterned poly-L-lysine template. *Appl. Surf. Sci.* 252, 7337–7342.
- Chang, J. C., Brewer, G. J., and Wheeler, B. C. (2003). A modified microstamping technique enhances polylysine transfer and neuronal cell patterning. *Biomaterials* 24, 2863–2870.
- Charrier, A., Martinez, D., Monette, R., Comas, T., Movileanu, R., Py, C., Denhoff, M., Krantis, A., and Mealing, G. (2010). Cell placement and guidance on substrates for neurochip interfaces. *Biotechnol. Bioeng.* 105, 368–373.
- Charrier, A., Porri, T. J., Murphy, C. J., and Nealey, P. F. (2006). A new method to characterize chemically and topographically nanopatterned surfaces. *J. Biotechnol.* 126, 196–204.
- Chen, C., and Folch, A. (2006). A high-performance elastomeric patch clamp chip. *Lab Chip* 6, 1338–1345.
- Chen, C.-Y., Tu, T.-Y., Chen, C.-H., Jong, D.-S., and Wo, A. M. (2009). Patch clamping on plane glass – fabrication of hourglass aperture and high-yield ion channel recording. *Lab Chip* 9, 2370–2380.
- Chen, C.-Y., Tu, T.-Y., Jong, D.-S., and Wo, A. M. (2011). Ion channel electrophysiology via integrated planar patch-clamp chip with on-demand drug exchange. *Biotechnol. Bioeng.* 108, 1395–1403.
- Conte Camerino, D., Tricarico, D., and Desaphy, J. -F. (2007). Ion channel pharmacology. *Neurotherapeutics* 4, 184–198.
- Craig, A., Graf, E., and Linhoff, M. (2006). How to build a central synapse: clues from cell culture. *Trends Neurosci.* 29, 8–20.
- Curtis, J. C., Baldwin, K., Dworak, B. J., Stevenson, T. J. M., Delivopoulos, E., MacLeod, N. K., and Murray, A. F. (2008). Seal formation in silicon planar patch-clamp microstructures. *J. Microelectromech. Syst.* 17, 974–983.
- Dan, Y., and Poo, M. (2004). Spike timing-dependent plasticity of neural circuits. *Neuron* 44, 23–30.
- Diaz-Quijada, G., Maynard, C., Comas, T., Monette, R., Py, C., Krantis, A., and Mealing, G. (2011). Surface patterning with chemisorbed chemical cues for advancing neurochip applications. *Ind. Eng. Chem. Res.* 50, 10029–10035.
- Diaz-Quijada, G. A., Peytavi, R., Nantel, A., Roy, E., Bergeron, M. G., Dumoulin, M. M., and Veres, T. (2007). Surface modification of thermoplastics-towards the plastic biochip for high throughput screening devices. *Lab Chip* 7, 856–862.
- Dunlop, J., Bowlby, M., Peri, R., Vasilyev, D., and Arias, R. (2008). High-throughput electrophysiology: an emerging paradigm for ion-channel

- screening and physiology. *Nat. Rev. Drug Discov.* 7, 358–368.
- Egert, U., Okujeni, S., Nisch, W., Stett, A., Boven, K. -H., Rudolf, R., and Gottschlich, N. (2005). *Perforated Microelectrode Arrays Optimize Oxygen Availability and Signal-to-Noise Ratio in Brain Slice Recordings*. Freiburg: Micro System Technic Kongress.
- Faid, K., Voicu, R., Bani-Yaghou, M., Tremblay, R., Mealing, G., Py, C., and Barjovanu, R. (2005). Rapid fabrication and chemical patterning of polymer microstructures and their applications as a platform for cell cultures. *Biomed. Microdevices* 7, 179–184.
- Falconnet, D., Csucs, G., Grandin, H. M., and Textor, M. (2006). Surface engineering approaches to micropattern surfaces for cell-based assays. *Biomaterials* 27, 3044–3063.
- Feldner, J., Bredt, W., and Kahane, I. (1983). Influence of cell shape and surface charge on attachment of *Mycoplasma pneumoniae* to glass surfaces. *J. Bacteriol.* 153, 1–5.
- Feng, Z., Klumperman, J., Lukowiak, K., and Syed, N. (1997). In vitro synaptogenesis between the somata of identified *Lymnaea* neurons requires protein synthesis but not extrinsic growth factors or substrate adhesion molecules. *J. Neurosci.* 17, 7839–7849.
- Fertig, N., George, M., Klau, M., Meyer, C., Tilke, A., Sobotta, C., Blick, R. H., and Behrends, J. C. (2003). Microstructured apertures in planar glass substrates for ion channel research. *Recept. Channels* 9, 29–40.
- Fertig, N., Meyer, C., Blick, R. H., Trautmann, C., and Behrends, J. C. (2001). Microstructured glass chip for ion-channel electrophysiology. *Phys. Rev. E* 64, 040901 (R).
- Fertig, N., Tilke, A., Blick, R. H., Kotthaus, J. P., Behrends, J. C., and Bruggencate, G. t. (2000). Stable integration of isolated cell membrane patches in a nanomachined aperture. *Appl. Phys. Lett.* 77, 1218–1220.
- Frey, U., Egert, U., Heer, F., Hafizovic, S., and Hierlemann, A. (2009). Microelectronic system for high-resolution mapping of extracellular electric fields applied to brain slices. *Biosens. Bioelectron.* 24, 2191–2198.
- Fromherz, P. (2003). “Neuroelectronic Interfacing: semiconductor chips with ion channels, brain cells, and nerves,” in *Nanoelectronics and Information Technology*, Chapt. 32, ed. R. Waser (Berlin: Wiley), 781–810.
- Fromherz, P., Offenhausser, A., Vetter, T., and Weis, J. (1991). A neuron-silicon junction – a Retzius cell of the leech on an insulated-gate field-effect transistor. *Science* 252, 1290–1293.
- Gad-el-Hak, M. (2001). *The MEMS Handbook*. New York, NY: CRC Press.
- Graham, A. H. D., Robbins, J., Bowen, C. R., and Taylor, J. (2011). Commercialisation of CMOS integrated circuit technology in multi-electrode arrays for neuroscience and cell-based biosensors. *Sensors* 11, 4943–4971.
- Hai, A., Shappir, J., and Spira, M. E. (2010). In-cell recordings by extracellular microelectrodes. *Nat. Methods* 7, 200–202.
- Hamakawa, T., Woodin, M. A., Bjorgum, M. C., Painter, S. D., Takasaki, M., Lukowiak, K., Nagle, G. T., and Syed, N. I. (1999). Excitatory synaptogenesis between identified *Lymnaea* neurons requires extrinsic trophic factors and is mediated by receptor tyrosine kinases. *J. Neurosci.* 19, 9306–9312.
- Hamblin, M. N., Edwards, J. M., Lee, M. L., Woolley, A. T., and Hawkins, A. R. (2007). Electroosmotic flow in vapor deposited silicon dioxide and nitride microchannels. *Biomicrofluidics* 1, 034101.
- Hamill, O. P., Marty, A., Neher, E., Sakmann, B., and Sigworth, F. J. (1981). Improved patch-clamp techniques for high-resolution current recording from cells and cell-free membrane patches. *Pflügers Arch.* 391, 85–100.
- Hediger, S., Sayah, A., and Gijs, M. A. M. (1999). Fabrication of a novel microsystem for the electrical characterisation of cell arrays. *Sens. Actuators B Chem.* 56, 175–180.
- Honey, C. J., Thivierge, J. P., and Sporns, O. (2010). Can structure predict function in the human brain? *Neuroimage* 52, 766–776.
- Huys, R., Braeken, D., Van Meerbergen, B., Winters, K., Eberle, W., Loo, J., Tsvetanova, D., Chen, C., Severi, S., Yitzchaik, S., Spira, M., Shappir, J., Callewaert, G., Borghs, G., and Bartic, C. (2008). Novel concepts for improved communication between nerve cells and silicon electronic devices. *Solid State Electron.* 52, 533–539.
- Ionescu-Zanetti, C., Shaw, R. M., Seo, J., Jan, Y. -N., Jan, L. Y., and Lee, L. P. (2005). Mammalian electrophysiology on a microfluidic platform. *Proc. Natl. Acad. Sci. U.S.A.* 102, 9112–9117.
- Jones, I. L., Livi, P., Lewandowska, M. K., Fiscella, M., Roscic, B., and Hierlemann, A. (2011). The potential of microelectrode arrays and microelectronics for biomedical research and diagnostics. *Anal. Bioanal. Chem.* 399, 2313–2329.
- Katz, L., and Shatz, C. (1996). Synaptic activity and the construction of cortical circuits. *Science* 274, 1133–1138.
- Kaul, A. R., Syed, N. I., and Fromherz, P. (2004). Neuron-semiconductor chip with chemical synapse between identified neurons. *Phys. Rev. Lett.* 92, 381021–381024.
- Kiss, L., Bennett, P. B., Uebele, V. N., Koblan, K. S., Kane, S. A., Neagle, B., and Schroeder, K. (2003). High throughput ion-channel pharmacology: planar-array-based voltage clamp. *Assay Drug Dev. Technol.* 1(Suppl. 2), 127–135.
- Klemic, K. G., Klemic, J. F., Reed, M. A., and Sigworth, F. J. (2002). Micromolded PDMS planar electrode allows patch clamp electrical recordings from cells. *Biosens. Bioelectron.* 17, 597–604.
- Klemic, K. G., Klemic, J. F., and Sigworth, F. J. (2005). An air-molding technique for fabricating PDMS planar patch-clamp electrodes. *Pflügers Arch.* 449, 564–572.
- Kumar, A., Biebuyck, H. A., and Whitesides, G. M. (1994). Patterning self-assembled monolayers – applications in materials science. *Langmuir* 10, 1498–1511.
- Lambacher, A., Jenkner, M., Merz, M., Eversmann, B., Kaul, R. A., Hofmann, F., Thewes, R., and Fromherz, P. (2004). Electrical imaging of neuronal activity by multi-transistor-array (MTA) recording at 7.8 μm resolution. *Appl. Phys. A Mater. Sci. Process.* 79, 1607–1611.
- Lau, A., Hung, P., Wu, A., and Lee, L. (2006). Open-access microfluidic patch-clamp array with raised lateral cell trapping sites. *Lab Chip* 6, 1510–1515.
- Lehnert, T., Gijs, M. A. M., Netzer, R., Bischoff, U., and Evotec Oai Ag/Genion, D. H. (2002). Realization of hollow SiO_2 microneozles for electrical measurements on living cells. *Appl. Phys. Lett.* 81, 5063–5065.
- Lehnert, T., Nguyen, D., Baldi, L., and Gijs, M. (2007). Glass reflow on 3-dimensional micro-apertures for electrophysiological measurements on-chip. *Microfluid. Nanofluidics* 3, 109–117.
- Li, N. Z., and Folch, A. (2005). Integration of topographical and biochemical cues by axons during growth on microfabricated 3-D substrates. *Exp. Cell Res.* 311, 307–316.
- Li, X., Klemic, K. G., Reed, M. A., and Sigworth, F. J. (2006). Microfluidic system for planar patch clamp electrode arrays. *Nano Lett.* 6, 815–819.
- Lom, B., Healy, K. E., and Hockberger, P. E. (1993). A versatile technique for patterning biomolecules onto glass coverslips. *J. Neurosci. Methods* 50, 385–397.
- Luk, C., Naruo, H., Prince, D., Hassan, A., Doran, S., Goldberg, J., and Syed, N. (2011). A novel form of presynaptic CaMKII-dependent short-term potentiation between *Lymnaea* neurons. *Eur. J. Neurosci.* 34, 567–577.
- Lukowiak, K., and Syed, N. I. (1999). Learning, memory and a respiratory central pattern generator. *Comp. Biochem. Physiol. Mol. Integr. Physiol.* 124, 265–274.
- Madou, M. (1997). *Fundamentals of Microfabrication*. New York, NY: CRC Press LLC.
- Martina, M., Luk, C., Py, C., Martinez, D., Monette, R., Comas, T., Denhoff, M. W., Syed, N., and Mealing, G. A. R. (2011). Interrogation of cultured neurons using patch-clamp chips. *J. Neural Eng.* 8, 034002.
- Martinez, D., Martina, M., Kremer, L., Monette, R., Comas, T., Salim, D., Py, C., Denhoff, M. W., and Mealing, G. (2010a). Development of patch-clamp chips for mammalian cell applications. *Micro Nanosystems* 2, 274–279.
- Martinez, D., Py, C., Denhoff, M., Martina, M., Monette, R., Comas, T., Luk, C., Syed, N., and Mealing, G. (2010b). High-fidelity patch-clamp recordings from neurons cultured on a polymer microchip. *Biomed. Microdevices* 12, 977.
- Matthews, B., and Judy, J. W. (2006). Design and fabrication of a micro-machined planar patch-clamp substrate with integrated microfluidics for single-cell measurements. *J. Microelectromech. Syst.* 15, 214–222.
- MEA Meeting. (2010). “See for example papers within Neuronal dynamics and plasticity,” in *Proceedings of the 7th International Meeting on Substrate-integrated Microelectrode Arrays*, June 29–July 2, Reutlingen.
- Mealing, G., Bani-Yaghou, M., Py, C., Voicu, R., Barjovanu, R., Tremblay, R., Monette, R., Mielke, J., and Faid, K. (2005a). “Application of polymer microstructures with controlled surface chemistries as a platform for creating and interfacing with synthetic neural networks,” in *International Joint Conference on Neural Networks 2005 Conference Proceedings*, Montreal, CA, 3116–3120.
- Mealing, G., Py, C., Denhoff, M., Dowlatshahi, R., Faid, K., Voicu, R., and Bani, M. (2005b). PCT patent application PCT/CA2005/000682.

- Merz, M., and Fromherz, P. (2005). Silicon chip interfaced with a geometrically defined net of snail neurons. *Adv. Funct. Mater.* 15, 739–744.
- Metz, S., Holzer, R., and Renaud, P. (2001). Polyimide-based microfluidic devices. *Lab Chip* 1, 29–34.
- Milligan, C. J., Li, J., Sukumar, P., Majeed, Y., Dallas, M. L., English, A., Emery, P., Porter, K. E., Smith, A. M., McFadzean, I., Beccano-Kelly, D., Bahnasi, Y., Cheong, A., Naylor, J., Zeng, F., Liu, X., Gamper, N., Jiang, L.-H., Pearson, H. A., Peers, C., Robertson, B., and Beech, D. J. (2009). Robotic multiwell planar patch-clamp for native and primary mammalian cells. *Nat. Protoc.* 4, 244–255.
- Milo, R., Shen-Orr, S., Itzkovitz, S., Kashtan, N., Chklovskii, D., and Alon, U. (2002). Network motifs: simple building blocks of complex networks. *Science* 298, 824–827.
- Morales, R., Riss, M., Wang, L., Gavín, R., Del Río, J. A., Alcubilla, R., and Claverol-Tinturé, E. (2008). Integrating multi-unit electrophysiology and plastic culture dishes for network neuroscience. *Lab Chip* 8, 1896–1905.
- Nagarah, J. M., Paek, E., Luo, Y., Wang, P., Hwang, G. S., and Heath, J. R. (2010). Batch fabrication of high-performance planar patch-clamp devices in quartz. *Adv. Mater.* 22, 4622–4627.
- Neher, E., and Sakmann, B. (1976). Single-channel currents recorded from membrane of denervated frog muscle fibers. *Nature* 260, 799–802.
- Offenhausser, A., Bocker-Meffert, S., Decker, T., Helpenstein, R., Gasteier, P., Groll, J., Moller, M., Reska, A., Schafer, S., Schulte, P., and Vogt-Eisele, A. (2007). Microcontact printing of proteins for neuronal cell guidance. *Soft Matter* 3, 290–298.
- Ogi, H., Fukunishi, Y., Nagai, H., Okamoto, K., Hirao, M., and Nishiyama, M. (2009). Nonspecific-adsorption behavior of polyethyleneglycol and bovine serum albumin studied by 55-MHz wireless-electrodeless quartz crystal microbalance. *Biosens. Bioelectron.* 24, 3148–3152.
- Ong, W.-L., Tang, K.-C., Agarwal, A., Nagarajan, R., Luo, L.-W., and Yobas, L. (2007). Microfluidic integration of substantially round glass capillaries for lateral patch clamping on chip. *Lab Chip* 7, 1357–1366.
- Ong, W.-L., Yobas, L., and Ong, W.-Y. (2006). A missing factor in chip-based patch clamp assay: gigaseal. *J. Phys.* 34, 187.
- Palop, J. J., Chin, J., and Mucke, L. (2006). A network dysfunction perspective on neurodegenerative diseases. *Nature* 443, 768–773.
- Pandey, S., Mehrotra, R., Wykosky, S., and White, M. H. (2004). Characterization of a MEMS BioChip for planar patch-clamp recording. *Solid State Electron.* 48, 2061–2066.
- Pantoja, R., Nagarah, J. M., Starace, D. M., Melosh, N. A., Blunck, R., Bezanilla, F., and Heath, J. R. (2004). Silicon chip-based patch-clamp electrodes integrated with PDMS microfluidics. *Biosens. Bioelectron.* 20, 509–517.
- Patolsky, F. (2007). Detection, stimulation, and inhibition of neuronal signals with high-density nanowire transistor arrays. *Science* 313, 1100–1104.
- Picollet, D. h. N., Sordel, T., Garnier, R. S., Sauter, F., Ricoul, F., Pudda, C., Marcel, F., and Chatelain, F. (2004). A silicon-based multi patch device for ion channel current sensing. *Sens. Lett.* 2, 91–94.
- Pleasure, D., Hardy, M., Johnson, G., Lisak, R., and Silberberg, D. (1981). Oligodendroglial glycerophospholipid synthesis: incorporation of radioactive precursors into ethanolamine glycerophospholipids by calf oligodendroglia prepared by a Percoll procedure and maintained in suspension culture. *J. Neurochem.* 37, 452–460.
- Priel, A., Gil, Z., Moy, V., Magleby, K., and Silberberg, S. (2007). Ionic requirements for membrane-glass adhesion and giga seal formation in patch-clamp recording. *Biophys. J.* 92, 3893–3900.
- Py, C., Denhoff, M., Martina, M., Monette, R., Comas, T., Ahuja, T., Martinez, D., Wingar, S., Caballero, J., Laframboise, S., Mielke, J., Bogdanov, A., Luk, C., Syed, N., and Mealing, G. (2010). A novel silicon patch-clamp chip permits high-fidelity recording of ion channel activity from functionally defined neurons. *Biotechnol. Bioeng.* 107, 593–600.
- Py, C., Mealing, G., Denhoff, M., Charrier, A., Monette, R., Comas, T., Ahuja, T., Martinez, D., Krantis, A., and Wingar, S. (2008). “A multiple recording patch clamp chip with integrated subterranean microfluidic channels for cultured neuronal networks,” in *Micro-Total Analysis Systems*, San Diego, CA, 507–509.
- Py, C., Salim, D., Monette, R., Comas, T., Fraser, J., Martinez, D., Martina, M., and Mealing, G. (2011). Cell to aperture interaction in patch-clamp chips visualized by fluorescence microscopy and focused-ion beam sections. *Biotechnol. Bioeng.* 108, 1395–1403.
- Qin, D., Xia, Y. N., and Whitesides, G. M. (2010). Soft lithography for micro- and nanoscale patterning. *Nat. Protoc.* 5, 491–502.
- Ruuslahti, E., and Pierchbacker, M. (1986). Arg-Gly-Asp: a versatile cell recognition signal. *Cell Motil. Cytoskeleton* 44, 517–518.
- Sachs, F., and Qin, F. (1993). Gated, ion-selective channels observed with patch pipettes in the absence of membranes: novel properties of a gigaseal. *Biophys. J.* 65, 1101–1107.
- Scheiffele, P. (2003). Cell-cell signaling during synapse formation in the CNS. *Annu. Rev. Neurosci.* 26, 485–508.
- Schmidt, C., Mayer, M., and Vogel, H. (2000). A chip-based biosensor for the functional analysis of single ion channels. *Angew. Chem. Int. Ed. Engl.* 39, 3137–3140.
- Schnizler, K., Kuster, M., and Methfessel, C. (2003). The roboocyte: automated cDNA/mRNA injection and subsequent TEVC recording on *Xenopus Oocytes* in 96-well microtiter plates. *Recept. Channels* 9, 41–48.
- Seeley, W. W., Crawford, R. K., Zhou, J., Miller, B. L., and Greicius, M. D. (2009). Neurodegenerative diseases target large-scale human brain networks. *Neuron* 62, 42–52.
- Seo, J., Ionescu-Zanetti, C., Diamond, J., Lal, R., and Lee, L. P. (2004). Integrated multiple patch-clamp array chip via lateral cell trapping junctions. *Appl. Phys. Lett.* 84, 1973–1975.
- Shatz, C. (1990). Impulse activity and the patterning of connections during CNS development. *Neuron* 5, 745–756.
- Sigworth, F. J., and Klemic, K. G. (2005). Microchip technology in ion-channel research. *IEEE Trans. Nanobioscience* 4, 121–127.
- Song, S., Sjöström, P. J., Reigl, M., Nelson, S., and Chklovskii, D. B. (2005). Highly nonrandom features of synaptic connectivity in local cortical circuits. *PLoS Biol.* 3, e68. doi:10.1371/journal.pbio.0030068
- Sordel, T., Garnier-Raveaud, S., Sauter, F., Pudda, C., Marcel, F., De-Waard, M., Arnoult, C., Vivaudou, M., Chatelain, F., and Piccollet-D’ahan, N. (2006). Hourglass SiO₂ coating increases the performance of planar patch-clamp. *J. Biotechnol.* 125, 142–154.
- Sordel, T., Kermarrec, F., Sinquin, Y., Fontelle, I., Labeau, M., Sauter-Starace, F., Pudda, C., de Crécy, F., Chatelain, F., De Waard, M., Arnoult, C., and Piccollet-D’ahan, N. (2010). The development of high quality seals for silicon patch-clamp chips. *Biomaterials* 31, 7398–7410.
- Sorkin, R., Greenbaum, A., David-Pur, M., Anava, S., Ayali, A., Ben-Jacob, E., and Hanein, Y. (2009). Process entanglement as a neuronal anchorage mechanism to rough surfaces. *Nanotechnology* 20, 015101.
- Stett, A., Egert, U., Guenther, E., Hofmann, F., Meyer, T., Nisch, W., and Haemmerle, H. (2003a). Biological application of microelectrode arrays in drug discovery and basic research. *Anal. Bioanal. Chem.* 377, 486–495.
- Stett, A., Burkhardt, C., Weber, U., van Stiphout, P., and Knott, T. (2003b). Cytoentering: a novel technique enabling automated cell-by-cell patch clamping with the cytopatch chip. *Recept. Channels* 9, 59–66.
- Stett, A., Bucher, V., Burkhardt, C., Weber, U., and Nisch, W. (2003c). Patch-clamping of primary cardiac cells with micro-openings in polyimide films. *Med. Biol. Eng. Comput.* 41, 233–240.
- Suchyna, T., Markin, V., and Sachs, F. (2009). Biophysics and structure of the patch and the gigaseal. *Biophys. J.* 97, 738–747.
- Taketani, M., and Baudry, M. (2006). *Advances in Network Electrophysiology: Using Multi-Electrode Arrays*. Secaucus, NJ: Springer.
- Tang, K. C., Reboud, J., Kwok, Y. L., Peng, S. L., and Yobas, L. (2010). Lateral patch-clamping in a standard 1536-well microplate format. *Lab Chip* 10, 1044–1050.
- Unger, M. A., Chou, H. P., Thorsen, T., Scherer, A., and Quake, S. R. (2000). Monolithic microfabricated valves and pumps by multilayer soft lithography. *Science* 288, 113–116.
- Vicario-Abejo’n, C., Collin, C., McKay, R., and Segal, M. (1998). Neurotrophins induce formation of functional excitatory and inhibitory synapses between cultured hippocampal neurons. *J. Neurosci.* 18, 7256–7271.
- Vogt, A. K., Brewer, G. J., and Offenhausser, A. (2005). Connectivity patterns in neuronal networks of experimentally defined geometry. *Tissue Eng.* 11, 1757–1767.
- Voicu, R., Faid, K., Farah, A. A., Bensebaa, F., Barjovanu, R., Py, C., and Tao, Y. (2007). Nanotemplating for two-dimensional molecular imprinting. *Langmuir* 23, 5452–5458.

- Wang, X., and Li, M. (2003). Automated electrophysiology: high throughput of art. *Assay Drug Dev. Technol.* 1, 695–708.
- Wheeler, B. C., and Brewer, G. J. (2010). Designing neural networks in culture. *Proc. IEEE* 98, 398–406.
- Wheeler, B. C., Brewer, G. J., Branch, D. W., Chang, J., and Venkateswar, K. (1999). Rational design of in vitro neural networks using patterned self-assembled monolayers. *Abstr. Pap. Am. Chem. Soc.* 217, 014-BTEC.
- Witchel, H. (2010). Emerging trends in ion channel-based assays for predicting the cardiac safety of drugs. *Idrugs* 13, 90–96.
- Woodin, M. A., Hamakawa, T., Takasaki, M., Lukowiak, K., and Syed, N. I. (1999). Trophic factor-induced plasticity of synaptic connections between identified *Lymnaea* neurons. *Learn. Mem.* 6, 307–316.
- Woodin, M. A., Munno, D. W., and Syed, N. (2002). Trophic factor-induced excitatory synaptogenesis involves postsynaptic modulation of nicotinic acetylcholine receptors. *J. Neurosci.* 22, 505–514.
- Wyart, C., Ybert, C., Bourdieu, L., Herr, C., Prinz, C., and Chatenay, D. (2002). Constrained synaptic connectivity in functional mammalian neuronal networks grown on patterned surfaces. *J. Neurosci. Methods* 117, 123–131.
- Zhao, Y., Chee, C. L., Sawyer, D. B., Liao, R., and Zhang, X. (2007). Simultaneous orientation and cellular force measurements in adult cardiac myocytes using three-dimensional polymeric microstructures. *Cell Motil. Cytoskeleton* 64, 718–725.
- Zhou, Z., and Kang, H.-G. (2000). Patch clamp noise from seal impedance and the pipette capacitance. *Annu. Int. Conf. IEEE Eng. Med. Biol. Soc.* 12, 1679–1680.
- Conflict of Interest Statement:** The authors declare that the research was conducted in the absence of any commercial or financial relationships that could be construed as a potential conflict of interest.
- Received: 13 July 2011; paper pending published: 29 July 2011; accepted: 05 September 2011; published online: 03 October 2011.
- Citation: Py C, Martina M, Diaz-Quijada GA, Luk CC, Martinez D, Denhoff MW, Charrier A, Comas T, Monette R, Krantis A, Syed NI and Mealing GAR (2011) From understanding cellular function to novel drug discovery: the role of planar patch-clamp array chip technology. *Front. Pharmacol.* 2:51. doi: 10.3389/fphar.2011.00051
- This article was submitted to *Frontiers in Pharmacology of Ion Channels and Channelopathies*, a specialty of *Frontiers in Pharmacology*.
- Copyright © 2011 Py, Martina, Diaz-Quijada, Luk, Martinez, Denhoff, Charrier, Comas, Monette, Krantis, Syed and Mealing. This is an open-access article subject to a non-exclusive license between the authors and Frontiers Media SA, which permits use, distribution and reproduction in other forums, provided the original authors and source are credited and other Frontiers conditions are complied with.



The importance of being profiled: improving drug candidate safety and efficacy using ion channel profiling

Gregory J. Kaczorowski¹, Maria L. Garcia¹, Jacob Bode², Stephen D. Hess² and Umesh A. Patel^{2*}

¹ Kanalis Consulting, Limited Liability Company, Edison, NJ, USA

² Millipore Corporation, Billerica, MA, USA

Edited by:

Ralf Franz Kettenhofen, Axiogenesis AG, Germany

Reviewed by:

Gary Gintant, Abbott, USA

*Correspondence:

Umesh A. Patel, Millipore Corporation, 15 Research Park Drive, St. Charles, MO 63304, USA.
e-mail: umesh.patel@merckgroup.com

Profiling of putative lead compounds against a representative panel of relevant enzymes, receptors, ion channels, and transporters is a pragmatic approach to establish a preliminary view of potential issues that might later hamper development. An early idea of which off-target activities must be minimized can save valuable time and money during the preclinical lead optimization phase if pivotal questions are asked beyond the usual profiling at hERG. The best data for critical evaluation of activity at ion channels is obtained using functional assays, since binding assays cannot detect all interactions and do not provide information on whether the interaction is that of an agonist, antagonist, or allosteric modulator. For ion channels present in human cardiac muscle, depending on the required throughput, manual-, or automated-patch-clamp methodologies can be easily used to evaluate compounds individually to accurately reveal any potential liabilities. The issue of expanding screening capacity against a cardiac panel has recently been addressed by developing a series of robust, high-throughput, cell-based counter-screening assays employing fluorescence-based readouts. Similar assay development approaches can be used to configure panels of efficacy assays that can be used to assess selectivity within a family of related ion channels, such as Nav1.X channels. This overview discusses the benefits of *in vitro* assays, specific decision points where profiling can be of immediate benefit, and highlights the development and validation of patch-clamp and fluorescence-based profiling assays for ion channels (for examples of fluorescence-based assays, see Bhavé et al., 2010; and for high-throughput patch-clamp assays see Mathes, 2006; Schröder et al., 2008).

Keyword: ion channel

WHY USE *IN VITRO* PROFILING ASSAYS TO UNDERSTAND LEAD SELECTIVITY AND SPECIFICITY?

The drug discovery and development process is long, and resource-intensive, often fraught with unforeseeable pitfalls, and historically challenged by low probability of success (Tollman et al., 2011). However, vast unmet medical needs justify the efforts expended in this area of research, and new methodologies are always being explored to streamline the research process and improve the success rate of drug registration. Perhaps the most important factor at the beginning of any drug discovery project, regardless of the target, is the identification of the best lead structure amongst the collection of hits discovered either using *in silico* or through high-throughput screening techniques to target the process of interest (Rudolph and Knoflach, 2011).

Many factors must be taken into account during lead selection, such as chemical tractability, chemical stability, physical-chemical properties, metabolic stability, PK characteristics, protein binding, and suitability for formulation, in addition to potency and mechanism of action. However, none are more important than the specificity and selectivity of the initial compound. Subjecting putative leads to thorough scrutiny with respect to potential off-target pharmacological activities can identify liabilities, some of them potentially fatal, early on in a program, and thereby allow medicinal chemists to explore the feasibility of correcting these

problems during exploratory analoging studies. Thus, broad profiling of early hits to determine selectivity, and then use of this information to prioritize compounds for follow-up, rather than simply rank-ordering hits based solely on chemical tractability, can prevent wasting time and effort due to making a poor initial decision based on a limited and incomplete data set. As an example, Millipore offers a wide variety of profiling services that utilize biochemical assays for over 300 kinases and phosphatases and cell-based functional assays for over 150 G-protein coupled receptors (GPCRs) and over 50 ion channels that can be utilized to query compounds at any development stage for specificity and selectivity for primary targets, related family members, and for cardiac safety.

SELECTIVITY AND SPECIFICITY SCREENING

The most straightforward means of generating selectivity data on a group of hits is to test for activity against a panel of similar targets from the same and closely related super families of proteins (e.g., classes of related enzymes, GPCRs, nuclear receptors, ion channels, etc.). Such studies provide important data for medicinal chemists and help focus their structure-activity determinations as part of a feasibility assessment of a compound's potential as a lead candidate. In addition, these studies also immediately identify molecules that are non-selective in their mechanism of action because such

agents often display pleiotropic activities across an entire family of related proteins. Functional assays are the preferred methodology to use for these analyses (see below).

In general, two other means are commonly employed initially to gather specificity data (i.e., to identify activities on proteins/processes unrelated to the initial target, some of which could cause serious adverse drug side effects) on a series of hits (c.f. Coburger et al., 2010). One is to profile test compounds *in vivo* in an animal efficacy model and determine therapeutic index based on comparing exposure for efficacy versus observed side effects. The other is to profile hits employing a panel of enzyme and receptor binding assays, gather the respective profile of off-target activities predicted for each compound, and assess their profile *in vivo*, in an animal model chosen to reveal ancillary pharmacological activities. Usually, it is assumed that if no untoward activities are observed *in vivo*, the risk of any predictable ancillary pharmacology will be minimal.

LIMITATIONS OF *IN VIVO* SPECIFICITY AND SELECTIVITY ASSESSMENT

There are a number of confounding aspects related to using such *in vivo* assessment approaches, and the data generated can be highly misleading without a thorough understanding gained from *in vitro* assays (e.g., Raehal et al., 2011). First, animal experiments are usually done in rodents, either mice or rats, and while these species are adequate for tolerability studies to reveal frank toxicity, they may not be useful for detecting subtle changes in physiology. In addition, limited exposure and high clearance rates (typical in rodents) can result in a misleading sense of ancillary pharmacology. Taken together with the facts that some physiological response pathways are species-dependent, high protein binding can mask ancillary pharmacology, and that poly pharmacy of compounds can cause compensation by altering a number of inter-related pathways whose individual modulation might otherwise produce serious consequences, an unremarkable initial *in vivo* profile could produce a false sense of security. But most importantly, the rodent cardiovascular (CV) system is a poor predictor of CV side effects in humans. This is due to very high heart rates in the rodent and distinct complements/contributions of ion channels in the two species (e.g., the cardiac action potential wave forms are much different when comparing rodent and human species). Therefore, rodent data, by itself, can yield false-negative misinformation with respect to adverse CV effects. We do recognize the utility of rat models for understanding cardiotoxicity (Herman et al., 2011); however in general we advise caution when using this species to assess potential pro-arrhythmic liabilities (i.e., prolongation of QTc intervals, see below). Indeed, this is one of the reasons that CV liabilities of late stage development candidates are traditionally assessed in a dog model, which is more predictive than rodent of CV safety liabilities in humans. However, it is not routinely feasible to profile putative lead structures in the dog due to the need for large quantities of test compound to initiate both tolerability studies and CV measurements. Employment of cardiomyocytes derived from embryonic or induced pluripotent stem cells that display the electrophysiological and biochemical properties of normal human heart cells is currently being explored as a more predictive *in vitro* model

system for testing a compound's potential cardiotoxicity, but this approach is still under development (Braam et al., 2010; Peng et al., 2010). Therefore, a more informative approach is required to carry out a formal risk analysis of a lead compound's potential liabilities than to simply use cursory rodent *in vivo* data. It is critical to have some early means to identify potential problems that could arise during development of a drug candidate and to minimize such hazards by selecting the most appropriate lead class for the focus of medicinal chemists. Moreover, if potential liabilities exist in an otherwise favorable lead compound, predictive, high-capacity assays must be employed to support Medicinal Chemistry efforts to dial out these unwanted activities in real time during the course of structure–activity relationship (SAR) studies.

It is important to consider the contribution of multiple mechanisms to a physiological response when developing *in vivo* models to evaluate specificity and selectivity and obtaining proof of concept for novel compounds targeting new mechanisms of action. As the drug industry searches for new druggable targets based on human genetics, rodent genetic paradigms, and reverse pharmacology approaches, it is important to check new leads for poly pharmacy before initiating Medicinal Chemistry campaigns, just to confirm that pharmacodynamic responses correlate strictly with the desired molecular action (Weinglass et al., 2008a,b). For example, the search for agonists of the high-conductance, calcium-activated potassium channel (maxi-K; KCa1.1) has often revealed compounds in the past which activate the channel, promote smooth muscle relaxation, and lower blood pressure in rodents, i.e., the phenotype expected for a KCa1.1 agonist. However, to date, all publicly disclosed channel agonists have been observed to have ancillary pharmacology (e.g., calcium entry blocker activity, phosphodiesterase inhibitory activity) that promote smooth muscle relaxation and blood pressure lowering as well, which confounds proof-of-concept arguments that a selective KCa1.1 agonist will have therapeutic utility in reversing pathophysiology associated with smooth muscle hyper-excitability (Garcia et al., 2007). The importance of profiling lead compounds directed against new mechanisms for ancillary pharmacological activity cannot be overemphasized.

CROSS-TARGET PROFILING: THE ADVANTAGES OF FUNCTIONAL ASSAYS

Profiling a putative lead compound against a panel representing a consensus of important enzymes, receptors, ion channels, and transporters is an excellent way to establish a preliminary view of potential issues that might hamper development, and which off-target activities must be minimized accordingly. However, although enzyme assays are activity-based measurements (N. B., their interpretation is subject to the conditions chosen for the assay, especially levels of substrate), the use of binding assays to assess interaction of test compound with receptors, channels, or transporters is not as informative as are functional measurements. The same issues exist, but to a greater extent, with ion channel proteins. The ability of test compounds to interfere with binding of specific ligand probes developed for individual ion channels is often used as a guide for determining potential drug liabilities. However, it is well known that, unless the sites at which test

agents interact with a channel are identical or strongly allosterically coupled to that region where the radiolabel probe binds, potential channel interactions can be missed. Tetrodotoxin (TTX) is a very potent and selective inhibitor of many voltage-gated sodium channels. However, except for similar congeners that compete for binding to this inhibitor's site in the external pore of the TTX-sensitive sodium channel subtype, the rich pharmacology known to exist with this channel family (i.e., the extensive number of both agonists and antagonists that have previously been well-characterized) is completely undetectable using the TTX binding reaction (Cestele and Catterall, 2009). Similarly, using omega conotoxin as a probe for Cav2.2, charybdotoxin as a probe for Kv1.X or KCa1.1 channels, apamin as a probe for KCa2.X channels, or sulfonylureas as a probe of K-ATP channels, are additional insensitive means to determine potential off-target activities directed against these proteins. Indeed, it is known that conotoxin binding is highly refractory to modulation by most small molecule Cav2.2 inhibitors (Abbadie et al., 2010). In the case of sulfonylureas, binding is to a regulatory subunit associated with Kir6.2, the pore-forming subunit of the K-ATP channel complex, and monitoring effects on that binding reaction is conceptually a poor way to detect direct modulators of the Kir6 channel (see relevant sections in Hibino et al., 2010). The same criticism could be applied to many of the probes used to assess interactions with ligand-gated ion channels or transporters. In the case of transporters, there is no guarantee that using ligands which interact at a carrier's substrate binding site is a sensitive means to detect all compounds that affect transporter function. Thus, there is no *bona fide* substitute to definitively identify putative ion channel or transporter modulators other than by direct measurement of protein function. This is especially true when evaluating novel chemical structures without previous pharmacological history, because many examples of false negatives and false positives have been noted when using binding protocols to profile such compound decks.

EXAMPLES OF PROFILING COMPOUNDS ACROSS TARGETS AND ACROSS CHANNEL FAMILIES

While drug discovery programs typically test the activity of lead compounds against other related family member targets, and may also include some critical cardiac targets, a much wider profiling can yield a better understanding of potential liabilities of the structural class of compounds under consideration. As an example, BIRB0796, which was developed as an allosteric inhibitor of p38 MAP kinase (aka SAPK2A/SAPK2B; Pargellis et al., 2002) was profiled at a single concentration of 10 μ M in a functional Safety and Liability Screening Panel consisting of 125 targets (76 GPCRs, 39 Kinases, two Phosphatases, and eight Cardiac Ion Channels). **Table 1** summarizes the activity of BIRB0796 in biochemical assays employing the kinases and phosphatases. BIRB0796 inhibits the SAPK2a/SAPK2b enzyme at a novel "DFG-out" allosteric site as determined from studies of the compound bound to non-activated human p38 MAP kinase, and has weak or no inhibition of 15 other kinases (Pargellis et al., 2002). In our studies greater than 50% inhibition of four kinases, including SAPK2B, was observed. In addition, 10 μ M BIRB0796 inhibited five GPCRs (**Table 2**) and two of seven Cardiac Ion Channels, hERG, and Kv1.5 (**Figure 1**), by

Table 1 | Activity expressed as percentage inhibition of 10 μ M BIRB0796 on 39 kinases and 2 phosphatases within Millipore's Safety and Liability Panel.

Kinase/phosphatase	Percentage inhibition
Abl(h)	80
AMPK(r)	1
CaMKII β (h)	22
CaMKII γ (h)	11
CaMKII δ (h)	22
CDK1/cyclinB(h)	-6
CDK2/cyclinA(h)	-6
CDK2/cyclinE(h)	-11
CDK3/cyclinE(h)	-10
CDK5/p25(h)	1
CDK5/p35(h)	-26
CDK7/cyclinH/MAT1(h)	17
CDK9/cyclin T1(h)	-17
Flt1(h)	96
GSK3 β (h)	-6
IR(h)	-3
LKB1(h)	10
Lyn(h)	81
MAPK1(h)	-3
MAPK2(h)	-10
p70S6K(h)	39
PhK γ 2(h)	-1
PKA(h)	6
PKB β (h)	-15
PKC μ (h)	13
PKC α (h)	9
PKC β I(h)	-17
PKC β II(h)	-11
PKC γ (h)	7
PKC δ (h)	-15
PKC ϵ (h)	16
PKC ζ (h)	-3
PKC η (h)	-14
PKC θ (h)	-29
PKC ι (h)	3
PKG1 α (h)	15
PKG1 β (h)	13
ROCK-II(h)	-3
SAPK2a(h)	94
PTP1B(h)	18
TCPTP(h)	17

The 39 kinases are arranged alphabetically from Abl (top) to SAPK2a (near bottom). The two phosphatases are PTP1B and TCPTP. Except for the rat AMPK, all enzymes and phosphatases were the human form. Red font is used to highlight the targets where the inhibition observed was > 50%.

≥50%. Inhibition of hERG and Kv1.5 channels could raise a flag of potential cardiac safety concern for this compound. All these data on BIRB0796, derived from a combination of biochemical and cell-based functional assays, provide a better insight into the putative compound's liabilities than would have been obtained from

Table 2 | Activity expressed as percentage inhibition of 10 μ M BIRB0796 on 76 GPCRs within Millipore's Safety and Liability Panel.

GPCR	Percentage inhibition
5-HT1A	31.0
5-HT2A	99.5
5-HT2B	18.5
5-HT2C	5.5
A1	19.5
A3	20.5
Alpha1A	6.0
Alpha1D	3.5
Alpha2A	-4.0
AT1	-2.5
B2	-4.5
BB2	0.0
Beta 1	-6.0
Beta 2	-9.5
BLT1	8.5
C5aR	-5.5
CB1	9.0
CB2	80.0
CCK2	2.0
CCR1	-6.0
CCR2B	0.0
CGRP1	0.0
CRF1	13.0
CX3CR1	-12.0
CXCR1	-1.5
CysLT1	2.0
D1	23.0
D2L	53.5
D5	14.0
DP	12.5
EP2	2.5
EP3	7.5
ETA	-4.0
ETB	11.0
FP	20.5
FPR1	-4.5
GAL1	-1.5
GnRH/LHRH	-20.5
GPR109A	-1.0
H1	-1.5
H2	-5.5
H3	91.5
IP1	12.5
LPA1	6.5
LPA3	5.0
M1	46.5
M2	34.5
M3	5.0
MC5	2.0
Motilin receptor	94.5
NK1	12.0

(Continued)

GPCR	Percentage inhibition
NK3	17.5
NMU1	22.5
NTR1	-12.0
OPRD1	8.5
OPRK1	-19.0
OPRM1	-2.5
OT	12.5
OX1	12.0
P2Y1	10.5
PAC1 long isoform	3.5
PAF	19.5
PK1	-6.5
PRP	3.0
PTH1	0.0
S1P3	-1.5
SST4	-5.5
TP	32.0
Trypsin-mediated PARs	9.0
TSH	-4.0
UT/GPR14	18.5
V1A	2.0
V2	1.0
VPAC1	-2.0
VPAC2	-4.0
Y2	-13.5

Red font is used to highlight the targets where the inhibition observed was > 50%. All GPCRs within Millipore's Safety and Liability Panel are full length human isoforms.

the use of binding assays alone. This example illustrates the need to broadly characterize any potential drug discovery compound in functional assays to better understand its potential off-target activities.

For functional assays to be able to provide accurate and decision-enabling information, it is important to understand how these assays perform over an extended period of time. This is best illustrated in the case of Nav channels, where some specific channel members, such as Nav1.7 and Nav1.8 are of interest for development of novel analgesics, but where such compounds must display restricted activity at the brain Nav1.1 and Nav1.2, and cardiac Nav1.5 isoforms. To identify novel chemical entities with the desired properties, i.e., state- and use-dependence to effectively block peripheral Nav1.7 or Nav1.8 channels involved in pain signaling, while sparing block at the cardiac Nav1.5 channel, drug discovery programs use both biochemical-based assays as well as manual patch-clamp and automated EPhys assays (Felix et al., 2004; Kaczorowski et al., 2008). Using IonWorks and PatchXpress platforms, Millipore can provide rapid turnaround times (within 7 business days from the date of compound receipt) for routine profiling against Nav1.1, Nav1.2, Nav1.3, Nav1.4, Nav1.5, Nav1.6, and Nav1.7 channels since these assays are sufficiently validated and quality control is followed rigorously. In addition, when development of assays using automated platforms is problematic because the amount of current remaining in cells held at $V_{1/2}$ inactivation

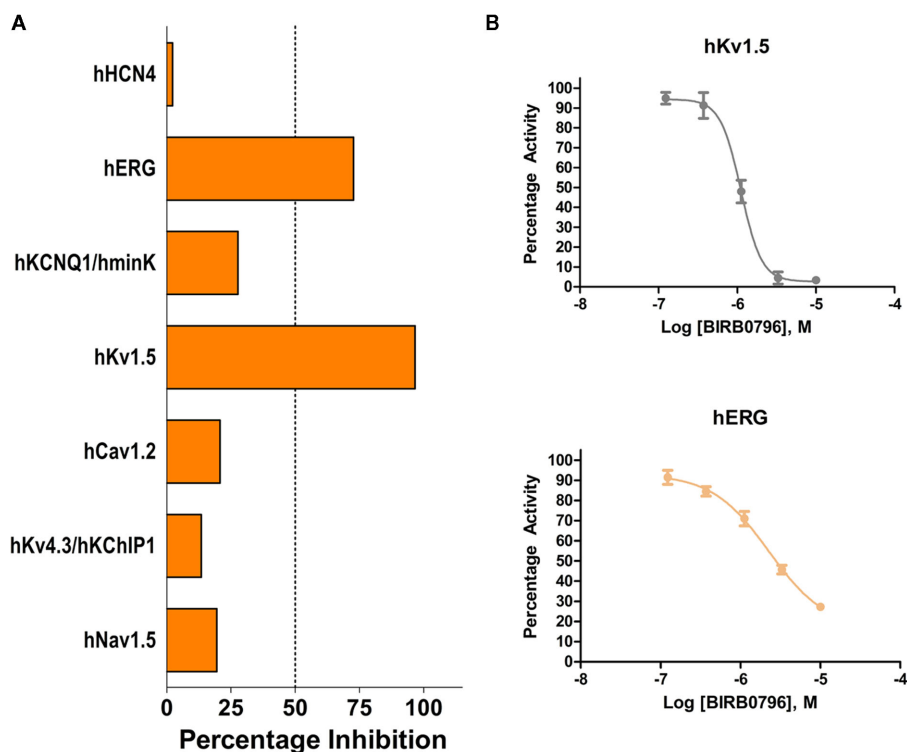


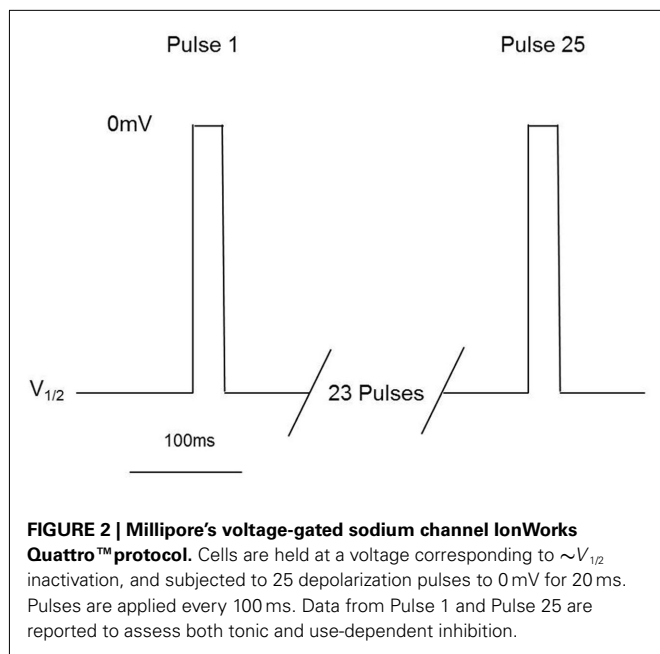
FIGURE 1 | (A) Activity of 10 μ M BIRB0796 on cardiac ion channels within Millipore's Safety and Liability Panel. **(B)** Because of the significant inhibition observed at 10 μ M, full concentration response curves for hERG and Kv1.5 were carried out with BIRB0796. Calculated IC_{50} values were 2.3 and 1.1 μ M for hERG and Kv1.5, respectively.

is not sufficient to enable robust and reliable IonWorks assays, additional assays can be provided using manual patch-clamp (e.g., Nav1.8).

These assays utilize stable cell lines (e.g., Burbidge et al., 2002; Clare et al., 2009) and voltage-clamp protocols designed to assess multiple features of compounds' interaction with the Nav channels (Figure 2). A parameter often desired is use-dependent block, a condition where block accumulates due to high frequency firing that can be assayed using multiple-pulse protocols. Block of the inactivated-state of the channel, also known as tonic block, which is thought to be relevant in the disease state, can also be determined by selecting a holding potential that inactivates a certain fraction of the channels, so that one can estimate the affinity of the test compound for the inactivated state (K_i) and compare it with resting state block (K_r ; see Hondeghem and Katzung, 1977; Bean et al., 1983). The protocol illustrated in Figure 2 was designed to efficiently profile both modes of interaction of test compounds with Nav1.x channels. Quality-control data for this protocol are shown in Figure 3, where the activity at pulse 25 for two concentrations of the reference compound, and the solvent control are shown. Robust-performing stable cell lines are crucial for these assays; the criteria for initial validation of these cell lines include current amplitude (we set a typical threshold of greater than 250 pA), seal resistance on automated patch-clamp platforms (i.e., is high enough relative to the current amplitude obtained with the assay protocol to give acceptable

current resolution; this ranges from hundreds of $M\Omega$ to a few $G\Omega$ depending on the seal substrate) percent of cells expressing the current (the higher, the better) and continued performance at these levels over at least 25 passages in culture. Data collected over a 6-month time period show that the assays are robust and reproducible (Figure 3). Rigorous quality control checks ensure week-to-week consistencies which are necessary to support Drug Discovery programs.

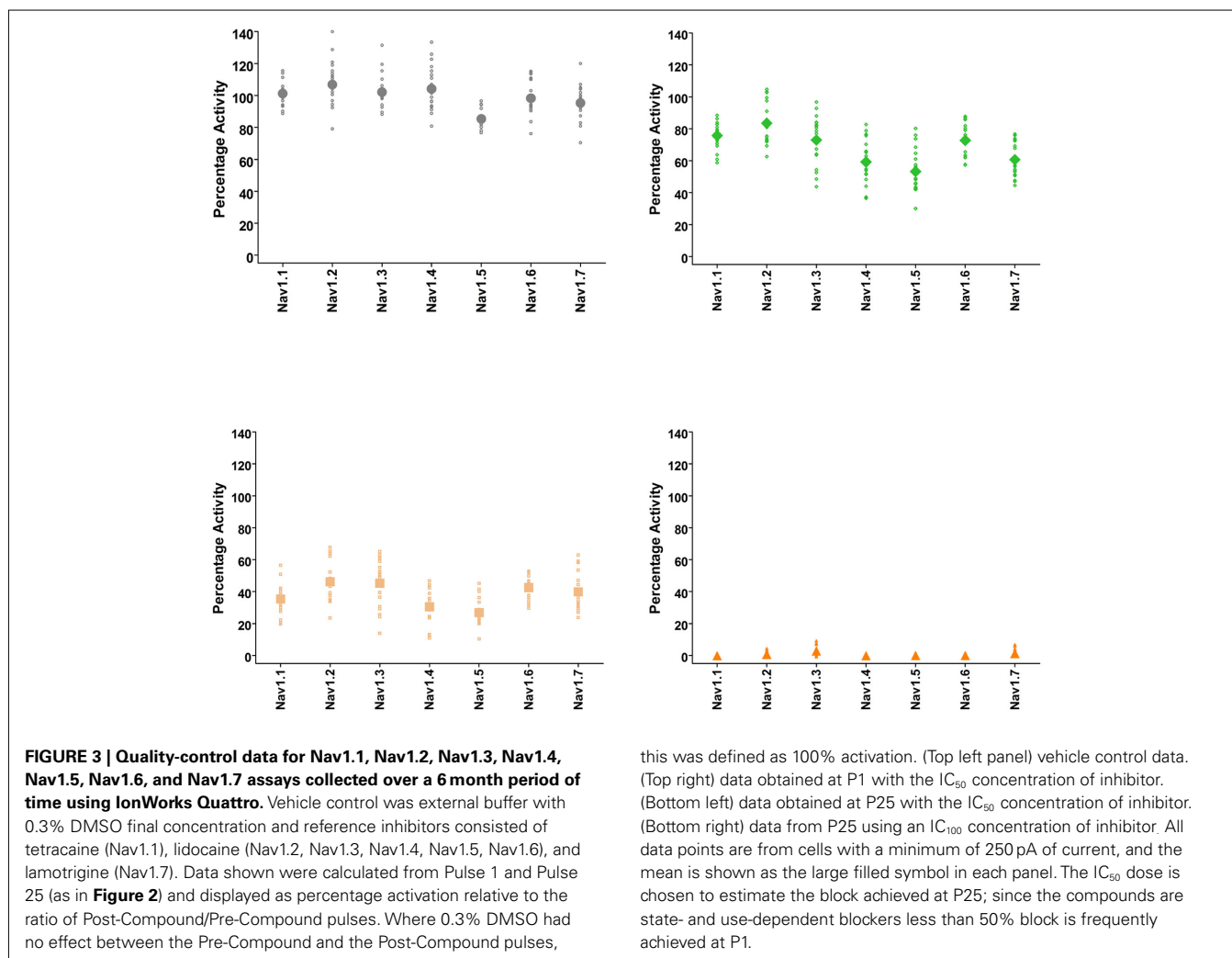
Additional specific custom automated patch-clamp protocols (see example in Figure 4) can be rapidly developed to identify inhibitors of Nav1.X channels that preferentially bind to the inactivated-state of the channel (Hondeghem and Katzung, 1977; Bean et al., 1983). We have developed custom protocols, with all validation data required, in as little as 3 weeks. Example data obtained using this protocol for seven Nav standards on three Nav1.X channels, Nav1.2, Nav1.5, and Nav1.6, are summarized in Table 3 and example data for Nav1.5 are shown in Figure 5. Lidocaine, tetracaine, lamotrigine, carbamazepine, and riluzole displayed a large leftward shift in their concentration–response curve at pulse 2, consistent with the use-dependent mechanism of block by these agents. Flecainide, on the other hand, displayed a more modest shift in affinity when comparing pulse 1 and 2, whereas for phenytoin there is essentially no block at pulse 1 and pronounced block at pulse 2. These data illustrate that reliable and efficient automated Ephys assays exist which can support Medicinal Chemistry programs targeting Nav channels. Similar



protocols are in development for other voltage-gated channels, including Kv channels.

IMPORTANCE OF MEASURING ACTIVITY OF DRUG CANDIDATES ON ION CHANNELS FOR CARDIAC SAFETY

Off-target activities of drug candidates are particularly relevant to ion channels expressed in the heart. Untoward modulation of many of these proteins can result in major safety issues, including lethality. Ion channels control conduction of electrical activity over the heart. They are responsible for efficiently orchestrating both cardiac rate and synchronous contraction of cardiac muscles comprising the atria and ventricle to allow efficient pumping of blood thorough the body's vascular system. Identification of compounds found to alter normal cardiac electrocardiogram (ECG) waveforms, thereby signaling propensity for chronotropic, ionotropic, or arrhythmogenic activities, typically stops development. Therefore, early testing of all drug target lead candidates against a panel of critical cardiac ion channel targets (e.g., Kv11.1, Kv7.1, Kir2.1, Nav1.5, and Cav1.2) can add substantial value in prioritizing initial screening hits, assessing lead specificity, supporting real-time Medicinal Chemistry SAR studies on selected leads in the process of identifying development candidates, rescuing programs



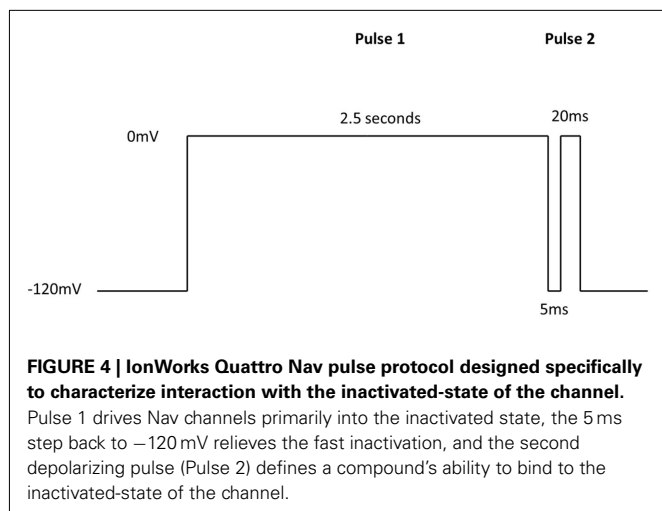


Table 3 | Potency values for reference Nav inhibitors as determined with the 2-pulse protocol.

Reference compound	Predicted IC ₅₀ potency values (μ M)					
	Nav1.2		Nav1.5		Nav1.6	
	P1	P2	P1	P2	P1	P2
Lidocaine	–	8.2	–	4	270	4.7
Tetracaine	18	0.12	19	0.17	9.4	0.08
Lamotrigine	–	8.6	–	8.8	–	5.2
Carbamazepine	–	12	–	5.7	–	4.6
Flecainide	11	3.2	9.1	3	9.7	2.7
Phenytoin	–	5.8	–	6.5	–	7
Riluzole	38	4.7	39	0.77	32	1.4

See **Figure 4** for the protocol.

with potential major cardiac safety liabilities that are usually only revealed at the end of preclinical development, and supporting final stage drug registration efforts. Medicinal chemists find real value in having access to such selectivity data from a cardiac ion channel panel during lead optimization efforts.

The human ventricular cardiac action potential waveform (**Figure 6**, top) is shaped primarily by the activity of six different ion channels; Nav1.5, Cav1.2, Kv4.2/4.3, Kv7.1 (KCNQ1/KCNE1 channel complex), Kv11.1 (hERG; the Kv11.1 protein is thought to underlie the IKr current), and Kir2.1 (Roden et al., 2002). Additional channels (Kv1.5, Kir3.1/3.4) also contribute to the action potential waveform in atria. The summation of action potential waveforms over the entire structure of the heart gives rise to the measurements made in a surface ECG (**Figure 6**, bottom). Human genetics demonstrate that mutations in most of the ventricular ion channels listed above can have profound effects on ECG parameters, such as QTc, QRS, and PR intervals, which thereby signal potential cardiac safety issues (Nattel and Carls-son, 2006; Lu et al., 2008). Some of these waveform alterations may have fatal consequences (e.g., QTc prolongation can lead to *torsades de pointes*, which can lead to ventricular fibrillation,

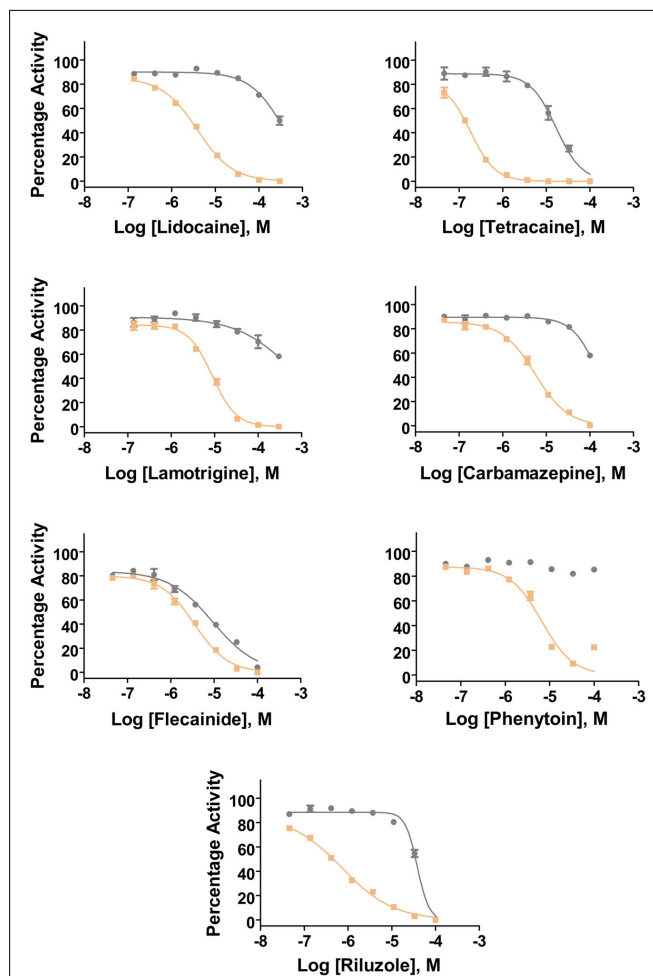
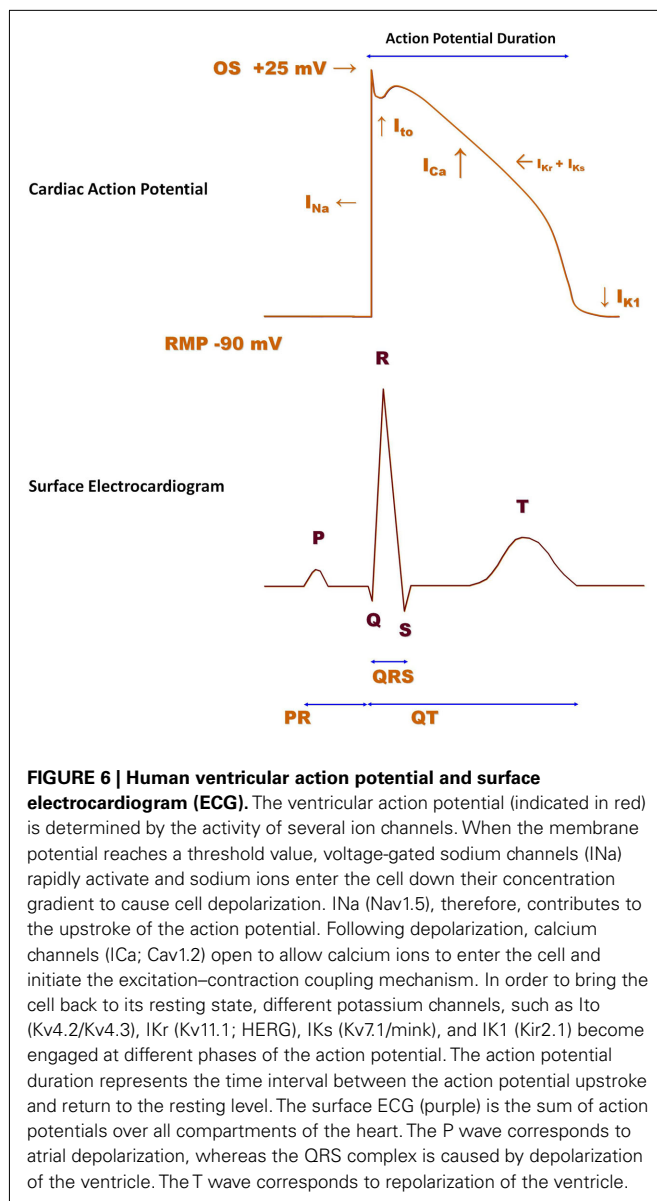


FIGURE 5 | Inhibition of Nav1.5 channels by Nav1.X channel standards using the inactivated-state IonWorks Quattro protocol (Figure 4). Pulse 1 (P1) and Pulse 2 (P2) data were calculated from the maximum inward Nav current amplitudes from each depolarizing pulse and are presented as percentage activation relative to the ratio of Post-Compound/Pre-Compound pulses. Gray symbols and lines are data from P1, and tan symbols and lines are from P2.

which can result in sudden cardiac death). Importantly, reduction of the cardiac rapid delayed rectifier potassium channel caused by loss-of-function mutations of the hERG channel will prolong the ventricular action potential, elongate the QTc interval, and cause a lethal arrhythmia. Gain-of-function mutations in hERG produce the opposite functional effects on action potentials and QTc intervals, but could result in either atrial fibrillation (Hong et al., 2005) or ventricular fibrillation; each condition is potentially lethal. Loss-of-function mutations in the cardiac sodium channel, Nav1.5 (Brugada Syndrome), increases QRS interval, slows conduction and may result in initiation of lethal arrhythmias, while gain-of-function mutations prolong QTc, thereby increasing probability of the same fatal end point. Inhibition of the cardiac slow delayed rectifier potassium channel due to loss-of-function of either the pore-forming subunit, KCNQ1, or of the beta regulatory subunit, KCNE1, prolongs QTc, while activation



of this channel through gain-of-function mutations in KCNQ1 shortens QTc. Both phenotypes increase the probability of sudden cardiac death. The same spectrum, with respect to effects on QTc interval and arrhythmogenic potential, is also produced by loss- or gain-of-function mutations in the cardiac inwardly rectifying potassium channel, Kir2.1. Finally, gain-of-function mutations (Timothy Syndrome) in the L-type calcium channel, Cav1.2, leads to QTc prolongation, ventricular, and atrial arrhythmias, and can be fatal, while loss of Cav1.2 function shortens QTc intervals and increases the possibility of sudden cardiac death, as well. Taken together, data from studies of human genetics demonstrate that the consequences of altering function of the major ion conduction pathways in the heart often result in an increase in mortality. Thus, drugs which affect these targets can similarly elicit fatal events (Roden, 2004; Knollmann and Roden, 2008) and it is critical to identify such liabilities as early as possible in development and take

corrective actions. Indeed as little as 20% block of hERG current by some drugs that do not affect other cardiac currents can produce dangerous prolongation of the ventricular action potential (for a comprehensive analysis of drugs that prolong QT interval, see Redfern et al., 2003). As an example for another cardiac ion channel, we recently profiled a compound from a non-cardiac ion channel program and detected antagonist activity at KCNQ1/minK channels, which could cause delayed ventricular repolarization *in vivo*. At this stage, profiling of different chemical series and multiple representatives of these chemical series can be performed to provide structure activity relationship data that provided a path forward in the project. CardiacProfiler™ functional patch-clamp assays offered by Millipore provide a convenient path to understand potential cardiac liability of potential lead compounds at the most important eight cardiac ion channels and can serve as an important component of integrated cardiac risk management.

DETERMINING ACTIVITY ON hERG, Nav1.5, AND Cav1.2 CHANNELS: LIMITATIONS OF LIGAND-BINDING ASSAYS

Several methodologies have been adopted to routinely probe for interactions of test compounds with three of the major cardiac ion channel liability targets; hERG, Nav1.5, and Cav1.2. Historically, the most commonly used technique involves monitoring the effects of test compounds on binding of selective ligands for each of these channels to identify potential safety risks. Of these targets, hERG is the most important to be evaluated, given that: (1) hERG modulation can produce mortality; (2) as little as 20% hERG block can have an effect on QTc interval; (3) some drugs have been withdrawn from the market or received a cautionary warning because of safety issues (lethal arrhythmias) found to be associated with their activity against hERG (Table 4); (4) regulatory agencies will not approve registration of new drugs without a data package demonstrating a minimal hERG liability; (5) the Kv11.1 channel is the most promiscuous ion channel ever characterized in terms of its molecular pharmacology – it is blocked by a wide variety of molecules, perhaps because the channel's inner cavity located below the selectivity filter can accommodate such a wide range of structures – so there is high probability that some interaction with novel test compounds might be observed (Fermini and Fossa, 2003). Although hERG binding assays have been used in the field for many years, this approach is conceptually flawed when compared with profiling actives directly on hERG function. Many instances of hERG binding by drug candidates have yielded both false positive and false-negative data during testing of novel structural series. False positives can be sorted out by subsequent evaluation in a functional assay. However, false negatives can have disastrous program consequences if the hERG liability is not detected until a potential preclinical candidate is profiled *in vivo* in a CV dog. The time wasted and lack of SAR information on the newly discovered hERG activity usually results in termination of development efforts. The risk of using hERG binding assays as the only support for Medicinal Chemistry is simply not warranted when alternatives exist for employing medium- and high-capacity functional hERG assay formats.

Similarly, it may be misleading to monitor the effect of test compounds on batrachotoxin (BTX) binding to Nav1.2 channels in brain tissue as a surrogate for identifying potential interactions

Table 4 | Drugs withdrawn due to QT-prolongation.

Drug	Date withdrawn	Reference
Terodiline	1991	Shah (2006)
Terfenadine (seldane)	1998	Shah (2006)
Mibefradil (posicor)	1998	Shah (2006)
Sertindole	1998	Shah (2006)
Astemizole (hismanal)	1999	Shah (2006)
Grepafloxacin (raxar)	1999	Shah (2006)
Cisapride (propulsid)	2000	http://www.medscape.com/viewarticle/446682
Droperidol	2001	Shah (2006)
Sparfloxacin (zagam)	2001	Fluoroquinolones and QT-prolongation research continues http://www.infectiousdiseaseneews.com/article/33493.aspx
Levacyclmethadol	2001	Shah (2006)
Dofetilide	2004	Shah (2006)
Thioridazine	2005	Shah (2006)
Quinidine	2006	Olsson (2010)
Halofantrine	?	Lin et al. (2011)
Anzemet (injection form)	2011	Sanofi Aventis (2011)
Pimozide (orap)	?	Lin et al. (2011)
Haloperidol (haldol)	?	Lin et al. (2011)
Erythromycin	?	Lin et al. (2011)
Lidoflazine	?	Oshiro et al. (2010)

with the cardiac sodium channel. Because (1) the BTX site is not coupled to all other drug binding sites on sodium channels (Cestele and Catterall, 2009), (2) the channels under investigation are distinct (Nav1.5 versus Nav1.2), (3) sodium channel subtype-selective inhibitors exist (Williams et al., 2007; Schmalhofer et al., 2008), and (4) electrical environment/biophysical properties can specifically influence Nav1.5 block, testing compounds directly on Nav1.5 function is a much more meaningful approach.

Lastly, monitoring binding of representative ligands for the L-type calcium channel from the dihydropyridine, phenylalkylamine, and benzothiazepine classes to probe for potential Cav1.2 interactions is likewise flawed. Out of the three ligand classes, the diltiazem binding assay is probably the most sensitive means to detect possible channel modulators; however, this assay still yields false positives and negatives. Such findings support use of a functional assay to replace ligand-binding for evaluating potential Cav1.2 interactions.

DEVELOPMENT OF HIGH-THROUGHPUT FUNCTIONAL ASSAYS FOR ION CHANNEL MODULATION

Depending on the required throughput, manual, or automated patch-clamp methods can be used to evaluate compounds individually against each of the six to eight critical ion channels present in human cardiac muscle to accurately reveal any potential liabilities. However, using such techniques to assess large numbers of compounds can be tedious, time-consuming, and costly. The issue of expanding screening capacity against a cardiac panel has recently been addressed by developing a series of robust, high-throughput, cell-based counter-screening assays employing fluorescence-based readouts. For example, assay conditions were developed and optimized to establish a high-capacity 384- and 1536-well functional thallium flux assay for the hERG channel

that recapitulates the molecular pharmacology of a wide range of standard, well-characterized, channel blockers based on their activities measured in electrophysiological protocols (Schmalhofer et al., 2010). These studies were further extended to the analysis of approximately 1000 compounds randomly chosen to represent diverse structural classes from ongoing Medicinal Chemistry programs, where the activities in thallium flux or in a hERG ligand-binding assay were compared with data obtained from electrophysiology determinations made on the same compound deck. Subsequent correlations reveal that the thallium flux inhibitory values correlate more closely with electrophysiology data than do the ligand-binding results for this series of compounds (Figure 7). Thus, use of a well-controlled thallium flux assay is an excellent high-capacity predictive assay of *in vitro* hERG blocking activity. Such an assay has supported Medicinal Chemistry efforts to significantly dial out problematic off-target interactions with Kv11.1, while potency was simultaneously enhanced on the primary target (Garcia and Kaczorowski, unpublished observations).

Robust HTS assays have been developed for Kir2.1, Nav1.5, and Cav1.2 channels, as well. For example, a HEK hKir2.1 thallium flux assay operant in 384- or 1536-well format has been established, validated, and routinely used as a counter-screen in efforts to develop the molecular pharmacology of other inwardly rectifying potassium channel targets (Garcia and Kaczorowski, unpublished observations). It is expected that a similar HTS assay could be configured with the KCNQ1/KCNE1 channel complex as a probe for modulators of the cardiac slow delayed rectifier potassium current. Using either FRET dye pairs or single fluorescence dyes to monitor membrane potential, a routine, robust, and sensitive hNav1.5 HTS assay has been configured that is operant in formats that can support high-density screening with 1536-well plates (Felix et al., 2004). Use of an agonist initiation protocol allows configuration of

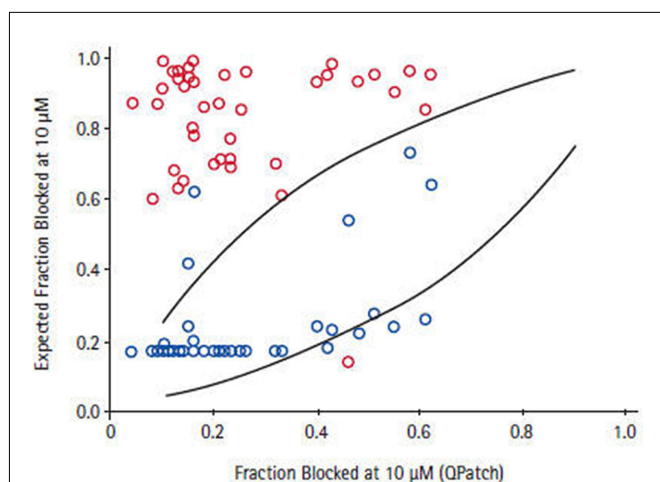


FIGURE 7 | Correlation between QPatch and high-throughput hERG assays. For a subset of compounds for which two high-throughput hERG assays, thallium flux (blue symbol), and ^{35}S -MK499 binding (red symbol) showed >7-fold difference in potency, the estimated fraction of block in QPatch hERG recordings correlates to a greater degree with the thallium flux data Schmalhofer et al. (2010).

assay conditions which yield pharmacologically faithful data when compared to $K_{\text{inactivation}}$ values of literature standards. Finally, a calcium influx assay was developed to detect state-dependent Cav1.2 blockers by stably expressing the Cav1.2 channel subunits ($\alpha 1\text{C}$, $\alpha 2\delta 1$, $\beta 2\text{a}$) along with an inward rectifier potassium channel, Kir2.3, in HEK cells (Dai et al., 2008; Abbadie et al., 2010). Cell membrane potential is controlled by bath external potassium concentrations due to the presence of Kir2.3 and the equilibrium between different Cav1.2 states is shifted by controlling cell

membrane potential. By incubating cells with test compounds at different potassium concentrations, triggering channel opening by depolarizing cells with high potassium, and measuring increases in internal calcium with a calcium-sensitive dye, state-dependent Cav1.2 blockers can be detected in an accurate, facile, and reproducible fashion. Importantly, pharmacological sensitivity data from all these protocols display good correlation with patch-clamp results.

This functional HTS approach to assay cardiac ion channels can reduce the risk of unwanted side effects and eliminate such liability early in lead development. The implementation of high-capacity, robust, facile, accurate, and cost effective, cellular-fluorescence-based ion channel counter-screening methodologies can support data delivery on a weekly basis to support Medicinal Chemistry SAR efforts. Moreover, this strategy can be extended to developing a CNS liability panel including functional assays for Kv1.X, Kv2.X, Kv3.X, Kv4.X, Cav2.X, Cav3.X, and KCNQ2-3 using the same general cell-based approach.

CONCLUSION

Attention to identifying serious off-target activities and supporting Medicinal Chemistry efforts to minimize these activities are as important as the other efforts that go into identifying a potential drug development candidate. Eliminating ancillary pharmacology helps to improve therapeutic index which will be beneficial during clinical trials supporting new drug registration. Often, drug failures in the clinic result from non-mechanism-based side effects which could have been identified and eliminated by proper profiling of lead candidates. Utilizing comprehensive, sensitive, and well-validated profiling assays provides drug developers the ability to ask the crucial questions early and often during the preclinical development process, which should save time, money, and avoid nasty surprises.

REFERENCES

- Abbadie, C., McManus, O. B., Sun, S.-Y., Bugianesi, R. M., Dai, G., Haedo, R. J., Herrington, J. B., Kaczorowski, Smith, M. M., Swensen, A. M., Warren, V. A., Williams, B., Arneric, S. P., Eduljee, C., Snutch, T. P., Tringha, E. W., Jochnowitz, N., Liang, A., MacIntyre, D. E., McGowan, E., Mistry, S., White, V. V., Hoyt, S. B., London, C., Lyons, K. A., Bunting, P. B., Volksdorf, S., and Duffy, J. L. (2010). Analgesic effects of substituted *N*-triazole oxindole (TROX-1), a state-dependent, voltage-gated calcium channel 2 blocker. *J. Pharmacol. Exp. Ther.* 334, 545–555.
- Bean, B. P., Cohen, C. J., and Tsien, R. W. (1983). Lidocaine block of sodium channels. *J. Gen. Physiol.* 81, 613–642.
- Bhave, G., Loneragan, D., Chauder, B. A. II., and Denton, J. S. (2010). Small-molecule modulators of inward rectifier K^+ channels: recent advances and future possibilities. *Future Med. Chem.* 2, 757–774.
- Braam, S. R., Tertoolen, L., van de Stolpe, A., Meyer, T., Passier, R., and Mummery, C. L. (2010). Prediction of drug-induced cardiotoxicity using human embryonic stem cell-derived cardiomyocytes. *Stem Cell Res.* 4, 107–116.
- Burbidge, S. A., Dale, T. J., Powell, A. J., Whitaker, W. R., Xie, X. M., Romanos, M. A., and Clare, J. J. (2002). Molecular cloning, distribution and functional analysis of the Na(V)1.6 voltage-gated sodium channel from human brain. *Brain Res. Mol. Brain Res.* 103, 80–90.
- Cestele, S., and Catterall, W. A. (2009). “Toxins targeting mammalian sodium channels,” in *Animal Toxins: State of the Art; Perspectives in Health and Biotechnology*, ed. M. E de Lima (Belo Horizonte: UFMV), 99–121.
- Clare, J. J., Chen, M. X., Downie, D. L., Trezise, D. J., and Powell, A. J. (2009). Use of planar array electrophysiology for the development of robust ion channel cell lines. *Comb. Chem. High Throughput Screen.* 12, 96–106.
- Coburger, C., Wollmann, J., Krug, M., Baumert, C., Seifert, M., Molnár, J., Lage, H., and Hilgeroth, A. (2010). Novel structure-activity relationships and selectivity profiling of cage dimeric 1,4-dihydropyridines as multidrug resistance (MDR) modulators. *Bioorg. Med. Chem.* 18, 4983–4990.
- Dai, G., Haedo, R. J., Warren, V. A., Ratliff, K. S., Bugianesi, R. M., Rush, A., Williams, M., Herrington, J. J., Smith, M. M., McMann, O. B., and Swensen, A. M. (2008). A high-throughput assay for evaluating state dependence and subtype selectivity of Cav2 calcium channel inhibitors. *Assay Drug Dev. Technol.* 6, 195–212.
- Felix, J. P., Williams, B. S., Priest, B. T., Brochu, R. M., Dick, I. E., Warren, V. A., Yan, L., Slaughter, R. S., Kaczorowski, G. J., Smith, M. M., and Garcia, M. L. (2004). Functional assay of voltage-gated sodium channels using membrane potential-sensitive dyes. *Assay Drug Dev. Technol.* 2, 260–268.
- Fermini, B., and Fossa, A. A. (2003). The impact of drug-induced QT interval prolongation on drug discovery and development. *Nat. Rev. Drug Discov.* 2, 439–447.
- Garcia, M. L., Shen, D.-M., and Kaczorowski, G. J. (2007). High-conductance calcium-activated potassium channels: validated targets for smooth muscle relaxants? *Expert Opin. Ther. Pat.* 17, 1–12.
- Herman, E. H., Knapton, A., Rosen, E., Thompson, K., Rosenzweig, B., Estis, J., Agee, S., Lu, Q. A., Todd, J. A., Lipshultz, S., Hasinoff, B., and Zhang, J. (2011). A multifaceted evaluation of imatinib-induced cardiotoxicity in the rat. *Toxicol. Pathol.* 39, 1091–1106.

- Hibino, H., Inanobe, A., Furutani, K., Murakami, S., Findlay, I., and Kurachi, Y. (2010). Inwardly rectifying potassium channels: their structure, function, and physiological roles. *Physiol. Rev.* 90, 291–366.
- Hondeghem, L. M., and Katzung, B. G. (1977). Time- and voltage-dependent interactions of antiarrhythmic drugs with cardiac sodium channels. *Biochem. Biophys. Acta* 472, 373–398.
- Hong, K., Bjerregaard, P., Gussak, I., and Brugada, R. (2005). Short QT syndrome and atrial fibrillation caused by mutation in KCNH2. *J. Cardiovasc. Electrophysiol.* 16, 394–396.
- Kaczorowski, G. J., McManus, O. B., Priest, B. T., and Garcia, M. L. (2008). Ion channels as drug targets: the next GPCRs. *J. Gen. Physiol.* 131, 399–405.
- Knollmann, B. C., and Roden, D. M. (2008). A genetic framework for improving arrhythmia therapy. *Nature* 451, 929–936.
- Lin, Y. L., Hsiao, C. L., Wu, Y. C., and Kung, M. F. (2011). Electrophysiology, pharmacokinetic, and pharmacodynamic values indicating a higher risk of torsades de pointes. *J. Clin. Pharmacol.* 51, 819–829.
- Lu, H. R., Vlamincx, E., Hermans, A. N., Rohrbacher, J., Van Ammel, K., Towart, R., Pugsley, M., and Gallacher, D. J. (2008). Predicting drug-induced changes in QT interval and arrhythmias: QT-shortening drugs point to gaps in the ICHS7B Guidelines. *Br. J. Pharmacol.* 154, 1427–1438.
- Mathes, C. (2006). QPatch: the past, present and future of automated patch clamp. *Expert Opin. Ther. Targets* 10, 319–327.
- Nattel, S., and Carlsson, L. (2006). Innovative approaches to antiarrhythmic drug therapy. *Nat. Rev.* 5, 1034–1049.
- Olsson, G. (2010). To the editor—market withdrawal of quinidine bisulfate (Kinidin Durules) in 2006. *Heart Rhythm* 7, 864.
- Oshiro, C., Thorn, C. F., Roden, D. M., Klein, T. E., and Altman, R. B. (2010). KCNH2 pharmacogenomics summary. *Pharmacogenet. Genomics* 20, 775–777.
- Pargellis, C., Tong, L., Churchill, L., Cirrilo, P. F., Gilmore, T., Graham, A. G., Grob, P. M., Hickey, E. R., Moss, N. Pav, S., and Regan, J. (2002). Inhibition of p38 MAP kinase by utilizing a novel allosteric binding site. *Nat. Struct. Biol.* 9, 268–272.
- Peng, S., Lacerda, A. E., Kirsch, G. E., Brown, A. M., and Bruening-Wright, A. (2010). The action potential and comparative pharmacology of stem cell-derived human cardiomyocytes. *J. Pharmacol. Toxicol. Methods* 61, 277–286.
- Raeal, K. M., Schmid, C. L., Groer, C. E., and Bohn, L. M. (2011). Functional selectivity at the μ -opioid receptor: implications for understanding opioid analgesia and tolerance. *Pharmacol. Rev.* 63, 1001–1019.
- Redfern, W., Carlsson, L., and Davis, A. S., Lynch, W. G., MacKenzie, I., Palethorpe, S., Siegl, P. K. S., Strang, I., Sullivan, A. T., Wallis, R., Camm, A. J., and Hammond, T. G. (2003). Relationships between preclinical cardiac electrophysiology, clinical QT interval prolongation and torsade de pointes for a broad range of drugs: evidence for a provisional safety margin in drug development. *Cardiovasc. Res.* 58, 32–45.
- Roden, D. M., Balser, J. R., George, A. L., and Anderson, M. E. (2002). Cardiac ion channels. *Annu. Rev. Physiol.* 64, 431.
- Roden, D. M. (2004). Drug-induced prolongation of the QT interval. *N. Engl. J. Med.* 350, 1013–1022.
- Rudolph, U., and Knoflach, F. (2011). Beyond classical benzodiazepines: novel therapeutic potential of GABAA receptor subtypes. *Nat. Rev. Drug Discov.* 10, 685–697.
- Sanofi Aventis. (2011). Available at: <http://online.wsj.com/article/BT-CO-20110215-704422.html>
- Schmalhofer, W., Calhoun, J., Burrows, R., Bailey, T., Kohler, M. G., Weinglass, A. B., Kaczorowski, G. J., Garcia, M. L., Koltzenburg, M., and Priest, B. T. (2008). ProTx-II, a selective inhibitor of NaV1.7 sodium channels, blocks action potential propagation in nociceptors. *Mol. Pharmacol.* 74, 1476–1484.
- Schmalhofer, W. A., Swensen, A., Williams, B. S., Felix, J. P., Haedo, R., Solly, K., Kiss, L., Kaczorowski, G. J., and Garcia, M. L. (2010). A pharmacologically validated, high capacity, functional thallium flux assay for the herg channel. *Assay Drug Dev. Technol.* 8, 714–726.
- Schröder, R. L., Friis, S., Sunesen, M., Mathes, C., and Willumsen, N. J. (2008). Automated patch-clamp technique: increased throughput in functional characterization and in pharmacological screening of small-conductance Ca^{2+} release-activated Ca^{2+} channels. *J. Biomol. Screen* 13, 638–647.
- Shah, R. R. (2006). Can pharmacogenetics help rescue drugs withdrawn from the market? *Pharmacogenomics* 7, 889–908.
- Tollman, P., Morieux, Y., Murphy, J. K., and Schulze, U. (2011). Identifying R&D outliers. *Nat. Rev. Drug Discov.* 10, 653–654.
- Weinglass, A. B., Köhler, M. G., Nketiah, E. O., Liu, J., Schmalhofer, W., Thomas, A., Williams, B., Beers, L., Smith, L., Hafey, M., Bleasby, K., Leone, J., Tang, Y. S., Braun, M., Ujjainwalla, F., McCann, M. E., Kaczorowski, G. J., and Garcia, M. L. (2008a). Madin-Darby canine kidney II cells: a pharmacologically validated system for NPC1L1-mediated cholesterol uptake. *Mol. Pharmacol.* 73, 1072–8473.
- Weinglass, A. B., Kohler, M., Schulte, U., Liu, J., Nketiah, E. O., Thomas, A., Schmalhofer, W., Williams, B., Bildl, W., McMasters, D. R., Dai, K., Beers, L., McCann, M. E., Kaczorowski, G. J., and Garcia, M. L. (2008b). Extracellular loop C of NPC1L1 is important for binding to ezetimibe. *Proc. Natl. Acad. Sci. U.S.A.* 105, 11140–11145.
- Williams, B. S., Felix, J. P., Priest, B. T., Brochu, R. M., Dai, K., Hoyt, S. B., London, C., Tang, Y. S., Duffy, J. L., Parsons, W. H., Kaczorowski, G. J., and Garcia, M. L. (2007). Characterization of a new class of potent inhibitors of the voltage-gated sodium channel NaV1.7. *Biochemistry* 46, 14693–14703.

Conflict of Interest Statement: Gregory J. Kaczorowski and Maria L. Garcia are President and CEO and Vice President, respectively, of Kanalis Consulting, L. L. C. Jacob Bode, Stephen D. Hess, and Umesh A. Patel are employees of the Millipore Corporation.

Received: 16 August 2011; accepted: 19 November 2011; published online: 13 December 2011.

Citation: Kaczorowski GJ, Garcia ML, Bode J, Hess SD and Patel UA (2011) The importance of being profiled: improving drug candidate safety and efficacy using ion channel profiling. *Front. Pharmacol.* 2:78. doi: 10.3389/fphar.2011.00078

This article was submitted to *Frontiers in Pharmacology of Ion Channels and Channelopathies*, a specialty of *Frontiers in Pharmacology*.

Copyright © 2011 Kaczorowski, Garcia, Bode, Hess and Patel. This is an open-access article distributed under the terms of the Creative Commons Attribution Non Commercial License, which permits non-commercial use, distribution, and reproduction in other forums, provided the original authors and source are credited.



Automated electrophysiology makes the pace for cardiac ion channel safety screening

Clemens Möller^{1*} and Harry Witchel²

¹ InViTe Research Institute, Albstadt-Sigmaringen University, Sigmaringen, Germany

² Brighton and Sussex Medical School, Brighton, UK

Edited by:

Ralf Franz Kettenhofen, Axiogenesis AG, Germany

Reviewed by:

Anthony Bahinski, Wyss Institute for Biologically Inspired Engineering at Harvard University, USA

Herbert Himmel, Bayer Pharma AG, Germany

Timm Danker, NMi TT GmbH, Germany

*Correspondence:

Clemens Möller, InViTe Research Institute, Albstadt-Sigmaringen University, 72488 Sigmaringen, Germany.

e-mail:

office@biophysicalconsulting.de

The field of automated patch-clamp electrophysiology has emerged from the tension between the pharmaceutical industry's need for high-throughput compound screening versus its need to be conservative due to regulatory requirements. On the one hand, hERG channel screening was increasingly requested for new chemical entities, as the correlation between blockade of the ion channel coded by hERG and torsades de pointes cardiac arrhythmia gained increasing attention. On the other hand, manual patch-clamping, typically quoted as the "gold-standard" for understanding ion channel function and modulation, was far too slow (and, consequently, too expensive) for keeping pace with the numbers of compounds submitted for hERG channel investigations from pharmaceutical R&D departments. In consequence it became more common for some pharmaceutical companies to outsource safety pharmacological investigations, with a focus on hERG channel interactions. This outsourcing has allowed those pharmaceutical companies to build up operational flexibility and greater independence from internal resources, and allowed them to obtain access to the latest technological developments that emerged in automated patch-clamp electrophysiology – much of which arose in specialized biotech companies. Assays for nearly all major cardiac ion channels are now available by automated patch-clamping using heterologous expression systems, and recently, automated action potential recordings from stem-cell derived cardiomyocytes have been demonstrated. Today, most of the large pharmaceutical companies have acquired automated electrophysiology robots and have established various automated cardiac ion channel safety screening assays on these, in addition to outsourcing parts of their needs for safety screening.

Keywords: hERG, cardiac ion channel, LQT, torsades de pointes, automated patch-clamp, planar patch-clamp, action potential, stem cell

ION CHANNEL ACTIVITY DETERMINES ECG-DETECTABLE CARDIOVASCULAR RISK

The coordinated electrical activity of the heart determines its ability to beat and pump oxygenated blood successfully, and the overall electrical activity is determined by the cellular action potentials (APs) at the level of the cardiomyocyte. Ion channels mediate transmembrane currents controlling the duration of cardiomyocyte APs, which en masse can be detected at the skin via the electrocardiogram (ECG; Sanguinetti and Tristani-Firouzi, 2006; Witchel, 2011). The QT interval, which is measured as an *in vivo* ECG parameter, has been shown to be an imperfect surrogate marker for arrhythmogenic risk (Roden et al., 1996; Witchel et al., 2003; Hondeghem, 2006). If prolonged in the presence of a drug, it may indicate that a compound could cause acquired long QT syndrome (aLQTS), and thus have a cardiac safety liability (Roden, 2004). aLQTS is a potentially fatal drug-induced disorder associated with the risk of sudden cardiac death mediated by the polymorphic ventricular tachyarrhythmia *torsades de pointes* (TdP; Viskin, 1999). In many cases the pathophysiological basis of aLQTS is based on a drug (or combination of drugs) interfering with the activity or production of either one or a range of

ion channels; thus, the testing of drugs for effects on ion channels has become a major concern (and industry) within drug development (Brown, 2008). For drug development programs that must establish cardiac safety profiles to achieve regulatory approval, the QT interval, therefore, remains one of the most important ECG parameters.

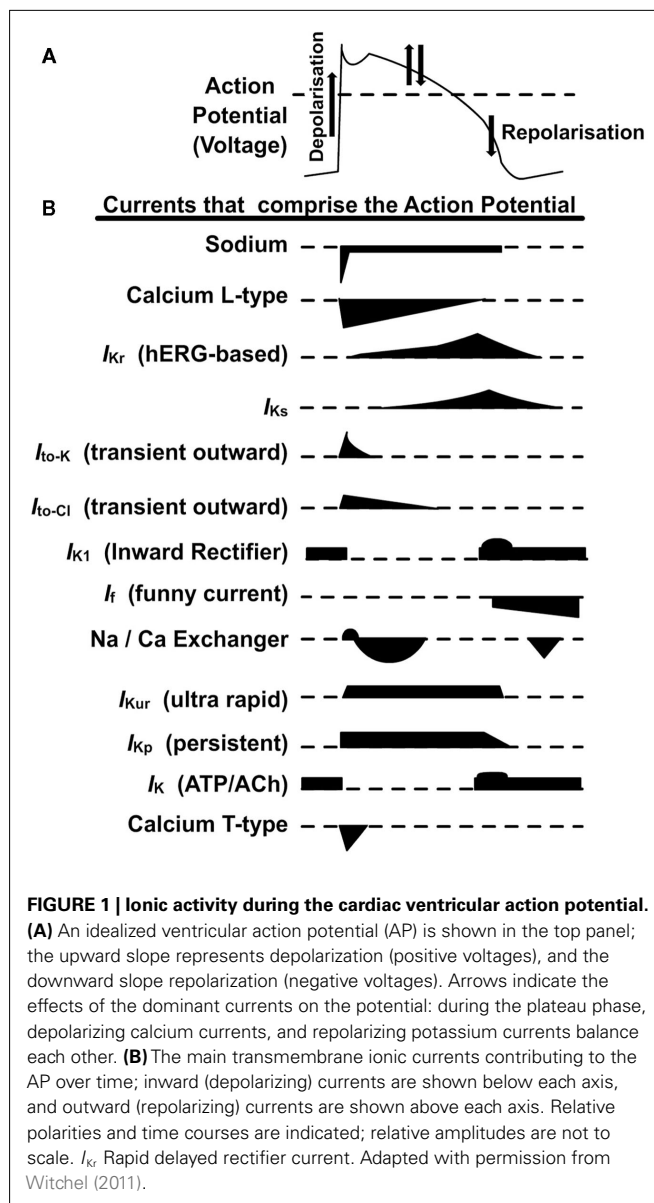
Control of the duration of the cardiac ventricular AP is mediated by the equilibrium between inward and outward currents across the cell membrane (Carmeliet, 1993). Under physiological conditions the AP progresses through the phases of depolarization, plateau phase, and repolarization over the course of 200–300 ms, but in LQTS repolarization is delayed and the AP duration at times will be substantially prolonged. Electrophysiologically, this delay in repolarization implies a deviation from the usual balance of currents across the myocyte membrane responsible for normal repolarization. Thus, prolongation of the AP could theoretically arise from an increase in inward (depolarizing) current, or alternatively, from a decrease in outward (repolarizing) current carried by potassium ions. Both of these conditions have been found to exist as the genetic basis of pathology in various familial LQTS patients (Splawski et al., 2000).

Potassium channels play prominent roles in AP repolarization, as well as during the plateau phase. The rate of net K^+ efflux, and by extension the rate of repolarization, is determined by the density and gating properties of different K^+ channels. K^+ channels mediating an inwardly rectifying current (I_{K1}) are important in maintaining the normal resting potential of ventricular cardiomyocytes, and during the final stage of AP repolarization (Carmeliet, 1993). A rapidly activating and inactivating transient outward current (I_{to}) contributes to early AP repolarization and underlies the initial “notch” before the plateau phase. Of particular relevance to the AP plateau is the delayed rectifier current (I_K) comprised of rapid (I_{Kr}) and slow (I_{Ks}) components mediated by distinct channel subtypes with distinct kinetic properties (Sanguinetti and Jurkiewicz, 1990; Sanguinetti and Keating, 1997). I_K develops gradually during the plateau phase, opposing the inward currents underlying sustained depolarization. As the net balance of current alters, and net outward current exceeds inward current, repolarization occurs. I_K and I_{K1} can be considered to regulate ventricular AP repolarization over the plateau range, and final rapid repolarization phase, respectively (Sanguinetti and Keating, 1997). A schematic showing the ventricular AP and the currents that comprise it are shown in **Figure 1**.

The cellular electrophysiological testing of drugs for cardiac safety tends to involve cardiac potassium channels, the cardiac sodium channel and the L-type calcium channel, because the association of these channels with LQTS is well-established. The protein comprising the pore of I_{Kr} is made from four hERG1a alpha subunits, and when these are expressed heterologously, the channel mediating the resulting transmembrane current is commonly referred to as the hERG channel. The hERG channel is the most commonly tested ion channel for cardiac liability of new drugs. Other ion channels that are relevant to the cardiac AP (**Figure 1**) are also tested commercially, including I_{Ks} (the slow component of the delayed rectifier current in cardiac myocytes), I_{K1} (the inward component), I_{Kur} (the ultra rapid component), I_{Kto} (the transient outward component), and I_f (the “funny current”). Sympathetic influences also affect arrhythmogenic risk, and β -adrenergic effects (using GPCR-screening methods) can thus also be tested for.

The most notorious ion channel associated with an aLQTS liability is the hERG (originally named human Ether-à-go-go related gene, also now known as Kv11.1) potassium (K^+) channel; the reason so many drugs were linked to aLQTS mediated by hERG is presumed to be due to the structure of the channel’s inner cavity, which allows the channel to make promiscuous interactions with many different small molecules (Mitcheson, 2008). Mutations in this alpha subunit were initially shown to be the cause of genetic long QT syndrome, and it was proposed that iatrogenic inhibition of the channel could lead to pathology by failing to protect against calcium-induced early after depolarizations (EADs) that could initiate arrhythmogenic electrical activity (January and Moscucci, 1992; Curran et al., 1995; Sanguinetti et al., 1995; Sanguinetti and Keating, 1997).

For many years the only test of drug-induced channel blockade that was viewed as critical for cardiac safety by drug regulators was for hERG (Committee for Proprietary Medicinal Products, 1997),



despite the fact that an ensemble of currents contributes to the AP (and the ECG). It is generally understood that changing the activity of ion channels on the cell surface of cardiac myocytes can both contribute to arrhythmogenesis and to its amelioration (Bril et al., 1996; ICH, 2005; Hansen et al., 2007), and that although blockade of hERG may increase the substrate for arrhythmogenesis, that concurrent blocking of L-type calcium channels may serve to reduce EADs and the arrhythmogenic substrate (January and Riddle, 1989; Bril et al., 1998; Chouabe et al., 1998). A number of investigators pointed out that extrapolating the net drug-induced effects on a range of channels based on measuring only one type of current can give false picture (Witchel et al., 2003). The pharmaceutical industry is therefore concerned with developing *in vitro* cardiac safety assays that provide an early measure of cardiac safety, integrating more than only the hERG ion channel current (Moeller, 2011).

AUTOMATED PATCH-CLAMP ELECTROPHYSIOLOGY ALLEVIATES A BOTTLENECK IN CARDIAC ION CHANNEL SAFETY SCREENING

AUTOMATED PATCH-CLAMP ELECTROPHYSIOLOGY PROVIDES A DIRECT BIOPHYSICAL READOUT OF ION CHANNEL FUNCTION

The flux of ions through transmembrane channels is accompanied by a charge transfer across the biological membrane. This charge transfer can be measured by biophysical readouts, and the manual patch-clamp technique (Neher and Sakmann, 1976; Hamill et al., 1981) is typically referred to as the “gold-standard” method for achieving this. Attempts to automate and simplify the classical, relatively slow, and technically challenging patch-pipette-based approach unfolded at NeuroSearch in the late 1990s with the development of NeuroPatch, later introduced as Apatchi-1 (Asmild et al., 2003). Subsequently, a few other systems have been developed that automate the classical method of pipette-based patch-clamping; however, none of these appear to have yielded a major revolution in patch-clamp throughput.

The technical realization that cells could form high-resistance (gigaseal) connections to planar glass substrates allowed for the introduction of chip-based systems for automated patch-clamp electrophysiology. This finding, approximately 10 years ago (Fertig et al., 2001, 2002; Sigworth and Klemic, 2002), has allowed scientists to increase the throughput of automated patch-clamping to the next level, and has started a technological revolution that alleviated the major bottleneck of throughput in ion channel patch-clamp research. A couple of biotech startup companies were launched and then contributed to bringing this (or a closely related) new technology to the market [including Nanion Technologies GmbH, Munich; Cytocentrics AG, Rostock; Flyion GmbH, Tübingen; Essen Instruments (now Essen BioScience, Inc.), Cytion SA (Lausanne, acquired by Molecular Devices, LLC); Cellectricon AB (Mölnådal); Sophion A/S (Copenhagen); Fluxion LLC (San Francisco)], and the technology was also a part of development activities in established companies [especially Axon Instruments, now part of Molecular Devices, LLC (MDS)].

THE REQUIREMENT FOR HERG CHANNEL DATA FOSTERED THE DEVELOPMENT OF AUTOMATED PATCH-CLAMP ROBOTS

Around the beginning of this century, awareness for the relevance of a blockade of the cardiac hERG ion channel for the development of drug-induced cardiac arrhythmias arose and was reflected in regulatory guidelines (ICH S7A, ICH S7B). Consequently the pharmaceutical industry was in huge need of hERG channel safety screening data of new drug candidates. A couple of small and medium-sized university spin-offs and biotech companies started to offer this kind of investigations for pharmaceutical companies, by employing different technologies: high-throughput assays (e.g., Fluorescence, binding, or flux assays: these represent an indirect readout, but are relatively cheap and offer a relatively high throughput), or manual patch-clamp assays (with only low compound throughput, and consequently at relatively high costs per data point). Some of these companies presented a showcase for a time-matched introduction of a scientifically sound and highly relevant expert service, which the pharmaceutical industry was

in dire need of, and which in some cases developed into a great commercial success. With increasing demand for hERG channel data, it is not surprising that the hERG ion channel was one of the first channels for which an assay was established on the newly developed automated patch-clamp instruments (Kiss et al., 2003), and in turn the need for high-throughput hERG channel patch-clamp data was a major accelerator in the further advancement of automated patch-clamp robots.

PROTOCOLS FOR AUTOMATED PATCH-CLAMP ASSAYS NEED TO BE CAREFULLY SET UP AND VALIDATED

Patch-clamp robots available today typically employ planar substrates on which cells delivered from suspension can form gigaseals (for an excellent review on automated patch-clamp instruments, see Dunlop et al., 2008). Protocols and details for the investigation of a number of different cell types by automated patch-clamp are given in the excellent paper by Milligan et al. (2009). Since its first application to measuring the hERG channel for safety screening (Kiss et al., 2003), this technique has been well validated for a number of robots. It is now widely applied to reduce the liability of compound series' towards the hERG channel as part of safety pharmacology assessment early during medicinal chemistry compound development (Kutchinsky et al., 2003; Davenport et al., 2010; Riether et al., 2011; Tye et al., 2011). Reported correlations of biophysical channel properties (Figure 2) as well as pharmacological compound properties between automated (planar, chip-based) and manual (pipette-based) patch-clamp investigations are generally excellent (Kutchinsky et al., 2003; Xu et al., 2003; Tao et al., 2004; Bridgland-Taylor et al., 2006; Jones et al., 2009; Davenport et al., 2010; Golden et al., 2011). The reported discrepancies between manual and automated patch-clamping have been well investigated, and a number of reasons for reported discrepancies have been identified. It is important to note that all of these reported discrepancies are not attributed to the technological principle of chip-based patch-clamping. Rather, one or several of the following points have been identified as the major source of potential discrepancies (Mathes, 2006; Ly et al., 2007; Farre et al., 2009; Mo et al., 2009; Davenport et al., 2010; Möller and Slack, 2010) if automated patch-clamp assays are not well validated: (1) Plate material in automated robots: in manual patch-clamping, test solutions are typically prepared in relatively large quantities and are continuously perfused, while in automated robots, microtiter plates with a smaller volume are used, and relatively small volumes of test solutions are added (one or several times) to the patched cells. The unfavorable surface-to-volume ratio in microtiter plates can lead to a potential reduction of compound concentrations in automated patch-clamping, especially if a hydrophobic plate material is employed. This would lead to a shift of IC₅₀ curves to larger nominal compound concentrations. It has therefore become good practice to use glass plates in automated electrophysiology robots, in particular for all aqueous solutions. In this context it is important to also consider the material of the patch-clamp chip. (2) Timing of compound preparation: in manual patch-clamp experiments, it is relatively easy to prepare test solutions directly before the patch-clamp experiment. This time-matched preparation of test solutions can become a challenge in automated experiments, due to the higher throughput, and the corresponding

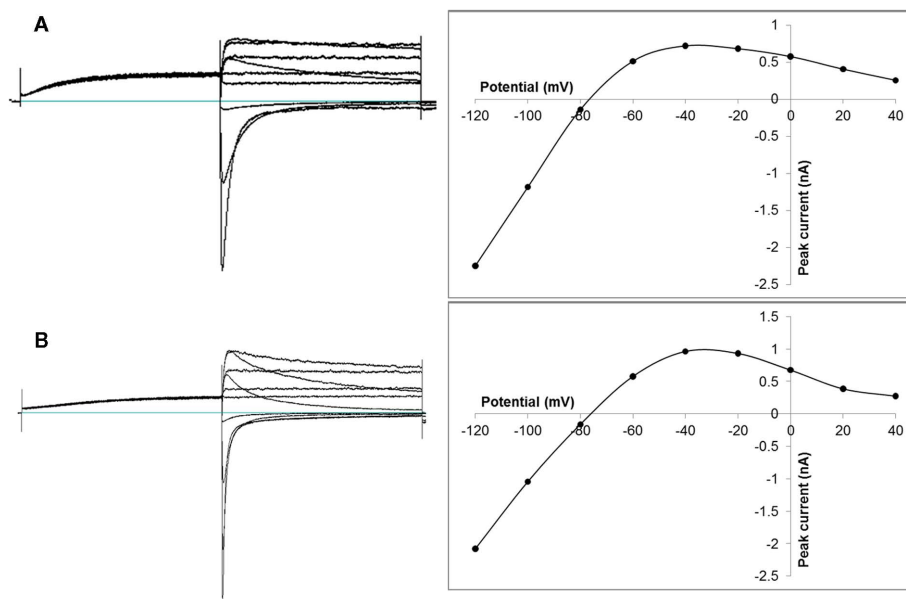


FIGURE 2 | Representative hERG channel whole-cell current-voltage relationships by manual and automated patch-clamp electrophysiology from CHO cells stably expressing the channel. The characteristic

bell-shaped current-voltage relation can be clearly seen during both partial repolarization phases [different current-voltage protocols for recording hERG channel currents have been described in the literature (e.g., Hancox et al., 1998; Su et al., 2004, 2009; Deisemann et al., 2008)]. (A) Recorded by manual patch-clamp using the following stimulation protocol: cells were held

at -80 mV, depolarized to $+20$ mV for 1 s, and repolarized in steps from -120 to $+40$ mV in 10 mV intervals for 1 s each. Stimulation frequency was 0.1 Hz.

(B) Recorded by automated planar patch-clamp on the Patchliner (Nanion Technologies) using the following stimulation protocol: cells were held at -80 mV, depolarized to $+40$ mV for 500 ms, and repolarized in steps from -140 to $+40$ mV in 20 mV intervals for 500 ms each. Stimulation frequency was 0.1 Hz. Adapted with permission from Moeller (2010). For more experimental details see Davenport et al. (2010).

requirement of a larger number of different test solutions. A time lag between the preparation of test solutions and the experiment can however result in a precipitation of compounds in test solution over time, resulting in IC_{50} curves shifted to larger nominal compound concentrations. (3) Buffer compositions: the ionic strength of buffers can shift pharmacological profiles of compounds (e.g., different ions can have an effect on channel gating, and certain compounds interact preferably with certain states of the channel). Consequently, it appears advisable to use buffers that mimic physiological conditions as closely as possible. (4) It is important to note that also manually measured compound IC_{50} values often span a relatively large range between different labs, often owing to different voltage protocols that are applied, or to different experimental temperatures.

Technological developments have further increased the throughput of automated patch-clamp robots during the past years. This has happened on the one hand by increasing parallelization of measurement electrodes, thereby allowing the execution of more patch-clamp recordings in parallel in one experimental run. In a different approach, it has been shown that an increased experiment success rate could be reached if seals with reduced resistance are included into the data evaluation. This notion has allowed reducing the technological demands for controlled seal formation, and has thereby facilitated an even higher rate of parallelization, albeit at potentially reduced data quality owing to the lack of high-resistance gigaseals. Interestingly, the development of ensemble patch-recordings (Finkel et al., 2006), as used

in various of today's instruments, averages out biological variability of individual cells, and thereby increases data consistency and reproducibility even in low-resistance experiments for most cell systems and ion channels (Finkel et al., 2006; Cao et al., 2010).

AUTOMATED PATCH-CLAMP ASSAYS GO BEYOND hERG

Most of the relevant cardiac ion channel safety targets that are discussed above have been shown to be amenable to measurements on different electrophysiological platforms in heterologous expression systems (Wible et al., 2008; Balasubramanian et al., 2009; Farre et al., 2009; Cao et al., 2010; Penniman et al., 2010), and form a standard resource within safety departments of many pharmaceutical companies. In addition, a number of competitive specialized Biotech Contract Research Organizations (CRO) are offering investigations of cardiac (and other) ion channels using well validated automated patch-clamp electrophysiology assays under fee-for-service or alliance contract agreements (e.g., Chantest, OH, USA; Millipore, MA, USA (now part of Merck KGaA); AvivaBioSciences, California; Evotec AG, Hamburg). Thereby these companies are offering an established flexible resource to meet outsourcing requirements of the pharmaceutical and the biotech industry.

It has been described that some compounds are more potent hERG-inhibitors at physiological temperature as compared to room temperature: measurements at the (higher) physiological temperature might affect the IC_{50} s for the many open-state hERG

channel blockers (e.g., methanesulfonanilides), as the faster kinetics at the higher temperature would make more of the channel available for open-state blockade (Zhou et al., 1998). This is especially relevant for safety investigations, where compounds could be incorrectly classified as non-hERG active if they are investigated at room temperature. It has therefore become good practice to perform hERG investigations (especially the relatively late-stage GLP) at (or near) physiological temperature. While the first automated patch-clamp instruments were only capable of operating at room temperature, some manufacturers of automated patch-clamp equipment have responded to this need for automated patch-clamp investigations at (or near) physiological temperature (Farre et al., 2007; Golden et al., 2011).

AUTOMATED PATCH-CLAMPING OF CARDIOMYOCYTES PROVIDES PHYSIOLOGICALLY RELEVANT ACTION POTENTIAL DATA

As discussed above, the cardiac AP is comprised of a well-orchestrated ensemble of individual ion channel currents. Considering only selected ion channels for cardiac risk assessment can therefore give a false picture, as effects of compounds on several channels can potentiate or alleviate a potential arrhythmic effect (Witchel et al., 2003; Fenichel et al., 2004; Moeller, 2011). Patch-clamp recordings in cardiomyocytes have been shown to provide a picture of the effect of compounds on the whole ensemble of cardiac ion channel currents, and to reproduce the effects of selected reference compounds on the AP. With improved protocols to differentiate stem-cells of various sources into a homogeneous cardiomyocyte population, the availability of cardiomyocytes increases, and the suitability of stem-cell derived cardiomyocytes for pharmacological investigations by patch-clamping has been convincingly demonstrated (Harding et al., 2007; Zhang et al., 2009; Kuryshv et al., 2010; Foldes et al., 2011). Recently, stem-cell derived cardiomyocytes from mouse have been applied to planar patch-clamp chips, and the pharmacology of a set of reference compounds was reproduced in AP recordings (Stoelzle et al., 2011). Also, data from human iPS-derived cardiomyocytes were shown (Anson, 2011). This proves the potential of such recordings and certainly represents an extremely interesting and physiologically potentially highly relevant approach. It should however be considered that (automated) AP recordings from myocytes still require a more thorough validation before their sensitivity and the correlation of the data to adult cardiac physiology and pharmacology is better understood. In particular two potential problems with data from stem-cell derived cardiomyocytes need to be considered: (1) Studies have given evidence that iPS and ES derived cardiomyocytes, depending on their age, most likely represent a neonatal state, and thus contain an ion channel population that most likely does not represent the adult one (Binah et al., 2007; Xi et al., 2010). This would certainly also influence the AP response and pharmacology. (2) While stem-cell derived cardiac myocytes certainly represent a more physiological test system than heterologous expression systems, it must be considered that in automated patch-clamp setups the cells reside out of their physiological surrounding, in (more or less) artificial buffer solutions. Also, the cells have lost their cell–cell network contacts, and therefore require an artificial stimulation to activate their AP.

AUTOMATED CARDIAC SAFETY ION CHANNEL PATCH-CLAMP ELECTROPHYSIOLOGY: *QUO VADIS?*

The automated patch-clamp electrophysiology technology has been referred to as an “enabling technology” for ion channel drug discovery and research. Never before has it been practically possible for pharmaceutical companies to screen compounds on the order of tens of thousands against an ion channel target by use of a direct functional readout, and thus avoiding the potential false positives and/or negatives associated to other, more indirect (such as fluorescence assay or binding techniques), high-throughput screening methods. This has allowed drug developers to move cardiac ion channel safety screening earlier into the drug development pipeline, and to mitigate potential cardiac safety liabilities of potent compound series (Davenport et al., 2010; Riether et al., 2011; Tye et al., 2011).

The two currently known instruments with the highest rate of parallelization and the largest throughput are – at the time of writing this manuscript – the SyncroPatch 96 (Nanion Technologies) and the IonWorks Barracuda (MDS). While the SyncroPatch is capable of handling up to 96 parallel high-quality Gigaseal recordings under continuous voltage control (using 96 well plates), the Barracuda can perform 384 parallel recordings – albeit potentially at the price of reduced data quality or limited voltage control, as the Barracuda relies on low-resistance seals and employs the population patch-clamp (PPC) technology (Finkel et al., 2006).

Furthermore, customer suggestions have led to other new developments to the existing automated patch-clamp robots. Recently there have been further improvements of the seal rates and seal stabilities (e.g., by optimizing chip substrates) as well as the addition of more sophisticated automated cell culture preparations on board of some instruments (Mathes et al., 2009). In the future there is likely to be even further increases in throughput, which could be achieved by an additional increase in parallelization.

Other expected development steps concern the biological side, as well as the pharmacological relevance of the data obtained by automated patch-clamping: at the time of writing this manuscript, only a few of the amplifiers from automated patch-clamp instruments are capable of operating in current clamp mode, and thus are able to perform AP recordings from cardiomyocytes, which are of great interest to the safety pharmacology community. Although neither drug-induced prolongation nor triangulation of AP in cardiac myocytes (e.g., Purkinje fibers) are perfect surrogates of risk (Gintant et al., 2001; Martin et al., 2006), if affordable and capable of high-throughput, these measures might become valuable complementary surrogates for QT prolongation (or for the need to provide a warning label) compared to hERG safety margins alone (Gintant, 2011). With improved robust protocols to differentiate stem-cells into cardiomyocytes, and increasing availability of cardiomyocytes from commercial sources, we expect that more comparative and validation data from these cells will be published. This will certainly help the safety pharmacology community to better assess the physiological relevance of automated AP recordings by patch-clamping, and evaluate the implications of these data for safety pharmacology investigations.

REFERENCES

- Anson, B. (2011). Pure human iPS-derived cardiomyocytes; a potential source of cardiomyocytes for automated patch-clamp screening. *Presentation at the Nanion Technologies User Meeting*, Munich.
- Asmild, M., Oswald, N., Krzykowski, K. M., Friis, S., Jacobsen, R. B., Reuter, D., Taboryski, R., Kutchinsky, J., Vestergaard, R. K., Schroder, R. L., Sorensen, C. B., Bech, M., Korsgaard, M. P., and Willumsen, N. J. (2003). Upscaling and automation of electrophysiology: toward high throughput screening in ion channel drug discovery. *Receptors Channels* 9, 49–58.
- Balasubramanian, B., Imredy, J. P., Kim, D., Penniman, J., Lagrutta, A., and Salata, J. J. (2009). Optimization of Ca(v)1.2 screening with an automated planar patch clamp platform. *J. Pharmacol. Toxicol. Methods* 59, 62–72.
- Binah, O., Dolnikov, K., Sadan, O., Shilkut, M., Zeevi-Levin, N., Amit, M., Danon, A., and Itskovitz-Eldor, J. (2007). Functional and developmental properties of human embryonic stem cells-derived cardiomyocytes. *J. Electrocardiol.* 40, S192–S196.
- Bridgland-Taylor, M. H., Hargreaves, A. C., Easter, A., Orme, A., Henthorn, D. C., Ding, M., Davis, A. M., Small, B. G., Heapy, C. G., Abi-Gerges, N., Persson, F., Jacobson, I., Sullivan, M., Albertson, N., Hammond, T. G., Sullivan, E., Valentin, J. P., and Pollard, C. E. (2006). Optimisation and validation of a medium-throughput electrophysiology-based hERG assay using IonWorks HT. *J. Pharmacol. Toxicol. Methods* 54, 189–199.
- Bril, A., Forest, M. C., Cheval, B., and Faivre, J. F. (1998). Combined potassium and calcium channel antagonistic activities as a basis for neutral frequency dependent increase in action potential duration: comparison between BRL-32872 and azimilide. *Cardiovasc. Res.* 37, 130–140.
- Bril, A., Gout, B., Bonhomme, M., Landais, L., Faivre, J. F., Linee, P., Poyser, R. H., and Ruffolo, R. R. J. (1996). Combined potassium and calcium channel blocking activities as a basis for antiarrhythmic efficacy with low proarrhythmic risk: experimental profile of BRL-32872. *J. Pharmacol. Exp. Ther.* 276, 637–646.
- Brown, A. M. (2008). High throughput functional screening of an ion channel library for drug safety and efficacy. *Eur. Biophys. J.* 38, 273–278.
- Cao, X., Lee, Y. T., Holmqvist, M., Lin, Y., Ni, Y., Mikhailov, D., Zhang, H., Hogan, C., Zhou, L., Lu, Q., Digan, M. E., Urban, L., and Erdemli, G. (2010). Cardiac ion channel safety profiling on the IonWorks Quattro automated patch clamp system. *Assay Drug Dev. Technol.* 8, 766–780.
- Carmeliet, E. (1993). Mechanisms and control of repolarization. *Eur. Heart J.* 14, 3–13.
- Chouabe, C., Drici, M. D., Romey, G., Barhanin, J., and Lazdunski, M. (1998). HERG and KvLQT1/IsK, the cardiac K⁺ channels involved in long QT syndromes, are targets for calcium channel blockers. *Mol. Pharmacol.* 54, 695–703.
- Committee for Proprietary Medicinal Products. (1997) “Points to consider: the assessment for the potential for QT prolongation by non-cardiovascular medicinal products,” in *European Agency for the Evaluation of Medicinal Products*, London.
- Curran, M. E., Splawski, I., Timothy, K. W., Vincent, G. M., Green, E. D., and Keating, M. T. (1995). A molecular basis for cardiac arrhythmia: HERG mutations cause long QT syndrome. *Cell* 80, 795–803.
- Davenport, A. J., Moller, C., Heifetz, A., Mazanetz, M. P., Law, R. J., Ebnet, A., and Gemkow, M. J. (2010). Using electrophysiology and in silico three-dimensional modeling to reduce human Ether-a-go-go related gene K(+) channel inhibition in a histamine H₃ receptor antagonist program. *Assay Drug Dev. Technol.* 8, 781–789.
- Deisemann, H., Ahrens, N., Schlobohm, I., Kirchhoff, C., Netzer, R., and Moller, C. (2008). Effects of common antitussive drugs on the hERG potassium channel current. *J. Cardiovasc. Pharmacol.* 52, 494–499.
- Dunlop, J., Bowlby, M., Peri, R., Vasilyev, D., and Arias, R. (2008). High-throughput electrophysiology: an emerging paradigm for ion-channel screening and physiology. *Nat. Rev. Drug Discov.* 7, 358–368.
- Farre, C., Haythornthwaite, A., Haarmann, C., Stoelzle, S., Kreir, M., George, M., Bruggemann, A., and Fertig, N. (2009). Port-a-patch and patchliner: high fidelity electrophysiology for secondary screening and safety pharmacology. *Comb. Chem. High Throughput Screen.* 12, 24–37.
- Farre, C., Stoelzle, S., Haarmann, C., George, M., Bruggemann, A., and Fertig, N. (2007). Automated ion channel screening: patch clamping made easy. *Expert Opin. Ther. Targets* 11, 557–565.
- Fenichel, R. R., Malik, M., Antzelevitch, C., Sanguinetti, M., Roden, D. M., Priori, S. G., Ruskin, J. N., Lipicky, R. J., and Cantilena, L. R. (2004). Drug-induced torsades de pointes and implications for drug development. *J. Cardiovasc. Electrophysiol.* 15, 475–495.
- Fertig, N., Blick, R. H., and Behrends, J. C. (2002). Whole cell patch clamp recording performed on a planar glass chip. *Biophys. J.* 82, 3056–3062.
- Fertig, N., Meyer, C., Blick, R. H., Trautmann, C., and Behrends, J. C. (2001). Microstructured glass chip for ion-channel electrophysiology. *Phys. Rev. E Stat. Nonlin. Soft Matter Phys.* 64, 040901.
- Finkel, A., Wittel, A., Yang, N., Handran, S., Hughes, J., and Constantin, J. (2006). Population patch clamp improves data consistency and success rates in the measurement of ionic currents. *J. Biomol. Screen.* 11, 488–496.
- Foldes, G., Mioulane, M., Wright, J. S., Liu, A. Q., Novak, P., Merkely, B., Gorelik, J., Schneider, M. D., Ali, N. N., and Harding, S. E. (2011). Modulation of human embryonic stem cell-derived cardiomyocyte growth: a testbed for studying human cardiac hypertrophy? *J. Mol. Cell. Cardiol.* 50, 367–376.
- Gintant, G. (2011). An evaluation of hERG current assay performance: translating preclinical safety studies to clinical QT prolongation. *Pharmacol. Ther.* 129, 109–119.
- Gintant, G. A., Limberis, J. T., McDermott, J. S., Wegner, C. D., and Cox, B. F. (2001). The canine Purkinje fiber: an in vitro model system for acquired long QT syndrome and drug-induced arrhythmogenesis. *J. Cardiovasc. Pharmacol.* 37, 607–618.
- Golden, A. P., Li, N., Chen, Q., Lee, T., Nevill, T., Cao, X., Johnson, J., Erdemli, G., Ionescu-Zanetti, C., Urban, L., and Holmqvist, M. (2011). IonFlux: a microfluidic patch clamp system evaluated with human ether-a-go-go related gene channel physiology and pharmacology. *Assay Drug Dev. Technol.* doi: 10.1089/adt.2010.0362. [Epub ahead of print].
- Hamill, O. P., Marty, A., Neher, E., Sakmann, B., and Sigworth, F. J. (1981). Improved patch-clamp techniques for high-resolution current recording from cells and cell-free membrane patches. *Pflugers Arch.* 391, 85–100.
- Hancox, J. C., Levi, A. J., and Witchel, H. J. (1998). Time course and voltage dependence of expressed HERG current compared with native “rapid” delayed rectifier K current during the cardiac ventricular action potential. *Pflugers Arch.* 436, 843–853.
- Hansen, R. S., Olesen, S. P., and Grunnet, M. (2007). Pharmacological activation of rapid delayed rectifier potassium current suppresses bradycardia-induced triggered activity in the isolated guinea pig heart. *J. Pharmacol. Exp. Ther.* 321, 996–1002.
- Harding, S. E., Ali, N. N., Brito-Martins, M., and Gorelik, J. (2007). The human embryonic stem cell-derived cardiomyocyte as a pharmacological model. *Pharmacol. Ther.* 113, 341–353.
- Hondeghem, L. M. (2006). Thorough QT/QTc not so thorough: removes torsadogenic predictors from the T-wave, incriminates safe drugs, and misses probrillatory drugs. *J. Cardiovasc. Electrophysiol.* 17, 337–340.
- ICH. (2005). “The non-clinical evaluation of the potential for delayed ventricular repolarization (QT interval prolongation) by human pharmaceuticals: S7B,” in *Proceedings of the Expert Working Group (Safety) of the International Conference on Harmonisation of Technical Requirements for Registration of Pharmaceuticals for Human Use and the FDA (Food and Drug Administration, USA)*, Rockville, MD.
- January, C. T., and Moscucci, A. (1992). Cellular mechanisms of early afterdepolarizations. *Ann. N. Y. Acad. Sci.* 644, 23–32.
- January, C. T., and Riddle, J. M. (1989). Early afterdepolarizations: mechanism of induction and block. A role for L-type Ca²⁺ current. *Circ. Res.* 64, 977–990.
- Jones, K. A., Garbati, N., Zhang, H., and Large, C. H. (2009). Automated patch clamping using the QPatch. *Methods Mol. Biol.* 565, 209–223.
- Kiss, L., Bennett, P. B., Uebele, V. N., Koblan, K. S., Kane, S. A., Neagle, B., and Schroeder, K. (2003). High throughput ion-channel pharmacology: planar-array-based voltage clamp. *Assay Drug Dev. Technol.* 1, 127–135.
- Kuryshv, Y. A., Bruening-Wright, A., Brown, A. M., and Kirsch, G. E. (2010). Increased cardiac risk in concomitant methadone and diazepam treatment: pharmacodynamic interactions in cardiac ion channels. *J. Cardiovasc. Pharmacol.* 56, 420–430.
- Kutchinsky, J., Friis, S., Asmild, M., Taboryski, R., Pedersen, S., Vestergaard, R. K., Jacobsen, R. B., Krzykowski, K., Schroder, R. L., Ljungstrom, T., Helix, N., Sorensen, C. B., Bech, M., and Willumsen, N. J. (2003). Characterization of potassium channel modulation with QPatch automated patch-clamp technology: system characteristics and performance. *Assay Drug Dev. Technol.* 1, 685–693.

- Ly, J. Q., Shyy, G., and Misner, D. L. (2007). Assessing hERG channel inhibition using PatchXpress. *Clin. Lab. Med.* 27, 201–208.
- Martin, R. L., Su, Z., Limberis, J. T., Palmatier, J. D., Cowart, M. D., Cox, B. F., and Gintant, G. A. (2006). In vitro preclinical cardiac assessment of tolterodine and terodiline: multiple factors predict the clinical experience. *J. Cardiovasc. Pharmacol.* 48, 199–206.
- Mathes, C. (2006). QPatch: the past, present and future of automated patch clamp. *Expert Opin. Ther. Targets* 10, 319–327.
- Mathes, C., Friis, S., Finley, M., and Liu, Y. (2009). QPatch: the missing link between HTS and ion channel drug discovery. *Comb. Chem. High Throughput Screen.* 12, 78–95.
- Milligan, C. J., Li, J., Sukumar, P., Majeed, Y., Dallas, M. L., English, A., Emery, P., Porter, K. E., Smith, A. M., McFadzean, I., Beccano-Kelly, D., Bahnasi, Y., Cheong, A., Naylor, J., Zeng, F., Liu, X., Gamper, N., Jiang, L. H., Pearson, H. A., Peers, C., Robertson, B., and Beech, D. J. (2009). Robotic multiwell planar patch-clamp for native and primary mammalian cells. *Nat. Protoc.* 4, 244–255.
- Mitcheson, J. S. (2008). hERG potassium channels and the structural basis of drug-induced arrhythmias. *Chem. Res. Toxicol.* 21, 1005–1010.
- Mo, Z. L., Faxel, T., Yang, Y. S., Gallavan, R., Messing, D., and Bahinski, A. (2009). Effect of compound plate composition on measurement of hERG current IC(50) using PatchXpress. *J. Pharmacol. Toxicol. Methods* 60, 39–44.
- Moeller, C. (2010). Challenging automated patch-clamping: *quo vadis?* Presentation at the Nanion Technologies User Meeting, Munich.
- Moeller, C. (2011). Keeping the Rhythm: hERG and beyond in Cardiovascular Safety Pharmacology. *Expert Rev. Clin. Pharmacol.* 3, 321–329.
- Moller, C., and Slack, M. (2010). Impact of new technologies for cellular screening along the drug value chain. *Drug Discov. Today* 15, 384–390.
- Neher, E., and Sakmann, B. (1976). Single-channel currents recorded from membrane of denervated frog muscle fibres. *Nature* 260, 799–802.
- Penniman, J. R., Kim, D. C., Salata, J. J., and Imredy, J. P. (2010). Assessing use-dependent inhibition of the cardiac Na(+/-) current (I(Na)) in the PatchXpress automated patch clamp. *J. Pharmacol. Toxicol. Methods* 62, 107–118.
- Riether, D., Wu, L., Cirillo, P. F., Berry, A., Walker, E. R., Ermann, M., Noya-Marino, B., Jenkins, J. E., Albaugh, D., Albrecht, C., Fisher, M., Gemkow, M. J., Grbic, H., Lobbe, S., Moller, C., O'Shea, K., Sauer, A., Shih, D. T., and Thomson, D. S. (2011). 1,4-Diazepane compounds as potent and selective CB2 agonists: optimization of metabolic stability. *Bioorg. Med. Chem. Lett.* 21, 2011–2016.
- Roden, D. M. (2004). Drug-induced prolongation of the QT interval. *N. Engl. J. Med.* 350, 1013–1022.
- Roden, D. M., Lazzara, R., Rosen, M., Schwartz, P. J., Towbin, J., and Vincent, G. M. (1996). Multiple mechanisms in the long-QT syndrome. Current knowledge, gaps, and future directions. The SADS Foundation Task Force on LQTS. *Circulation* 94, 1996–2012.
- Sanguinetti, M. C., Jiang, C., Curran, M. E., and Keating, M. T. (1995). A mechanistic link between an inherited and an acquired cardiac arrhythmia: HERG encodes the IKr potassium channel. *Cell* 81, 299–307.
- Sanguinetti, M. C., and Jurkiewicz, N. K. (1990). Two components of cardiac delayed rectifier K⁺ current. Differential sensitivity to block by class III antiarrhythmic agents. *J. Gen. Physiol.* 96, 195–215.
- Sanguinetti, M. C., and Keating, M. T. (1997). Role of delayed rectifier potassium channels in cardiac repolarization and arrhythmias. *News Physiol. Sci.* 12, 152–157.
- Sanguinetti, M. C., and Tristani-Firouzi, M. (2006). hERG potassium channels and cardiac arrhythmia. *Nature* 440, 463–469.
- Sigworth, F. J., and Klemic, K. G. (2002). Patch clamp on a chip. *Biophys. J.* 82, 2831–2832.
- Splawski, I., Shen, J., Timothy, K. W., Lehmann, M. H., Priori, S., Robinson, J. L., Moss, A. J., Schwartz, P. J., Towbin, J. A., Vincent, G. M., and Keating, M. T. (2000). Spectrum of mutations in long-QT syndrome genes. KVLQT1, HERG, SCN5A, KCNE1, and KCNE2. *Circulation* 102, 1178–1185.
- Stoelzel, S., Haythornthwaite, A., Kettenhofen, R., Kolosov, E., Bohlen, H., George, M., Bruggemann, A., and Fertig, N. (2011). Automated patch clamp on mESC-derived cardiomyocytes for cardiotoxicity prediction. *J. Biomol. Screen.* 16, 910–916.
- Su, Z., Limberis, J., Souers, A., Kym, P., Mikhail, A., Houseman, K., Diaz, G., Liu, X., Martin, R. L., Cox, B. F., and Gintant, G. A. (2009). Electrophysiologic characterization of a novel hERG channel activator. *Biochem. Pharmacol.* 77, 1383–1390.
- Su, Z., Martin, R., Cox, B. F., and Gintant, G. (2004). Mesoridazine: an open-channel blocker of human ether-a-go-go-related gene K⁺ channel. *J. Mol. Cell. Cardiol.* 36, 151–160.
- Tao, H., Santa, A. D., Guia, A., Huang, M., Ligutti, J., Walker, G., Sithipong, K., Chan, F., Guoliang, T., Zozulya, Z., Saya, S., Phimmachack, R., Sie, C., Yuan, J., Wu, L., Xu, J., and Ghatti, A. (2004). Automated tight seal electrophysiology for assessing the potential hERG liability of pharmaceutical compounds. *Assay Drug Dev. Technol.* 2, 497–506.
- Tye, H., Mueller, S. G., Prestle, J., Scheuerer, S., Schindler, M., Nosse, B., Prevost, N., Brown, C. J., Heifetz, A., Moeller, C., Pedret-Dunn, A., and Whittaker, M. (2011). Novel 6,7,8,9-tetrahydro-5H-1,4,7,10a-tetraaza-cyclohepta[f]indene analogues as potent and selective 5-HT(2C) agonists for the treatment of metabolic disorders. *Bioorg. Med. Chem. Lett.* 21, 34–37.
- Viskin, S. (1999). Long QT syndromes and torsade de pointes. *Lancet* 354, 1625–1633.
- Wible, B. A., Kuryshv, Y. A., Smith, S. S., Liu, Z., and Brown, A. M. (2008). An ion channel library for drug discovery and safety screening on automated platforms. *Assay Drug Dev. Technol.* 6, 765–780.
- Witchel, H. J. (2011). Drug-induced hERG Block and Long QT Syndrome. *Cardiovasc. Ther.* 29, 251–259.
- Witchel, H. J., Hancox, J. C., and Nutt, D. J. (2003). Psychotropic drugs, cardiac arrhythmia, and sudden death. *J. Clin. Psychopharmacol.* 23, 58–77.
- Xi, J., Khalil, M., Shishechian, N., Hannes, T., Pfannkuche, K., Liang, H., Fatima, A., Hausteine, M., Suhr, F., Bloch, W., Reppel, M., Saric, T., Wernig, M., Janisch, R., Brockmeier, K., Hescheler, J., and Pillekamp, F. (2010). Comparison of contractile behavior of native murine ventricular tissue and cardiomyocytes derived from embryonic or induced pluripotent stem cells. *FASEB J.* 24, 2739–2751.
- Xu, J., Guia, A., Rothwarf, D., Huang, M., Sithipong, K., Ouang, J., Tao, G., Wang, X., and Wu, L. (2003). A benchmark study with sealchip planar patch-clamp technology. *Assay Drug Dev. Technol.* 1, 675–684.
- Zhang, J., Wilson, G. E., Soerens, A. G., Koonce, C. H., Yu, J., Palecek, S. P., Thomson, J. A., and Kamp, T. J. (2009). Functional cardiomyocytes derived from human induced pluripotent stem cells. *Circ. Res.* 104, e30–e41.
- Zhou, Z., Gong, Q., Ye, B., Fan, Z., Makielski, J. C., Robertson, G. A., and January, C. T. (1998). Properties of hERG channels stably expressed in HEK 293 cells studied at physiological temperature. *Biophys. J.* 74, 230–241.

Conflict of Interest Statement: The authors declare that the research was conducted in the absence of any commercial or financial relationships that could be construed as a potential conflict of interest.

Received: 15 August 2011; paper pending published: 17 September 2011; accepted: 06 November 2011; published online: 23 November 2011.

Citation: Möller C and Witchel H (2011) Automated electrophysiology makes the pace for cardiac ion channel safety screening. *Front. Pharmacol.* 2:73. doi: 10.3389/fphar.2011.00073

This article was submitted to *Frontiers in Pharmacology of Ion Channels and Channelopathies*, a specialty of *Frontiers in Pharmacology*.

Copyright © 2011 Möller and Witchel. This is an open-access article subject to a non-exclusive license between the authors and Frontiers Media SA, which permits use, distribution and reproduction in other forums, provided the original authors and source are credited and other Frontiers conditions are complied with.



Toward a new gold standard for early safety: automated temperature-controlled hERG test on the PatchLiner®

Liudmila Polonchuk *

Non-Clinical Safety, Pharma Research, F. Hoffmann-La Roche Ltd., Basel, Switzerland

Edited by:

Ralf Franz Kettenhofen, Axiogenesis AG, Germany

Reviewed by:

Clemens Möller, Albstadt-Sigmaringen University, Germany
Jean-Marie Chambard, Sanofi, France
Aurore Colomar, Union chimique belge, Belgium

*Correspondence:

Liudmila Polonchuk, Non-Clinical Safety, Pharma Research, F. Hoffmann-La Roche Ltd., Grenzacherstr. 124, Building, 73/R. 103b, CH-4070 Basel, Switzerland.
e-mail: liudmila.polonchuk@roche.com

The Patchliner® temperature-controlled automated patch clamp system was evaluated for testing drug effects on potassium currents through human ether-à-go-go related gene (hERG) channels expressed in Chinese hamster ovary cells at 35–37°C. IC₅₀ values for a set of reference drugs were compared with those obtained using the conventional voltage clamp technique. The results showed good correlation between the data obtained using automated and conventional electrophysiology. Based on these results, the Patchliner® represents an innovative automated electrophysiology platform for conducting the hERG assay that substantially increases throughput and has the advantage of operating at physiological temperature. It allows fast, accurate, and direct assessment of channel function to identify potential proarrhythmic side effects and sets a new standard in ion channel research for drug safety testing.

Keywords: hERG, Patchliner®, automated patch clamp, physiological temperature

INTRODUCTION

The cardiac proarrhythmic liability of new pharmacological entities is a major concern for pharmaceutical companies and regulatory agencies. Remarkably, many if not most compounds exert their arrhythmogenic effects through the same electrophysiological mechanism: blockade of repolarizing currents through human ether-à-go-go related gene (hERG) K⁺ channels located in ventricular myocytes (Sanguinetti and Tristani-Firouzi, 2006). As a result, *in-vitro* hERG assay has been introduced into the drug development process to test the proarrhythmic potential of small molecules (International Conference on Harmonisation, 2005). The assay evaluates the acute effects of new therapeutic agents on hERG channels stably expressed in mammalian cell lines (such as HEK293 and CHO cells). By directly measuring a compound's ability to block hERG K⁺ channels it evaluates the proarrhythmic liability associated with this fairly common arrhythmogenic mechanism.

The gold standard for assessing ion channel functionality is the patch clamp technique. The high-resolution conventional manual method involves a glass micropipette filled with an ionic solution that electrically connects an electrode wire to a small patch of cell membrane. Considerable expertise is needed and throughput is low as only one cell can be recorded at a time. In addition, accurate drug safety assessment requires a highly sensitive temperature-controlled patch clamp since the current kinetics is temperature-dependent and inappropriate experimental temperature may compromise the pharmacological properties of the hERG current (Vandenberg et al., 2006). Thus thorough analysis of hERG liabilities under physiological conditions has only been possible to date for advanced compounds using the conventional manual patch clamp technique. However, the high attrition rate due to cardiovascular adverse effects

indicated a strong need for a high-quality electrophysiological method for early hERG profiling of a larger number of drug candidates.

Fortunately, automation has entered the area of experimental electrophysiology over the past few years. The first automated patch clamp instruments focused on increasing throughput by the parallel formation of high-resistance seals using the planar patch clamp at ambient temperature (reviewed in Möller, 2010). Various companies have recently launched second-generation automated platforms, including the Patchliner® (Nanion Technologies GmbH, Munich, Germany), a fully automated patch clamp system with integrated temperature control. The planar NPC® chip electrode combined with temperature control add-on is designed to control giga-Ohm seal formation at 35–37°C and accurately maintain temperatures over an experiment. By recording from up to eight cells simultaneously at physiological temperature, the Patchliner® claims to substantially increase throughput without compromising data quality.

The objective of the present study was to transfer the hERG assay at physiological temperature to the Patchliner® and evaluate the automated platform for its ability to correctly determine potency and IC₅₀ values for reference compounds including known hERG blockers and negative controls.

MATERIALS AND METHODS

CELL CULTURE

The CHO crelox hERG cell line (ATCC reference Nr. PTA-6812) was generated and validated at Roche (Guthrie et al., 2005). Recombinant hERG K⁺ channels originally cloned from human heart were stably expressed in CHO cells grown in sterile tissue flasks in DMEM/F-12 (1:1) medium (Invitrogen, USA) supplemented with 10% (v/v) heat-inactivated fetal calf serum (FCS)

(Hyclone, USA) and 500 $\mu\text{g/ml}$ gentamycin solution (Gibco, UK) at 35–37°C in 5% CO_2 .

Confluent cell cultures were subcultured every 2–3 days using Accumax (Innovative Cell Technologies Inc., USA). Before electrophysiological experiments, cells were treated with Accumax for 3–5 min at 42°C, harvested, and centrifuged at 1000 rpm for 1 min. The pellet was gently resuspended in the extracellular solution and directly used for electrophysiological recording.

SOLUTIONS

The extracellular solution contained (mM): NaCl 150; KCl 4; CaCl_2 1.2; MgCl_2 1; HEPES 10; pH 7.2–7.6 with NaOH, osmolarity 290–330 mOsm. The internal solution contained (mM): KCl, 50; KF, 60; NaCl, 10; HEPES, 10; EGTA, 20; pH 7.0–7.4 with KOH, osmolarity 260–300 mOsm.

All solutions were filtered through 0.2 μM GP Millipore Express PLUS membrane and stored in aliquots at +2–8°C.

COMPOUNDS

Olanzapine was synthesized by Roche (Basel, Switzerland). Amiodarone, astemizole, bepridil, clemastine, haloperidol, terfenadine, and verapamil were purchased from Sigma (USA), cisapride from Research Diagnostic Inc. (USA), E-4031 from Wako Chemicals (Japan), quinidine from Aldrich Chemicals (USA), D,L-Sotalol from Bristol-Myers-Squibb (USA), amoxicillin, fluoxetine, isradipine, and tamoxifen from USP (USA), glyburide/glibenclamide from Calbiochem (USA), ibuprofen from ICN Biomedicals Inc. (USA), moxifloxacin from APIChem Technologies Co. (China), and erythromycin and captopril from Fluka (Switzerland).

Selection of test concentrations for each compound was done based on the hERG potency data and the solubility in the extracellular solution. Stock solutions of compounds were freshly prepared in DMSO. Test solutions were made such that solvent concentrations were kept constant throughout the experiment (0.1%). Compound solutions were transferred to 4 mL glass vials that were placed in the compound plate holder of the patch clamp system (Figure 1).

AUTOMATED PATCH CLAMP PROCEDURES ON THE PATCHLINER®

On the day of the experiment, an aliquot of the cell suspension in the extracellular solution was placed in the cell hotel (Figure 1). Cells were added to each chip well and attracted to the holes by suction applied by a pressure controller. Once a stable whole-cell configuration was obtained, the experimental protocol was initiated. K^+ currents were measured with a patch-voltage-clamp technique in the whole-cell configuration at 35–37°C using the QuadroEPC-10 amplifier (HEKA Elektronik GmbH, Germany) and associated software (Patch MasterPro). Currents were low-pass filtered using the internal Bessel filter of the EPC-10 and digitized at 50 kHz. Series resistance was typically 2–4 M Ω and compensated 70–80%.

Cells were held at a resting voltage of –80 mV and stimulated by a voltage pattern to activate hERG channels and conduct outward IK_{hERG} current (Figure 2, bottom panel), at a stimulation frequency of 0.1 Hz (6 bpm). The reported current amplitudes represent the maximal peak tail current. After the cells stabilized

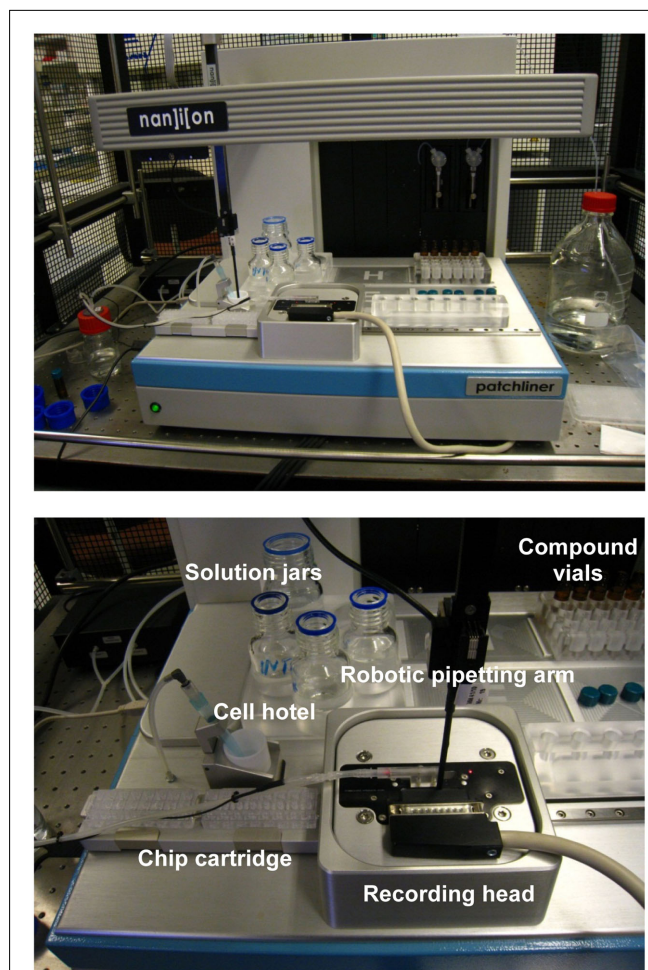


FIGURE 1 | The Patchliner® is shown at the top panel and a closer view of the working area is presented below.

for a few minutes and currents were steady, IK_{hERG} amplitude and kinetics were recorded under control conditions (vehicle control) for 3–5 min. Thereafter, a single test item concentration was added and incubated for at least 3 min until a new steady state current level was reached (see Figures 3 and 4 for the experimental procedure). At the end of the compound incubation, a 1 μM solution of standard IK_{hERG} blocker E-4031 was applied twice to each cell for 1 min to suppress IK_{hERG} entirely.

IK_{hERG} amplitudes were recorded at four to five drug concentrations. The hERG current was measured as the average current from five sweeps collected at the end of vehicle or compound addition. After subtracting current levels from that of full block (i.e., positive control) they were compared to the vehicle control values (taken as 100%) to define fractional blocks. The fractional block values at single concentrations were saved in the appropriate.xls file generated by PatchControlHT software (Nanion). Data were expressed as mean \pm SEM for each drug concentration and were used to determine the concentration–response relationship for the test compounds. The effect of the solvent (DMSO) on the hERG K^+ current was studied in a vehicle control group.

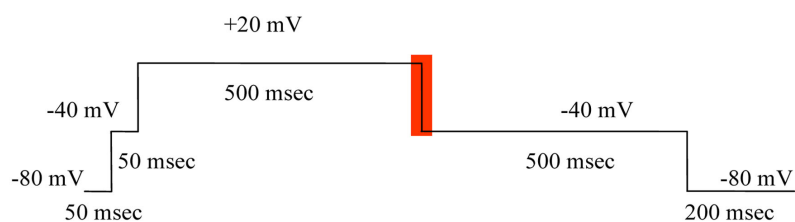
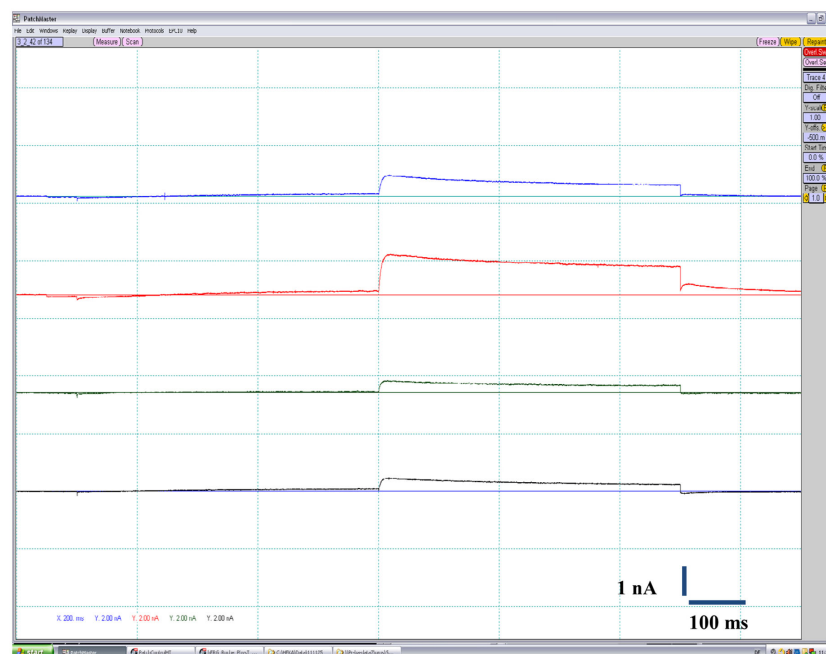


FIGURE 2 | The top panel shows typical outward K^+ current traces elicited in CHO-hERG cells by the voltage pulse depicted at the bottom panel (the area for the peak current measurement is highlighted in red).

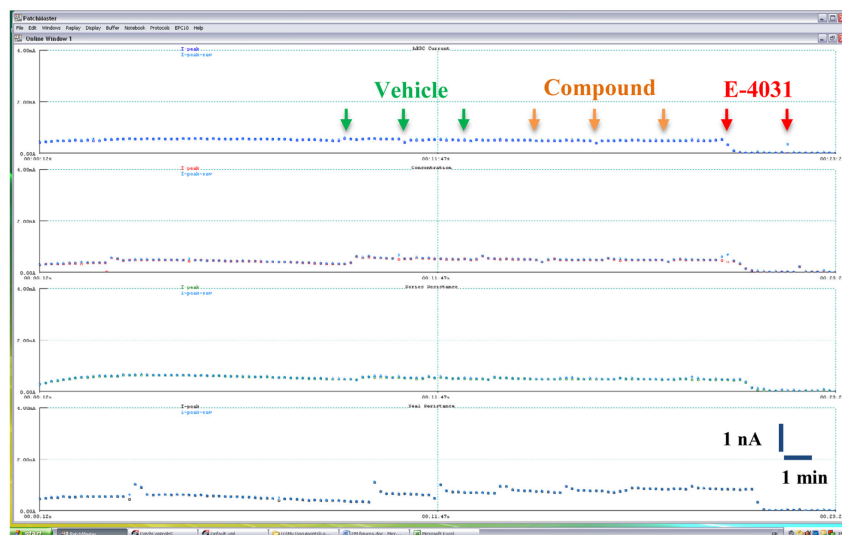


FIGURE 3 | Time course of hERG K^+ current amplitude recorded in a representative vehicle control experiment on the Patchliner®. Cells were

exposed sequentially to vehicle (0.1% v/v DMSO), compound (0.1% v/v DMSO), and 1 μ M E-4031. Arrows indicate compound additions.

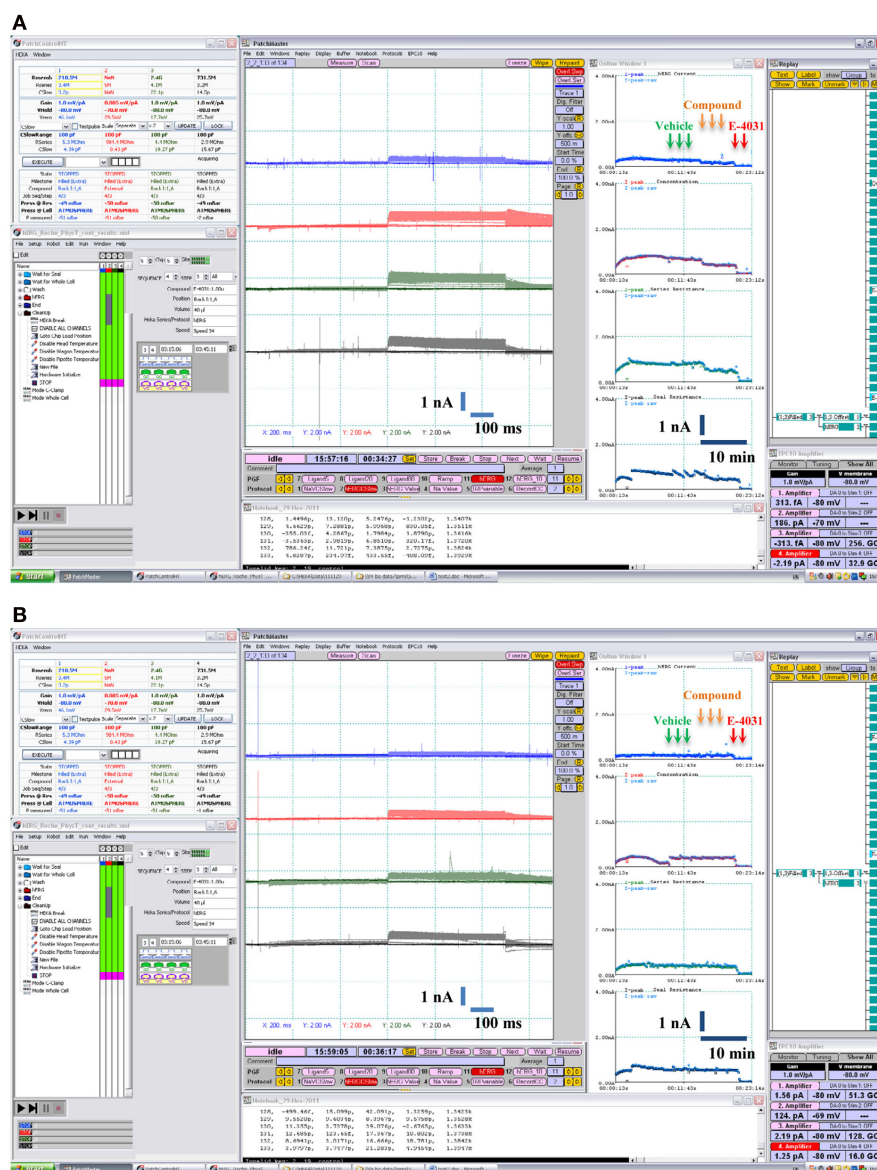


FIGURE 4 | Examples of pharmacological experiments on the Patchliner®. Recordings from four cells were performed in parallel. Original traces are shown in the middle with the on-line analysis window showing the time course of a compound effect on the peak

hERG K⁺ current to the right. Arrows indicate compound additions for vehicle (0.1% v/v DMSO), test item single concentration [0.3 μM quinidine in (A) and 6 μM glibenclamide in (B)] and positive control (1 μM E-4031).

DATA ANALYSIS

If the effect of a drug on the currents was $\leq 20\%$ at the highest concentration tested, IC₅₀ was reported as exceeding the highest concentration value. If the effect of a drug on the currents exceeded 20% at the highest concentration tested, then concentration–response data from three to five cells were normalized to vehicle and 100% blocking levels and the resulting data fitted with the following relationship:

$$I(C) = \frac{100}{1 + (C/IC_{50})^h}$$

where C was the concentration, IC₅₀ the 50% inhibitory concentration, h the Hill coefficient.

Concentration–response curves were fitted by non-linear regression analysis using the XL fit add-in (IDBS Ltd., UK). Data were fitted using a four-parameter logistic model [fit = $(A + (B/(1 + ((x/C)^D))))$], where $A = 0$ and $B = 100$.

Statistical analysis was performed using two-way ANOVA with the Bonferroni post-test, applying the correction for multiple comparison at a significance level of $p < 0.05$ with GraphPad Prism 5 for Windows (GraphPad Software, USA). Correlation between assays [Pearson's coefficient (r)] and values

for statistical significance (p) were determined using GraphPad Prism.

RESULTS

The Patchliner® work station shown in **Figure 1** uses NPC-16 borosilicate glass chips with a microfluidic cartridge for parallel seal formation and patch clamp recordings from up to eight different wells. In this study, a simultaneous recording from four cells exposed to the same compound concentration was performed, resulting in a four-point dose–response curve with one chip cartridge, containing 16 recording wells in total. After priming, cells were captured on the holes of the chip by applying continuous vacuum pressure. After allowing current to stabilize in the whole-cell configuration, a quality control check was performed before starting treatment to ensure that only recordings with true giga-Ohm-seals and a minimum current of 300 pA were included in the experiment. The seal resistance varied between 3.9 ± 2.6 GΩ at the start and 3.2 ± 2.1 GΩ at the end of the experiment while the average current amplitude was 0.9 ± 0.6 nA (mean \pm SD, $n = 297$ cells). Typical examples of the hERG current traces are shown in **Figure 2**. The recordings remained stable for over 30 min at physiological temperature enabling subsequent conduction of compound incubation followed by exposure to the positive control at each concentration with an overall success rate $>70\%$. Cells were maintained in suspension for over 2 h in a cell hotel with no associated decline in patch properties. The sealing quality was very high with the giga-Ohm-seal formation and the whole-cell transition rates almost reaching 100% on the Patchliner®. On average, three out of four cells maintained giga-Ohm-seals and stable currents until the end of the experiments.

Vehicle effect (0.1% v/v DMSO) on the hERG current was studied in time-matched vehicle control groups (**Figure 3**). These control measurements were performed once a week during the validation period. The largest reduction in the outward K⁺ current magnitude (mean \pm SEM) produced by the subsequent application of a vehicle alone to the CHO cells expressing recombinant hERG K⁺ channels was $6 \pm 1\%$ (**Table 1**). This indicates that exposure to solvent may produce only a slight significant effect on the current with time. Therefore, the relative current values were corrected appropriately to the mean vehicle effect at each test item concentration as follows:

$$I_{\text{corrected}} (\%) = \frac{I_{\text{test}}}{\text{mean} I_{\text{vehicle}}} \times 100$$

where I was the relative current amplitude.

To validate the utility of the Patchliner® for the hERG assay, the actions of reference drugs on the hERG current were examined at physiological temperature. A set of 21 compounds including known hERG blockers and negative controls was evaluated. Examples of pharmacological experiments on the Patchliner® are shown in **Figure 4**. Obtained IC₅₀ values (**Table 2**) were plotted against those obtained using the conventional voltage clamp technique. Manual patch clamp data for reference drugs were either generated in-house using the CHO–hERG cells and identical experimental conditions (solutions and voltage step protocol) or taken from published literature. Literature hERGIC₅₀ values were carefully selected to match such key experimental parameters as temperature, expression system, and voltage protocol.

Table 1 | Effects of 0.1% (v/v) DMSO on the hERG K⁺ current.

	hERG current (% of control)			
	Mean	SD	N	p
30 min	98	7	17	>0.05
60 min	97	6	19	>0.05
90 min	94	5	19	<0.001
120 min	94	6	14	<0.001

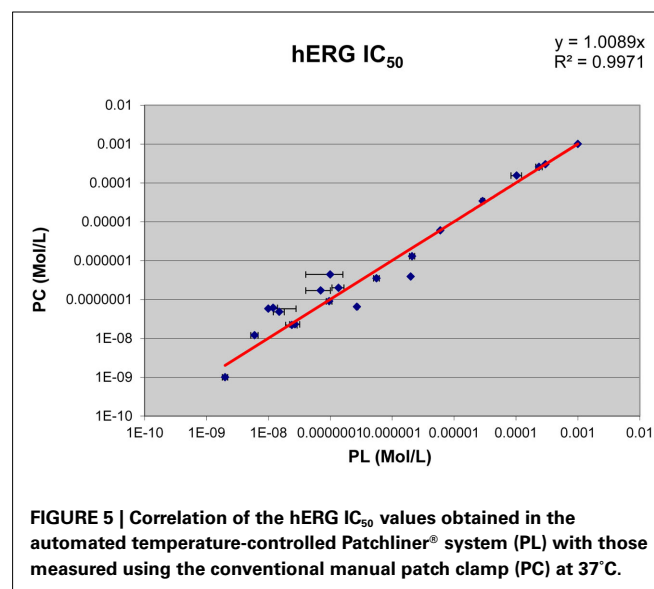


FIGURE 5 | Correlation of the hERG IC₅₀ values obtained in the automated temperature-controlled Patchliner® system (PL) with those measured using the conventional manual patch clamp (PC) at 37°C.

The hERG potencies of all reference drugs were correctly identified. Amiodarone, astemizole, cisapride, clemastine, E-4031, and terfenadine were by far the strongest hERG inhibitors of the compounds tested, with IC₅₀ values in the low and mid-nanomolar range. Some drugs, such as olanzapine, moxifloxacin, sotalol, tamoxifen, and verapamil, showed an intermediate effect on the hERG current. Captopril, ibuprofen, and glibenclamide did not affect the hERG current up to the highest concentration tested. Comparison of the results showed statistically significant correlation ($r = 0.9989$, $p < 0.0001$) between the data obtained at physiological temperature on the Patchliner® and those using the conventional patch clamp rig at the same temperature (**Figure 5**).

DISCUSSION

The hERG test has become the routine *in vitro* approach for assessing the cardiac safety of new drugs in early development. Since some compounds exhibit temperature-dependent potency shifts (Yao et al., 2005), performing experiments at physiological temperature improves the relevance of pharmacological data and ensures more accurate cardiac risk assessment *in vivo*. Until recently, the manual patch clamp was the only technique for conducting temperature-controlled electrophysiological measurements. However, its low throughput hampered functional early profiling of large compound series for proper clinical candidate selection. The availability of a predictive cost–effective hERG assay based on efficient high-resolution technology is thus of major importance

Table 2 | Effects of reference drugs on the hERG K⁺ current.

Compound	Test conc. PL (μM)	hERGIC ₅₀ PL (μM) Mean ± SE	hERG IC ₅₀ PC (μM)
Amiodarone	0.01–0.03–0.1–0.3	0.17 ± 0.03	0.070 (Ridley et al., 2004)
Astemizole	0.001–0.003–0.01–0.03	0.012 ± 0.0008	0.006
Bepidil	0.01–0.03–0.1–0.3	0.065 ± 0.012	0.27
Captopril	1–10–100–1000	>1000	>1000
Cisapride	0.001–0.01–0.1–1	0.022 ± 0.005	0.024 (Walker et al., 1999)
Clemastine	0.001–0.01–0.1–1	0.006 ± 0.002	0.012 (Ridley et al., 2006)
Dofetilide	0.001–0.01–0.1–1	0.058 ± 0.018	0.01 (Du et al., 2011)
E-4031	0.0003–0.003–0.03–0.3	0.001 ± 0.0002	0.002
Erythromycin	1–10–100–1000	257 ± 28	236
Fluoxetine	0.1–0.3–1–3	0.39 ± 0.05	2.0
Glibenclamide	0.2–0.6–2–6	>6	>6
Haloperidol	0.001–0.01–0.1–1	0.023 ± 0.005	0.027
Ibuprofen	0.3–3–30–300	>300	>300
Moxifloxacin	0.3–3–30–300	34 ± 2	29 (Alexandrou et al., 2006)
Olanzapine	0.3–1–3–10	1.3 ± 0.2	2.1
Quinidine	0.1–0.3–1–3	0.35 ± 0.06	0.6
d,l-Sotalol	0.3–3–30–300	103 ± 20	154
Tamoxifen	0.1–0.3–1–3	0.44 ± 0.06	0.1 (Yuill et al., 2004)
Terfenadine	0.003–0.01–0.03–0.3	0.05 ± 0.01	0.015
Thioridazine	0.03–0.1–0.3–1–3	0.09 ± 0.003	0.096 (Kirsch et al., 2004)
Verapamil	0.01–0.003–0.1–0.3	0.2 ± 0.03	0.136 (Kirsch et al., 2004)

for the pharmaceutical industry. A recent publication by Golden et al. (2011) described a first attempt to evaluate the hERG channel physiology at 37°C using an automated sub-giga-Ohm planar patch clamp IonFlux system from Fluxion with a satisfactory outcome. The present study aimed to evaluate the Nanion Patchliner®, a novel automated electrophysiological workstation, for hERG testing under physiological conditions.

The Patchliner® has been successfully introduced as a high-quality medium throughput automated planar patch clamp platform for ion channel research in drug discovery and safety (review in Farre et al., 2009). A unique feature is its ability to conduct stable recordings at different temperatures in the 22–60°C range. The results of the present study showed that the Patchliner® gives high-quality patch clamp recordings in CHO-hERG cells, with a high success rate of giga-Ohm-seals lasting up to an hour at 37°C. Such performance makes the system a powerful tool for studying hERG channel pharmacology at physiological temperature.

In this work, a systematic comparison of diverse panel of reference drugs spanning a broad hERG potency range was performed to validate the Patchliner® for temperature-controlled hERG assay. The obtained IC₅₀s values were compared with their manual patch clamp counterparts. The main finding was that the potency data generated on the Patchliner® matched those obtained by the conventional method (Pearson $r = 0.9989$, $p < 0.0001$). It is important to note that among the drugs tested, the inhibitory effects of D,L-sotalol and erythromycin (Kirsch et al., 2004) were correctly identified at 37°C. The Patchliner® system allowed fast and accurate electrophysiological characterization of ion channels, e.g., for determining the IC₅₀ values of ion channel blockers.

In addition to the standard test, the Patchliner® could be a useful tool for studying temperature-dependent potency shifts and new mechanisms of compound action, e.g., the kinetics of recovery after full inhibition of the hERG current that may provide valuable guidance for drug candidate identification (Swinney, 2009). An additional advantage of the system is that experiments can be preprogrammed and executed in a stand-alone mode. Thus the results of the present study indicate that the Patchliner® can be successfully used to produce high-quality data similar to those obtained by means of the current gold standard, the manual patch clamp. The system is unique in combining the features of high-quality patch clamp recordings with increased physiological relevance of the collected data, resulting in the enhanced safety profiling of new chemical entities.

CONCLUSION

The Patchliner® workstation provides stable currents and high-quality giga-Ohm-seal recordings at 37°C. Based on the validation results, this automated electrophysiology workstation can be used for conducting an advanced hERG assay for new compounds at physiological temperature and may eventually become a new gold standard for ion channel research in safety pharmacology.

ACKNOWLEDGMENTS

The author would like to thank the Nanion Technologies GmbH team, especially Drs. David Guinot and Alison Haythornthwaite, for their help. I am also grateful to Drs. Silvio Albertini, Claudia McGinnis, Susanne Mohr, and Thomas Weiser from Roche Non-Clinical Safety for supporting the acquisition and validation of the system, and to Fabian Häusermann for technical assistance.

REFERENCES

- Alexandrou, A., Duncan, R., Sullivan, A., Hancox, J., Leishman, D., Witchel, H., and Leaney, J. (2006). Mechanism of hERG K⁺ channel blockade by the fluoroquinolone antibiotic moxifloxacin. *Br. J. Pharmacol.* 147, 905–916.
- Du, C. Y., El Harchi, A., Zhang, Y. H., Orchard, C. H., and Hancox, J. C. (2011). Pharmacological inhibition of the HERG potassium channel is modulated by extracellular but not intracellular acidosis. *J. Cardiovasc. Electrophysiol.* 22, 1163–1670.
- Farre, C., Haythornthwaite, A., Haarmann, C., Stoelzle, S., Kreir, M., George, M., Brüggemann, A., and Fertig, N. (2009). Port-a-patch and Patchliner: high fidelity electrophysiology for secondary screening and safety pharmacology. *Comb. Chem. High Throughput Screen.* 12, 24–37.
- Golden, A. P., Li, N., Chen, Q., Lee, T., Nevill, T., Cao, X., Johnson, J., Erdemli, G., Ionescu-Zanetti, C., Urban, L., and Holmqvist, M. (2011). IonFlux: a microfluidic patch clamp system evaluated with human ether-à-go-go related gene channel physiology and pharmacology. *Assay Drug Dev. Technol.* 9, 608–619.
- Guthrie, H., Livingston, F. S., Gubler, U., and Garippa, R. (2005). A place for high-throughput electrophysiology in cardiac safety: screening hERG cell lines and novel compounds with the ion works HTTM system. *J. Biomol. Screen.* 10, 832–840.
- International Conference on Harmonisation. (2005). ICH S7B: the non-clinical evaluation of the potential for delayed ventricular repolarization (QT interval prolongation) by human pharmaceuticals. CHMP/ICH/423/02. *Fed. Regist.* 70, 61133–61134.
- Kirsch, G. E., Trepakova, E. S., Brimacombe, J. C., Sidach, S. S., Erickson, H. D., Kochan, M. C., Shyja, L. M., Lacerda, A. E., and Brown, A. M. (2004). Variability in the measurement of hERG potassium channel inhibition: effects of temperature and stimulus pattern. *J. Pharmacol. Toxicol. Methods* 50, 93–101.
- Möller, C. (2010). Impact of new technologies for cellular screening along the drug value chain. *Drug Discov. Today* 15, 384–390.
- Ridley, J., Milnes, J., Hancox, J., and Witchel, H. (2006). Clemastine, a conventional antihistamine, is a high potency inhibitor of the HERG K⁺ channel. *J. Mol. Cell Cardiol.* 40, 107–118.
- Ridley, J., Milnes, J., Witchel, H., and Hancox, J. (2004). High affinity HERG K⁺ channel blockade by the antiarrhythmic agent dronedarone: resistance to mutations of the S6 residues Y652 and F656. *Biochem. Biophys. Res. Commun.* 325, 883–891.
- Sanguinetti, M. C., and Tristani-Firouzi, M. (2006). hERG potassium channels and cardiac arrhythmia. *Nature* 440, 463–469.
- Swinney, D. C. (2009). The role of binding kinetics in therapeutically useful drug action. *Curr. Opin. Drug Discov. Devel.* 12, 31–39.
- Vandenberg, J. I., Varghese, A., Lu, Y., Bursill, J. A., Mahaut-Smith, M. P., and Huang, C. L. (2006). Temperature dependence of ether-a-go-go-related gene K⁺ currents. *Am. J. Physiol. Cell Physiol.* 291, C165–C175.
- Walker, B., Singleton, C., Bursill, J., Wyse, K., Valenzuela, S., Qiu, M., Breit, S., and Campbell, T. (1999). Inhibition of the human ether-a-go-go-related gene (HERG) potassium channel by cisapride: affinity for open and inactivated states. *Br. J. Pharmacol.* 128, 444–450.
- Yao, J. A., Du, X., Lu, D., Daharsh, E., and Atterson, P. (2005). Estimation of potency of hERG channel blockers: impact of voltage protocol and temperature. *J. Pharmacol. Toxicol. Methods* 52, 146–153.
- Yuill, K. H., Borg, J. J., Ridley, J. M., Milnes, J. T., Witchel, H. J., Paul, A. A., Kozłowski, R. Z., and Hancox, J. C. (2004). Potent inhibition of human cardiac potassium (HERG) channels by the anti-estrogen agent clomiphene-without QT interval prolongation. *Biochem. Biophys. Res. Commun.* 318, 556–561.

Conflict of Interest Statement: The author declares that the research was conducted in the absence of any commercial or financial relationships that could be construed as a potential conflict of interest.

Received: 16 August 2011; accepted: 06 January 2012; published online: 26 January 2012.

Citation: Polonchuk L (2012) Toward a new gold standard for early safety: automated temperature-controlled hERG test on the PatchLiner®. *Front. Pharmacol.* 3:3. doi: 10.3389/fphar.2012.00003

This article was submitted to *Frontiers in Pharmacology of Ion Channels and Channelopathies*, a specialty of *Frontiers in Pharmacology*.

Copyright © 2012 Polonchuk. This is an open-access article distributed under the terms of the Creative Commons Attribution Non Commercial License, which permits non-commercial use, distribution, and reproduction in other forums, provided the original authors and source are credited.



Screening action potentials: the power of light

Lars Kaestner^{1,2*} and Peter Lipp^{1,2}

¹ Institute for Molecular Cell Biology, School of Medicine, Saarland University, Homburg/Saar, Germany

² Research Center for Molecular Imaging and Screening, Saarland University, Homburg/Saar, Germany

Edited by:

Ralf Franz Kettenhofen, Axiogenesis AG, Germany

Reviewed by:

Erik Renström, Lund University, Sweden

William A. Coetzee, NYU School of Medicine, USA

*Correspondence:

Lars Kaestner, Institute for Molecular Cell Biology, School of Medicine, Building 61, 66421 Homburg/Saar, Germany.
e-mail: lars_kaestner@me.com

Action potentials reflect the concerted activity of all electrogenic constituents in the plasma membrane during the excitation of a cell. Therefore, the action potential is an integrated read out and a promising parameter to detect electrophysiological failures or modifications thereof in diagnosis as well as in drug screens. Cellular action potentials can be recorded by optical approaches. To fulfill the pre-requirements to scale up for, e.g., pharmacological screens the following preparatory work has to be provided: (i) model cells under investigation need to represent target cells in the best possible manner; (ii) optical sensors that can be either small molecule dyes or genetically encoded potential probes need to provide a reliable read out with minimal interaction with the naive behavior of the cells and (iii) devices need to be capable to stimulate the cells, read out the signals with the appropriate speed as well as provide the capacity for a sufficient throughput. Here we discuss several scenarios for all three categories in the field of cardiac physiology and pharmacology and provide a perspective to use the power of light in screening cardiac action potentials.

Keywords: cardiac action potentials, membrane potential dyes, genetically encoded membrane potential sensors, human cardiac myocytes, optical screens

INTRODUCTION

Pharmacological screening of ion channels is traditionally performed by the patch-clamp technique, related tools, and their automated incarnations or indirect fluorescence as well as luminescence based end-point measurements. There are good reasons why the patch-clamp technique is the gold standard in investigating ion channels, such as the possibility to isolate specific currents or to characterize single channels. However, there are scientific questions, pharmacological approaches, or medical requirements, when the concert of electrogenic membrane transport entities are of particular interest. Such a situation is, e.g., the measurement of action potentials for cardiac safety issues. The action potential duration can be regarded as a cellular equivalent of the QT-Interval in electrocardiograms (Arrigoni and Crivori, 2007). Since the investigation of action potential considers all electrogenic elements and is thus not limited to a single entity, e.g., hERG channels, the screening of action potentials bears a conceptional advantage. Action potentials can be measured optically for almost four decades (Salzberg et al., 1973). Beside the measurement of action potentials in isolated primary cells, optical methods can follow cellular action potentials and their interplay in tissue slices and entire organs (e.g., Jin et al., 2002; Lee et al., 2011). Here we describe recent advances and promising perspectives in screening cardiac action potentials.

CELLULAR SYSTEMS

When it comes to cellular systems for cardiac safety screens we find an inherent conflict; on one hand cells should be as close as possible to human situation and on the other hand simplicity of operation. Since optical approaches operate contact free, they bear the potential to screen even very fragile cells like human

atrial myocytes as depicted in **Figure 1A**. Human cardiomyocytes, either atrial myocytes from appendages after surgery involving heart-lung machines (Kaestner and Lipp, 2007) or ventricular myocytes taken from biopsies, facilitate screening drugs for personalized medication. However, for pharmacological safety screens one would need to switch to animal models: for adult ventricular myocytes we recently described a reliable isolation procedure (Kaestner et al., 2009) as well as optimized culture conditions (Viero et al., 2008; Hammer et al., 2010). Furthermore we compared neonatal and adult cardiomyocytes in a basic pharmacological profiling (Tian et al., 2011), showing that neonatal cells do not reflect the adult situation at all. The present guidelines of FDA and EMEA for cardiac safety screens (Food and Drug Administration, HHS, 2005) explicitly exclude rodents for such investigations because adult animals almost completely lack hERG expression. However, neonatal cardiomyocytes express hERG (Kaestner et al., 2011a; Tian et al., 2011) and therefore the guidelines may need a revision. Furthermore, it might have to be considered that during aging and many cardiac diseases re-expression of fetal and/or neonatal genes might change this situation. Very promising are the ongoing developments and refinements to differentiate cardiac myocytes from embryonic or pluripotent stem cells (e.g., Kettenhofen and Bohlen, 2008) and (Moretti et al., 2010), respectively. The years to come will show to what extent stem cell derived cardiomyocytes will enter cardiac safety screens – the potential is enormous.

OPTICAL SENSORS

Since action potentials in cardiomyocytes are convolved by cellular contraction artifacts optical read out need to be performed in a quantitative manner, e.g., based on ratiometric or fluorescence

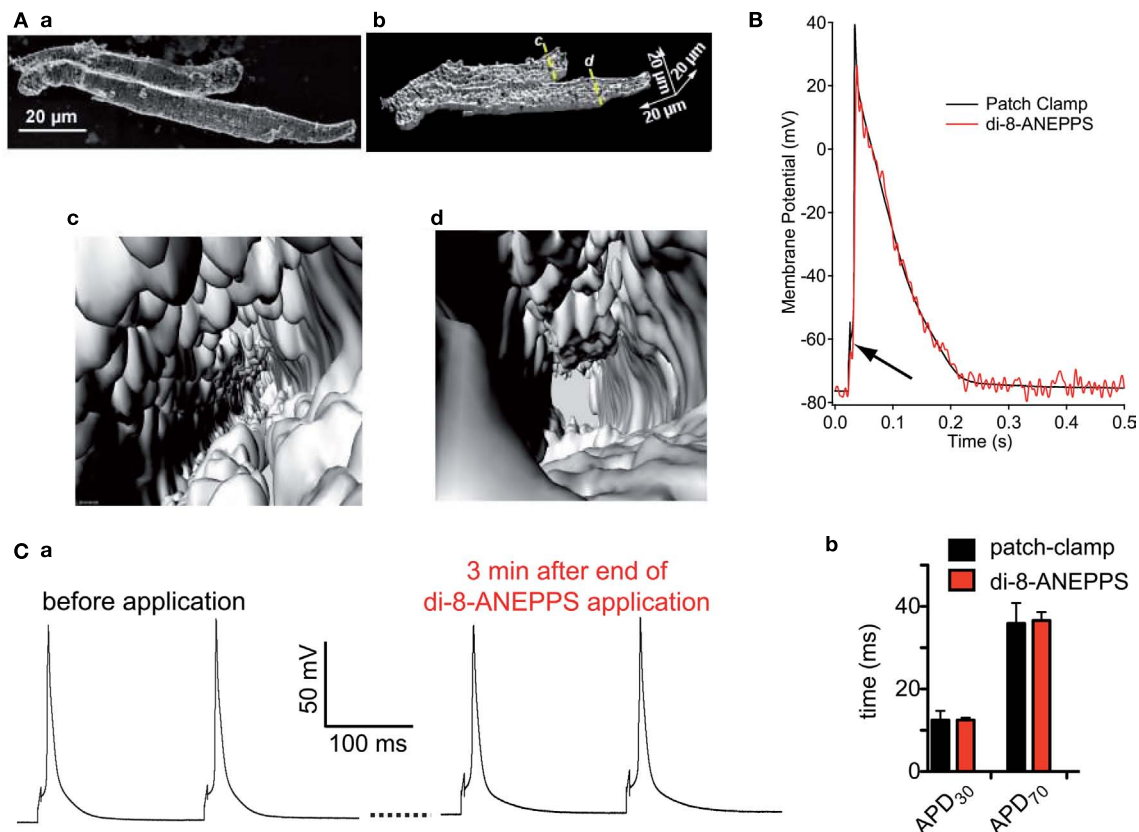


FIGURE 1 | (A) Depicts isolated human atrial myocytes loaded with the membrane potential dye di-8-ANEPPS. Image (a) displays a max. intensity projection of a confocal z-stack of two atrial myocytes, while image (b) depicts a cut open 3D-reconstruction of the same cells. The cells are virtually cut open along the lines c,d in image (b) and the view into the cells from that position is displayed in images (c,d), respectively. (B) Illustrates that the patch-clamp technique (black line) and the optical sensor (red line) measure exactly the same potential. Even the stimulation artifact of the patch-clamp

technique to induce an action potential translates into the optical signal (black arrow). (C) Shows that the di-8-ANEPPS, when applied at a concentration of 5 μ M for 7 min, does not disturb the naive action potential. (a) Displays action potentials recorded by patch-clamp before and after the di-8-ANEPPS staining procedure. (b) Depicts a statistical analysis of action potential duration in cells measured by the patch-clamp technique ($n = 94$) and measured by the optical di-8-ANEPPS read out ($n = 214$). (B,C) are reproduced from Tian et al. (2011) with friendly permission of S. Karger AG (Basel, Switzerland).

lifetime approaches. Alternatively, contractions can be suppressed, but this is problematic since compounds such as BDM or cytochalasin D prolong the action potential in the required concentrations (discussed in Tian et al., 2011). Blebbistatin is a more promising drug, but is easily photoconverted (Tian et al., 2011). For quantitative read-out fluorescence lifetime imaging is inherently too slow (Kaestner et al., 2011b). Therefore we regard ratio-metric approaches as the method of choice. Small molecule dyes such as di-4-ANEPPS or di-8-ANEPPS can be used in an excitation or emission ratio-metric manner. Although, with the availability of diode based light sources switching times between excitation wavelengths can be fairly short (Lee et al., 2011), emission ratio-metric scenarios generate both channels simultaneously allowing at least two times the acquisition speed. For di-8-ANEPPS it was shown that (a) it resembles action potentials from current clamp recordings (e.g., Figure 1B) and (b) the naive action potential is not influenced by the probe, if applied appropriately (Figure 1C; Tian et al., 2011). A promising development is a novel dye, called di-4-ANBDQPP (Matiukas

et al., 2007; Lee et al., 2011), that shows bathochromely shifted spectra and therefore may be used in the presence of GFP, that is often expressed, e.g., as cardiac marker in stem cell environments.

Yet another approach to potential sensitive sensors are genetically encoded potential probes. We published a recent review with particular emphasize on their application in cardiac myocytes (Kaestner et al., 2011b). One of the most promising candidates, the FRET based “Mermaid,” is introduced in Figure 2. The use of novel fluorescent proteins (Figure 2A) requires unusual detection channels when compared to the “classical” FRET pair CFP/YFP (Figure 2B). Especially since the mKusabira orange_K is prone to rapid bleaching it is not easy to get the best out of Mermaid (Atsushi Miyawaki and Hidekatsu Tsutsui, personal communication). Since there have been conflicting reports about the amino acid sequence of the linker in Mermaid (Tsutsui et al., 2008; Mutoh et al., 2009), we provide the sequence of the construct (Figure 2C) that was used in our previous studies (Kaestner et al., 2011a; Tian et al., 2011) as well as in Figure 2D. However, genetically

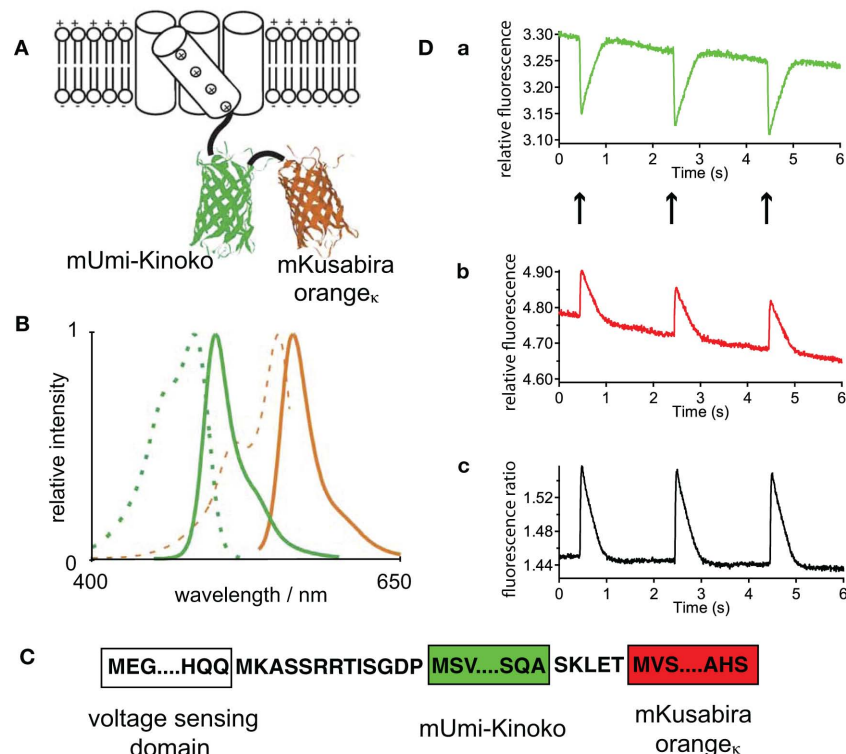


FIGURE 2 | (A) Is a schematic illustration of the FRET based sensor Mermaid containing two coral derived fluorescence proteins, whereas the voltage sensor containing a phosphatase of the sea squirt *Ciona intestinalis*, provides the base for the conformational change. The spectral properties of these fluorescent proteins are given in **(B)** (mUmi-Kinoko green lines and mKusabira orange_K, orange lines; excitation spectra dashed lines and fluorescence spectra solid lines). **(A,B)** are reprinted by permission from Macmillan Publishers Ltd: Nature Methods (Tsutsui et al., 2008), copyright (2008). Since

there have been conflicting reports concerning the linker sequences of Mermaid (Tsutsui et al., 2008; Mutoh et al., 2009), in **(C)** we provide the linker sequence of the construct used for our investigations [cp. **(D)**]. **(D)** Depicts action potential recordings from viral transduced Mermaid in isolated ventricular myocytes. **(a,b)** Are traces of the fluorescence intensity of the two spectral channels, while **(Dc)** presents the ratio of **(a,b)**. **(D)** Is a reprint from Tian et al. (2011) with friendly permission of S. Karger AG (Basel, Switzerland).

encoded potential sensors bear a potential for further improvements, especially with respect to their kinetic properties (Kaestner et al., 2011b).

DEVICES

To perform optical screens there are several requirements for the hardware, comprising three major components: (i) cell substrate and cavity that meet the conditions for optical screens, (ii) a microscope for imaging and (iii) a robotic system that handles the workflow:

- (i) A suitable substrate with oleophobic properties compatible with oil immersion objectives on the outside and elastic coating to mimic extracellular matrix on the inside was introduced recently (Muller et al., 2010). This was implemented in 24-well plates, as shown in **Figure 3A**, but would need further integration into 96 well plates and beyond. For electrical field stimulation of the cells this particular model used carbon electrodes incorporated into the lid. This method has the disadvantage of producing unwanted electrolytic by-products that need to be taken care of, e.g., by more frequent change

of the medium. Alternative concepts include cell stimulation by electromagnetic fields with an appropriate coil. Since such a coil would need proximity to the cells there are spatial conflicts with the objective. Another promising alternative to excite cardiomyocytes is the optogenetic manipulation by the expression of channelrhodopsin, a light-activated cation channel, that can induce action potentials (Bruegmann et al., 2010).

- (ii) As mentioned above fast read out of membrane potentials requires emission ratiometric approaches that in the past were only performed with photometric techniques (e.g., Hardy et al., 2009; Kaestner et al., 2011a,b). To increase the throughput many cells need to be measured simultaneously. Such properties are offered by systems employing array detectors. **Figure 3B** depicts a design of a microscope with an integrated image splitter projecting two spectral channels on one camera chip. Recent developments of CMOS camera chips (Coates et al., 2009; **Figure 3Ca**) provide a technology unifying high acquisition speed (**Figure 3Bb**) and good quantum efficiency (**Figure 3Bc**). Within the near future the latter parameter will improve even further since back thinned scientific CMOS chips will become available.

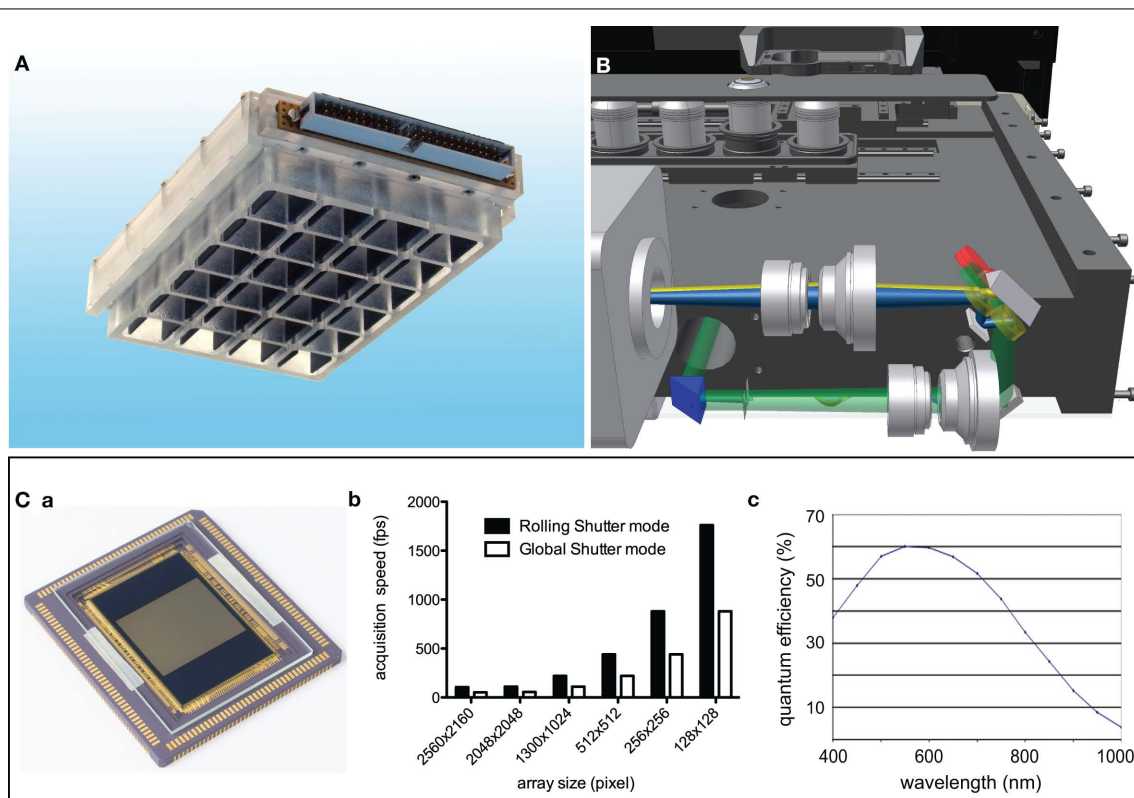


FIGURE 3 | Hardware enabling optical action potential screens. (A)

Depicts a 24-well plate allowing an electrical field stimulation of cardiac myocytes under the application of high numerical aperture oil immersion objectives. For a detailed description refer to Muller et al. (2010)). **(B)** Shows a design of a prototype microscope, which is representative for a new generation of microscopes allowing a precise screen of standard multi-well

plates and be able to detect two emission channels simultaneously on array detectors like CCD or CMOS based cameras. **(B)** Is a courtesy from Prof. Rainer Uhl (TILL I.D. GmbH, Gräfelfing, Germany). **(C)** Shows the state of the art scientific CMOS sensor **(a)** and key specifications of that sensor, what are frame rates in the range of 1 kHz **(b)** and a quantum efficiency of 60% around 550 nm **(c)**. **(D)** Is modified from Coates et al. (2009).

- (iii) To perform screens an automated plate and liquid handling, electrical stimulation (see above), and a complex microscopy protocol are compulsory. Although each of the elements is readily available on its own, a device combining the necessary hardware and an advanced software allowing online analysis and feedback into the acquisition procedure remains to be developed.

CONCLUSION

Beside the conceptional advantages of screening action potentials as outlined in the introduction, optical screens have a minimal requirement for the cellular system, since cells do not need to be mechanically manipulated. Therefore it is a very flexible screening approach and eventually the only one that can be applied to intact adult cardiomyocytes, in addition to model cells and stem cell derived cardiomyocytes. Action

potential screening can be combined with other optical measurements, such as those employing GFP for identifying stem cell derived cardiomyocytes (see above) or for imaging calcium (Lee et al., 2011). Additionally, optical screening that takes advantage of genetically encoded potential sensors allows experimental regimes in which cells can be revisited, even after a couple of days. Taken together, the possibilities of optical action potential screening may enable novel fields of application beyond cardiac safety.

ACKNOWLEDGMENTS

We like to thank Dr. Sandra Ruppenthal for assistance with the sequencing of Mermaid and Mrs. Sarah Schwarz for isolating the human atrial myocytes. This work was supported by the German Federal Ministry for Education and Research (BMBF) and the German Research Foundation (KFO 196).

REFERENCES

- Arrigoni, C., and Crivori, P. (2007). Assessment of QT liabilities in drug development. *Cell Biol. Toxicol.* 23, 1–13.
- Bruegmann, T., Malan, D., Hesse, M., Beiert, T., Fuegemann, C. J., Fleischmann, B. K., and Sasse, P. (2010). Optogenetic control of heart muscle in vitro and in vivo. *Nat. Methods* 7, 897–900.
- Coates, C., Fowler, B., and Holst, G. (2009). *Scientific CMOS Technology – A High-Performance Imaging Breakthrough*. Belfast: Andor Technology PLC, Fairchild Imaging, PCO AG, 1–14.
- Food and Drug Administration, HHS. (2005). ICH: S7B nonclinical evaluation of the potential for delayed ventricular repolarization (QT interval prolongation) by human pharmaceuticals. *Fed. Regist.* 70, 61133–61134.
- Hammer, K., Ruppenthal, S., Viero, C., Scholz, A., Edelmann, L., Kaestner, L., and Lipp, P. (2010). Remodelling of Ca²⁺ handling organelles in adult

- rat ventricular myocytes during long term culture. *J. Mol. Cell. Cardiol.* 49, 427–437.
- Hardy, M. E. L., Pollard, C. E., Small, B. G., Bridgland-Taylor, M., Woods, A. J., Valentin, J., and Abi-Gerges, N. (2009). Validation of a voltage-sensitive dye (di-4-ANEPPS)-based method for assessing drug-induced delayed repolarisation in Beagle dog left ventricular midmyocardial myocytes. *J. Pharmacol. Toxicol. Methods* 60, 94–106.
- Jin, W., Zhang, R.-J., and Wu, J.-Y. (2002). Voltage-sensitive dye imaging of population neuronal activity in cortical tissue. *J. Neurosci. Methods* 115, 13–27.
- Kaestner, L., and Lipp, P. (2007). “Non-linear and ultra high-speed imaging for explorations of the murine and human heart,” in *Optics in Life Science*, Vol. 6633, eds J. Popp and G. von Bally (Munich: SPIE), 66330K–1–66330K–10.
- Kaestner, L., Scholz, A., Hammer, K., Vecerdea, A., Ruppenthal, S., and Lipp, P. (2009). Isolation and genetic manipulation of adult cardiac myocytes for confocal imaging. *J. Vis. Exp.* 31. doi: 10.3791/1433
- Kaestner, L., Tian, Q., and Lipp, P. (2011a). “Cardiac safety screens: molecular, cellular and optical advancements,” in *Biomedical Optics III*, Vol. 8089, eds C. P. Lin and V. Ntziachistos (Munich: SPIE), 80890H–1–80890H–6.
- Kaestner, L., Tian, Q., and Lipp, P. (2011b). “Action potentials in heart cells,” in *Fluorescent Proteins II Application of Fluorescent Protein Technology*, ed. G. Jung (Heidelberg: Springer), doi: 10.1007/4243_2011_28. [Epub ahead of print].
- Kettenhofen, R., and Bohlen, H. (2008). Preclinical assessment of cardiac toxicity. *Drug Discov. Today* 13, 702–707.
- Lee, P., Bollensdorff, C., Quinn, T. A., Wuskell, J. P., Loew, L. M., and Kohl, P. (2011). Single-sensor system for spatially-resolved, continuous and multi-parametric optical mapping of cardiac tissue. *Heart Rhythm*. doi: 10.1016/j.hrthm.2011.03.061. [Epub ahead of print].
- Matiukas, A., Mitrea, B. G., Qin, M., Pertsov, A. M., Shvedko, A. G., Warren, M. D., Zaitsev, A. V., Wuskell, J. P., Wei, M. D., Watras, J., and Loew, L. M. (2007). Near-infrared voltage-sensitive fluorescent dyes optimized for optical mapping in blood-perfused myocardium. *Heart Rhythm* 4, 1441–1451.
- Moretti, A., Bellin, M., Welling, A., Jung, C. B., Lam, J. T., Bott-Flügel, L., Dorn, T., Goedel, A., Höhnke, C., Hofmann, F., Seyfarth, M., Sinnecker, D., Schömig, A., and Laugwitz, K. L. (2010). Patient-specific induced pluripotent stem-cell models for long-QT syndrome. *N. Engl. J. Med.* 363, 1397–1409.
- Muller, O., Tian, Q., Zantl, R., Kahl, V., Lipp, P., and Kaestner, L. (2010). A system for optical high resolution screening of electrical excitable cells. *Cell Calcium* 47, 224–233.
- Mutoh, H., Perron, A., Dimitrov, D., Iwamoto, Y., Akemann, W., Chudakov, D. M., and Knöpfel, T. (2009). Spectrally-resolved response properties of the three most advanced FRET based fluorescent protein voltage probes. *PLoS ONE* 4, e4555. doi: 10.1371/journal.pone.0004555
- Salzberg, B. M., Davila, H. V., and Cohen, L. B. (1973). Optical recording of impulses in individual neurones of an invertebrate central nervous system. *Nature* 246, 508–509.
- Tian, Q., Oberhofer, M., Ruppenthal, S., Scholz, A., Buschmann, V., Tsutsui, H., Miyawaki, A., Zeug, A., Lipp, P., and Kaestner, L. (2011). Optical action potential screening on adult ventricular myocytes as an alternative QT-screen. *Cell. Physiol. Biochem.* 27, 281–290.
- Tsutsui, H., Karasawa, S., Okamura, Y., and Miyawaki, A. (2008). Improving membrane voltage measurements using FRET with new fluorescent proteins. *Nat. Methods* 5, 683–685.
- Viero, C., Kraushaar, U., Ruppenthal, S., Kaestner, L., and Lipp, P. (2008). A primary culture system for sustained expression of a calcium sensor in preserved adult rat ventricular myocytes. *Cell Calcium* 43, 59–71.

Conflict of Interest Statement: The authors declare that the research was conducted in the absence of any commercial or financial relationships that could be construed as a potential conflict of interest.

Received: 15 June 2011; paper pending published: 27 June 2011; accepted: 12 July 2011; published online: 28 July 2011.

Citation: Kaestner L and Lipp P (2011) Screening action potentials: the power of light. *Front. Pharmacol.* 2:42. doi: 10.3389/fphar.2011.00042

This article was submitted to *Frontiers in Ion Channels and Channelopathies*, a specialty of *Frontiers in Pharmacology*. Copyright © 2011 Kaestner and Lipp. This is an open-access article subject to a non-exclusive license between the authors and Frontiers Media SA, which permits use, distribution and reproduction in other forums, provided the original authors and source are credited and other Frontiers conditions are complied with.



Targeting GIRK channels for the development of new therapeutic agents

Kenneth B. Walsh*

Department of Pharmacology, Physiology and Neuroscience, School of Medicine, University of South Carolina, Columbia, SC, USA

Edited by:

Ralf Franz Kettenhofen, Axiogenesis AG, Germany

Reviewed by:

Maurizio Tagliatela, University of Molise, Italy

Owen McManus, Johns Hopkins

University, USA

Gregory John Kaczorowski, Kanalis Consulting, L.L.C., USA

*Correspondence:

Kenneth B. Walsh, Department of Pharmacology, Physiology and Neuroscience, School of Medicine, University of South Carolina, Columbia, SC 29208, USA.
e-mail: walsh@uscmcd.sc.edu

G protein-coupled inward rectifier K⁺ (GIRK) channels represent novel targets for the development of new therapeutic agents. GIRK channels are activated by a large number of G protein-coupled receptors (GPCRs) and regulate the electrical activity of neurons, cardiac myocytes, and β -pancreatic cells. Abnormalities in GIRK channel function have been implicated in the patho-physiology of neuropathic pain, drug addiction, cardiac arrhythmias, and other disorders. However, the pharmacology of these channels remains largely unexplored. In this paper we describe the development of a screening assay for identifying new modulators of neuronal and cardiac GIRK channels. Pituitary (AtT20) and cardiac (HL-1) cell lines expressing GIRK channels were cultured in 96-well plates, loaded with oxonol membrane potential-sensitive dyes and measured using a fluorescent imaging plate reader. Activation of the endogenous GPCRs in the cells caused a rapid, time-dependent decrease in the fluorescent signal; indicative of K⁺ efflux through the GIRK channels (GPCR stimulation versus control, Z'-factor = 0.5–0.7). As expected this signal was inhibited by addition of Ba²⁺ and the GIRK channel toxin tertiapin-Q. To test the utility of the assay for screening GIRK channel blockers, cells were incubated for 5 min with a compound library of Na⁺ and K⁺ channel modulators. Ion transporter inhibitors such as 5-(N,N-hexamethylene)-amiloride and SCH-28080 were identified as blockers of the GIRK channel at sub-micromolar concentrations. Thus, the screening assay will be useful for expanding the limited pharmacology of the GIRK channel and in developing new agents for the treatment of GIRK channelopathies.

Keywords: GIRK channel, clonal cell lines, drug screening, neuropathic pain, atrial fibrillation

INTRODUCTION

G protein-coupled inward rectifier K⁺ (GIRK) channels function as cellular mediators of a wide range of hormones and neurotransmitters and are expressed in the brain, heart, skeletal muscle, and endocrine tissue (Hibino et al., 2010; Lusscher and Slesinger, 2010). GIRK channels are members of the super-family of proteins known as inward rectifier K⁺ (Kir) channels (Hibino et al., 2010; Lusscher and Slesinger, 2010) that function to stabilize the cell resting membrane potential near the K⁺ equilibrium potential (E_K). Four GIRK channel subunits are expressed in mammals: GIRK1 (Kir3.1), GIRK2 (Kir3.2), GIRK3 (Kir3.3), and GIRK4 (Kir3.4; Hibino et al., 2010; Lusscher and Slesinger, 2010). The GIRK1, GIRK2, and GIRK3 subunits are expressed in a number of regions of the brain including the hippocampus, cerebellum, substantia nigra, locus coeruleus, and ventral tegmental area (Lusscher and Slesinger, 2010). In addition, GIRK1 and GIRK2 subunits are expressed in the superficial layers of the spinal dorsal horn and are enriched in the postsynaptic membranes of substantia gelatinosa neurons (Lusscher and Slesinger, 2010). In neuronal tissue GIRK subunits combine to form both heterotetrameric (e.g., GIRK1/GIRK2, GIRK1/GIRK3, etc.) and homotetrameric (GIRK2/GIRK2) channels. In the atrial myocardium and sinus and atrioventricular nodes of the heart, GIRK channels are composed of heteromers of GIRK1 and GIRK4 subunits (Hibino et al., 2010).

G protein-coupled inward rectifier K⁺ channels become activated following the binding of ligands to their cognate G protein-coupled receptors (GPCRs). This binding causes the dissociation of the $\beta\gamma$ subunits of pertussis toxin-sensitive G proteins which subsequently bind to and activate the GIRK channel. Once opened the GIRK channel allows the movement of K⁺ out of the cell causing the resting membrane potential to become more negative. As a consequence, GIRK channel activation in neurons decreases spontaneous action potential formation and inhibits the release of excitatory neurotransmitters. In the heart, activation of the GIRK channel inhibits pacemaker activity thereby slowing the heart rate.

G protein-coupled inward rectifier K⁺ channels represent novel targets for the development of new therapeutic agents for the treatment of neuropathic pain, drug addiction, cardiac arrhythmias, and other disorders. However, the pharmacology of these channels remains largely unexplored. Although a number of drugs including anti-arrhythmic agents, antipsychotic drugs, and antidepressants block the GIRK channel (Kobayashi and Ikeda, 2006), this inhibition is non-selective and occurs at relatively high drug concentrations. In this paper we describe the development of a screening assay for identifying new modulators of neuronal and cardiac GIRK channels. Pituitary (AtT20) and cardiac (HL-1) cell lines expressing GIRK channels were analyzed using patch clamp recording procedures and fluorescent imaging plate reader

measurements. Application of the GPCR ligands somatostatin (AtT20 cells) and carbachol (HL-1 cells) activated whole-cell GIRK currents that were blocked by the Kir channel selective toxin tertiapin-Q. In cells loaded with the membrane potential-sensitive fluorescent dye HLB 021-152, GPCR stimulation caused a rapid, time-dependent decrease in the fluorescent signal. This GPCR-induced decrease in fluorescence was blocked by BaCl₂ and tertiapin-Q. A preliminary screen of the GIRK channel fluorescent assay identified several ion transporter inhibitors as blockers of the channel. Thus, the GIRK channel screening assay will be useful for expanding the limited pharmacology of the channel and for developing new agents for the treatment of GIRK channelopathies.

MATERIALS AND METHODS

CELL CULTURE AND PLATING

The immortalized cardiac HL-1 cell line was generously supplied by Dr. William Claycomb (LSU Medical Center, New Orleans, LA, USA). HL-1 cells were maintained in Claycomb/DMEM media supplemented with 10% fetal bovine serum, penicillin/streptomycin, and L-glutamine (Sigma-Aldrich). The AtT20 pituitary cell line was obtained from Dr. Ken Mackie (Indiana University) and grown in DMEM media with 10% horse serum. Cells were plated on gelatin- (HL-1 cells) or poly L-lysine- (AtT20 cells) coated glass coverslips (5,000 cells per coverslip; patch clamp recording) and in black 96-well plates (Corning; 30,000 cells per well; plate reader measurements). Cells were stored in an incubator at 37°C (5% O₂/95% CO₂) and used on days 2–4 after plating.

PATCH CLAMP RECORDING OF GIRK CURRENTS

The patch clamp method (Hamill et al., 1981) was used to record the whole-cell, GIRK currents using L/M EPC-7 (Adams and List Associates) and Axopatch 200 (Axon Instruments) amplifiers. Our procedures for measuring K⁺ channels have been described (Walsh and Zhang, 2008; Walsh, 2010). Pipettes were made from borosilicate glass capillaries (World Precision Instruments) and had resistances of 1–2 Mohm when filled with internal solution. All experiments were conducted on isolated, non-coupled cells at room temperature (22–24°C). For the measurement of GIRK currents, cells were placed in a normal buffer solution consisting of; 132 mM NaCl, 5 mM KCl, 1 mM CaCl₂, 1 mM MgCl₂, 5 mM dextrose, 5 mM HEPES, pH 7.4 (with NaOH; 280 mOsm). The internal solution consisted of; 50 mM KCl, 60 mM K⁺-glutamate, 2 mM MgCl₂, 1 mM CaCl₂, 11 mM EGTA, 3 mM ATP, 0.1 mM GTP, 10 mM HEPES, pH 7.3 (with KOH; 280 mOsm). Upon establishment of the whole-cell configuration, the cell was perfused with a high K⁺ buffer solution containing; 107 mM NaCl, 30 mM KCl, 1 mM CaCl₂, 1 mM MgCl₂, 5 mM dextrose, 5 mM HEPES, pH 7.4. Following the measurement of the cell background current, GIRK channels were activated by the addition of the GPCR ligands carbachol (10 μM; HL-1 cells) or somatostatin (200 nM; AtT20 cells) using a rapid perfusion system. In each case the GIRK current was defined as the BaCl₂-sensitive current (see Figure 1).

GIRK CHANNEL FLUORESCENT PLATE READER ASSAY

For measuring changes in the membrane potential, cells were incubated for 1 h in normal buffer solution containing the

oxonol dye HLB 021-152 (5 μM; AnaSpec) and fluorescent signals recorded using a Synergy2 microplate reader (Biotek) at 28°C. Test compounds were dissolved in DMSO at a stock concentration of 10 mM, diluted to various concentrations and applied to the cells for 5 min prior to the fluorescent measurements. DMSO, up to 1% in normal buffer solution, had no adverse effects on the cell response. Carbachol, somatostatin, or control solution (20 μL) was added to each well (total volume = 220 μL) at time zero using the Synergy2 injector system. Data points were collected at 10 s intervals over a 300-s sampling period at excitation and emission wavelengths of 520 and 560 nm, respectively. Z'-factors (Zhang et al., 1999) were obtained by (1) comparing the fluorescent signal between wells injected with control solution and wells injected with the GPCR ligand and (2) comparing the signal in wells injected with the GPCR ligand in the presence and absence of 2 mM BaCl₂. The Z'-factor is defined as: $Z' = 1 - (3\sigma_P + 3\sigma_N) / |\mu_P - \mu_N|$, where μ_P and μ_N are the means of the positive control and negative control signals, and σ_P and σ_N are the SD of the positive control and negative control signals, respectively (Zhang et al., 1999). Plates used for Z'-factor determination contained two rows each of positive and negative controls. Dose-response curves for selected compounds were obtained and drug potencies determined by fitting the data with the curve: $\text{Max} / (1 + ([\text{drug}] / \text{IC}_{50})^k)$, where the IC₅₀ is the concentration of the compound producing a 50% decrease in the maximal GPCR response (Max) and k is the slope factor. Interference of the test compounds with the HLB 021-152 fluorescence was determined in the absence of cells by adding various concentrations of the compounds to buffer solution containing the dye.

DRUGS AND CHEMICALS

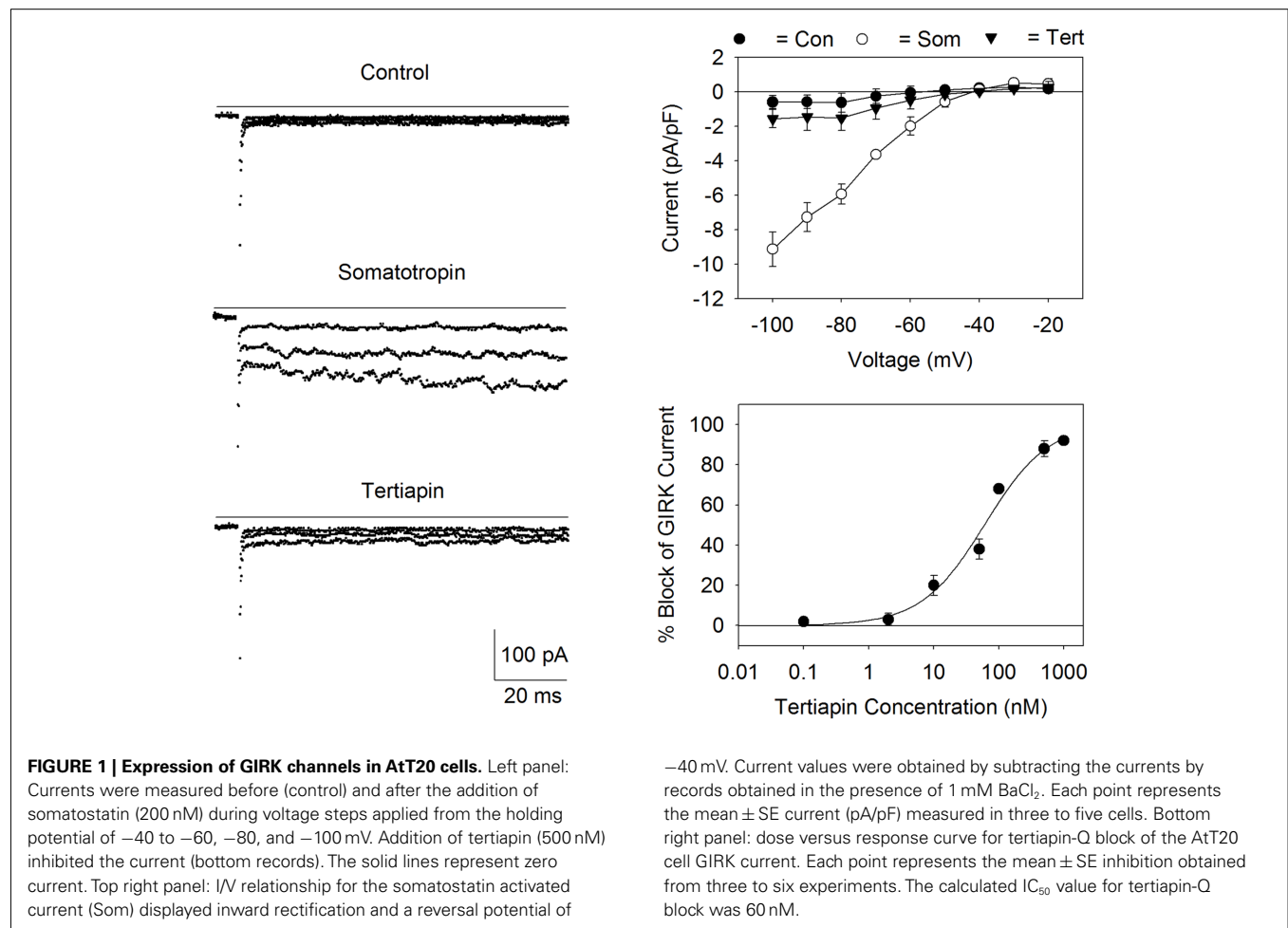
Carbachol, somatostatin, and a Na⁺, K⁺ channel modulator kit (catalog # LO2220), containing 68 compounds, were purchased from Sigma-Aldrich Chemical Corp. Tertiapin-Q (synthetic formulation) was obtained from Alomone Labs.

RESULTS

MEASUREMENT OF GIRK CURRENTS IN AtT20 CELLS

G protein-coupled inward rectifier K⁺ channels are highly expressed in the central and peripheral nervous system as well as in endocrine tissue. The AtT20 cell line was originally derived from a mouse pituitary tumor and expresses the somatostatin type 2 and 5 receptors (SSTR2 and SSTR5), voltage-gated Ca²⁺ channels, and GIRK1/GIRK2 channels (Mackie et al., 1995; Kuzhikan-dathil et al., 1998). Although the AtT20 cells were first thought to be related to pituitary corticotrophs, recent evidence indicates that these cells have functional and structural features more in common with neuropeptide-secreting neurons. Thus, the AtT20 cells provide a good model system for studying neuronal signaling.

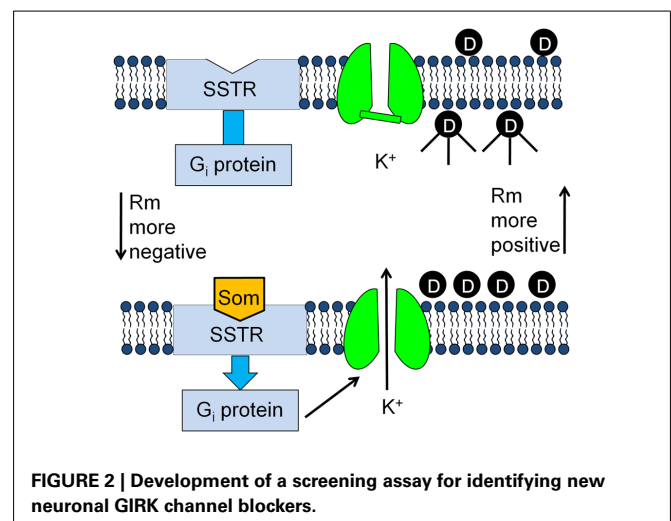
Figure 1 displays GIRK currents measured in the AtT20 cells using the whole-cell arrangement of the patch clamp technique. Cells were bathed in the high K⁺ buffer solution (30 mM KCl) and the internal (pipette) solution contained KCl/K⁺-glutamate (140 mM K⁺) with GTP. Application of somatostatin to the recording chamber resulted in the activation of a Ba²⁺-sensitive,



inward rectifying current (Figure 1). The somatostatin-activated current was blocked by addition of the GIRK channel blocker tertiapin-Q (Jin and Lu, 1998; Figure 1). Tertiapin-Q blocked the current with an IC₅₀ of 60 nM (Figure 1). The reversal potential (E_{rev}) for the current (-40 mV) was close to the calculated Nernst equilibrium potential (E_K ; -39 mV) for a K⁺-selective channel under the conditions of the experiment. Thus, the inward rectifying current versus voltage relationship, the tertiapin-Q-sensitivity, and the K⁺ selectivity of the channel are all consistent with the expression of GIRK channels in the AtT20 cells (Mackie et al., 1995; Kuzhikandathil et al., 1998).

DEVELOPMENT OF A GIRK CHANNEL SCREENING ASSAY

Having confirmed the presence of GIRK channels in the AtT20 cell line, it was determined if these cells could be used for drug screening. The experimental design of the screening assay is outlined in Figure 2. AtT20 cells were cultured in 96-well plates and loaded with the fluorescent membrane potential-sensitive dye HLB 021-152 (AnaSpec). Membrane potential-sensitive dyes such as HLB 021-152 (D) distribute across the plasma membrane when cells are in the rested state and reach equilibrium (Figure 2, top panel). The dye molecules inside the cells become strongly fluorescent upon binding to intracellular proteins and other cytoplasmic components. Treatment of the cells with somatostatin (Som), which binds



to the somatostatin receptor (SSTR), activates the G inhibitory protein (G_i) stimulating the GIRK channels to open (Figure 2, bottom panel). The resulting efflux of K⁺ out of the cell (resting potential of -50 to -60 mV for AtT20 cells) causes the resting membrane potential (R_m) to become more negative and the HLB

021-152 molecules to redistribute to the outside of the cell. As a result the cell fluorescent signal is decreased.

The applicability of the GIRK channel fluorescent assay for drug discovery was evaluated in the experiments displayed in **Figure 3**. Each figure plots the HLB 021-152 fluorescence signal measured over time in the 96-well plates using a microplate reader. As predicted by the experimental model, addition of somatostatin (200 nM) to the AtT20 cells caused a rapid, time-dependent decrease in the HLB 021-152 fluorescent signal (**Figure 3**). In contrast, addition of control solution produced only a small instantaneous rise in the fluorescence (**Figure 3**). Comparison of peak fluorescent values in wells injected with control and somatostatin solutions gave a Z' -factor of 0.7. The Z' -factor is used to quantify the reliability of the assay (Zhang et al., 1999). Z' -factors

in the range of 0.5–1.0 indicate that the quality of the assay is excellent (Zhang et al., 1999). In order to quantify the GIRK channel fluorescent signal, the averaged control measurement, obtained in each 96-well plate, was subtracted from the records measured in the presence of somatostatin (Som – Con; **Figure 3**). This control-subtracted fluorescent signal (i.e., the somatostatin-sensitive component) was subsequently obtained and analyzed throughout the rest of the study. As shown in the top panel of **Figure 3**, somatostatin activated the AtT20 cell GIRK channel in a concentration dependent manner with a half-maximal effective concentration (EC_{50}) of 4 nM. At a concentration of 200 nM somatostatin caused a fluorescent change (F/F_0) of -0.088 ($n = 6$ wells). In comparison, addition of 10, 20, and 30 mM KCl, to depolarize the cell membrane, produced fluorescent changes of 0.058,

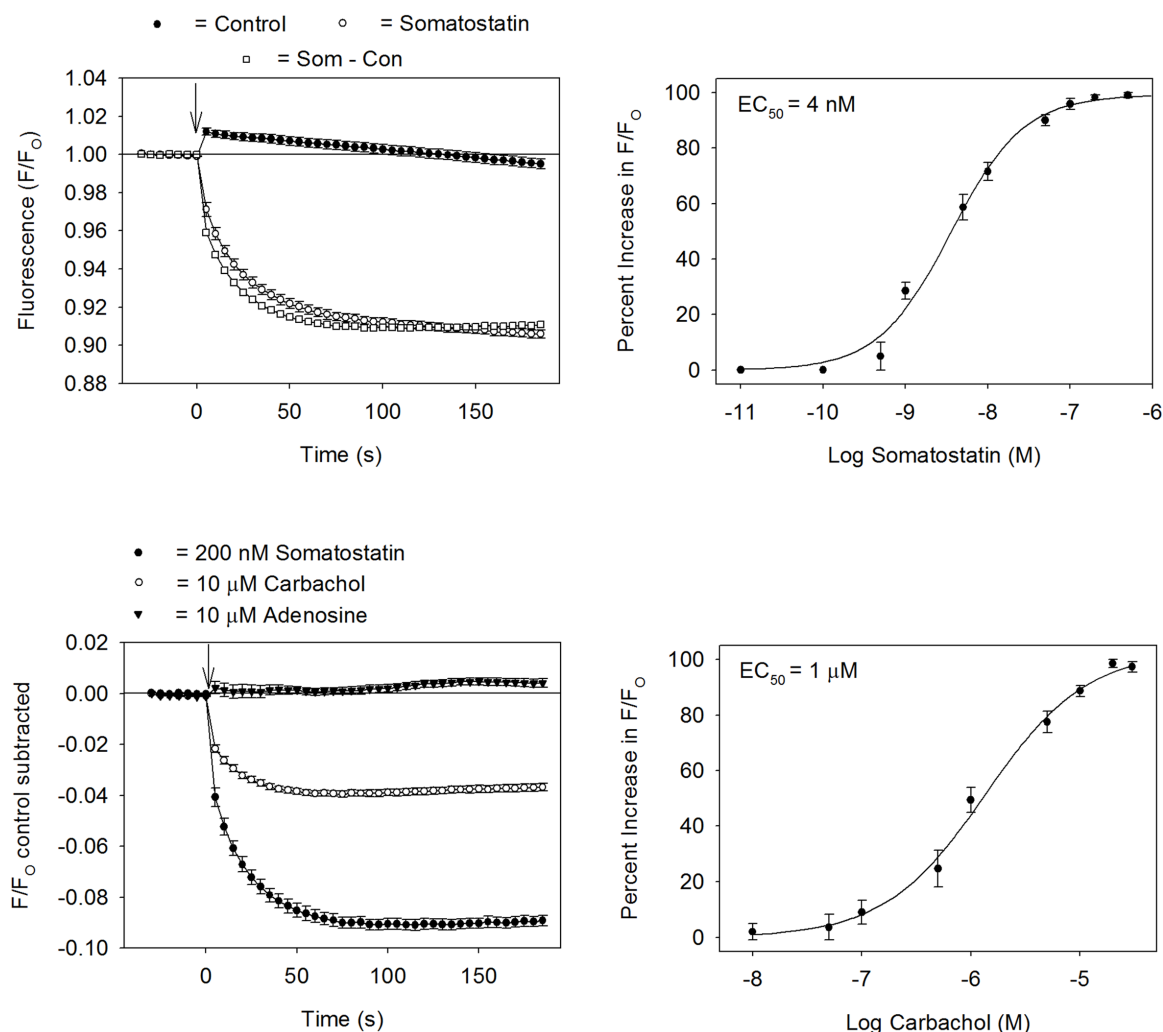


FIGURE 3 | Development of a GIRK channel blocker screening assay. Top left panel: HLB 021-152 fluorescent intensities obtained in AtT20 cells in the presence or absence of somatostatin. The ratio of the fluorescent intensity (F/F_0) was calculated by dividing the signal in the presence (F) of somatostatin (or control solution) by the baseline signal measured before (F_0) addition of somatostatin (or control solution). Each point represents the mean \pm SE obtained in six to eight wells. Somatostatin was added at time

zero (\downarrow). Top right panel: dose–response curve for the somatostatin-sensitive fluorescent signal ($EC_{50} = 4$ nM). Each point represents the mean \pm SE of six measurements. Bottom left panel: changes in fluorescent signal obtained during injection of somatostatin, carbachol, and adenosine. Each point represents the mean \pm SE obtained in six wells. Bottom right panel: dose–response curve for the carbachol-sensitive fluorescent signal ($EC_{50} = 1$ μ M). Each point represents the mean \pm SE of six measurements.

0.13, and 0.15, respectively ($n=6$ wells for each KCl concentration). It was also determined if stimulation of other G_i -coupled GPCRs might activate the AtT20 cell GIRK channels. Application of the muscarinic agonist carbachol resulted in a peak fluorescent change of -0.037 ($n=6$ wells; **Figure 3**, bottom panel). The EC_{50} for carbachol activation of the channel was $1\ \mu\text{M}$ (**Figure 3**, bottom panel). In contrast, application of $10\ \mu\text{M}$ adenosine caused no change in the fluorescent signal.

IDENTIFICATION OF GIRK CHANNEL BLOCKERS IN AtT20 CELLS AND CARDIAC HL-1 CELLS

It was next determined if the fluorescent assay system could be utilized for screening drugs that block GIRK channels. Inhibition of the GIRK channel should reduce somatostatin-mediated changes in Rm by preventing K^+ efflux from the cells. To provide proof of concept, the AtT20 cells were incubated for 5 min with either BaCl_2 or tertiapin-Q prior to somatostatin addition. As expected for a signal arising from GIRK channel activation, treatment with BaCl_2 (2 mM) or tertiapin (500 nM) produced a complete inhibition of the somatostatin-mediated fluorescent change (**Figure 4**). BaCl_2 at concentrations of 0.5 and 1 mM reduced the fluorescent change by $67 \pm 4\%$ and $92 \pm 2\%$ ($n=6$ wells each), respectively.

We previously demonstrated that the GIRK channel fluorescent assay could be utilized to study the pharmacology of the GIRK1/GIRK4 channel in cardiac HL-1 cells (Walsh, 2010). The HL-1 cells are an immortalized atrial cell line that displays an adult-like cardiac genotype and contracts spontaneously in cell culture (Whit et al., 2004). The cardiac GIRK channel is strongly blocked by tertiapin (Nobles et al., 2010; Walsh, 2010). In **Figure 4** the concentration versus inhibition response of tertiapin-Q on the GIRK channel fluorescent signal was compared in the AtT20 and HL-1 cells. Tertiapin-Q was nearly a 100-fold more potent in blocking the GIRK channel in the HL-1 cells ($IC_{50} = 1.4\ \text{nM}$) as compared to the AtT20 cells ($IC_{50} = 102\ \text{nM}$).

G protein-coupled inward rectifier K^+ channels are non-specifically blocked by a number of drugs including anti-arrhythmic agents, antipsychotic drugs, and antidepressants (Kobayashi and Ikeda, 2006). As a first step in expanding the limited pharmacology of the channel, the AtT20 and HL-1 cells were screened against a small compound library of Na^+ and K^+ channel modulators. Dose versus response curves were obtained for compounds producing a 50% or greater inhibition of the GPCR ligand-induced signal when tested at a concentration of $1\ \mu\text{M}$. Several ion transporter inhibitors were identified as GIRK channel blockers. The Na^+/H^+ exchange inhibitors 5-(*N,N*-hexamethylene)-amiloride (HMEA; **Figure 5**) and 5-(*N*-ethyl-*N*-isopropyl)-amiloride (EIPA) blocked the GIRK channel with IC_{50} s of $1\ \mu\text{M}$ in both the AtT20 and HL-1 cells. In contrast, the parent compound amiloride had no blocking effect when tested up to a concentration of $10\ \mu\text{M}$. The gastric H^+/K^+ transport inhibitor SCH-28080 (2-methyl-8-(phenylmethoxy)imidazo[1,2-*A*]pyridine-3-acetonitrile) potently reduced the GPCR-sensitive fluorescent signal ($IC_{50} = 0.2\ \mu\text{M}$ for the AtT20 cells; $IC_{50} = 0.3\ \mu\text{M}$ for the HL-1 cells; **Figure 5**). However, no change in fluorescence was measured during treatment with the structurally related transport inhibitor omeprazole (**Figure 5**).

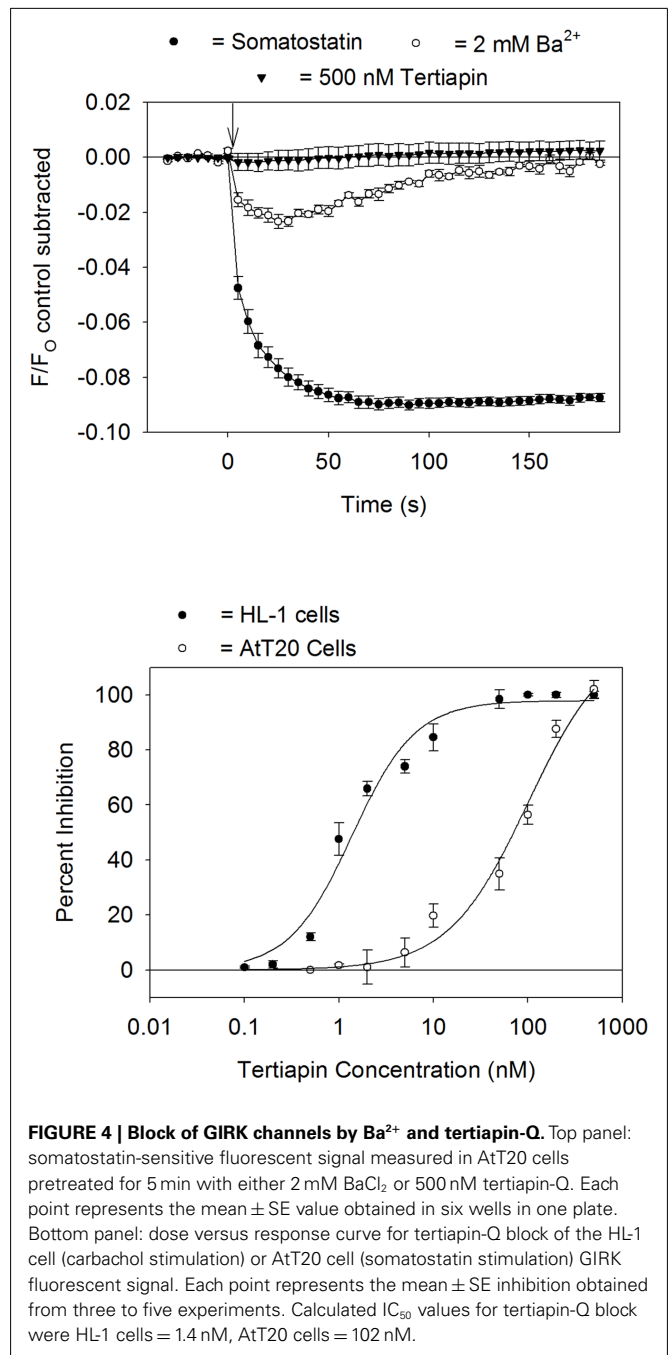
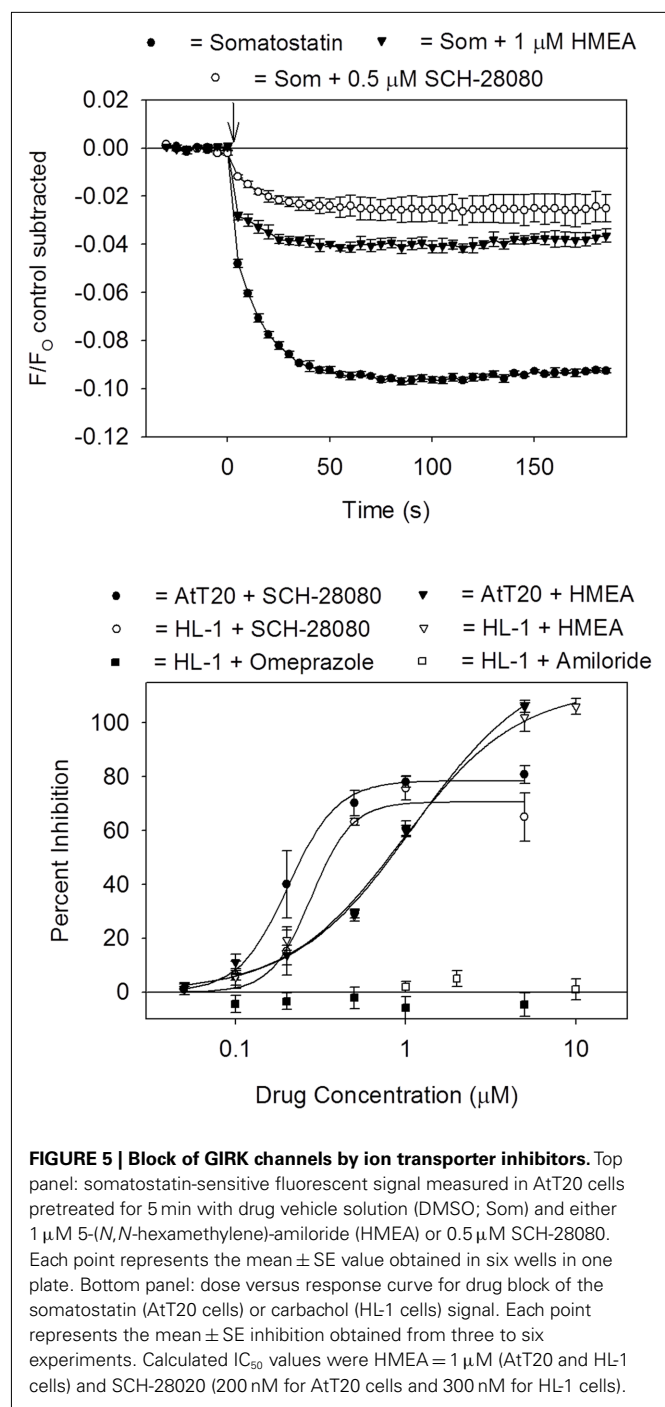


FIGURE 4 | Block of GIRK channels by Ba^{2+} and tertiapin-Q. Top panel: somatostatin-sensitive fluorescent signal measured in AtT20 cells pretreated for 5 min with either 2 mM BaCl_2 or 500 nM tertiapin-Q. Each point represents the mean \pm SE value obtained in six wells in one plate. Bottom panel: dose versus response curve for tertiapin-Q block of the HL-1 cell (carbachol stimulation) or AtT20 cell (somatostatin stimulation) GIRK fluorescent signal. Each point represents the mean \pm SE inhibition obtained from three to five experiments. Calculated IC_{50} values for tertiapin-Q block were HL-1 cells = 1.4 nM, AtT20 cells = 102 nM.

DISCUSSION

GIRK CHANNELS AS TARGETS FOR DRUG THERAPY

The goal of this study was to develop a screening assay for identifying modulators of neuronal and cardiac GIRK channels. For this purpose immortalized pituitary AtT20 and cardiac HL-1 cells were cultured in 96-well plates, loaded with an oxonol membrane potential-sensitive dye and analyzed with a fluorescent plate reader. Activation of the endogenous GPCRs in the cells, through application of either somatostatin or carbachol, caused a rapid, time-dependent decrease in the fluorescent signal. This change in the fluorescent signal was blocked by treatment with



the GIRK channel blockers Ba^{2+} and tertiapin-Q. Thus, the GIRK channel fluorescent assay provides a fast, reliable, and inexpensive procedure for identifying drugs that modulate GIRK channels.

G protein-coupled inward rectifier K^+ channel dysfunction has been implicated in the patho-physiology of a number of disorders including neuropathic pain, drug addiction, and cardiac arrhythmias. Support for a role of GIRK channels in these disorders has come primarily from studies with GIRK channel knockout mice. For example, GIRK channel knockout mice display a

reduced sensitivity to analgesics (Lusscher and Slesinger, 2010). Dose-response curves for morphine-induced analgesia are shifted to higher doses in both GIRK2 and GIRK1 subunit knockout mice (Marker et al., 2004). Anti-nociceptive effects of ethanol, oxotremorine (muscarinic agonist), nicotine, baclofen (GABA agonist), clonidine (α_2 -adrenergic agonist), and WIN 55,212 (cannabinoid agonist) are also diminished in GIRK2 null mice (Blednov et al., 2003; Mitrovic et al., 2003). Koor et al. (2001) demonstrated that mice lacking the GIRK4 subunit are less susceptible to the development of atrial fibrillation. This finding is supported by recent studies indicating that the GIRK channel is constitutively activated in patients with atrial fibrillation (Dobrev et al., 2005). Therefore, although GIRK channels represent desirable targets for pharmacological therapy, drug development has been hampered by the absence of a cell-based screening system.

DEVELOPMENT OF A GIRK CHANNEL SCREENING ASSAY

The traditional approach to ion channel drug discovery has involved the expression of recombinant channels in heterologous cell lines such as HEK-293 and CHO cells. However, these cells often lack the relevant “physiological environment” that is present in native tissues, and required for normal pharmacological responses (Numann and Negulescu, 2001; Eglen and Reisine, 2010). Of particular concern, the expression profile of G proteins and ion channels in HEK-293 cells differs from that found in muscle and nerve (Numann and Negulescu, 2001; Eglen and Reisine, 2010). Thus, recent interest has focused on the suitability of primary cells, embryonic stem cells and clonal cell lines for drug discovery (Eglen and Reisine, 2010).

In the present study, GIRK channels were screened using the membrane potential-sensitive dye HLB 021-152. Membrane potential-sensitive dyes have previously been used to study Kir channels (Wolff et al., 2003). More recently, HEK-293 cells over-expressing GIRK channels were successfully utilized to screen for metabotropic glutamate receptor ligands using the thallium flux assay (Niswender et al., 2008). During the course of our experiments we performed preliminary experiments using the thallium flux assay with the fluorescent dye BTC-AM. Application of the thallium containing solution to the HL-1 and AtT20 cells produced large non-linear background increases in the BTC fluorescence. This background signal was larger than the subsequent fluorescent change produced by addition of the GPCR ligand. HL-1 cells express the ether-à-go-go related gene (ERG) channel and other K^+ channels (Whit et al., 2004) that may allow thallium influx under basal conditions. Therefore, the thallium influx assay is not currently suitable for the AtT20 and HL-1 cell lines.

The AtT20 and HL-1 cell lines represent ideal systems for GIRK channel drug discovery. AtT20 cells express the GIRK1 and GIRK2 subunits as well as SSTR2 and SSTR5. HL-1 cells express the GIRK1 and GIRK4 subunits along with the muscarinic type2 (M2) receptor. Whole-cell acetylcholine-activated K^+ currents ($I_{K,ACh}$; GIRK1/GIRK4 channel) are blocked by 100 nM tertiapin-Q in the HL-1 cells (Nobles et al., 2010; Walsh, 2010). In the present study, tertiapin-Q was nearly 100-fold more potent in blocking the HL-1 cell GIRK channel fluorescent signal (Figure 4). Lu and colleagues (Jin and Lu, 1998; Ramu et al., 2004) identified a short sequence

of amino acids (approximately 10 amino acid residues), located in the M1–M2 linker of Kir subunits, that determines the binding affinity of tertiapin. Slight variances in this region greatly alter the potency of tertiapin in blocking Kir channels (Ramu et al., 2004). When expressed in *Xenopus* oocytes, homomeric GIRK1 and GIRK4 channel constructs are blocked by tertiapin-Q with K_d values of 20 μ M and 2 nM, respectively (Ramu et al., 2004). Variances in this linker sequence may also account for the different IC_{50} s that were measured with tertiapin in the AtT20 and HL-1 cells.

Despite the different potencies of GIRK channel inhibition produced by tertiapin-Q in the two cell lines, both cell types displayed a similar sensitivity to the ionic transport inhibitors HMEA, EIPA, and SCH-28080. GIRK channels are blocked by a wide range of pharmacological agents including volatile anesthetics (halothane, isoflurane, and enflurane), antipsychotic drug (clozapine, pimozide, and haloperidol), and antidepressants (imipramine, amitriptyline, and clomipramine; Kobayashi and Ikeda, 2006; Lusscher and Slesinger, 2010). Furthermore, a number of anti-arrhythmic agents including amiodarone, flecainide,

quinidine, and propafenone block GIRK channels in primary cultures of atrial myocytes (Inomata et al., 1993; Watanabe et al., 1996; Hashimoto et al., 2006) and in HL-1 cells (Walsh, 2010). However, GIRK channel inhibition by these agents typically requires drug concentrations in the micromolar range. Recently, two benzopyran derivatives, NIP-151 and NTC-801, were demonstrated to block GIRK1/GIRK4 channels at nanomolar concentrations (Hashimoto et al., 2008; Machida et al., 2011). When tested in a canine model of atrial fibrillation, both compounds decreased atrial excitability and converted AF to sinus rhythm (Hashimoto et al., 2008; Machida et al., 2011). While the clinical efficacy of these agents is yet to be established, the results of these studies support the further development of new and selective GIRK channel modulators.

ACKNOWLEDGMENTS

The author thanks Ms. Charity Fix and Mr. David Stepp for their excellent technical assistance. This work was supported by US Public Health Service award NS-071530 and a grant from the University of South Carolina.

REFERENCES

- Blednov, Y. A., Stoffel, M., Alva, H., and Harris, R. A. (2003). A pervasive mechanism for analgesia: activation of GIRK2 channels. *Proc. Natl. Acad. Sci. U.S.A.* 100, 277–282.
- Dobrev, D., Friedrich, A., Voigt, N., Jost, N., Wettwer, E., Christ, T., Knaut, M., and Ravens, U. (2005). The G protein-gated potassium current $I_{K,ACh}$ is constitutively active in patients with chronic atrial fibrillation. *Circulation* 112, 3697–3706.
- Eglen, R., and Reisine, T. (2010). Primary cells and stem cells in drug discovery: emerging tools for high-throughput screening. *Assay Drug Dev. Technol.* 9, 108–124.
- Hamill, O. P., Marty, A., Neher, E., Sakmann, B., and Sigworth, J. (1981). Improved patch-clamp techniques for high resolution current recordings from cells and cell-free membrane patches. *Pflugers Arch.* 391, 85–100.
- Hashimoto, N., Yamashita, T., and Nobutomo, T. (2008). Characterization of in vivo and in vitro electrophysiological and antiarrhythmic effects of a novel $I_{K,ACh}$ blocker, NIP-151: a comparison with an IKr-blocker dofetilide. *J. Cardiovasc. Pharmacol.* 51, 162–169.
- Hashimoto, N., Yamashita, T., and Tsuruzoe, N. (2006). Tertiapin, a selective $I_{K,ACh}$ blocker, terminates atrial fibrillation with selective atrial effective refractory period prolongation. *Pharmacol. Res.* 54, 136–141.
- Hibino, H., Inanobe, A., Furutani, K., Murakami, S., Findlay, I., and Kurachi, Y. (2010). Inward rectifying potassium channels: their structure, function and physiological roles. *Physiol. Rev.* 90, 291–366.
- Inomata, N., Ohno, T., Ishihara, K., and Akaiki, N. (1993). Antiarrhythmic agents act differently on the activation phase of the ACh-response in guinea pig atrial myocytes. *Br. J. Pharmacol.* 108, 111–115.
- Jin, W., and Lu, Z. (1998). A novel high-affinity inhibitor for inward-rectifier K^+ channels. *Biochemistry* 37, 13291–13299.
- Kobayashi, T., and Ikeda, K. (2006). G protein-activated inwardly rectifying potassium channels as potential therapeutic targets. *Curr. Pharm. Des.* 12, 4513–4523.
- Kovoor, P., Wickman, K., Maguire, C., Pu, W., Gehrmann, J., Berul, C., and Clapham, D. E. (2001). Evaluation of the role of $I_{K,ACh}$ in atrial fibrillation using a mouse knockout model. *J. Am. Coll. Cardiol.* 37, 2136–2143.
- Kuzhikandathil, E. V., Yu, W., and Oxford, G. S. (1998). Human dopamine D3 and D2L receptors couple to inward rectifier potassium channels in mammalian cell lines. *Mol. Cell. Neurosci.* 12, 390–402.
- Lusscher, C., and Slesinger, P. A. (2010). Emerging roles for G protein-gated inwardly rectifying potassium (GIRK) channels in health and disease. *Nat. Rev. Neurosci.* 11, 301–315.
- Machida, T., Hashimoto, N., Kuwahara, I., Ogino, Y., Matsuura, J., Yamamoto, W., Itano, Y., Zamma, A., Matsumoto, R., Kamon, J., Kobayashi, T., Ishiwata, N., Yamashita, T., Ogura, T., and Nakaya, H. (2011). Effects of a highly selective acetylcholine-activated K^+ channel blocker on experimental atrial fibrillation. *Circ. Arrhythm. Electrophysiol.* 4, 94–102.
- Mackie, K., Lai, Y., Westenbroek, R., and Mitchell, R. (1995). Cannabinoids activate an inwardly rectifying potassium conductance and inhibit Q-type calcium currents in AtT20 cells transfected with rat brain cannabinoid receptor. *J. Neurosci.* 15, 6552–6561.
- Marker, C. L., Stoffel, M., and Wickman, K. (2004). Spinal G-protein-gated K^+ channels formed by GIRK1 and GIRK2 subunits modulate thermal nociception and contribute to morphine analgesia. *J. Neurosci.* 24, 2806–2812.
- Mitrovic, I., Margeta-Mitrovic, M., Bader, S., Stoffel, M., Jan, L. Y., and Basbaum, A. I. (2003). Contribution of GIRK2-mediated postsynaptic signaling to opiate and α_2 -adrenergic analgesia and analgesic sex differences. *Proc. Natl. Acad. Sci. U.S.A.* 100, 271–276.
- Niswender, C. M., Johnson, K. A., Luo, Q., Ayala, J. E., Kim, C., Conn, P. J., and Weaver, C. D. (2008). A novel assay of $G_{i/o}$ -linked G protein-coupled receptor coupling to potassium channels provides new insights into the pharmacology of the group III metabotropic glutamate receptors. *Mol. Pharmacol.* 73, 1213–1224.
- Nobles, M., Sebastian, S., and Tinker, A. (2010). HL-1 cells express an inwardly rectifying K^+ current activated via muscarinic receptors comparable to that in mouse atrial myocytes. *Pflugers Arch.* 460, 99–108.
- Numann, R., and Negulescu, P. (2001). High throughput screening strategies for cardiac ion channels. *Trends Cardiovasc. Med.* 11, 54–59.
- Ramu, Y., Klem, A. M., and Lu, Z. (2004). Short variable sequence acquired in evolution enables selective inhibition of various inward-rectifier K^+ channels. *Biochemistry* 43, 10701–10709.
- Walsh, K. B. (2010). A real-time screening assay for GIRK1/4 channel blockers. *J. Biomol. Screen.* 15, 1229–1237.
- Walsh, K. B., and Zhang, J. (2008). Neonatal rat cardiac fibroblasts express three types of voltage-gated K^+ channels: regulation of a transient outward current by protein kinase C. *Am. J. Physiol. Cell Physiol.* 294, H1010–H1017.
- Watanabe, Y., Hara, Y., Tamagawa, M., and Nakaya, H. (1996). Inhibitory effect of amiodarone on the muscarinic acetylcholine receptor-operated potassium current in guinea pig atrial cells. *J. Pharmacol. Exp. Ther.* 279, 617–624.
- Whit, S. M., Constantin, P. E., and Claycomb, W. C. (2004). Cardiac physiology at the cellular level: use of cultured HL-1 cardiomyocytes for studies of cardiac muscle cell structure and function. *Am. J. Physiol. Heart Circ. Physiol.* 286, H823–H829.
- Wolff, C., Fuks, B., and Chatelain, P. (2003). Comparative study of membrane potential-sensitive fluorescent probes and their use in ion channel screening assays. *J. Biomol. Screen.* 8, 533–543.
- Zhang, J.-H., Chung, T. D. Y., and Oldenburg, K. R. (1999). A simple

statistical parameter for use in evaluation and validation of high throughput screening assays. *J. Biomol. Screen.* 4, 67–73.

Conflict of Interest Statement: The author declares that the research was

conducted in the absence of any commercial or financial relationships that could be construed as a potential conflict of interest.

Received: 29 June 2011; accepted: 04 October 2011; published online: 31 October 2011.

Citation: Walsh KB (2011) Targeting GIRK channels for the development of new therapeutic agents. *Front. Pharmacol.* 2:64. doi: 10.3389/fphar.2011.00064
This article was submitted to *Frontiers in Pharmacology of Ion Channels and Channelopathies*, a specialty of *Frontiers in Pharmacology*.

Copyright © 2011 Walsh. This is an open-access article subject to a non-exclusive license between the authors and Frontiers Media SA, which permits use, distribution and reproduction in other forums, provided the original authors and source are credited and other Frontiers conditions are complied with.



Finding inward rectifier channel inhibitors: why and how?

Marcel A. G. van der Heyden*

Division Heart and Lungs, Department of Medical Physiology, University Medical Center, Utrecht, Netherlands

*Correspondence: m.a.g.vanderheyden@umcutrecht.nl

A commentary on

Discovery, characterization, and structure–activity relationships of an inhibitor of inward rectifier potassium (Kir) channels with preference for Kir2.3, Kir3.X, and Kir7.1

by Raphemot, R., Lonergan, D. F., Nguyen, T. T., Utley, T., Lewis, L. M., Kadakia, R., Weaver, C. D., Gogliotti, R., Hopkins, C., Lindsley, C. W., and Denton, J. S. (2011). *Front. Pharmacol.* 2:75. doi: 10.3389/fphar.2011.00075

The eukaryotic inward rectifier potassium (Kir) channel family is part of an ancient class of ion channels evolved in prokaryotes (Durell and Guy, 2001). Kir proteins have two transmembrane domains encompassing the pore loop region. Subunit tetramerization, either homo- or hetero-typic, results in the formation of a functional channel. The 16 known mammalian Kir channel proteins are divided over seven different families, each having their own specific expression pattern and functional characteristics (De Boer et al., 2010; Hibino et al., 2010). In general, Kir channels allow more inward potassium flow at membrane potentials negative from the potassium equilibrium potential (E_K) than outward flow at equivalent membrane potentials positive of E_K , a characteristic known as inward rectification. Within the superfamily, strong and weak rectifiers exist. Strong rectifying channels are most apparent in excitable tissues, where they are responsible for a stable and negative resting membrane potential, and due to their strong rectification, prevent extensive potassium loss during action potential formation. Weak rectifiers are expressed in numerous other tissue types and organs and have a role in processes like potassium homeostasis, insulin release, and signal transduction. Despite the long evolutionary history only a few inhibitors are known, of which most show limited specificity at their best. One of the most widely used Kir inhibitors is Ba^{2+} . However, as it blocks all Kir chan-

nels at concentrations differing not even two orders of magnitude, its severe effects in whole animal studies or poisoning cases are difficult to ascribe to a given Kir family member (De Boer et al., 2010). Given the fact that most cell types express more than one Kir channel protein, lack of specific inhibitors therefore strongly hinders our understanding of their contribution and working mechanism in normal physiology and pathology. The presence of disease causing mutations in human Kir channels that lead to severe syndromes, e.g., Bartter's syndrome (Kir1.1), Andersen Tawil syndrome (Kir2.1), SeSAME syndrome (Kir4.1), neonatal diabetes (Kir6.2), Snowflake vitreoretinal degeneration (Kir7.1) illustrate their importance in human pathology, while many more milder Kir related channelopathies probably remain unaccounted for at this moment. An excellent illustration of the potential of inward rectifier channel inhibitors comes from the field of neonatal diabetes where recognition of disease causing gain-of-function mutations in Kir6.2 (Gloyn et al., 2004) and its regulatory subunit Sur1 (Ellard et al., 2007) provided new insights to treat the disease with Kir6/Sur inhibitors (Pearson et al., 2006). One of the diseases that affects significant numbers of the aging human population, and has been correlated to Kir2.X and Kir3.X dysfunction, is atrial fibrillation. Increased Kir channel activity in the atria shortens atrial action potential durations and thereby allows formation of multiple re-entry circuits in the atrial tissue fueling rapid arrhythmia. Furthermore, ventricular Kir2.1 overexpression in mice results in rotor driven tachycardia's. These mechanisms are likely to have a role in initiation and perpetuation of the process of atrial fibrillation. Therefore, pharmacological intervention by means of Kir channel modifying drugs may be a new and valuable treatment option in this disease (Ehrlich, 2008).

Standard single cell patch clamp methods allow highly detailed characterization of the inhibiting capacity and its underlying

mechanisms of new compounds for virtually every ion channel of interest, including Kir channels. However, procedures are time consuming and therefore not compatible with large screening procedures. Automated patching techniques to a large extent overcome these throughput limitations (Dunlop et al., 2008). Alternatively, the last decade, a number of non-electrophysiological Kir assay systems have been developed that allow large scale screening assays also. Systems are either based on membrane potential sensitive dyes (e.g., Walsh, 2011) or thallium flux (e.g., Niswender et al., 2008). The latter makes use of a thallium sensitive fluorescent probe loaded into Kir expressing cells. Upon stimulation of channel opening, thallium from the bath medium enters the cell through Kir channels, resulting in increased fluorescence. Co-application of different test compounds to the bath medium than enables identification of potent Kir channel inhibitors, and dependent on the assay conditions, activators. New lead compounds for every Kir class will likely be derived from screening efforts of public, academic, or private owned compound libraries (e.g., Wang et al., 2011), or from development of existing drugs displaying Kir channel block as an apparent side effect (Van der Heyden and Sánchez-Chapula, 2011).

In this issue of *Frontiers in Pharmacology of Ion Channel and Channelopathies*, Raphemot et al. (2011) describe the results from a screen for compounds that can inhibit Kir3.X channels. For this purpose, they used a thallium flux assay in combination with a compound library originally used for discovery of new Kir1.1 inhibitors. They identified a lead compound, named VU573 that besides blocking Kir3.X, also demonstrate specificity for Kir2.3 channels over Kir2.1. Subsequent cross validation using patch clamp assays in *Xenopus* oocytes and HEK293 cells reached similar conclusions. However, VU573 showed also inhibiting action on Kir7.1. Next, making clever use of a Kir7.1 mutant, they developed and validated a Kir7.1 thallium flux assay,

and in combination with a medicinal chemistry approach, this yielded a VU573 analog that lost affinity for Kir7.1 and Kir1.1, but retained reasonable inhibition of Kir3.X and Kir2.3. This makes an interesting combination from the perspective of atrial fibrillation therapy, since Kir3.1/3.4 and Kir2.3 are predicted channels involved in atrial fibrillation (Ehrlich, 2008) as mentioned before.

New questions are arising now. What is the nature of Kir inhibition by VU573? As pointed out by the authors, drugs can directly plug the channel pore inhibiting potassium flow, interfere with lipid [i.e., phosphatidylinositol 4,5-bisphosphate (PIP₂)] dependent Kir activation or both. The preference of VU573 for Kir2.3 over Kir2.1 might indicate a role for PIP₂ interference, but extensive studies using channel structure models, Kir mutations affecting PIP₂ binding, and application of PIP₂ during patch clamp experiments are required first to answer this intriguing question. Secondly, what is the long term effect of VU573 or its derivatives on ion channel trafficking? An increasing number of drugs, regardless whether they block the channel directly, affect channel protein trafficking resulting in decreased amounts of functional channels on the plasma membrane which may pose an arrhythmogenic risk (Van der Heyden et al., 2008). Thirdly, is a combined Kir3.X and Kir2.3 block effective indeed against atrial fibrillation without affecting ventricular electrophysiological parameters? Dedicated *in vitro* and *in vivo* models are essential here to answer these questions.

The data reported by Raphemot et al. (2011) are another step in the development of subtype specific I_{K1} modifiers that eventually will provide valuable insights into

the roles of I_{K1} in normal physiology and may offer clinicians new treatment options for a diverse set of genetic syndromes and acquired diseases.

ACKNOWLEDGMENTS

I thank Dr. T. P. de Boer for careful reading of the manuscript. This work was supported by a grant from the Dondersfonds (Utrecht, The Netherlands).

REFERENCES

- De Boer, T. P., Houtman, M. J. C., Compier, M., and Van der Heyden, M. A. G. (2010). The mammalian KIR2.x inward rectifier ion channel family: expression pattern and pathophysiology. *Acta Physiol. (Oxf.)* 199, 243–256.
- Dunlop, J., Bowlby, M., Peri, R., Vasilyev, D., and Arias, R. (2008). High-throughput electrophysiology: an emerging paradigm for ion-channel screening and physiology. *Nat. Rev. Drug Discov.* 7, 358–368.
- Durell, S. R., and Guy, H. R. (2001). A family of putative Kir potassium channels in prokaryotes. *BMC Evol. Biol.* 1, 14. doi: 10.1186/1471-2148-1-14
- Ehrlich, J. R. (2008). Inward rectifier potassium currents as a target for atrial fibrillation therapy. *J. Cardiovasc. Pharmacol.* 52, 129–135.
- Ellard, S., Flanagan, S. E., Girard, C. A., Patch, A. M., Harries, L. W., Parrish, A., Edghill, E. L., Mackay, D. J., Proks, P., Shimomura, K., Haberland, H., Carson, D. J., Shield, J. P., Hattersley, A. T., and Ashcroft, F. M. (2007). Permanent neonatal diabetes caused by dominant, recessive, or compound heterozygous SUR1 mutations with opposite functional effects. *Am. J. Hum. Genet.* 81, 375–382.
- Gloyn, A. L., Pearson, E. R., Antcliff, J. F., Proks, P., Bruining, G. J., Slingerland, A. S., Howard, N., Srinivasan, S., Silva, J. M., Molnes, J., Edghill, E. L., Frayling, T. M., Temple, I. K., Mackay, D., Shield, J. P., Sumnik, Z., Van Rhijn, A., Wales, J. K., Clark, P., Gorman, S., Aisenberg, J., Ellard, S., Njolstad, P. R., Ashcroft, F. M., and Hattersley, A. T. (2004). Activating mutations in the gene encoding the ATP-sensitive potassium-channel subunit Kir6.2 and permanent neonatal diabetes. *N. Engl. J. Med.* 350, 1838–1849.
- Hibino, H., Inanobe, A., Furutani, K., Murakami, S., Findlay, I., and Kurachi, Y. (2010). Inwardly rectifying potassium channels: their structure, function, and physiological roles. *Physiol. Rev.* 90, 291–366.
- Niswender, C. M., Johnson, K. A., Luo, Q., Ayala, J. E., Kim, C., Conn, P. J., and Weaver, C. D. (2008). A novel assay of Gi/o-linked G protein-coupled receptor coupling to potassium channels provides new insights into the pharmacology of the group III metabotropic glutamate receptors. *Mol. Pharmacol.* 73, 1213–1224.
- Pearson, E. R., Flechtner, I., Njolstad, P. R., Malecki, M. T., Flanagan, S. E., Larkin, B., Ashcroft, F. M., Klimes, I., Codner, E., Iotova, V., Slingerland, A. S., Shield, J., Robert, J. J., Holst, J. J., Clark, P. M., Ellard, S., Søvik, O., Polak, M., Hattersley, A. T., and Neonatal Diabetes International Collaborative Group. (2006). Switching from insulin to oral sulfonylureas in patients with diabetes due to Kir6.2 mutations. *N. Engl. J. Med.* 355, 467–477.
- Van der Heyden, M. A. G., and Sánchez-Chapula, J. A. (2011). Toward specific cardiac IK1 modulators for *in vivo* application: old drugs point the way. *Heart Rhythm* 8, 1076–1080.
- Van der Heyden, M. A. G., Smits, M. E., and Vos, M. A. (2008). Drugs and trafficking of ion channels: a new pro-arrhythmic threat on the horizon? *Br. J. Pharmacol.* 153, 406–409.
- Walsh, K. B. (2011). Targeting GIRK channels for the development of new therapeutic agents. *Front. Pharmacol.* 2:64. doi: 10.3389/fphar.2011.00064
- Wang, H. R., Wu, M., Yu, H., Long, S., Stevens, A., Engers, D. W., Sackin, H., Daniels, J. S., Dawson, E. S., Hopkins, C. R., Lindsley, C. W., Li, M., and McManus, O. B. (2011). Selective inhibition of the Kir2 family of inward rectifier potassium channels by a small molecule probe: the discovery, SAR, and pharmacological characterization of ML133. *ACS Chem. Biol.* 6, 845–856.

Received: 11 November 2011; accepted: 23 December 2011; published online: 09 January 2012.

Citation: van der Heyden MAG (2012) Finding inward rectifier channel inhibitors: why and how? *Front. Pharmacol.* 2:95. doi: 10.3389/fphar.2011.00095

This article was submitted to *Frontiers in Pharmacology of Ion Channels and Channelopathies*, a specialty of *Frontiers in Pharmacology*.

Copyright © 2012 van der Heyden. This is an open-access article distributed under the terms of the Creative Commons Attribution Non Commercial License, which permits non-commercial use, distribution, and reproduction in other forums, provided the original authors and source are credited.



Discovery, characterization, and structure–activity relationships of an inhibitor of inward rectifier potassium (Kir) channels with preference for Kir2.3, Kir3.X, and Kir7.1

Rene Raphemot^{1,2†}, Daniel F. Loneragan^{1†}, Thuy T. Nguyen^{1,2}, Thomas Utley², L. Michelle Lewis³, Rishin Kadakia¹, C. David Weaver^{2,3}, Rocco Gogliotti^{2,4}, Corey Hopkins^{2,3,4,5,6}, Craig W. Lindsley^{2,3,4,5,6} and Jerod S. Denton^{1,2,3*}

¹ Department of Anesthesiology, Vanderbilt University School of Medicine, Nashville, TN, USA

² Department of Pharmacology, Vanderbilt University School of Medicine, Nashville, TN, USA

³ Vanderbilt Institute of Chemical Biology, Vanderbilt University, Nashville, TN, USA

⁴ Vanderbilt Center for Neuroscience Drug Discovery, Vanderbilt University School of Medicine, Nashville, TN, USA

⁵ Department of Chemistry, Vanderbilt University, Nashville, TN, USA

⁶ Vanderbilt Specialized Chemistry Center for Accelerated Probe Development, Molecular Libraries Probe Production Centers Network, Nashville, TN, USA

Edited by:

Ralf Franz Kettenhofen, Axiogenesis AG, Germany

Reviewed by:

Oscar Moran, Institute of Biophysics, National Research Council, Italy
Marcel Van Der Heyden, University Medical Center, Netherlands

*Correspondence:

Jerod S. Denton, Department of Anesthesiology, Vanderbilt University School of Medicine, T4208 Medical Center North, 1161 21st Avenue South, Nashville, TN 37232, USA.
e-mail: jerod.s.denton@vanderbilt.edu

[†] Rene Raphemot and Daniel F. Loneragan have contributed equally to this work.

The inward rectifier family of potassium (Kir) channels is comprised of at least 16 family members exhibiting broad and often overlapping cellular, tissue, or organ distributions. The discovery of disease-causing mutations in humans and experiments on knockout mice has underscored the importance of Kir channels in physiology and in some cases raised questions about their potential as drug targets. However, the paucity of potent and selective small-molecule modulators targeting specific family members has with few exceptions mired efforts to understand their physiology and assess their therapeutic potential. A growing body of evidence suggests that G protein-coupled inward rectifier K (GIRK) channels of the Kir3.X subfamily may represent novel targets for the treatment of atrial fibrillation. In an effort to expand the molecular pharmacology of GIRK, we performed a thallium (Tl⁺) flux-based high-throughput screen of a Kir1.1 inhibitor library for modulators of GIRK. One compound, termed VU573, exhibited 10-fold selectivity for GIRK over Kir1.1 (IC₅₀ = 1.9 and 19 μM, respectively) and was therefore selected for further study. In electrophysiological experiments performed on *Xenopus laevis* oocytes and mammalian cells, VU573 inhibited Kir3.1/3.2 (neuronal GIRK) and Kir3.1/3.4 (cardiac GIRK) channels with equal potency and preferentially inhibited GIRK, Kir2.3, and Kir7.1 over Kir1.1 and Kir2.1. Tl⁺ flux assays were established for Kir2.3 and the M125R pore mutant of Kir7.1 to support medicinal chemistry efforts to develop more potent and selective analogs for these channels. The structure–activity relationships of VU573 revealed few analogs with improved potency, however two compounds retained most of their activity toward GIRK and Kir2.3 and lost activity toward Kir7.1. We anticipate that the VU573 series will be useful for exploring the physiology and structure–function relationships of these Kir channels.

Keywords: GIRK, pharmacology, screening, thallium flux, fluorescence, electrophysiology, high throughput

INTRODUCTION

The inward rectifier family of potassium (Kir) channels is comprised of at least 16 family members exhibiting unique functional and regulatory properties that enable them to carry out important functions in most organ systems (Hebert et al., 2005; Hibino et al., 2010). Kir channels preferentially pass current in the inward direction at voltages more negative than the Nernst electrochemical equilibrium potential for potassium (E_K). Unlike their voltage-gated potassium channel counterparts, Kir channels lack discrete voltage-sensing domains that regulate pore opening. Rather, the rectification of the channel conductance–voltage relationship is due to voltage-dependent pore block by magnesium and polyamines at potentials more positive than E_K . The degree of rectification varies widely between family members and is used

to categorize them functionally into groups of strong versus weak rectifiers. In general, strong rectifiers are expressed in excitable cells such as neurons and muscle cells, whereas weak rectifiers are expressed in epithelial and other non-excitable cell types (Hibino et al., 2010). Some Kir channels are postulated therapeutic targets for common diseases (Bhave et al., 2010). Consequently, we have been working to develop small-molecule probes of clinically relevant Kir channels to provide sharper pharmacological tools with which to study their physiological roles and therapeutic potential.

The founding Kir channel family member Kir1.1, is a weak rectifier encoded by the gene *KCNJ1* (Ho et al., 1993; Zhou et al., 1994). Kir1.1 is expressed almost exclusively in epithelial cells of the renal tubule where it critically regulates salt and water balance

and hence blood volume and pressure (Welling and Ho, 2009). Autosomal recessive mutations in *KCNJ1* give rise to antenatal Bartter syndrome, a severe salt and water wasting disorder characterized by hypokalemic metabolic alkalosis and low to normal blood pressure (Simon et al., 1996). In contrast, heterozygous carriers of *KCNJ1* mutations have lower blood pressure but no overt evidence of disease (Ji et al., 2008). These genetic data raise the intriguing possibility that Kir1.1 represents a drug target for a novel class of diuretic. Consequently, our group recently employed high-throughput screening and medicinal chemistry to develop the first publicly disclosed small-molecule inhibitors of Kir1.1 (Lewis et al., 2009; Bhavé et al., 2011). These, as well as inhibitors recently disclosed by investigators at Merck (Pasternak et al., 2010), should be instrumental in assessing the therapeutic potential of Kir1.1 for the management of hypertension.

Another emerging drug target in the Kir channel family is the G protein-coupled inward rectifier potassium (GIRK) channel, which is expressed in the heart and throughout the nervous system (Hibino et al., 2010). The major cardiac form of GIRK is a heterotetrameric channel comprised of Kir3.1 and Kir3.4 subunits, which is expressed primarily in atrial but not ventricular myocytes. In the nervous system, heteromeric GIRK channels are primarily formed by Kir3.1 and Kir3.2. In the basal state, GIRK channels exhibit a low open-state probability and therefore contribute little to the resting membrane potassium conductance and potential. In the heart, sympathetic release of acetylcholine (ACh) onto M2 muscarinic receptors leads to G protein-dependent opening of GIRK channels, potassium efflux, and consequent membrane hyperpolarization. The ACh-induced increase in potassium conductance slows the rate of membrane depolarization, action potential generation, and heart rate. In patients with chronic atrial fibrillation, GIRK channels become constitutively active in atrial cardiomyocytes through mechanisms that are incompletely understood (Dobrev et al., 2005; Voigt et al., 2007; Makary et al., 2011). This background current hyperpolarizes the membrane potential, abbreviates the action potential, and increases the availability sodium channels for activation. A growing body of experimental and clinical data support the notion that electrical remodeling sets up high-frequency re-entrant current sources that perpetuate atrial fibrillation, suggesting that a specific blocker of GIRK could have anti-arrhythmic actions without the ventricular side effects commonly associated with current therapies (reviewed in Wakili et al., 2011). Similarly, the other Kir channel family member Kir2.3 is enriched in atrial cardiomyocytes and may also be a pharmaceutical target for atrial fibrillation (Ehrlich, 2008).

The molecular pharmacology of GIRK and most other inward rectifiers is limited. A high-throughput screen using a voltage-sensitive dye identified analogs of amiloride (a K⁺ sparing diuretic) and propafenone (a class 1c anti-arrhythmic) that inhibit GIRK with sub-micromolar potencies (Walsh, 2010). These and several cardiac and neurological drugs exhibiting weak off-target activity toward GIRK (reviewed in Bhavé et al., 2010) may be useful lead compounds for developing more specific inhibitors of GIRK. The bee venom toxin tertiapin is a nanomolar affinity GIRK antagonist that also inhibits Kir1.1 (Jin and Lu, 1998; Kitamura et al., 2000). Hashimoto et al. (2006) demonstrated that administration of tertiapin to cannulated dogs terminated induced atrial

fibrillation, providing some of the first experimental evidence that GIRK is a target for anti-arrhythmic therapeutics (Hashimoto et al., 2006). Nissan Chemical Industries developed a benzopyrene derivative, termed NIP-142, which inhibits Kir3.1/3.4 GIRK channels with sub-micromolar affinity and the cardiac Kv1.5 delayed rectifier current with equal potency (Matsuda et al., 2006; Tanaka and Hashimoto, 2007). NIP-142 has shown efficacy in terminating induced atrial fibrillation in dogs, but it is unknown whether the improvement in sinus rhythm is due to inhibition of GIRK, Kv1.5, or both. However, the low nanomolar inhibitor NTC-801, which is highly selective for GIRK over other cardiac channels, was shown recently to be effective in several models of atrial fibrillation (Machida et al., 2011).

In an effort to further expand the molecular pharmacology of GIRK, we employed a TI⁺ flux-based fluorescence assay to screen a Kir1.1 inhibitor focus library for antagonists of GIRK. One compound termed VU573 was found to preferentially inhibit GIRK (cardiac and neuronal forms), Kir2.3 and Kir7.1 over Kir1.1 and Kir2.1. We anticipate that VU573 and its analogs will be useful for investigating the physiology and structure–function relationships of inward rectifier potassium channels.

MATERIALS AND METHODS

EXPRESSION VECTORS

Plasmids used in this study are from the following sources: rat Kir1.1 (NM_017023; Chun Jiang, Georgia State University, Atlanta, GA, USA), human Kir2.1 (NM_000891.2; Al George, Vanderbilt University School of Medicine, Nashville, TN, USA), human Kir7.1 (NM_002242.2; David Clapham, Harvard Medical School, Cambridge, MA, USA). Human Kir1.1 (NM_000220), Kir3.1 (NM_002239.2), Kir3.2 (NM_002240.2), Kir3.4 (NM_000890.3), and Kir2.3 (NM_152868) were purchased from OriGene Technologies (Rockville, MD, USA). The M125R mutant of Kir7.1 was created using the QuickChange Site-Directed Mutagenesis Kit (Agilent Technologies). The open reading frame of Kir7.1 was fully sequenced to ensure that no spurious mutations were introduced during mutation of the intended codon.

CELL LINES

Monoclonal mGluR8/GIRK/HEK cells stably expressing Kir3.1/3.2, the M4 muscarinic receptor and rat mGlu8a were cultured as described previously (Niswender et al., 2008). Polyclonal stable T-REx-HEK-293 cell lines expressing Kir2.3 and Kir7.1-M125R under the control of a tetracycline-inducible promoter were established essentially as described in detail elsewhere (Fallen et al., 2009; Lewis et al., 2009). Monoclonal Kir2.3 cell lines were isolated through limiting dilution in 384-well plates and testing for tetracycline-inducible TI⁺ flux, as described below. Polyclonal Kir7.1-M125R cells were used in this study. The development of monoclonal C1 T-REx-HEK-293 cells expressing Kir1.1 (S44D) was described previously (Lewis et al., 2009). T-REx-HEK-293 lines were cultured in DMEM growth medium containing 10% FBS, 50 U/mL Penicillin, 50 µg/mL Streptomycin, 5 µg/mL Blasticidin S, and 250 µg/mL Hygromycin.

TWO-ELECTRODE VOLTAGE-CLAMP ANALYSIS

Stage V–VI oocytes were isolated from gravid *Xenopus laevis* frogs using sterile surgical techniques under tricaine anesthesia. All

methods were in accordance with the guidelines for the use of laboratory animals of Vanderbilt University School of Medicine. The oocyte follicle layer was removed by manual dissection following enzymatic treatment with 1 mg/mL collagenase (Type 1A Sigma) dissolved in calcium-free OR-2 of the following composition (in mM): 82.5 NaCl, 2 KCl, 1 MgCl₂, 5 HEPES, with pH 7.5 adjusted with NaOH. Oocytes were allowed to recover overnight at 16°C in modified L-15 media containing gentamicin sulfate (25 mg/mL).

pcDNA3.1(+) vectors carrying Kir1.1, human Kir2.1, 2.3, and 7.1 cDNA were used to synthesize channel cRNA from a T7 RNA polymerase and nucleotides provided in the mMESSAGE mMACHINE kit (Ambion, Austin, TX, USA) after linearization of the expression constructs. cRNA was purified by LiCl precipitation, diluted in RNAase-free water and used for injections. The oocytes were injected with 0.5–10 ng of cRNA of Kir1.1, Kir2.1, Kir2.3, and Kir7.1 using a Drummond digital microdispenser. Oocytes were incubated at 16°C in modified L-15 for 24–72 h prior to Kir channel recordings.

Whole-cell currents were recorded from *Xenopus* oocytes injected with Kir channel cRNA using the two-electrode voltage-clamp (TEVC) technique. Current and voltage commands were generated with a GeneClamp 600 amplifier, a Digidata 1200 A/D converter, and pCLAMP 8.0 software (Molecular Devices, Sunnyvale, CA, USA). The bath was actively clamped to 0 mV using a VG-2A bath clamp (Molecular Devices). Electrodes pulled from borosilicate glass (Sutter Instruments, Novato, CA, USA) using a PP-830 vertical puller (Narishige International, Narishige, Japan) had resistances of 0.5–5.0 MΩ when filled with 3 M KCl. The standard bath solution contained (in mM): 85 NaCl, 5 KCl, 10 HEPES, 2 MgCl₂, pH 7.4 with NaOH. After achieving stable current amplitude, VU573 was applied continuously. This was followed by application of the non-specific potassium channel blocker barium. For Kir current recordings, cells were voltage-clamped and stepped every 5 s from a holding potential of –70 to –100 mV for 200 ms, then ramped at a rate of 1.6 mV/ms to 60 mV before returning to –80 mV. All recordings were made at room temperature (20–23°C).

WHOLE-CELL PATCH CLAMP ELECTROPHYSIOLOGY

T-REx-HEK-293-Kir2.3 cells were patch clamped after overnight induction with tetracycline (1 µg/mL). GIRK (Kir3.1/3.2) and wild type Kir7.1 were studied in HEK-293 cells transiently co-transfected with the respective channel expression vectors and pcDNA3.1-EGFP (transfection marker) using Lipofectamine LTX/Plus reagent according to manufacturer's protocol (Invitrogen, Carlsbad, CA, USA). The standard intracellular solution contained 135 mM KCl, 2 mM MgCl₂, 1 mM EGTA, 10 mM HEPES-free acid, and 2 mM Na₂ ATP (Roche), pH 7.3, adjusted to 275 mOsmol/kg with sucrose. For Kir2.3 recordings, MgCl₂ was reduced to 1 mM to prevent channel rundown (Chuang et al., 1997). The standard bath solution contained 135 mM NaCl, 5 mM KCl, 2 mM CaCl₂, 1 mM MgCl₂, 5 mM glucose, and 10 mM HEPES-free acid, pH 7.4, 290 mOsmol/kg. In some experiments, a high-K⁺ bath was used that contained 90 mM NaCl, 50 mM KCl, 2 mM CaCl₂, 1 mM MgCl₂, 5 mM glucose, and 10 mM HEPES-free acid, pH 7.4, 290 mM mOsmol/kg. Kir current recordings were collected as previously described (Bhave et al., 2011). After

achieving stable whole-cell currents, VU573 was applied intermittently or continuously for 2–10 min, followed by application of 2 mM BaCl₂. Data acquisition and analysis were performed using pClamp 9.2 software (Molecular Devices). All recordings were made at room temperature (20–23°C).

TEST COMPOUND AND STIMULUS PLATE PREPARATION

Compound master antagonist plates were created by serial diluting compounds 1:3 from 10 mM stock in 100% DMSO using the BRAVO liquid handler (Agilent Technologies, Santa Clara, CA, USA). Assay daughter plates were created using the ECHO 555 liquid handler (Labcyte, Sunnyvale, CA, USA), transferring 240 nL from the master plate to the daughter plate for each well followed by addition of 40 µL of assay buffer resulting in antagonist compound concentration–response curves (CRC) starting at 60 µM (2× final concentration). Glutamate was diluted in TI⁺ buffer [125 mM sodium bicarbonate (added fresh the morning of the experiment), 1 mM magnesium sulfate, 1.8 mM calcium sulfate, 5 mM glucose, 12 mM TI⁺ sulfate, and 10 mM HEPES, pH 7.3] at 5× the final concentration to be assayed.

KINETIC IMAGING, DATA ANALYSIS, AND STATISTICS

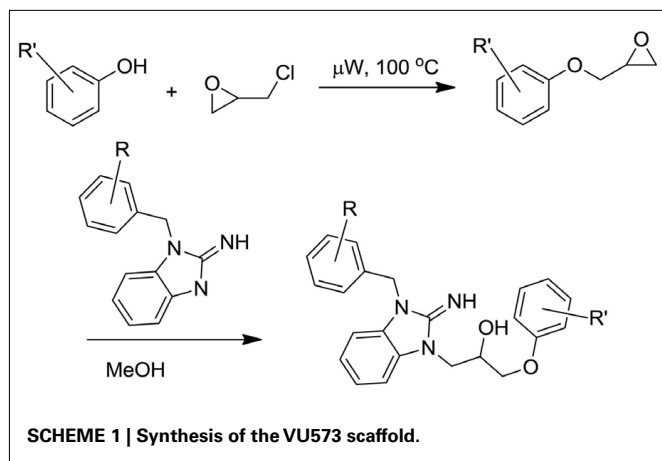
Cells were loaded with the TI⁺ sensitive fluorescent dye FluoZin-2 and plated in clear-bottom 384-well plates essentially as described previously (Lewis et al., 2009; Bhave et al., 2011). Cell plates and daughter compound plates were loaded onto a kinetic imaging plate reader (FDSS 6000; Hamamatsu Corporation, Bridgewater, NJ, USA). All recordings were made at room temperature (20–23°C). Appropriate baseline readings were taken (10 images at 1 Hz; excitation, 470 ± 20 nm; emission, 540 ± 30 nm) and 20 µL test compounds were added followed by 50 images at 1 Hz additional baseline. Following a 20-min incubation period, baseline readings were taken for 30 s followed by addition of 10 µL Glutamate at an EC₈₀ concentration. An additional 170 images were taken at 1 Hz. Glutamate EC₈₀ concentration was determined the day of the assay.

Data were analyzed using Excel (Microsoft Corp, Redmond, WA, USA). Raw data were opened in Excel and each data point in a given trace was divided by the first data point from that trace (static ratio). For experiments in which antagonists were added, data were again normalized by dividing each point by the fluorescence value immediately before the glutamate addition to correct for any subtle differences in the baseline traces after the compound incubation period. The slope of the fluorescence increase beginning 5 s after TI⁺/glutamate addition and ending 15 s after TI⁺/glutamate addition was calculated. The data were then plotted in Prism software (GraphPad Software, San Diego, CA, USA) to generate CRC after correcting for the slope values determined for baseline waveforms generated in the presence of vehicle controls. Potencies were calculated from fits using a four-parameter logistic equation.

CHEMICAL SYNTHESIS

General

All NMR spectra were recorded on a 400-MHz AMX Bruker NMR spectrometer. ¹H chemical shifts are reported in δ values in part per million downfield with the deuterated solvent as the internal standard. Data are reported as follows: chemical shift, multiplicity (s = singlet, d = doublet, t = triplet, q =



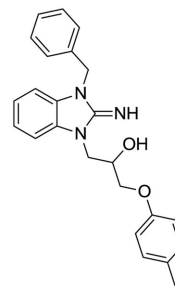
quartet, br = broad, m = multiplet), integration, coupling constant (Hz). Low resolution mass spectra were obtained on an Agilent 1200 series 6130 mass spectrometer with electrospray ionization. High-resolution mass spectra were recorded on a Waters Q-TOF API-US plus Acquity system with electrospray ionization. Analytical thin layer chromatography was performed on EM Reagent 0.25 mm silica gel 60-F plates. Samples were analyzed for $\geq 95\%$ purity using LC-UV/Vis-MS. Analytical HPLC was performed on an Agilent 1200 series with UV detection at 214 and 254 nm along with ELSD detection. LC/MS: method 1 = J-Sphere80-C18, 3.0 mm \times 50 mm, 4.1 min gradient, 5%[0.05%TFA/CH₃CN]:95%[0.05%TFA/H₂O] to 100% [0.05%TFA/CH₃CN]; method 2 = Phenomenex-C18, 2.1 mm \times 30 mm, 2 min gradient, 7%[0.1%TFA/CH₃CN]:93%[0.1%TFA/H₂O] to 100%[0.1%TFA/CH₃CN]; method 3 = Phenomenex-C18, 2.1 mm \times 30 mm, 1 min gradient, 7%[0.1%TFA/CH₃CN]:93%[0.1%TFA/H₂O] to 95%[0.1%TFA/CH₃CN]. Preparative purification was performed on a custom HP1100 purification system (Leister et al., 2003) with collection triggered by mass detection. Solvents for extraction, washing, and chromatography were HPLC grade. All reagents were purchased from Aldrich Chemical Co. and were used without purification.

Reagents. Substituted phenols were purchased from various commercial sources, 2-Amino-1-benzylbenzimidazole and 2-Amino-1-methylbenzimidazole were purchased from Acros Organics. 1-(4-Chlorophenylmethyl)-2-aminobenzimidazole was made using published procedures (Caroti et al., 1986).

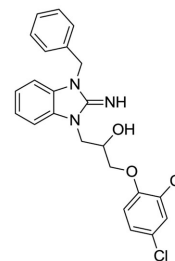
General synthetic procedure

The desired phenol (2 mmol) was dissolved in 0.4 mL NaOH (5 M) and then treated with epichlorohydrin (0.32 mL, 3.7 mmol; **Scheme 1**). The mixture was heated in a Biotage Initiator microwave reactor at 100°C for a 15-min period. The reaction was cooled to ambient temperature and diluted with dichloromethane. The aqueous layer was removed and the organic layer extracted with water. The mixture was dried and solvent removed under reduced pressure. The crude mixture was then treated with the desired 2-aminobenzimidazole (3 mL, 0.2 mmol, 0.7 M MeOH) dissolved in methanol (**Scheme 1**). The mixture was allowed to stir for 4 days at ambient temperature. The solvent was

removed under reduced pressure and the residue was diluted with dichloromethane. The mixture was extracted with water, dried, and concentrated under reduced pressure. The crude was purified using reverse phase chromatography (C18, Acetonitrile/H₂O 0.1% TFA).

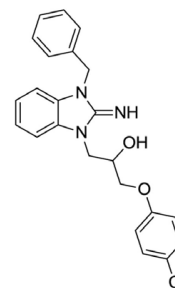


1-(3-benzyl-2-imino-2,3-dihydro-1H-benzo[d]imidazol-1-yl)-3-(p-tolyloxy)propan-2-ol (1). Purchased from ChemBridge.



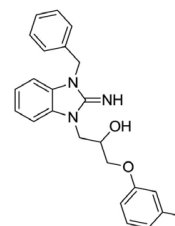
1-(3-benzyl-2-imino-2,3-dihydro-1H-benzo[d]imidazol-1-yl)-3-(2,4-dichlorophenoxy)propan-2-ol (2).

LCMS: Rt = 1.41 min., >98%, m/z = 443 [M + H].



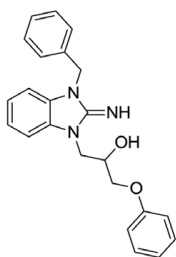
1-(3-benzyl-2-imino-2,3-dihydro-1H-benzo[d]imidazol-1-yl)-3-(4-chlorophenoxy)propan-2-ol (3).

LCMS: Rt = 1.38 min., >98%, m/z = 408 [M + H].



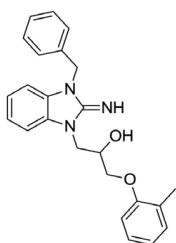
1-(3-benzyl-2-imino-2,3-dihydro-1H-benzo[d]imidazol-1-yl)-3-(m-tolyloxy)propan-2-ol (4).

Purchased from InterBioScreen.



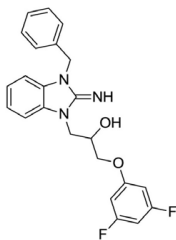
1-(3-benzyl-2-imino-2,3-dihydro-1*H*-benzo[d]imidazol-1-yl)-3-phenoxypropan-2-ol (5).

Purchased from ChemBridge.



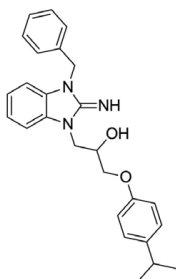
1-(3-benzyl-2-imino-2,3-dihydro-1*H*-benzo[d]imidazol-1-yl)-3-(*o*-tolylloxy)propan-2-ol (6).

Purchased from ChemBridge.



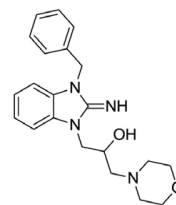
1-(3-benzyl-2-imino-2,3-dihydro-1*H*-benzo[d]imidazol-1-yl)-3-(3,5-difluorophenoxy)propan-2-ol (7).

LCMS: $R_t = 1.05$ min., >98%, $m/z = 410$ [M + H].



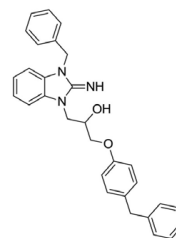
1-(3-benzyl-2-imino-2,3-dihydro-1*H*-benzo[d]imidazol-1-yl)-3-(4-isopropylphenoxy)propan-2-ol (8).

LCMS: $R_t = 1.14$ min., >98%, $m/z = 416$ [M + H].



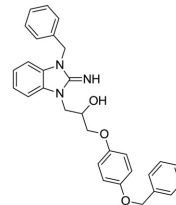
1-(3-benzyl-2-imino-2,3-dihydro-1*H*-benzo[d]imidazol-1-yl)-3-morpholinopropan-2-ol (9).

LCMS: $R_t = 0.67$ min., >98%, $m/z = 367$ [M + H].



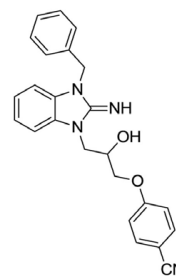
1-(3-benzyl-2-imino-2,3-dihydro-1*H*-benzo[d]imidazol-1-yl)-3-(4-benzylphenoxy)propan-2-ol (10).

LCMS: $R_t = 1.19$ min., >98%, $m/z = 464$ [M + H].



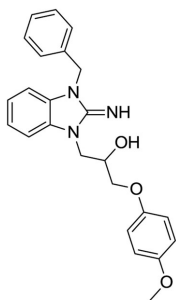
1-(3-benzyl-2-imino-2,3-dihydro-1*H*-benzo[d]imidazol-1-yl)-3-(4-(benzyloxy)phenoxy)propan-2-ol (11).

LCMS: $R_t = 1.16$ min., >98%, $m/z = 480$ [M + H].



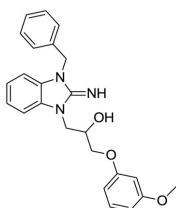
4-(3-(3-benzyl-2-imino-2,3-dihydro-1*H*-benzo[d]imidazol-1-yl)-2-hydroxypropoxy)benzonitrile (12).

LCMS: $R_t = 1.00$ min., >98%, $m/z = 399$ [M + H].



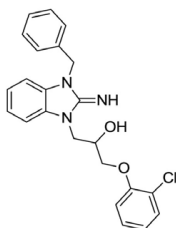
1-(3-benzyl-2-imino-2,3-dihydro-1*H*-benzo[d]imidazol-1-yl)-3-(4-methoxyphenoxy)propan-2-ol (13).

LCMS: Rt = 1.00 min., >98%, m/z = 404 [M + H].



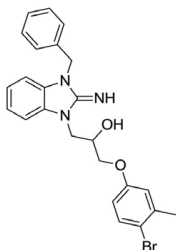
1-(3-benzyl-2-imino-2,3-dihydro-1*H*-benzo[d]imidazol-1-yl)-3-(3-methoxyphenoxy)propan-2-ol (14).

LCMS: Rt = 1.01 min., >98%, m/z = 404 [M + H].



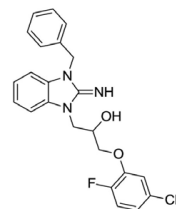
1-(3-benzyl-2-imino-2,3-dihydro-1*H*-benzo[d]imidazol-1-yl)-3-(2-chlorophenoxy)propan-2-ol (15).

LCMS: Rt = 1.08 min., 90%, m/z = 408 [M + H].



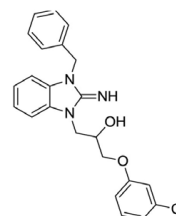
1-(3-benzyl-2-imino-2,3-dihydro-1*H*-benzo[d]imidazol-1-yl)-3-(4-bromo-3-methylphenoxy)propan-2-ol (16).

LCMS: Rt = 1.13 min., >98%, m/z = 466 [M + H].



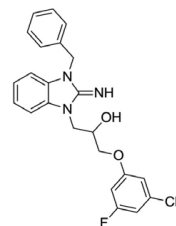
3-(3-(3-benzyl-2-imino-2,3-dihydro-1*H*-benzo[d]imidazol-1-yl)-2-hydroxypropoxy)-4-fluorobenzonitrile (17).

LCMS: Rt = 0.99 min., >98%, m/z = 417 [M + H].



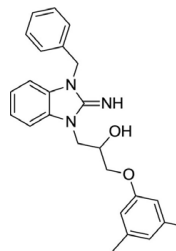
1-(3-benzyl-2-imino-2,3-dihydro-1*H*-benzo[d]imidazol-1-yl)-3-(3-chlorophenoxy)propan-2-ol (18).

LCMS: Rt = 1.06 min., >98%, m/z = 408 [M + H].



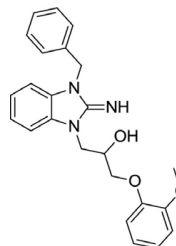
3-(3-(3-benzyl-2-imino-2,3-dihydro-1*H*-benzo[d]imidazol-1-yl)-2-hydroxypropoxy)-5-fluorobenzonitrile (19).

LCMS: Rt = 1.00 min., 90%, m/z = 417 [M + H].



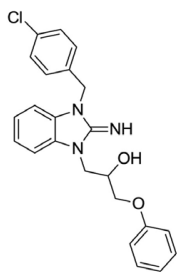
1-(3-benzyl-2-imino-2,3-dihydro-1*H*-benzo[d]imidazol-1-yl)-3-(3,5-dimethylphenoxy)propan-2-ol (20).

LCMS: Rt = 1.10 min., 93%, m/z = 402 [M + H].



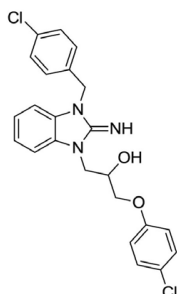
1-(3-benzyl-2-imino-2,3-dihydro-1*H*-benzo[d]imidazol-1-yl)-3-(2-methoxyphenoxy)propan-2-ol (21).

LCMS: Rt = 0.98 min., >98%, m/z = 404 [M + H].



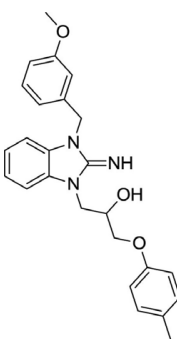
1-(3-(4-chlorobenzyl)-2-imino-2,3-dihydro-1*H*-benzo[d]imidazol-1-yl)-3-phenoxypropan-2-ol (22).

LCMS: Rt = 1.33 min., 87%, m/z = 408 [M + H].



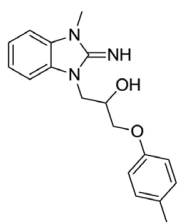
1-(3-(4-chlorobenzyl)-2-imino-2,3-dihydro-1*H*-benzo[d]imidazol-1-yl)-3-(4-chlorophenoxy)propan-2-ol (23).

LCMS: Rt = 1.38 min., >98%, m/z = 442 [M + H].



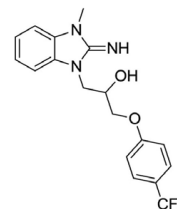
1-(2-imino-3-(3-methoxybenzyl)-2,3-dihydro-1*H*-benzo[d]imidazol-1-yl)-3-(*p*-tolylloxy)propan-2-ol (24).

LCMS: Rt = 1.05 min., >98%, m/z = 418 [M + H].



1-(2-imino-3-methyl-2,3-dihydro-1*H*-benzo[d]imidazol-1-yl)-3-(*p*-tolylloxy)propan-2-ol (25).

LCMS: Rt = 0.91 min., >98%, m/z = 312 [M + H].



1-(2-imino-3-methyl-2,3-dihydro-1*H*-benzo[d]imidazol-1-yl)-3-(4-(trifluoromethyl)phenoxy)propan-2-ol (26).

LCMS: Rt = 1.11 min., >98%, m/z = 442 [M + H].

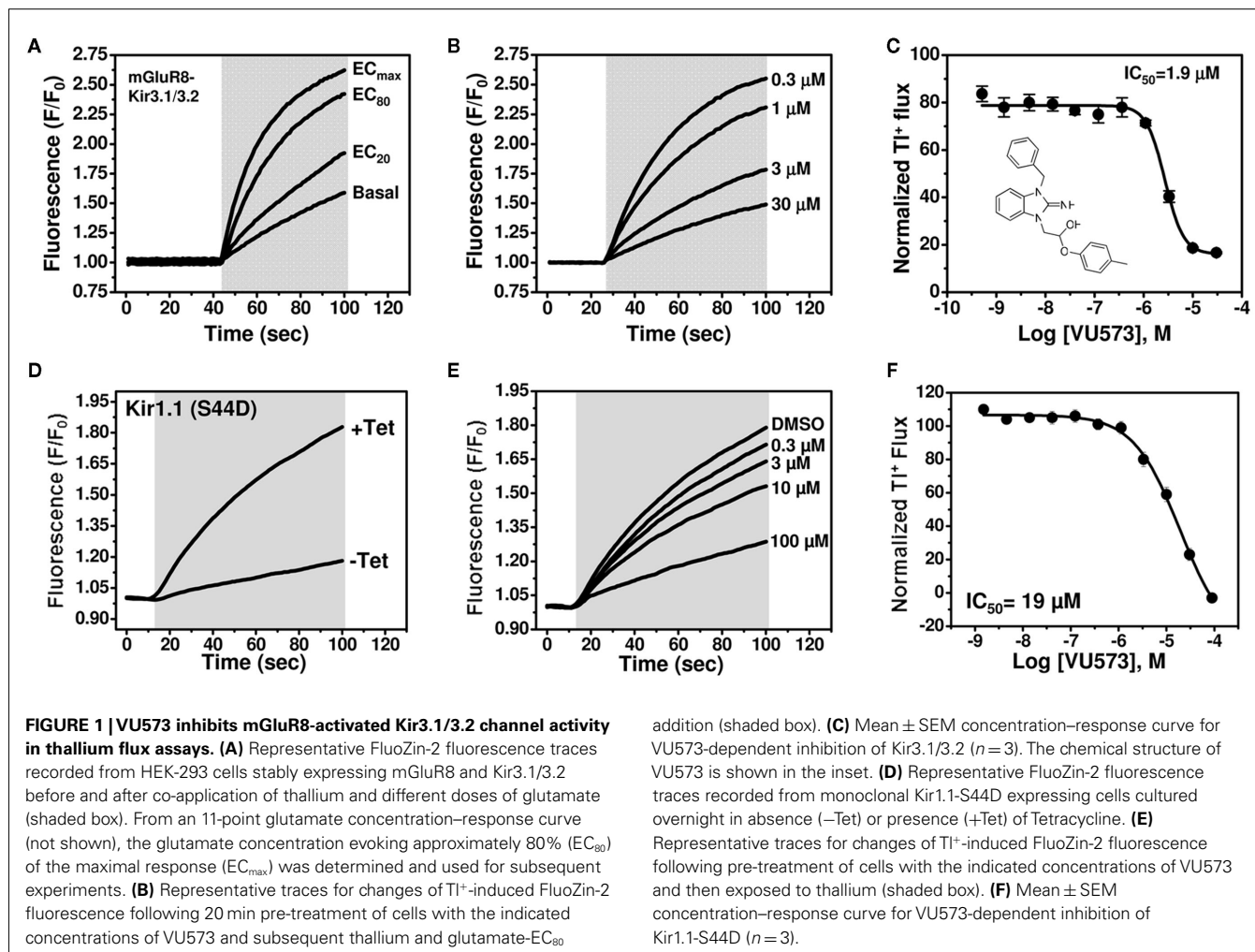
RESULTS

VU573: A WEAK Kir1.1 INHIBITOR THAT PREFERENTIALLY INHIBITS GIRK

We recently performed a high-throughput screen (HTS) for small-molecule modulators of Kir1.1 (Lewis et al., 2009), the founding member of the inward rectifier potassium (Kir) channel family (Ho et al., 1993; Zhou et al., 1994) and putative diuretic target (Simon et al., 1996; Ji et al., 2008; Pasternak et al., 2010). A focused library of reproducibly active inhibitors was assembled from the primary screen, with the goal of mining the library for antagonists of other inward rectifiers. As noted in the Introduction, a growing body of evidence suggests that GIRK channels expressed in atrial cardiomyocytes may represent a viable drug target for the treatment of atrial fibrillation. Given the paucity of potent and selective small-molecule inhibitors of GIRK and therapeutic interest in the channel, we screened the focus library for GIRK modulators using a Ti^+ flux-based fluorescence assay developed recently at Vanderbilt (Niswender et al., 2008). The assay reports Ti^+ flux through heteromeric Kir3.1/3.2 channels co-expressed in HEK-293 cells with the group III metabotropic glutamate receptor mGluR8. Intracellular Ti^+ concentration is reported using the commercially available Ti^+ -sensitive fluorescent dye FluoZin-2. As shown in **Figure 1A**, glutamate addition dose-dependently increased Ti^+ flux as GIRK channels are activated by mGluR8 stimulation. The focused library was screened at a single concentration of 10 μM using an 80% maximally effective concentration (EC_{80}) of glutamate. Several compounds were identified that preferentially inhibited GIRK over Kir1.1 (data not shown). One of these compounds, termed VU573, was selected for further study.

The chemical structure of VU573 is shown in the inset of **Figure 1C**. The potency of VU573 was evaluated in 11-point CRC using an EC_{80} of glutamate to activate GIRK. As shown in **Figure 1B**, VU573 inhibited GIRK-dependent Ti^+ flux in a dose-dependent manner with a 50% inhibition concentration (IC_{50}) of approximately 1.9 μM (**Figure 1C**).

To verify that VU573 is a more potent inhibitor of GIRK than Kir1.1, a full VU573 CRC was generated using an established Ti^+ flux assay for Kir1.1 (Lewis et al., 2009; Bhavé et al., 2011). The assay employs an inducible system in which Kir1.1 is expressed from a tetracycline-regulatable promoter. As shown in **Figure 1D**, extracellular Ti^+ addition produced a dramatic increase in FluoZin-2 fluorescence in cells cultured with



tetracycline, but not in uninduced cells. Thus, most of the Tl^{+} flux in tetracycline-induced cells occurs through Kir1.1. VU573 exhibited weak yet dose-dependent inhibition of Kir1.1 (Figure 1F), with an IC_{50} of approximately $19 \mu M$. Whole-cell patch clamp experiments confirmed that $20 \mu M$ VU573 inhibited Kir1.1 by $49.5 \pm 0.03\%$ ($n = 5$). Thus, VU573 is a preferential inhibitor of GIRK over Kir1.1.

VU573 SHOWS PREFERENCE FOR KIR2.3, GIRK, AND KIR7.1 OVER KIR1.1 AND KIR2.1

To further assess the selectivity of VU573, several members of the Kir channel family were expressed in *Xenopus* oocytes and screened for VU573 sensitivity using the TEVC technique. We first tested whether VU573 discriminates between Kir3.1/3.2 and Kir3.1/3.4 channels, the predominant heterotetrameric forms of GIRK found in the nervous system and heart, respectively (Hibino et al., 2010). Figure 2A illustrates a typical experiment performed on an oocyte co-injected with cRNA encoding Kir3.1 and Kir3.2. Current recorded at -80 mV is shown as a function of time. The oocyte was initially bathed in a potassium-free (0K) solution and then switched to one containing 90 mM K^{+} (90K) to activate GIRK. The dramatic increase in inward current in the presence of

90K buffer was not observed in water-injected oocytes (data not shown) and therefore largely reflects current through Kir3.1/3.2 channels. Bath application of $10 \mu M$ VU573 inhibited GIRK current by approximately 50%, which was significantly lower than expected from Tl^{+} flux experiments (Figure 1C). The residual current was blocked by Ba^{2+} . Figure 2F shows mean \pm SEM percentage block of Kir3.1/3.2 and Kir3.1/3.4 channels by 1, 10, and $25 \mu M$ VU573 or Ba^{2+} . The mean \pm SEM time constant (τ) for inhibition of Kir3.1/3.2 and Kir3.1/3.4 currents by $25 \mu M$ VU573 were 28 ± 4 s ($n = 6$) and 27 ± 5 s ($n = 6$), respectively. There were no significant ($P > 0.05$) differences in the degree of VU573-dependent block of Kir3.1/3.2 and Kir3.1/3.4 channels at any of the concentrations.

GIRK channels are co-expressed with other members of the Kir channel family in a tissue- and cell type-specific manner. As noted in the Introduction, there is growing evidence that inhibitors of cardiac GIRK channels may be therapeutically beneficial in patients with atrial fibrillation. However, Kir2.1 and Kir2.3 are also expressed in the heart (Hibino et al., 2010) and therefore represent potential off-targets for VU573 actions. GIRK, Kir2.1, and Kir2.3 are also co-expressed in various brain regions, as is one of the newest Kir channel family

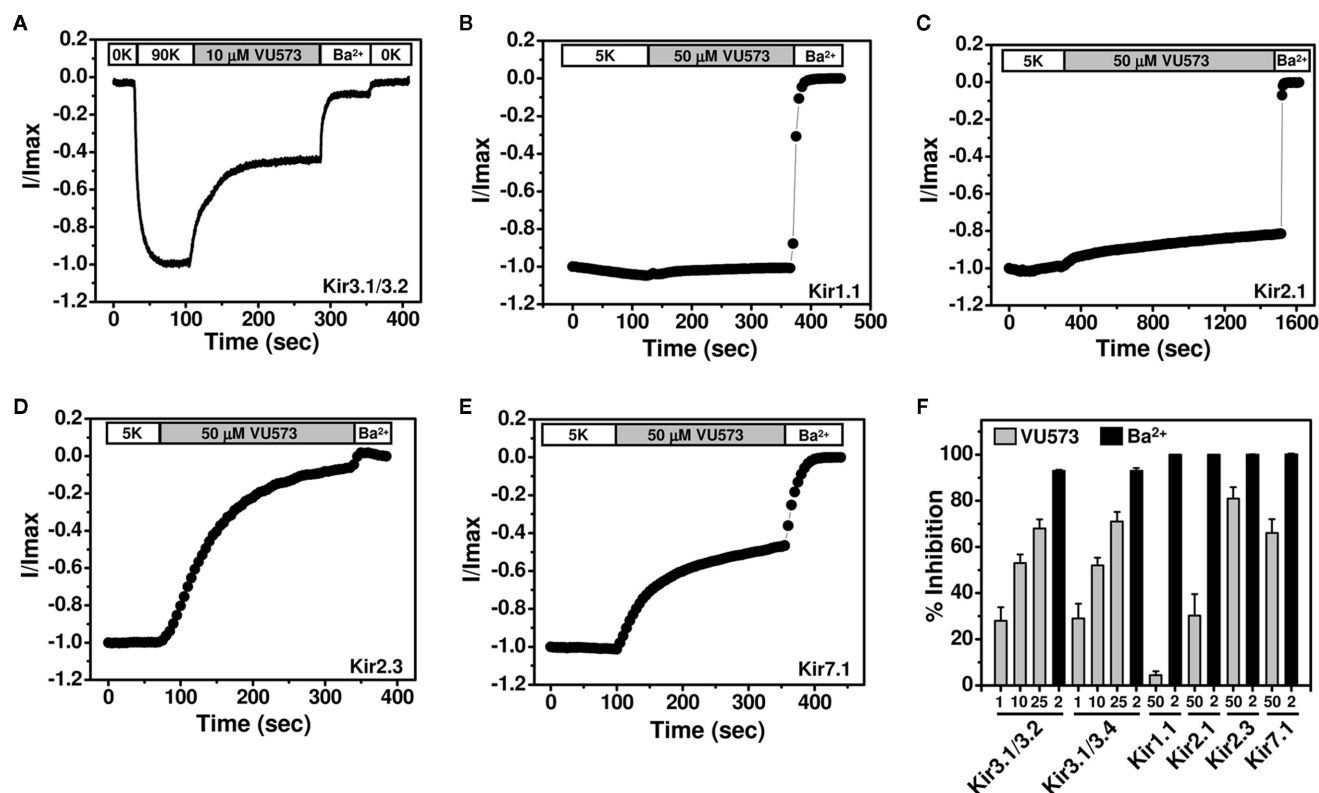


FIGURE 2 | Effect of VU573 on Kir channels expressed in oocytes. (A) Representative Kir3.1/3.2 current traces recorded from an oocyte using the two-electrode voltage-clamp technique. Oocytes were initially bathed in a potassium-free (0K) solution and then switched to one containing 90 mM potassium (90K) to activate Kir3.1/3.2. After reaching a steady-state, the oocyte was exposed to 10 μM VU573 (in 90K) bath to inhibit Kir3.1/3.2. Residual Kir3.1/3.2 currents were inhibited with 2 mM barium (Ba²⁺). A final

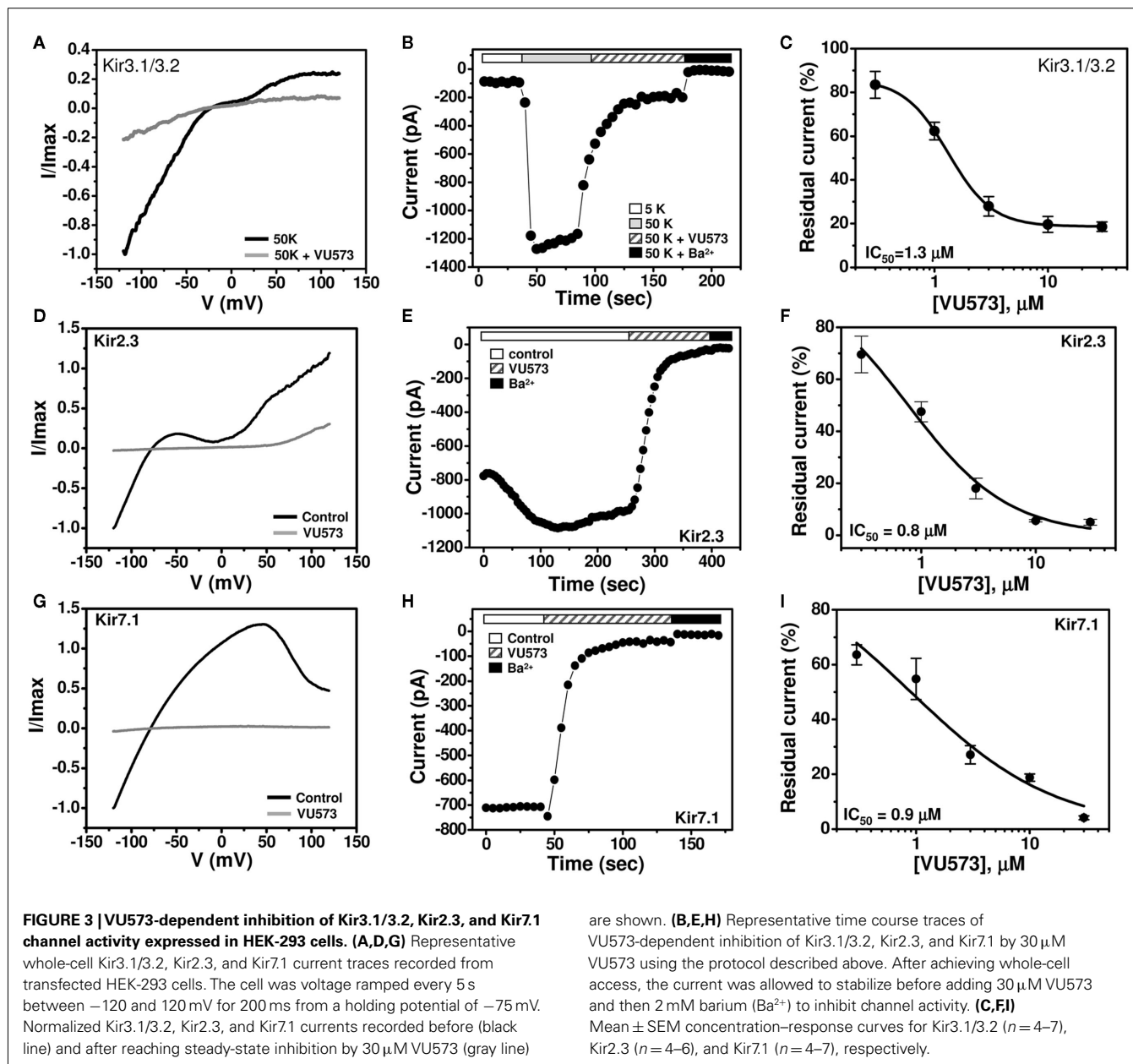
switch back to 0K was used to measure leak current at the end of each experiment. Representative whole-cell current traces recorded from oocytes expressing respectively (B) Kir1.1, (C) Kir2.1, (D) Kir2.3, and (E) Kir7.1 before and after application of 50 μM VU573. Residual Kir currents were inhibited with 2 mM barium (Ba²⁺). (F) Mean ± SEM percent inhibition of current evoked by Kir3.1/3.2, Kir3.1/3.4, Kir1.1, Kir2.1, Kir2.3, and Kir7.1 with the indicated concentrations of VU573 (■) or Ba²⁺ (■) *n* = 4–6.

members, Kir7.1 (Krapivinsky et al., 1998). We therefore determined whether VU573 inhibits any of these channels expressed in *Xenopus* oocytes. Kir1.1 was also expressed to confirm the results from TI⁺ flux and patch clamp experiments.

Representative TEVC recordings from oocytes expressing Kir1.1, Kir2.1, Kir2.3, or Kir7.1 are shown in **Figures 2B–E**. The oocytes were voltage-clamped at −75 mV and stepped for 200 ms every 5 s to −120 mV to evoke inward current. The current amplitude at −120 mV is shown as a function of time. Barium was again used at the end of each experiment as a control blocker. Consistent with the TI⁺ flux data showing greater potency toward GIRK than Kir1.1, 50 μM VU573 inhibited Kir1.1 by only $4.3 \pm 1.7\%$ with a time constant of 95 ± 15 s (*n* = 8). Kir2.1 was also relatively insensitive to VU573, and the time constant was very slow ($\tau = 735 \pm 85$ s; *n* = 4; **Figure 2C**). After 25 min of constant bath perfusion, 50 μM VU573 inhibited Kir2.1 by only $30.2 \pm 9.4\%$. In contrast, Kir2.3 was inhibited comparatively quickly ($\tau = 154 \pm 32$ s) by $80.9 \pm 5.0\%$ (*n* = 7). Similarly, Kir7.1 was inhibited by $66.0 \pm 6\%$ with a rapid time constant of 38 ± 6 s (*n* = 8).

PATCH CLAMP ANALYSIS OF VU573 POTENCY IN MAMMALIAN CELLS

GIRK is inhibited by VU573 with an IC₅₀ of approximately 2 μM in TI⁺ flux assays in HEK-293 (**Figure 1**) cells and 10 μM in TEVC experiments in oocytes (**Figure 2**). To determine if the discrepancy is due to the expression system or assay type, whole-cell patch clamp techniques were used to assess the potency of VU573 toward Kir3.1/3.2 GIRK channels expressed in HEK-293 cells. The cells were voltage-clamped at a holding potential of −75 mV and then stepped to −120 mV for 200 ms, after which the membrane potential was ramped between −120 and 120 mV at a rate of 2.4 mV/ms. As shown in **Figure 3B**, GIRK activity was low in the presence of 5 mM extracellular K⁺ (5K), but increased upon elevation of bath K⁺ to 50 mM (50K), paralleling the behavior of GIRK observed in oocytes. Consistent with TI⁺ flux data (**Figure 1C**), bath application of 30 μM VU573 led to a near complete inhibition of GIRK. As shown in the voltage ramp experiments in **Figure 3A**, VU573 inhibited GIRK across all potentials tested. The residual current was inhibited by barium (Ba²⁺; **Figure 3B**). The mean ± SEM time constant of inhibition was 16 ± 1 s (*n* = 5). A fit of the CRC data (**Figure 3C**) from patch clamp experiments yielded an IC₅₀



of $1.3 \mu\text{M}$, which is very near that derived from Ti^+ flux assays (Figure 1C).

We extended our patch clamp experiments to include Kir2.3 and Kir7.1 due to their strong inhibition by VU573 in oocytes (Figure 2F). A monoclonal stable T-Rex-HEK-293 cell line expressing Kir2.3 under the control of a tetracycline-inducible promoter was patch clamped following overnight induction with tetracycline. Kir7.1 was studied in transiently transfected HEK-293 cells (see Materials and Methods). The cells were subjected to the same voltage ramp protocol described above for GIRK. Steady-state Kir2.3 and Kir7.1 currents recorded before (black line) and after (gray line) bath application of $30 \mu\text{M}$ VU573 are shown in Figures 3D,G, respectively. Both channels were inhibited with a rapid time course (Figures 3E,H) and IC_{50} values of approximately

$1 \mu\text{M}$ (Figures 3E,I). The mean \pm SEM time constants for inhibition of Kir2.3 and Kir7.1 were 23 ± 2 and 14 ± 2 s, respectively ($n = 4$ each).

DEVELOPMENT OF Ti^+ FLUX ASSAYS FOR Kir2.3 AND Kir7.1-M125R

We next set out to employ medicinal chemistry in an effort to improve the potency and selectivity of VU573 toward GIRK, Kir2.3, and Kir7.1. Conventional electrophysiological methods are too slow and labor intensive to support a robust medicinal chemistry campaign, leading us to establish high-throughput Ti^+ flux assays for Kir2.3 and Kir7.1. As shown in Figure 4A, robust tetracycline-inducible Ti^+ flux was observed in monoclonal stable T-Rex-HEK-293 expressing Kir2.3. VU573 dose-dependently inhibited Ti^+ flux through Kir2.3 with an IC_{50} of

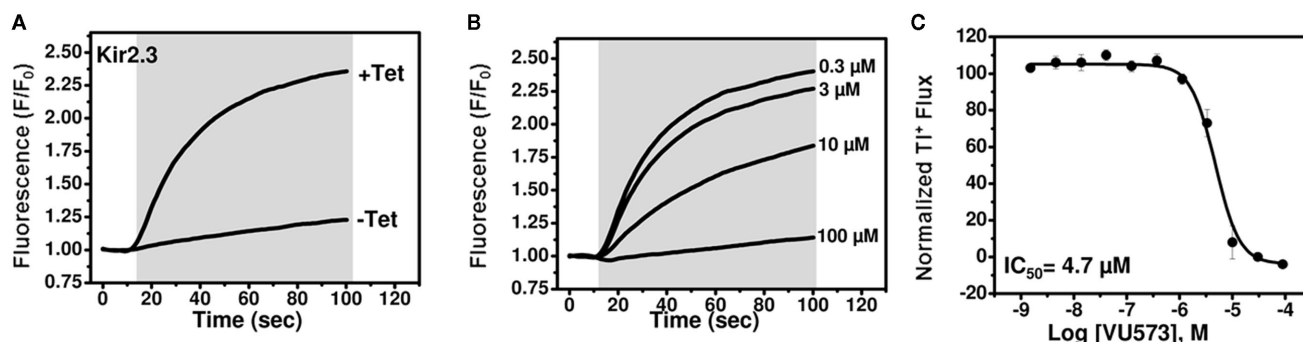


FIGURE 4 | Development of a thallium flux assay for Kir2.3. (A) Thallium flux-dependent FluoZin-2 fluorescence recorded from monoclonal Kir2.3 T-REx-HEK-293 cells cultured overnight in absence (–Tet) or presence (+Tet) of Tetracycline. The fluorescence emission was recorded before and after the addition of extracellular thallium (shaded box). (B) Representative traces for

changes of Ti^+ -induced FluoZin-2 fluorescence following 20 min pre-treatment of cells with the indicated concentrations of VU573. (C) CRC for VU573-dependent inhibition of Kir2.3 activity. Values are mean \pm SEM ($n = 3$). A fit of the CRC with a single-site four-parameter logistic function yielded IC_{50} of 4.7.

4.7 μM (Figures 4B,C), a value that is reasonably close to that derived from patch clamp experiments (Figure 3F).

In contrast, despite numerous attempts on multiple polyclonal and monoclonal cell lines, we were unable to detect Ti^+ flux through Kir7.1. Western blot analysis revealed that this was not due to lack of channel protein expression (data not shown), suggesting that other channel properties were responsible. Kir7.1 is unique among Kir channels in that it has a very small unitary conductance, which has been estimated from noise analysis to be on the order of 50 femptoSiemens (fS; Krapivinsky et al., 1998). We reasoned that this could keep Ti^+ flux through Kir7.1 below the limit of detection of FluoZin-2. The small conductance of the channel is due at least in part to a non-conserved Methionine (M) residue at position 125 located in the pore. Mutation of the residue to Arginine (R), which occupies the homologous position in all other Kir channels (not shown), has no effect on protein expression or targeting to the plasma membrane, but increases the single-channel conductance by approximately 20-fold (Krapivinsky et al., 1998). We therefore wondered if the M125R mutation could enable measurement of Ti^+ flux using FluoZin-2. As shown in Figure 5B, tetracycline-induced robust Ti^+ flux in polyclonal stable T-REx-HEK-293 cells expressing Kir7.1-M125R. VU573 induced concentration-dependent inhibition of Ti^+ flux with an IC_{50} of 4.9 μM (Figures 5C,D). The good correlation between IC_{50} values from patch clamp and Ti^+ flux experiments and the fact that the M125R mutation had no effect on the sensitivity to VU573 in patch clamp experiments (Figure 5A) indicated that the Kir7.1-M125R assays could be used as a screening tool to support medicinal chemistry efforts for VU573.

SYNTHESIS AND STRUCTURE–ACTIVITY RELATIONSHIPS OF VU573 ANALOGS

Lead optimization efforts directed at VU573 to improve its potency and selectivity toward Kir2.3, GIRK, and Kir7.1 were initiated by conserving the benzyl moiety and substituting the R group (Table 1). Structure–activity relationships (SAR) revealed few analogs with channel selectivity. Replacement of the phenoxy moiety with a morpholino group to the VU573 scaffold resulted in

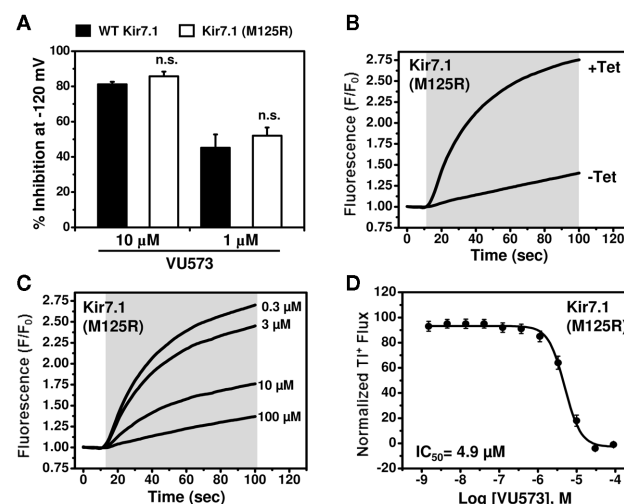
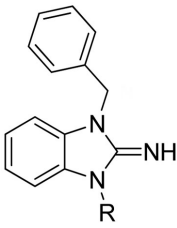
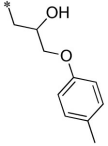
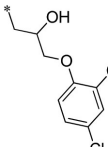
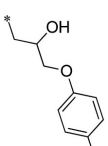
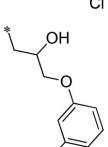
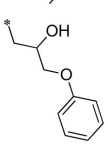
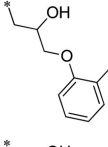
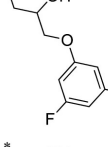
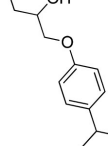


FIGURE 5 | Development of a thallium flux assay for Kir7.1 (M125R). (A) Mean \pm SEM % inhibition of wild type (closed bars; $n = 6-7$) or M125R mutant (open bars; $n = 4-6$) Kir7.1 by the indicated concentration of VU573. Note that the wild type data are reproduced from Figure 3. (B) Thallium flux-dependent FluoZin-2 fluorescence recorded from polyclonal Kir7.1 (M125R) T-REx-HEK-293 cells cultured overnight in absence (–Tet) or presence (+Tet) of Tetracycline. The fluorescence emission was recorded before and after the addition of extracellular thallium (shaded box). (C) Representative traces for changes of Ti^+ -induced FluoZin-2 fluorescence following 20 min pre-treatment of cells with the indicated concentrations of VU573. (D) CRC for VU573-dependent inhibition of Kir2.3 activity. Values are mean \pm SEM ($n = 3$). A fit of the CRC with a single-site four-parameter logistic function yielded IC_{50} of 4.9 μM .

compound (9), which lost activity (IC_{50} values $> 100 \mu\text{M}$) for Kir7.1 and Kir1.1. The IC_{50} values for Kir2.3 and GIRK were 24 and 15.3 μM , respectively. Substitution of the R group of the VU573 scaffold with a phenoxy benzyloxy functional group led to an analog (11), which was equipotent for Kir2.3 and GIRK, but lost activity toward Kir7.1 (IC_{50} values $> 100 \mu\text{M}$). An alternate functional group for the VU573 scaffold, a 4-cyanophenyl (12),

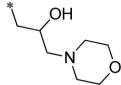
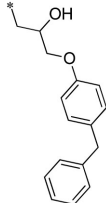
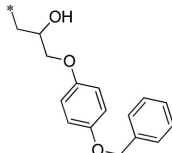
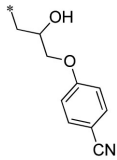
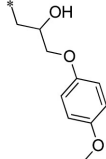
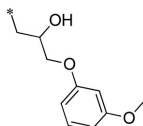
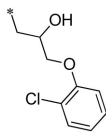
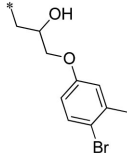
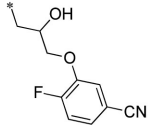
Table 1 | Structure–activity relationships and lead optimization summary.

RN1C(=N2C(=N1)c3ccccc32)Cc4ccccc4

Cmpd	R	VU#/Barcode	IC ₅₀ (μM)			
			Kir2.3	Kir7.1	GIRK	Kir1.1
1		VU0160573-1/IC4X	4.15 ± 0.35	4.77 ± 2.89	2.17 ± 0.40	10.8 ± 3.8
2		VU0403134-1/IC3Y	5.33 ± 2.08	4.73 ± 2.57	3.20 ± 0.71	7.07 ± 2.30
3		VU0403131-1/IC58	4.20 ± 1.25	5.17 ± 1.89	2.90 ± 1.10	6.57 ± 3.80
4		VU0340260-1/IC38	7.53 ± 2.34	8.00 ± 3.86	4.95 ± 1.80	11.2 ± 2.8
5		VU0026784-1/IC3L	3.43 ± 0.67	4.47 ± 2.40	1.95 ± 0.49	11.7 ± 4.1
6		VU0288495-1/IC39	5.33 ± 1.70	4.10 ± 1.93	1.95 ± 0.07	11.9 ± 2.2
7		VU0451348-1/R6P	3.53 ± 1.33	4.20 ± 0.95	1.40 ± 0.35	7.57 ± 2.20
8		VU0451344-1/R80	5.03 ± 1.96	6.03 ± 1.60	3.37 ± 0.70	6.77 ± 1.70

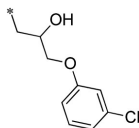
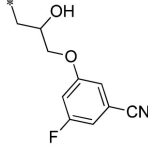
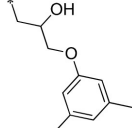
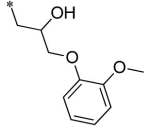
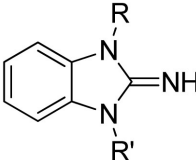
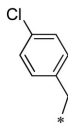
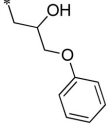
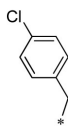
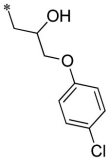
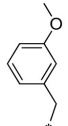
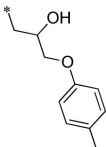

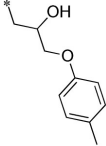
(Continued)

Table 1 | Continued

Cmpd	R	VU#/Barcode	IC ₅₀ (μM)			
			Kir2.3	Kir7.1	GIRK	Kir1.1
9		VU0451342-1/R70	24.0 ± 10.4	>100	15.3 ± 0.6	>100
10		VU0451341-1/R7M	2.80 ± 0.99	6.07 ± 2.71	3.83 ± 1.10	6.13 ± 0.23
11		VU0451340-1/R5C	2.33 ± 0.68	>100	3.17 ± 0.86	5.23 ± 0.59
12		VU0451339-1/R56	11.3 ± 1.2	19.7 ± 7.4	5.27 ± 0.40	15.7 ± 2.1
13		VU0066224-6/R7N	3.87 ± 1.40	6.70 ± 1.39	1.50 ± 0.44	12.7 ± 1.2
14		VU0451336-1/R5B	3.13 ± 1.45	3.47 ± 0.67	1.43 ± 0.25	10.1 ± 2.9
15		VU0451333-1/R5X	4.95 ± 1.34	5.33 ± 2.91	2.77 ± 0.60	8.60 ± 1.20
16		VU0451337-1/R5K	5.10 ± 1.27	6.10 ± 3.12	3.43 ± 0.21	8.53 ± 1.70
17		VU0451332-1/R7B	5.30 ± 1.56	4.33 ± 1.33	1.40 ± 0.30	8.27 ± 0.29

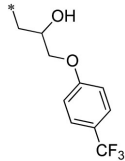
(Continued)

Table 1 | Continued

Cmpd	R	VU#/Barcode	IC ₅₀ (μM)				
			Kir2.3	Kir7.1	GIRK	Kir1.1	
18		VU0451338-1/R71	4.45 ± 0.92	5.63 ± 2.24	2.83 ± 0.42	11.7 ± 2.1	
19		VU0451330-1/R6J	7.15 ± 0.71	8.27 ± 2.37	1.93 ± 0.21	14.3 ± 1.5	
20		VU0451331-1/RKN	3.65 ± 0.21	3.03 ± 0.68	4.33 ± 0.68	16.0 ± 2.0	
21		VU0451846-2/R87	3.60 ± 0.28	8.50 ± 2.18	5.13 ± 1.60	19.3 ± 1.5	
							
Cmpd	R	R'	VU#/Barcode	IC ₅₀ (μM)			
				Kir2.3	Kir7.1	GIRK	Kir1.1
22			VU0401333-1/IC4L	7.20 ± 1.73	8.93 ± 3.53	4.80 ± 1.10	14.7 ± 2.1
23			VU0403132-1/IC48	5.70 ± 3.18	19.5 ± 28.2	3.35 ± 0.92	6.53 ± 3.90
24			VU0451343-1/RJ4	2.80 ± 0.89	3.00 ± 0.87	4.20 ± 0.69	13.7 ± 4.4
25			VU0451335-1/R5P	16.5 ± 0.7	25.3 ± 8.5	12.3 ± 2.5	13.0 ± 2.6

(Continued)

Table 1 | Continued

Cmpd	R	R'	VU#/Barcode	IC ₅₀ (μM)			
				Kir2.3	Kir7.1	GIRK	Kir1.1
26	/		VU0451334-1/R7L	4.90 ± 0.14	5.20 ± 1.82	2.87 ± 0.31	6.97 ± 2.00

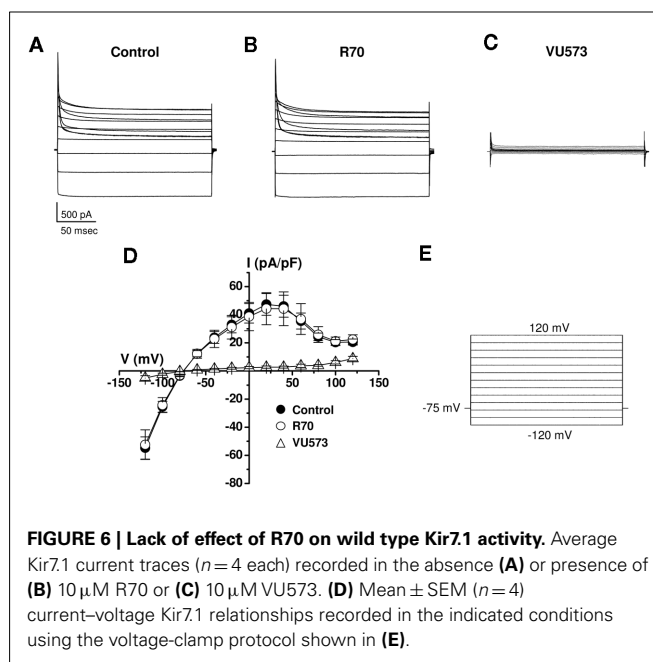
Summary of structure–activity relationships of VU573 analogs. Reported IC₅₀ values were measured by TI⁺ flux assay. Values are mean ± SEM (n = 3).

led to an analog compound with moderate selectivity for GIRK (IC₅₀ = 5.27 μM) and weak inhibition of Kir2.3 and Kir7.1, with IC₅₀ values of 11.3 and 19.7 μM, respectively. All other analogs in which substitutions were made at both R and R' groups led to similar potency among the Kir2.3, Kir7.1, and GIRK channels as compared to VU573, but with weak inhibition for Kir1.1. The development of two VU573 analogs, R70 and R5C (Table 1), that retain activity toward GIRK and Kir2.3 but have lost activity toward Kir7.1 suggest that chemically optimized analogs based on the VU573 scaffold can be developed to increase their selectivity.

To determine if the apparent loss of activity is an artifact of the TI⁺ flux assay or the use of the M125R mutant, we examined the effects of the VU573 analog R70 on wild type Kir7.1 currents in whole-cell patch clamp experiments. The cells were voltage-clamped between −120 and 120 mV in 20 mV increments from a −75-mV holding potential (Figure 6E). As illustrated in the average current traces recorded before (Figure 6A) or during bath application of 10 μM R70 (Figure 6B), the analog had no effect on wild type Kir7.1 activity. In contrast, subsequent addition of 10 μM VU573 led to a near complete inhibition of the channel (Figures 6C). The mean ± SEM current–voltage relationships recorded in the three conditions are shown in Figure 6D.

DISCUSSION

The TI⁺ flux assay developed by Weaver et al. (2004) and subsequently commercialized by Invitrogen under the FluxOR® label has had a major impact on high-throughput screening for potassium channels. The assay takes advantage of the fact that TI⁺ readily permeates most K⁺ channel pores. With the exception of wild type Kir7.1, the assay seems to be particularly well suited for inward rectifier K⁺ channels due to their high open probability near the resting membrane potential of a cell. This obviates the need for depolarizing the cell with a high-potassium step to open voltage-gated K⁺ channels. To date, TI⁺ flux assays have been reported for the inward rectifiers Kir1.1 (Lewis et al., 2009), Kir2.1 (Wang et al., 2010), Kir2.3 (this study), Kir3.1/3.2 (Niswender et al., 2008), and Kir7.1-M125R (this study). TI⁺ flux assays have also been developed for some ligand- and voltage-gated potassium channels, including SK3 and KCNQ2 (Weaver et al., 2004), KCNQ4 (Li et al., 2011), and hERG (Titus et al., 2009; Bridal et al., 2010; Huang et al., 2010; Schmalhofer et al., 2010; Zou et al., 2010). A TI⁺ flux assay was used to screen for modulators of the potassium-chloride co-transporter KCC2 (Delpire et al., 2009). This is notable



because KCC2 is electroneutral and therefore cannot be screened using voltage-sensitive dyes. Thus, the TI⁺ flux assay appears to be broadly adaptable to both electrogenic and electroneutral K⁺ transport proteins.

In the present study, TI⁺ flux- and electrophysiological-based counterscreens revealed a preferential inhibitor of GIRK, Kir2.3, and Kir7.1. It is unclear why IC₅₀ values are lower in oocytes compared to mammalian cells, but likely reflects differences in membrane properties or intracellular factors between the two cell types. VU573 inhibits GIRK independent of GPCR stimulation and does not discriminate between cardiac (Kir3.1/3.4) and neuronal (Kir3.1/3.2) forms of the channel. The latter observation suggests that the VU573 binding site is located within the Kir3.1 subunit, which is common to both heteromeric forms, or is shared between all three subunits. Pharmacology experiments on homotetrameric Kir3.1, Kir3.2, and Kir3.4 channels should help resolve the issue. Given the broad tissue distribution and important physiological functions of GIRK channels in multiple organ systems, the development of subtype selective modulators may be important for developing, for example, cardiac-specific

drugs to treat atrial fibrillation without toxic side effects on the nervous system. The availability of high-resolution crystal structures of the GIRK cytoplasmic domain (Nishida and Mackinnon, 2002), GIRK-bacterial Kir channel chimeras (Nishida et al., 2007) and now full-length mammalian Kir2.2 (Tao et al., 2009) should be helpful in guiding and interpreting experiments to define the molecular binding site for VU573 and other GIRK antagonists. The relatively flat SAR of VU573 against GIRK, Kir2.3, and Kir7.1 suggests that the VU573 scaffold may be amenable to the addition of diazirine or other light-reactive moieties for photoaffinity labeling of the channels for identification of the binding site using mass spectrometry. A detailed understanding of both unique and overlapping binding sites will provide novel insights into the molecular architecture of GIRK and should facilitate the development of subtype-specific inhibitors.

Members of the Kir2.X subfamily, including Kir2.1, Kir2.2, Kir2.3, Kir2.4, and Kir2.6, are broadly expressed in neurons, cardiac, skeletal and smooth muscle cells, endothelial cells, macrophages, and epithelial cells (De Boer et al., 2010a). Much of our understanding of the physiology of Kir2.X channels comes from studies of disease-causing mutations in humans (Plaster et al., 2001; Ryan et al., 2010) and knockout mice (Zaritsky et al., 2001). While it is clear from this work that Kir2.X channels are essential in many organ systems, pinpointing their individual roles has been difficult due to their overlapping expression profiles, propensity to form Kir2.X heterotetramers and poorly developed pharmacology. The development of subtype selective Kir2.X inhibitors would undoubtedly bolster efforts to understand the physiology and druggability of Kir2.X homo- and heteromeric channels. To date, however, the inhibitor pharmacology of Kir2.X channels is limited to barium, cesium, and a handful of non-specific drugs such as chloroquine (Rodriguez-Menchaca et al., 2008), mefloquine (Lopez-Izquierdo et al., 2011b), quinacrine (Lopez-Izquierdo et al., 2011a), carvedilol (Ferrer et al., 2011), tamoxifen (Ponce-Balbuena et al., 2009), and pentamidine (De Boer et al., 2010b). Pregnenolone sulfate (Kobayashi et al., 2009) and flecainide (Caballero et al., 2010) are activators of Kir2.3 and Kir2.1, respectively. Like VU573 (this study), mefloquine, quinacrine, tamoxifen, and carvedilol preferentially inhibit Kir2.3 over Kir2.1. Electrophysiological analysis of mutagenized channels suggests that chloroquine and pentamidine are cytoplasmic pore blockers, whereas mefloquine and carvedilol appear to disrupt channel interactions with the activating membrane phospholipid phosphatidylinositol 4,5-bisphosphate (PIP₂). There is evidence that quinacrine has a complex mechanism of action involving both pore block and disruption of channel-PIP₂ interactions. Because VU573 is also a preferential inhibitor of Kir2.3, we are currently testing if it shares a common mechanism of action and binding site(s) with these drugs. Looking ahead, it will be important to determine whether VU573 or any of the aforementioned drugs show preference for homomeric versus

heteromeric Kir2.X channels. These studies may help inform medicinal chemistry efforts to develop subtype-specific inhibitors of Kir2.X channels.

To our knowledge, VU573 is only the second and most potent Kir7.1 inhibitor available. We recently reported that the ~300 nM Kir1.1 inhibitor 7,13-bis[(4-nitrophenyl)methyl]-1,4,10-trioxo-7,13-diazacyclopentadecanedihydrochloride, or VU590, inhibits Kir7.1 with an IC₅₀ of approximately 8 μM, making VU590 the first publically disclosed small-molecule inhibitor of both Kir1.1 and Kir7.1 (Lewis et al., 2009). In the present study, we found that VU573 preferentially inhibits Kir7.1 (IC₅₀ ~ 1 μM) over Kir1.1 (IC₅₀ ~ 19 μM).

Kir7.1 is widely expressed in the brain, retinal pigment epithelial cells of the eye, the choroid plexus, and epithelial cells of the intestine, nephron, and inner ear (Krapivinsky et al., 1998; Nakamura et al., 1999; Ookata et al., 2000; Pondugula et al., 2006; Yang et al., 2008). Very little is known about the physiology of Kir7.1 due in part to the unusually small (i.e., ~50 fS) unitary conductance of the channel. This precludes the use of single-channel recording techniques to study its activity in native cell types, where other inward rectifiers of larger unitary conductances are often co-expressed. Whole-cell patch clamp recordings could conceivably be used to dissect out the relative contributions of Kir7.1 and other Kir channels to the macroscopic current provided that specific blockers were available. This scenario highlights the need for better pharmacological modulators of Kir7.1 and other members of the Kir channel family. The discovery of VU573 and its inactive analogs represent important steps toward filling this gap. Furthermore, and importantly, the development of a robust TI⁺ flux assay using the Kir7.1-M125R mutant will enable HTS for chemically diverse modulators of the channel.

Interestingly, heritable mutations in the Kir7.1-encoding gene *KCNJ13* were recently found in patients with two forms of retinal disease (Hejtmanick et al., 2008; Sergouniotis et al., 2011). These findings confirm the importance of Kir7.1 in retinal pigmented epithelia of the eye and raise questions regarding the detailed physiological roles of Kir7.1 in the eye and other organ systems. The development of potent and selective Kir7.1 antagonists will greatly facilitate those efforts.

ACKNOWLEDGMENTS

HEK-293 cells stably expressing GIRK 1, GIRK 2, and the human M4 muscarinic receptor (HEK/GIRK cells) were generously provided by Drs Huai Hu Chang and Lily Jan (University of California San Francisco, San Francisco, CA, USA). The authors would like to thank the B. H. Robbins Scholars Fellowship Program (Daniel F. Loneragan), NIH 1R01DK082884 (Jerod S. Denton), T32GM07628 (Thuy T. Nguyen), and NIH/MLPCN (5U54MH084659-02) for support of this research. Vanderbilt is a member of the MLPCN and houses the Vanderbilt Specialized Chemistry Center for Accelerated Probe Development.

REFERENCES

- Bhave, G., Chauder, B. A., Liu, W., Dawson, E. S., Kadakia, R., Nguyen, T. T., Lewis, L. M., Meiler, J., Weaver, C. D., Satlin, L. M., Lindsley, C. W., and Denton, J. S. (2011). Development of a selective small-molecule inhibitor of Kir1.1, the renal outer medullary potassium channel. *Mol. Pharmacol.* 79, 42–50.
- Bhave, G., Loneragan, D., Chauder, B. A., and Denton, J. S. (2010). Small-molecule modulators of inward rectifier K⁺ channels: recent advances and future possibilities. *Future Med. Chem.* 2, 757–774.
- Bridal, T. R., Margulis, M., Wang, X., Donio, M., and Sorota, S. (2010). Comparison of human Ether-a-go-go related gene screening assays based on IonWorks Quattro and thallium flux. *Assay Drug Dev. Technol.* 8, 755–765.
- Caballero, R., Dolz-Gaiton, P., Gomez, R., Amoros, I., Barana, A., Gonzalez De La Fuente, M., Osuna, L., Duarte, J., Lopez-Izquierdo, A., Moraleda, I., Galvez, E., Sanchez-Chapula, J. A.,

- Tamargo, J., and Delpon, E. (2010). Flecainide increases Kir2.1 currents by interacting with cysteine 311, decreasing the polyamine-induced rectification. *Proc. Natl. Acad. Sci. U.S.A.* 107, 15631–15636.
- Caroti, P., Ceccotti, C., Da Settimo, A., Palla, F., and Primofiore, G. (1986). A facile synthesis of 5,7-dihydro-5-oxopyrido[3',2':5,6]pyrimido[1,2-a]benzimidazoles. A new heterocyclic ring system. *J. Heterocycl. Chem.* 82, 1833–1836.
- Chuang, H. H., Jan, Y. N., and Jan, L. Y. (1997). Regulation of IRK3 inward rectifier K⁺ channel by m1 acetylcholine receptor and intracellular magnesium. *Cell* 89, 1121–1132.
- De Boer, T. P., Houtman, M. J., Compier, M., and Van Der Heyden, M. A. (2010a). The mammalian K(IR)2.x inward rectifier ion channel family: expression pattern and pathophysiology. *Acta Physiol. (Oxf.)* 199, 243–256.
- De Boer, T. P., Nalos, L., Stary, A., Kok, B., Houtman, M. J., Antoons, G., Van Veen, T. A., Beekman, J. D., De Groot, B. L., Ophof, T., Rook, M. B., Vos, M. A., and Van Der Heyden, M. A. (2010b). The anti-protozoal drug pentamidine blocks KIR2.x-mediated inward rectifier current by entering the cytoplasmic pore region of the channel. *Br. J. Pharmacol.* 159, 1532–1541.
- Delpire, E., Days, E., Lewis, L. M., Mi, D., Kim, K., Lindsley, C. W., and Weaver, C. D. (2009). Small-molecule screen identifies inhibitors of the neuronal K-Cl cotransporter KCC2. *Proc. Natl. Acad. Sci. U.S.A.* 106, 5383–5388.
- Dobrev, D., Friedrich, A., Voigt, N., Jost, N., Wettwer, E., Christ, T., Knaut, M., and Ravens, U. (2005). The G protein-gated potassium current I_{K,ACh} is constitutively active in patients with chronic atrial fibrillation. *Circulation* 112, 3697–3706.
- Ehrlich, J. R. (2008). Inward rectifier potassium currents as a target for atrial fibrillation therapy. *J. Cardiovasc. Pharmacol.* 52, 129–135.
- Fallen, K., Banerjee, S., Sheehan, J., Addison, D., Lewis, L. M., Meiler, J., and Denton, J. S. (2009). The Kir channel immunoglobulin domain is essential for Kir1.1 (ROMK) thermodynamic stability, trafficking and gating. *Channels (Austin)* 3, 57–68.
- Ferrer, T., Ponce-Balbuena, D., Lopez-Izquierdo, A., Arechiga-Figueroa, I. A., De Boer, T. P., Van Der Heyden, M. A., and Sanchez-Chapula, J. A. (2011). Carvedilol inhibits Kir2.3 channels by interference with PIP₂-channel interaction. *Eur. J. Pharmacol.* 668, 72–77.
- Hashimoto, N., Yamashita, T., and Tsuruzoe, N. (2006). Tertiapin, a selective IK_{ACh} blocker, terminates atrial fibrillation with selective atrial effective refractory period prolongation. *Pharmacol. Res.* 54, 136–141.
- Hebert, S. C., Desir, G., Giebisch, G., and Wang, W. (2005). Molecular diversity and regulation of renal potassium channels. *Physiol. Rev.* 85, 319–371.
- Hejtmancik, J. F., Jiao, X., Li, A., Sergeev, Y. V., Ding, X., Sharma, A. K., Chan, C. C., Medina, I., and Edwards, A. O. (2008). Mutations in *KCNJ13* cause autosomal-dominant snowflake vitreoretinal degeneration. *Am. J. Hum. Genet.* 82, 174–180.
- Hibino, H., Inanobe, A., Furutani, K., Murakami, S., Findlay, I., and Kurachi, Y. (2010). Inwardly rectifying potassium channels: their structure, function, and physiological roles. *Physiol. Rev.* 90, 291–366.
- Ho, K., Nichols, C. G., Lederer, W. J., Lytton, J., Vassilev, P. M., Kanazirska, M. V., and Hebert, S. C. (1993). Cloning and expression of an inwardly rectifying ATP-regulated potassium channel. *Nature* 362, 31–38.
- Huang, X. P., Mangano, T., Hufeisen, S., Setola, V., and Roth, B. L. (2010). Identification of human Ether-a-go-go related gene modulators by three screening platforms in an academic drug-discovery setting. *Assay Drug Dev. Technol.* 8, 727–742.
- Ji, W., Foo, J. N., O'Roak, B. J., Zhao, H., Larson, M. G., Simon, D. B., Newton-Cheh, C., State, M. W., Levy, D., and Lifton, R. P. (2008). Rare independent mutations in renal salt handling genes contribute to blood pressure variation. *Nat. Genet.* 40, 592–599.
- Jin, W., and Lu, Z. (1998). A novel high-affinity inhibitor for inward-rectifier K⁺ channels. *Biochemistry* 37, 13291–13299.
- Kitamura, H., Yokoyama, M., Akita, H., Matsushita, K., Kurachi, Y., and Yamada, M. (2000). Tertiapin potently and selectively blocks muscarinic K⁺ channels in rabbit cardiac myocytes. *J. Pharmacol. Exp. Ther.* 293, 196–205.
- Kobayashi, T., Washiyama, K., and Ikeda, K. (2009). Pregnenolone sulfate potentiates the inwardly rectifying K channel Kir2.3. *PLoS ONE* 4, e6311. doi:10.1371/journal.pone.0006311
- Krapivinsky, G., Medina, I., Eng, L., Krapivinsky, L., Yang, Y., and Clapham, D. E. (1998). A novel inward rectifier K⁺ channel with unique pore properties. *Neuron* 20, 995–1005.
- Leister, W., Strauss, K., Wisnoski, D., Zhao, Z., and Lindsley, C. (2003). Development of a custom high-throughput preparative liquid chromatography/mass spectrometer platform for the preparative purification and analytical analysis of compound libraries. *J. Comb. Chem.* 5, 322–329.
- Lewis, L. M., Bhawe, G., Chauder, B. A., Banerjee, S., Lornsen, K. A., Redha, R., Fallen, K., Lindsley, C. W., Weaver, C. D., and Denton, J. S. (2009). High-throughput screening reveals a small-molecule inhibitor of the renal outer medullary potassium channel and Kir7.1. *Mol. Pharmacol.* 76, 1094–1103.
- Li, Q., Rottlander, M., Xu, M., Christoffersen, C. T., Frederiksen, K., Wang, M. W., and Jensen, H. S. (2011). Identification of novel KCNQ4 openers by a high-throughput fluorescence-based thallium flux assay. *Anal. Biochem.* 418, 66–72.
- Lopez-Izquierdo, A., Arechiga-Figueroa, I. A., Moreno-Galindo, E. G., Ponce-Balbuena, D., Rodriguez-Martinez, M., Ferrer-Villada, T., Rodriguez-Menchaca, A. A., Van Der Heyden, M. A., and Sanchez-Chapula, J. A. (2011a). Mechanisms for Kir channel inhibition by quinacrine: acute pore block of Kir2.x channels and interference in PIP₂ interaction with Kir2.x and Kir6.2 channels. *Pflugers Arch.* 462, 505–517.
- Lopez-Izquierdo, A., Ponce-Balbuena, D., Moreno-Galindo, E. G., Arechiga-Figueroa, I. A., Rodriguez-Martinez, M., Ferrer, T., Rodriguez-Menchaca, A. A., and Sanchez-Chapula, J. A. (2011b). The antimalarial drug mefloquine inhibits cardiac inward rectifier K⁺ channels: evidence for interference in PIP₂-channel interaction. *J. Cardiovasc. Pharmacol.* 57, 407–415.
- Machida, T., Hashimoto, N., Kuwahara, I., Ogino, Y., Matsuura, J., Yamamoto, W., Itano, Y., Zamma, A., Matsumoto, R., Kamon, J., Kobayashi, T., Ishiwata, N., Yamashita, T., Ogura, T., and Nakaya, H. (2011). Effects of a highly selective acetylcholine-activated K⁺ channel blocker on experimental atrial fibrillation. *Circ. Arrhythm. Electrophysiol.* 4, 94–102.
- Makary, S., Voigt, N., Maguy, A., Wakili, R., Nishida, K., Harada, M., Dobrev, D., and Nattel, S. (2011). Differential protein kinase C isoform regulation and increased constitutive activity of acetylcholine-regulated potassium channels in atrial remodeling. *Circ. Res.* 109, 1031–1043.
- Matsuda, T., Ito, M., Ishimaru, S., Tsuruoka, N., Saito, T., Iida-Tanaka, N., Hashimoto, N., Yamashita, T., Tsuruzoe, N., Tanaka, H., and Shigenobu, K. (2006). Blockade by NIP-142, an antiarrhythmic agent, of carbachol-induced atrial action potential shortening and GIRK1/4 channel. *J. Pharmacol. Sci.* 101, 303–310.
- Nakamura, N., Suzuki, Y., Sakuta, H., Ookata, K., Kawahara, K., and Hirose, S. (1999). Inwardly rectifying K⁺ channel Kir7.1 is highly expressed in thyroid follicular cells, intestinal epithelial cells and choroid plexus epithelial cells: implication for a functional coupling with Na⁺, K⁺-ATPase. *Biochem. J.* 342(Pt 2), 329–336.
- Nishida, M., Cadene, M., Chait, B. T., and Mackinnon, R. (2007). Crystal structure of a Kir3.1-prokaryotic Kir channel chimera. *EMBO J.* 26, 4005–4015.
- Nishida, M., and Mackinnon, R. (2002). Structural basis of inward rectification: cytoplasmic pore of the G protein-gated inward rectifier GIRK1 at 1.8 Å resolution. *Cell* 111, 957–965.
- Niswender, C. M., Johnson, K. A., Luo, Q., Ayala, J. E., Kim, C., Conn, P. J., and Weaver, C. D. (2008). A novel assay of Gi/o-linked G protein-coupled receptor coupling to potassium channels provides new insights into the pharmacology of the group III metabotropic glutamate receptors. *Mol. Pharmacol.* 73, 1213–1224.
- Ookata, K., Tojo, A., Suzuki, Y., Nakamura, N., Kimura, K., Wilcox, C. S., and Hirose, S. (2000). Localization of inward rectifier potassium channel Kir7.1 in the basolateral membrane of distal nephron and collecting duct. *J. Am. Soc. Nephrol.* 11, 1987–1994.
- Pasternak, A. P., Shahipour, A., Tang, H., Teumelsan, N. H., Yang, L., Zhu, Y., and Walsh, S. P. (2010). Inhibitors of the renal outer medullary potassium channel. US patent number: US20100286123.
- Plaster, N. M., Tawil, R., Tristani-Firouzi, M., Canun, S., Bendahhou, S., Tsunoda, A., Donaldson, M. R., Iannaccone, S. T., Brunt, E., Barohn, R., Clark, J., Deymeier, F., George, A. L. Jr., Fish, F. A., Hahn, A., Nitu, A., Ozdemir, C., Serdaroglu, P., Subramony, S. H., Wolfe, G., Fu, Y. H., and Ptacek, L. J. (2001). Mutations in Kir2.1 cause the developmental and episodic electrical phenotypes of Andersen's syndrome. *Cell* 105, 511–519.

- Ponce-Balbuena, D., Lopez-Izquierdo, A., Ferrer, T., Rodriguez-Menchaca, A. A., Arechiga-Figueroa, I. A., and Sanchez-Chapula, J. A. (2009). Tamoxifen inhibits inward rectifier K^+ 2.x family of inward rectifier channels by interfering with phosphatidylinositol 4,5-bisphosphate-channel interactions. *J. Pharmacol. Exp. Ther.* 331, 563–573.
- Pondugula, S. R., Raveendran, N. N., Ergonul, Z., Deng, Y., Chen, J., Sanneman, J. D., Palmer, L. G., and Marcus, D. C. (2006). Glucocorticoid regulation of genes in the amiloride-sensitive sodium transport pathway by semicircular canal duct epithelium of neonatal rat. *Physiol. Genomics* 24, 114–123.
- Rodriguez-Menchaca, A. A., Navarro-Polanco, R. A., Ferrer-Villada, T., Rupp, J., Sachse, F. B., Tristani-Firouzi, M., and Sanchez-Chapula, J. A. (2008). The molecular basis of chloroquine block of the inward rectifier Kir2.1 channel. *Proc. Natl. Acad. Sci. U.S.A.* 105, 1364–1368.
- Ryan, D. P., Da Silva, M. R., Soong, T. W., Fontaine, B., Donaldson, M. R., Kung, A. W., Jongjaroenprasert, W., Liang, M. C., Khoo, D. H., Cheah, J. S., Ho, S. C., Bernstein, H. S., Maciel, R. M., Brown, R. H. Jr., and Ptacek, L. J. (2010). Mutations in potassium channel Kir2.6 cause susceptibility to thyrotoxic hypokalemic periodic paralysis. *Cell* 140, 88–98.
- Schmalhofer, W. A., Swensen, A. M., Thomas, B. S., Felix, J. P., Haedo, R. J., Solly, K., Kiss, L., Kaczorowski, G. J., and Garcia, M. L. (2010). A pharmacologically validated, high-capacity, functional thallium flux assay for the human Ether-a-go-go related gene potassium channel. *Assay Drug Dev. Technol.* 8, 714–726.
- Sergouniotis, P. I., Davidson, A. E., Mackay, D. S., Li, Z., Yang, X., Plagnol, V., Moore, A. T., and Webster, A. R. (2011). Recessive mutations in KCNJ13, encoding an inwardly rectifying potassium channel subunit, cause leber congenital amaurosis. *Am. J. Hum. Genet.* 89, 183–190.
- Simon, D. B., Karet, F. E., Rodriguez-Soriano, J., Hamdan, J. H., Dipietro, A., Trachtman, H., Sanjad, S. A., and Lifton, R. P. (1996). Genetic heterogeneity of Bartter's syndrome revealed by mutations in the K^+ channel, ROMK. *Nat. Genet.* 14, 152–156.
- Tanaka, H., and Hashimoto, N. (2007). A multiple ion channel blocker, NIP-142, for the treatment of atrial fibrillation. *Cardiovasc. Drug Rev.* 25, 342–356.
- Tao, X., Avalos, J. L., Chen, J., and Mackinnon, R. (2009). Crystal structure of the eukaryotic strong inward-rectifier K^+ channel Kir2.2 at 3.1 Å resolution. *Science* 326, 1668–1674.
- Titus, S. A., Beacham, D., Shahane, S. A., Southall, N., Xia, M., Huang, R., Hooten, E., Zhao, Y., Shou, L., Austin, C. P., and Zheng, W. (2009). A new homogeneous high-throughput screening assay for profiling compound activity on the human ether-a-go-go-related gene channel. *Anal. Biochem.* 394, 30–38.
- Voigt, N., Friedrich, A., Bock, M., Wettwer, E., Christ, T., Knaut, M., Strasser, R. H., Ravens, U., and Dobrev, D. (2007). Differential phosphorylation-dependent regulation of constitutively active and muscarinic receptor-activated $I_{K_{ACH}}$ channels in patients with chronic atrial fibrillation. *Cardiovasc. Res.* 74, 426–437.
- Wakili, R., Voigt, N., Kaab, S., Dobrev, D., and Nattel, S. (2011). Recent advances in the molecular pathophysiology of atrial fibrillation. *J. Clin. Invest.* 121, 2955–2968.
- Walsh, K. B. (2010). A real-time screening assay for GIRK1/4 channel blockers. *J. Biomol. Screen* 15, 1229–1237.
- Wang, H. R., Wu, M., Yu, H., Long, S., Stevens, A., Engers, D. W., Sackin, H., Daniels, J. S., Dawson, E. S., Hopkins, C. R., Lindsley, C. W., Li, M., and Mcmanus, O. B. (2010). Selective inhibition of the K(ir)2 family of inward rectifier potassium channels by a small molecule probe: the discovery, SAR, and pharmacological characterization of ML133. *ACS Chem. Biol.* 6, 845–856.
- Weaver, C. D., Harden, D., Dworetzky, S. I., Robertson, B., and Knox, R. J. (2004). A thallium-sensitive, fluorescence-based assay for detecting and characterizing potassium channel modulators in mammalian cells. *J. Biomol. Screen* 9, 671–677.
- Welling, P. A., and Ho, K. (2009). A comprehensive guide to the ROMK potassium channel: form and function in health and disease. *Am. J. Physiol. Renal Physiol.* 297, F849–F863.
- Yang, D., Zhang, X., and Hughes, B. A. (2008). Expression of inwardly rectifying potassium channel subunits in native human retinal pigment epithelium. *Exp. Eye Res.* 87, 176–183.
- Zaritsky, J. J., Redell, J. B., Tempel, B. L., and Schwarz, T. L. (2001). The consequences of disrupting cardiac inwardly rectifying K^+ current (I_{K1}) as revealed by the targeted deletion of the murine Kir2.1 and Kir2.2 genes. *J. Physiol.* 533, 697–710.
- Zhou, H., Tate, S. S., and Palmer, L. G. (1994). Primary structure and functional properties of an epithelial K channel. *Am. J. Physiol.* 266, C809–C824.
- Zou, B., Yu, H., Babcock, J. J., Chanda, P., Bader, J. S., Mcmanus, O. B., and Li, M. (2010). Profiling diverse compounds by flux- and electrophysiology-based primary screens for inhibition of human Ether-a-go-go related gene potassium channels. *Assay Drug Dev. Technol.* 8, 743–754.

Conflict of Interest Statement: The authors declare that the research was conducted in the absence of any commercial or financial relationships that could be construed as a potential conflict of interest.

Received: 07 October 2011; accepted: 07 November 2011; published online: 30 November 2011.

Citation: Raphemot R, Lonergan DF, Nguyen TT, Utley T, Lewis LM, Kadakia R, Weaver CD, Gogliotti R, Hopkins C, Lindsley CW and Denton JS (2011) Discovery, characterization, and structure–activity relationships of an inhibitor of inward rectifier potassium (Kir) channels with preference for Kir2.3, Kir3.X, and Kir7.1. *Front. Pharmacol.* 2:75. doi: 10.3389/fphar.2011.00075

This article was submitted to *Frontiers in Pharmacology of Ion Channels and Channelopathies*, a specialty of *Frontiers in Pharmacology*.

Copyright © 2011 Raphemot, Lonergan, Nguyen, Utley, Lewis, Kadakia, Weaver, Gogliotti, Hopkins, Lindsley and Denton. This is an open-access article distributed under the terms of the Creative Commons Attribution Non Commercial License, which permits use, distribution, and reproduction in other forums, provided the original authors and source are credited.



Voltage- and temperature-dependent allosteric modulation of $\alpha 7$ nicotinic receptors by PNU120596

Fabrizio Sitzia¹, Jon T. Brown¹, Andrew D. Randall¹ and John Dunlop^{2*}

¹ Pfizer Applied Neurophysiology Group, School of Physiology and Pharmacology, University of Bristol, Bristol, UK

² Neuroscience Research Unit, Pfizer, Groton, CT, USA

Edited by:

Ralf Franz Kettenhofen, Axiogenesis AG, Germany

Reviewed by:

Roger L. Papke, University of Florida, USA

Andrea Bruggemann, Nanion Technologies GmbH, Germany

*Correspondence:

John Dunlop, Neuroscience Research Unit, Pfizer, Eastern Point Road, Groton, CT 06340, USA.

e-mail: john.dunlop@pfizer.com

Alpha7 nicotinic acetylcholine receptors ($\alpha 7$ nAChR) are widely distributed throughout the central nervous system and are found at particularly high levels in the hippocampus and cortex. Several lines of evidence indicate that pharmacological enhancement of $\alpha 7$ nAChRs function could be a potential therapeutic route to alleviate disease-related cognitive deficits. A recent pharmacological approach adopted to increase $\alpha 7$ nAChR activity has been to identify selective positive allosteric modulators (PAMs). $\alpha 7$ nAChR PAMs have been divided into two classes: type I PAMs increase agonist potency with only subtle effects on kinetics, whereas type II agents produce additional dramatic effects on desensitization and deactivation kinetics. Here we report novel observations concerning the pharmacology of the canonical type II PAM, PNU120596. Using patch clamp analysis of acetylcholine (ACh)-mediated currents through recombinant rat $\alpha 7$ nAChR we show that positive allosteric modulation measured in two different ways is greatly attenuated when the temperature is raised to near physiological levels. Furthermore, PNU120596 largely removes the strong inward rectification usually exhibited by $\alpha 7$ nAChR-mediated responses.

Keywords: nicotinic receptors, electrophysiology, allosteric modulator, channel, patch clamp

INTRODUCTION

It has long been appreciated that activation of central nervous system (CNS) nicotinic receptors can produce a variety of behavioral changes, including improvements to cognitive function. The most abundant nicotinic acetylcholine receptor (nAChR) subtypes in the mammalian brain are $\alpha 7$ -subunit containing homomers ($\alpha 7$ nAChRs) and $\alpha 4\beta 2$ heteromers. Expression of $\alpha 7$ nAChRs receptors is predominantly, but not exclusively, observed in cortex and hippocampus, whereas $\alpha 4\beta 2$ receptors have a somewhat more widespread distribution (Lindstrom, 1996). At the cellular level $\alpha 7$ nAChRs are reported to be found on both neurons and glial cells (Gotti et al., 2006).

Pharmacological and molecular manipulation of both $\alpha 7$ - and $\alpha 4$ -containing nAChRs has indicated that they both potentially play a role in cognitive processes (Leiser et al., 2009). As a consequence of such findings, both receptors have become enthusiastically pursued drug targets, particularly for those seeking to normalize the cognitive deficits that contribute to the phenotype of devastating CNS diseases, such as schizophrenia and Alzheimer's disease (Olincy et al., 2006; Leiser et al., 2009; Hajos and Rogers, 2010; Haydar and Dunlop, 2010; Thomsen et al., 2010). These research efforts have produced a growing number of receptor subtype-selective compounds active at either $\alpha 7$ nAChRs or $\alpha 4\beta 2$ nAChRs receptors.

Our own research focus is the $\alpha 7$ nAChR. Evidence specifically implicating this particular nAChR in disease pathophysiology comes from a number of studies. Decreased $\alpha 7$ nAChR expression has been reported in brains from schizophrenia sufferers (Freedman et al., 2001a,b). Genetic linkage studies in schizophrenia implicate the region of the $\alpha 7$ nAChRs gene promoter where

polymorphisms result in diminished promoter efficacy to drive receptor expression *in vitro* (Leonard et al., 2002). Selective $\alpha 7$ nAChRs receptor agonists have also been shown to normalize sensory gating deficits in animal models of schizophrenia (Stevens et al., 1998; Simosky et al., 2001; Hajos et al., 2005), and a recent human study has provided proof-of-concept for the normalization of auditory gating deficits in schizophrenics (Olincy et al., 2006).

The $\alpha 7$ nAChRs is a homomeric Ca^{2+} -permeable ligand-gated channel. It is activated by ACh, choline, and (–)-nicotine and is antagonized by α -bungarotoxin and MLA. Kinetically, $\alpha 7$ nAChRs both activate and deactivate with fast kinetics, they also exhibit a very rapid and profound desensitization that is likely to have important functional consequences. Behavioral experiments suggest that increasing activation of $\alpha 7$ nAChR generates improved cognition in rodents (Arendash et al., 1995a,b; Levin et al., 1999). Recent efforts have led to the discovery of a number of novel full and partial $\alpha 7$ nAChR agonists that exhibit good selectivity over both other nicotinic receptors and a wide range of other targets (reviewed in Hajos and Rogers, 2010; Haydar and Dunlop, 2010).

An additional pharmacological approach to increasing $\alpha 7$ nAChR activity is through positive allosteric modulation (Bertrand and Gopalakrishnan, 2007). Broad spectrum positive allosteric modulators (PAMs) of nicotinic receptors have been available for some time. More recently agents with good selectivity for $\alpha 7$ nAChRs have been described. Based on their characterization in electrophysiological studies it has recently been proposed that $\alpha 7$ nAChRs PAMs can be subdivided into two classes. Type I PAMs predominantly affect apparent agonist affinity but can also enhance maximum responsiveness, whereas type II PAMs, such as PNU120596 (Hurst et al., 2005), additionally produce profound

changes to receptor kinetics, in particular desensitization and deactivation (Gronlien et al., 2007). Recent studies have extended the evaluation of PNU120596 potentiation of $\alpha 7$ nAChRs in some detail to suggest the presence of two distinct desensitization states, one PNU120596 sensitive and the other insensitive to PNU120596 (Williams et al., 2011), although the *in vivo* significance of such findings remains to be determined. The emerging behavioral properties of $\alpha 7$ nAChRs PAMs *in vivo* (Hurst et al., 2005; Gronlien et al., 2007; Ng et al., 2007; Timmermann et al., 2007; Dunlop et al., 2009) indicate they share the cognitive-enhancing and normalization of sensory gating properties previously described for $\alpha 7$ nAChR agonists.

In this study we have analyzed in detail the actions at recombinant rat $\alpha 7$ nAChRs of the canonical type II PAM PNU120596. We show for the first time that the pharmacology of these molecules has striking temperature dependence. Furthermore, PNU120596 largely removes the strong inward rectification usually exhibited by $\alpha 7$ nAChRs.

MATERIALS AND METHODS

CELL LINE AND CELL CULTURE

GH4C1 cells stably transfected with rat $\alpha 7$ nAChRs (GH4C1- $\alpha 7$ cells) were cultured and passaged in standard tissue culture flasks before being transferred to, and cultured on, glass coverslips. The culture medium consisted of Dulbecco's Modified Eagles Medium (DMEM, Cambrex) supplemented with 10% heat-inactivated fetal bovine serum (FBS, Biosera), 1% penicillin–streptomycin, and 200 μ g/ml hygromycin B (Invitrogen) at 37°C in a humidified atmosphere composed of 95% air and 5% CO₂.

ELECTROPHYSIOLOGY

A cell-bearing coverslip was broken into numerous pieces and a single shard placed into a continuously perfused chamber on the stage of an inverted microscope (Nikon Eclipse TE300). The extracellular solution was a standard HEPES-buffered saline (HBSS) consisting of: (in mM) NaCl, 135; KCl, 5; HEPES–NaOH, 10; MgCl₂, 1; CaCl₂, 2; D-glucose, 30; pH 7.3.

Standard whole-cell patch clamp recordings were made using an Axopatch-200B amplifier (Axon Instruments Inc.) under the control of the pClamp 9.2 software suite (Axon Instruments Inc.). Patch clamp electrodes were of resistance of 3–5 M Ω when filled with the intracellular solution which consisted of (in mM): CsCl, 120; HEPES–CsOH, 10; EGTA, 10; QX314-Br, 5; ATP disodium salt, 4; GTP-disodium salt, 0.3; MgCl₂, 4; (pH 7.3). The pairing of this solution with HBSS resulted in a calculated liquid junction potential error of 5 mV, which was arithmetically corrected for in analysis. Whole-cell voltage clamp recordings were established in GH4C1- $\alpha 7$ cells using standard methods. The holding potential was -75 mV except during the determination of current–voltage relationships where the membrane potential was increased stepwise from -75 in 20 mV increments. To permit rapid solution exchange cells were detached from, and lifted above the underlying coverslip and placed adjacent to the control barrel of a fast-switching multibarrel perfusion system (Warner Instruments). To apply drugs the barrels were translated horizontally so the cell was exposed to the drug-containing solution flow from a different, adjacent barrel. The temperature of the solutions

applied from all barrels of this device could be set at a single defined level using a commercially available multichannel temperature controller (Warner Instruments). Data are presented as mean \pm SEM.

DRUGS

Acetylcholine (ACh), choline, and (–)-nicotine were purchased from Sigma-Aldrich, UK. Methyllycaconitine (MLA), PNU120596 were purchased from Tocris Biosciences, UK.

RESULTS

PATCH CLAMP ANALYSIS OF $\alpha 7$ nAChR-MEDIATED RESPONSES

Application of ACh, (–)-nicotine, and choline all produced the expected inward currents in GH4C1- $\alpha 7$ cells voltage-clamped at -75 mV. At high concentrations of each of these agonists, inward currents rapidly appeared and then promptly desensitized (**Figure 1A**). The remaining work in this manuscript employs only ACh as an agonist, since this is likely to be the major physiological activator of $\alpha 7$ receptors *in vivo*.

The concentration–response behavior of ACh-mediated $\alpha 7$ nAChR activation was determined using 2 s agonist applications at concentrations between 10 and 3000 μ M. A plot of peak current versus concentration for such data pooled from seven cells is shown in **Figure 1B**. The mean EC₅₀ determined from fitting these datasets individually was 260 ± 31 μ M, while the mean Hill coefficient was 1.4 ± 0.1 . The kinetics of current responses were also strongly concentration-dependent with both activation and desensitization being faster at higher agonist concentrations. Deactivation following removal of 30 μ M ACh occurred with a mean time constant of 54.5 ± 9.1 ms, $n = 7$. Responses to 3 mM ACh were completely eliminated by MLA (100 nM; **Figure 1C**), confirming currents evoked by ACh in these cells are mediated solely by $\alpha 7$ nAChR. This antagonism was reversed upon MLA washout with a time constant of recovery of approximately 240 s (data not shown). An important caveat to note here is that the estimation of $\alpha 7$ nAChR peak current and kinetics of channel activation and desensitization are impacted profoundly by the kinetics of solution exchange. The $\alpha 7$ nAChR is unique among ligand-gated ion channels with respect to its extremely rapid activation and desensitization kinetics. Although we have employed a rapid perfusion system to activate $\alpha 7$ nAChR channels the estimation of ACh potency and kinetic parameters under such conditions is predominantly governed by the leading edge of the solution application.

Current–voltage relationships for $\alpha 7$ nAChR-mediated currents were obtained by varying the holding potential at which ACh was applied. In line with previous observations, under control conditions the peak current versus voltage plot exhibited strong inward rectification, with little outward current observed at positive potentials (**Figure 1D**). Similarly strong rectification was observed with all three different ACh concentrations, which produced approximately 10, 30, and 100% levels of peak response amplitude.

ELECTROPHYSIOLOGICAL ACTIONS OF PNU120596 AT ROOM TEMPERATURE

PNU120596 was first described as a PAM at $\alpha 7$ -AChR receptors by Hurst et al. (2005). It has more recently been put forward as

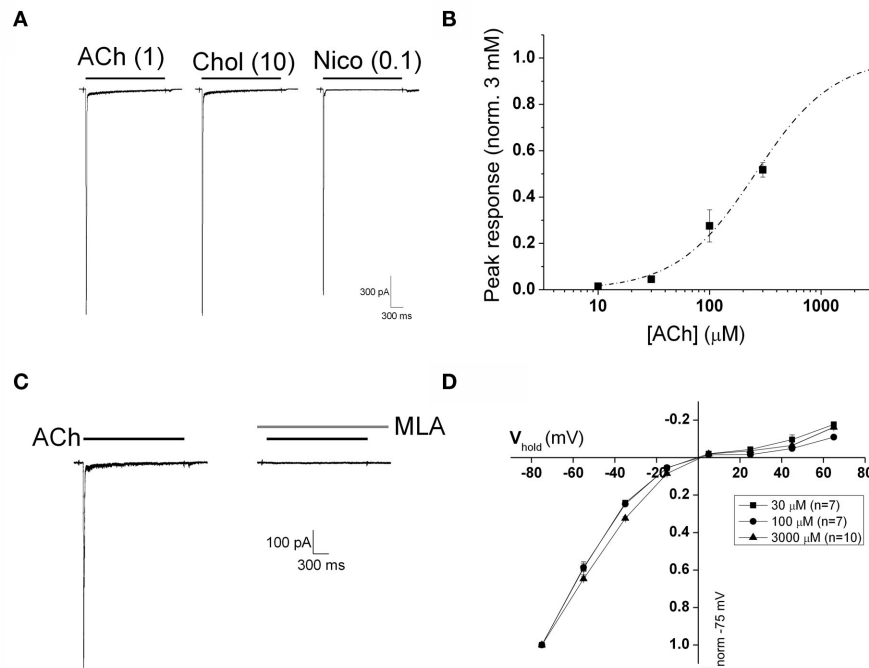


FIGURE 1 | Activation of recombinant $\alpha 7$ nAChR stably expressed in GH4C1 cells. (A) Two seconds duration applications of ACh (1 mM), choline (10 mM), and nicotine (100 μ M) elicited $\alpha 7$ nAChR-mediated fast inward currents that rapidly desensitize. **(B)** Pooled peak current versus concentration data from seven cells. All data from each cell were normalized to the response obtained with 3 mM ACh. The dashed line is a logistic fit to the concentration–response curve of ACh-evoked peak current

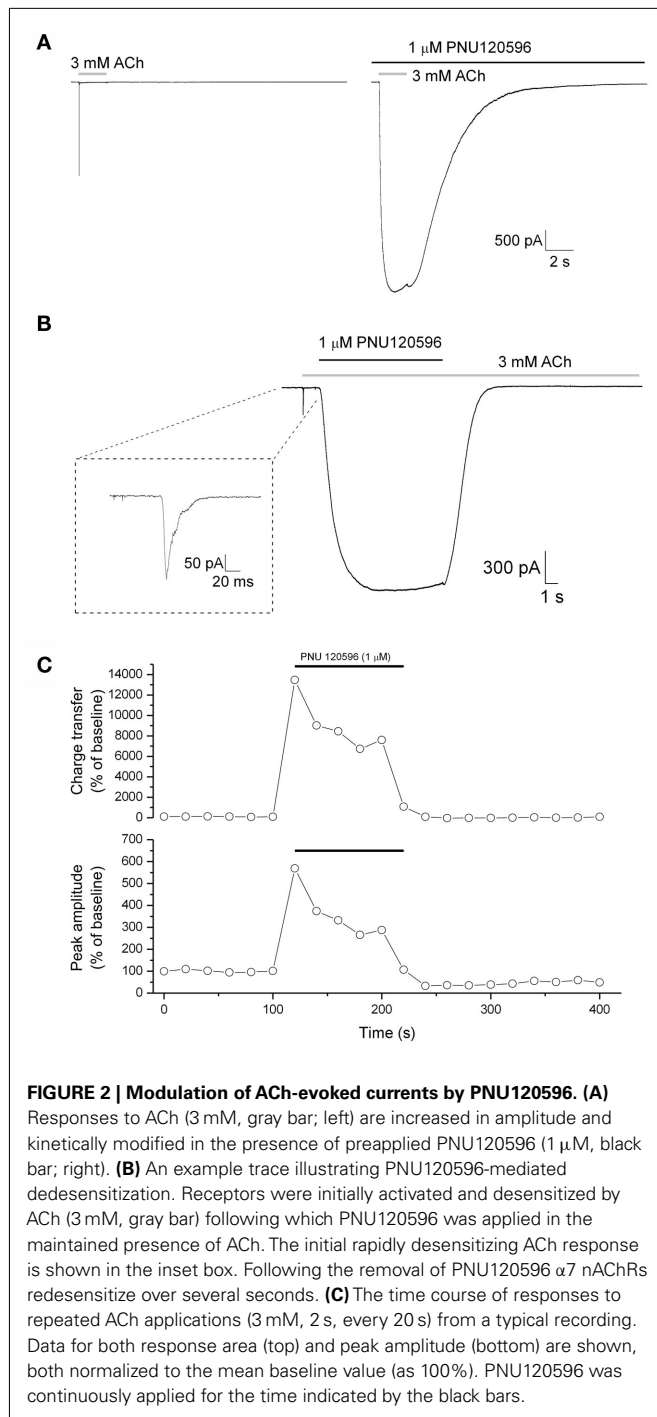
($EC_{50} = 260 \mu$ M; $n = 7$). **(C)** ACh-evoked currents (3 mM) are completely abolished by pre-application of the selective $\alpha 7$ nAChR blocker MLA (100 nM). **(D)** Current–voltage relationships of currents evoked by three different ACh concentrations [30 μ M ($n = 7$), 100 μ M ($n = 7$), and 3 mM, ($n = 10$)]. Responses are normalized to the response recorded at a holding potential of -75 mV. Note the strong inward rectification at all agonist concentrations.

a canonical example of so-called type II PAMs (Gronlien et al., 2007). In addition to enhancing agonist-induced currents and increasing apparent agonist affinity, type II PAMs produce dramatic effects on receptor kinetics. This behavior is illustrated in **Figure 2A** where responses to 3 mM ACh from the same cell recorded in either the absence (left) or maintained presence (right) of PNU120596 are compared. In the presence of PNU120596, the maximum current was larger, desensitization was largely eliminated and deactivation was massively slowed. The time constant of deactivation in the presence of PNU120596 (1 μ M) was 5211 ± 838 ms ($n = 10$), close to $100\times$ slower than that seen in the absence of this PAM. Application of PNU120596 produced no agonist effects in its own right.

In addition to slowing desensitization of agonist responses (**Figure 2A**), PNU120596 was also able to effectively dedesensitize $\alpha 7$ nAChRs previously completely desensitized by application of a high concentration of ACh. An example of this activity is shown in **Figure 2B**. Here the receptors were first activated and then desensitized by applying 3 mM ACh for 1 s, PNU120596 was applied then in the maintained presence of ACh. This elicited a large non-desensitizing current response that rose to peak with a time constant of 2300 ± 265 ms ($n = 17$); a rate that is likely to reflect the association kinetics of PNU120596 with its binding site (formally $[PNU].k_{on} + k_{off}$). The peak current generated by such dedesensitization was much larger (8.6 ± 2.0 -fold; $n = 17$)

than that produced by the initial desensitizing application of 3 mM ACh (an approximately EC_{99} agonist concentration when applied alone). Removal of PNU120596, in the maintained presence of ACh, caused the receptors to redensitize with a mean half time of 1456 ± 175 ms ($n = 9$). This redensitization rate is >300 times slower than the initial rate of desensitization (which has a half time below 5 ms), and thus the redensitization kinetics are likely to predominantly reflect the off-rate of PNU120596 from its binding site. In agreement with the rapid redensitization of $\alpha 7$ nAChR on PNU removal in the presence of ACh (**Figure 2B**), the effects of preapplied PNU120596 on both the amplitude and kinetics of ACh-evoked responses were rapidly reversed following PNU120596 washout (**Figure 2C**).

Using the pre-application protocol described above (**Figure 2A**) we were able to show that PNU120596 also produced a marked change in the voltage-dependence of $\alpha 7$ nAChR-mediated responses (**Figures 3A,B**). Thus, although current–voltage relationships of agonist responses (3 mM ACh) exhibited marked inward rectification (**Figures 1D and 3B**), the current–voltage relationship in the presence of PNU120596 was considerably more linear. This was quantified by calculating the rectification index which was 1.38 ± 0.1 for ACh responses in the presence of PNU120596 ($n = 5$) compared to 3.82 ± 0.3 for responses to 3 mM ACh alone ($n = 10$, **Figure 3C**). Consequently, the fold increase in peak current produced by PNU120596 was strongly voltage-dependent.



Like other effects of PNU120596 (**Figure 2C**), the linearization of the I–V relationship was reversed when this agent was removed.

We also noted that the rate of current deactivation on ACh removal in the presence of PNU120596, as well as being massively slowed, was voltage-dependent. Thus around three times faster deactivation being seen at positive membrane potentials than at a holding potential of -75 mV. This is readily apparent in the traces in **Figure 3A** as well as the pooled results of exponential fits in **Figure 3D**.

TEMPERATURE DEPENDENCE OF PNU120596 ACTIONS AT $\alpha 7$ nAChRs

The vast majority of patch clamp-based studies of ligand-gated channel pharmacology and biophysics are performed at room temperature, presumably because it is technically much simpler so to do. The findings of such studies are then frequently used to interpret studies in brain slices or *in vivo* which frequently involve higher temperatures (often around 33°C for brain slices and $\sim 37^{\circ}\text{C}$ *in vivo*). PNU120596 has documented *in vivo* actions and we are ultimately interested in understanding how these actions are generated at a circuit level. Consequently, we were motivated to understand how PNU120596 affected $\alpha 7$ nAChR gating at temperatures around 37°C . To do this we modified our stepping perfusion system such that we could warm the various solution streams, in parallel, to the same temperature.

Increasing the temperature from room temperature (22°C) to physiological temperature ($\sim 37^{\circ}\text{C}$) produced somewhat variable effects of the amplitude of ACh responses. On average, however, peak amplitude was $20 \pm 20\%$ smaller, a non-significant change. Charge transfer over 2 s was significantly reduced by $54 \pm 10\%$ ($n = 8$, **Figures 4A,B**), due to faster desensitization combined with the slightly reduced peak.

We initially studied the temperature dependence of the actions of PNU120596 using the dedesensitization protocol (**Figure 4C**). As described above (**Figure 2B**), this involves using a high agonist concentration to completely predesensitize the $\alpha 7$ nAChR population before co-applying PNU120596 to induce recovery (dedesensitization) of the receptor response in the maintained presence of agonist. As before, we quantified the effectiveness of a PAM in this assay by plotting the ratio of the dedesensitized response in the presence of the PAM (P2), to that of the initial ACh response prior to desensitization (P1). At room temperature this ratio was 34 ± 20 ($n = 4$). When we increased the experimental temperature in the same cells it was immediately apparent that PNU120596 became much less effective at dedesensitizing the $\alpha 7$ nAChRs. Thus the P2:P1 ratio fell below 1 (0.86 ± 2 ; $n = 4$) at temperature of $\sim 37^{\circ}\text{C}$ (**Figure 4D**).

As well as comparing the dedesensitization produced by PNU120596 at room and physiological temperature we also examined the temperature dependence of agonist responses at receptors pre-equilibrated with this PAM. From the example traces shown in **Figure 5A**, it is clear that the actions of the PNU120596 are greatly curtailed at higher temperatures. This is not only seen in the response amplitude in the presence of PNU120596 but also, for example, in the decreased PAM-mediated slowing of deactivation.

Figures 5B,C plot pooled data from six such experiments. Specifically these graphs plot, for three binned levels of elevated temperature, the relative amplitude (**Figure 5B**) and charge transfer (**Figure 5C**) seen in PNU120596 normalized to that seen at room temperature in the same cells. These indicate that the loss of the potentiating effect of the PNU120596 intimately depends on temperature and can be observed with just a few degrees change above room temperature. Together with the dedesensitization measurements in **Figure 4** these data provide good evidence that the allosteric actions of PNU120596 are strongly temperature-dependent within the range of standard biological experimentation.

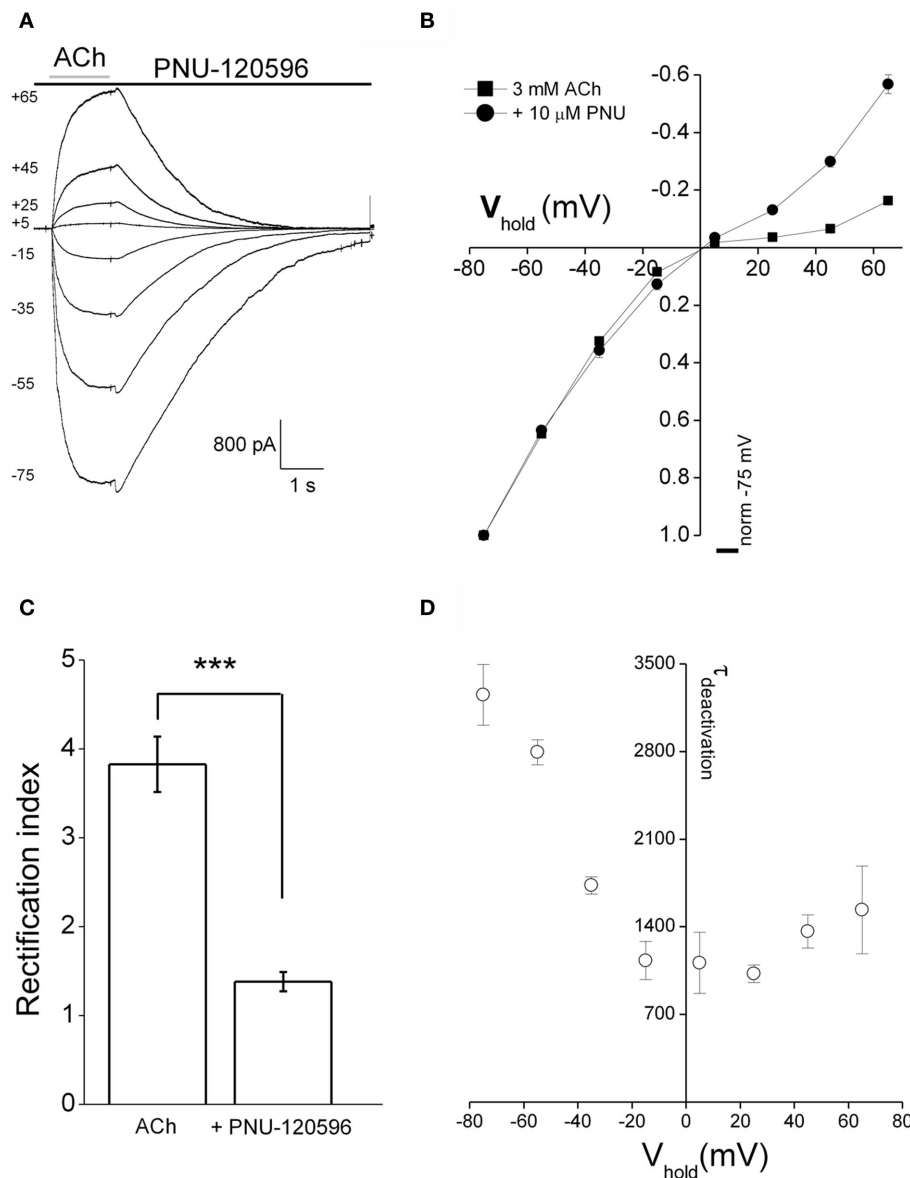


FIGURE 3 | PNU120596 alters voltage-dependence of $\alpha 7$ nAChR-mediated responses. (A) Currents from a standard I-V relationships in response to ACh (3 mM) applied in the continuous presence of 10 μ M PNU120596 at room temperature. The numbers to the left of the traces are the holding potential in millivolt. (B) Pooled I-V relationships for ACh alone (3 mM; $n = 10$, squares) and ACh + PNU120596 ($n = 5$, circles). PNU120596-modulated ACh-evoked currents have a more linear I-V relationship while currents recorded in ACh alone show classically strong inward rectification. (C) A comparison of rectification index of currents evoked by ACh alone ($n = 10$) and ACh applied in the

presence of PNU120596 ($n = 5$). Rectification index is defined as the chord conductance between -75 and -55 mV divided by that between $+45$ and $+65$ mV. Rectification ratios recorded in PNU120596 were different (***) $P < 0.001$, using Student's *T*-test) when compared to currents evoked by ACh (3 mM) alone. (D) A graph plotting the voltage-dependence of the deactivation time constant of ACh-induced currents recorded in the maintained presence of PNU120596. Time constant was determined by making single exponential fits to the current decay following ACh removal. As is visibly apparent in (A), deactivation is considerably faster at less negative membrane potentials.

Lastly, we were interested to determine if the temperature dependence of the positive allosteric modulation of $\alpha 7$ nAChR by PNU120596 extended to other structurally diverse $\alpha 7$ nAChR PAMs. We have previously reported on the $\alpha 7$ nAChR PAM activity of SB-206553 (Dunlop et al., 2009), a compound originally characterized as a 5-HT_{2B/C} receptor antagonist. **Figure 6** shows the

desensitization protocol evaluating the effect of SB-206553 on ACh-evoked $\alpha 7$ nAChR currents showing a strongly temperature-dependent effect, similar to PNU120596, with reduced desensitization at near physiological temperatures compared to room temperature. Similar to PNU120596, the magnitude of potentiation of $\alpha 7$ nAChR currents in response to ACh in cells

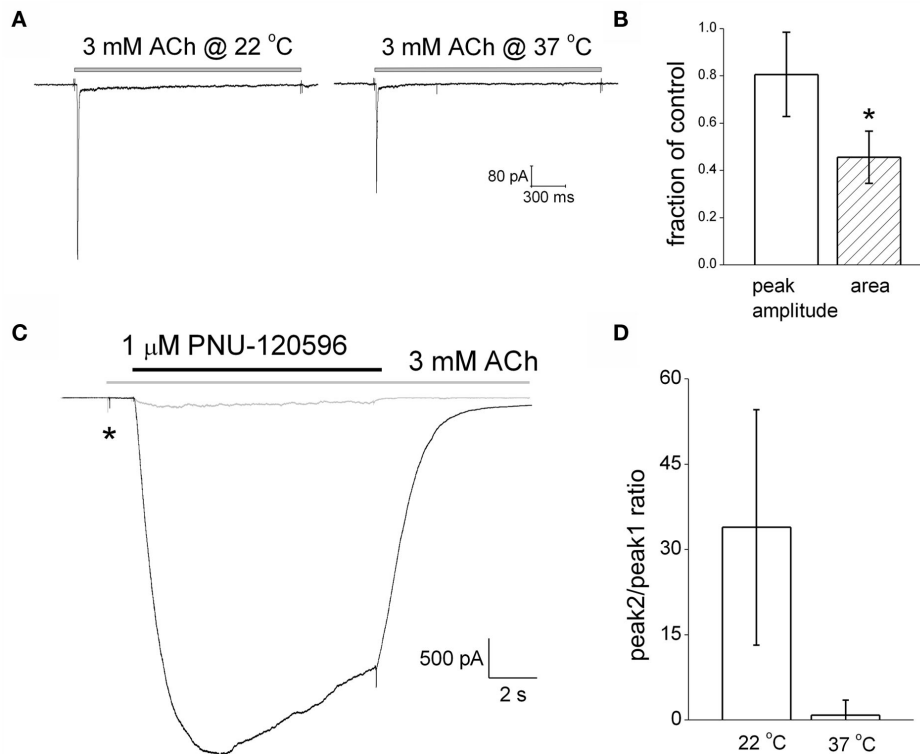


FIGURE 4 | PNU120596-mediated dedesensitization is strongly attenuated at physiological temperatures. (A) ACh-mediated current responses at room temperature and 37°C in the same example cell. **(B)** A graph plotting the changes in amplitude and charge transfer produced by increasing the recording temperature to 37°C. **(C)** Example traces showing

PNU120596-mediated reversal of ACh-evoked desensitization at room temperature (black trace) and 37°C (gray trace). **(D)** A histogram showing the ratio between the dedesensitized peak current (P2) evoked by PNU120596 and the initial desensitizing ACh response (P1) at room temperature and 37°C.

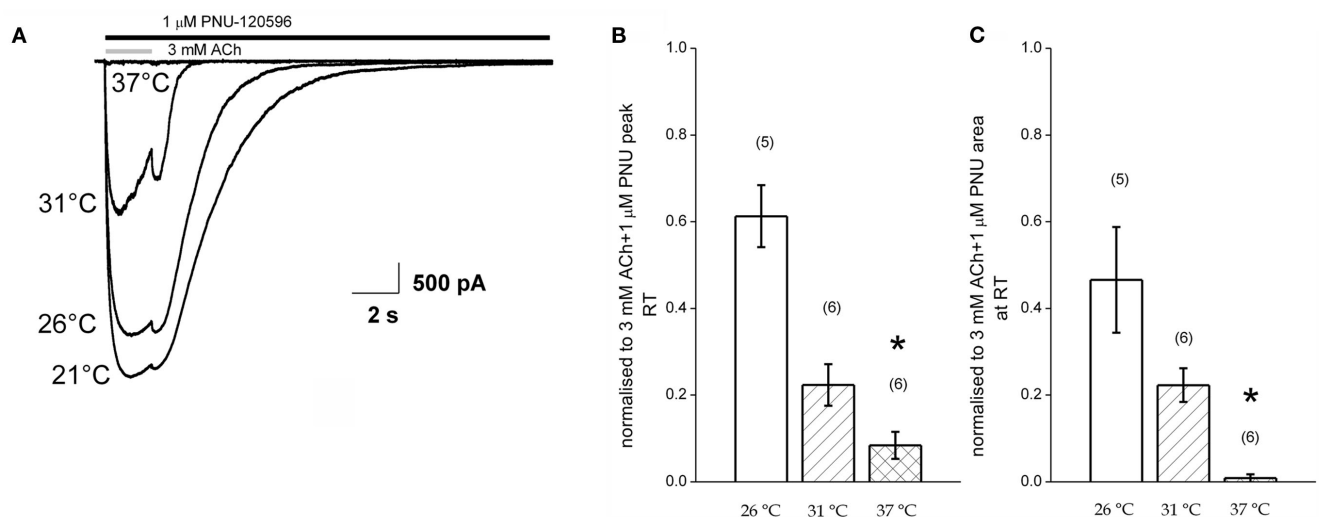
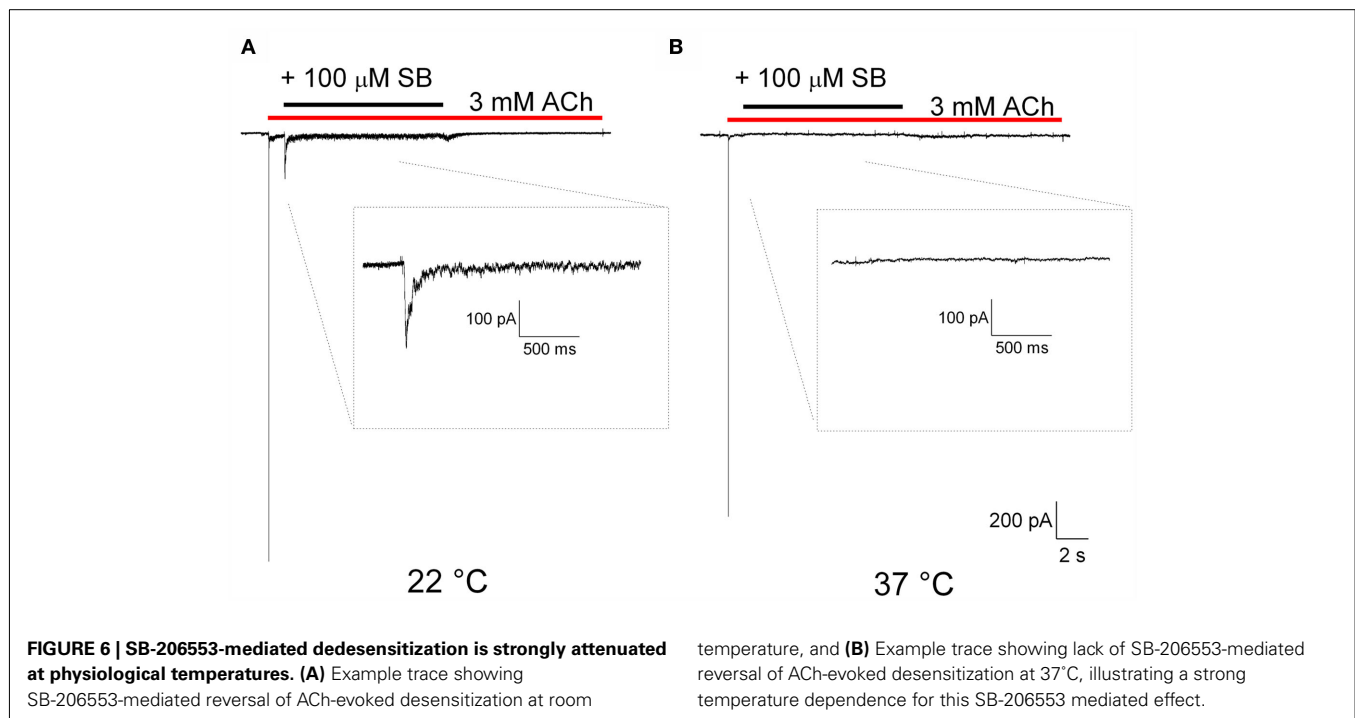


FIGURE 5 | Potentiation of agonist responses at receptors pre-equilibrated with PNU120596 is reduced at higher temperatures. (A) Example responses to 3 mM ACh in the maintained presence of PNU120596 at four different temperatures. **(B,C)** Pooled data plotting the

amplitude (left) and charge transfer (right) of response to ACh in the presence of PNU in three different recording temperature bins. Data are normalized to the corresponding responses recorded at room temperature.



pre-equilibrated with SB-206553 was reduced at physiological temperature compared to room temperature (data not shown).

DISCUSSION

Selective pharmacological manipulation of $\alpha 7$ nicotinic receptors holds considerable promise for the future pharmacotherapy of schizophrenia and other human diseases characterized by significant cognitive deficits (Leiser et al., 2009; Hajos and Rogers, 2010; Haydar and Dunlop, 2010; Thomsen et al., 2010). Furthermore, pharmacological modulation of $\alpha 7$ nAChR also has some potential promise as a neuroprotective strategy (Kihara et al., 2001; Hellstrom-Lindhall et al., 2004; Hu et al., 2007; Roncarati et al., 2009). The current over-arching view is that increasing activity of $\alpha 7$ nAChRs is the required route to improved cognitive function, a supposition that is supported by behavioral data using agonists, and to a lesser extent PAMs. It is this view-point that has shaped the recent extensive drug discovery efforts in many pharmaceutical companies around the world.

At room temperature, the type II PAM PNU120596 produces remarkable effects on gating of $\alpha 7$ receptors. As well as potentiating peak current generated by agonist concentrations that produce near maximal responses in the absence of a PAM, this agent almost eliminates desensitization and slows deactivation by around 100-fold (Figure 2A). Furthermore, this agent can completely dedesensitize $\alpha 7$ nAChRs that have been fully desensitized with a high agonist concentration (Figure 2B). At room temperature these effects are massive compared to the positive allosteric modulation of other neurotransmitter-gated channels by well known drugs, for example, the effects of benzodiazepines on GABA_A receptors and the actions of so-called “AMPAkines” on the AMPA subclass of glutamate receptors. Importantly, all of the effects of PNU120596 we observed in both activation and desensitization

assays were substantially reduced as temperature was increased toward physiological levels (Figures 4 and 5). Similarly, the profound temperature dependence for the $\alpha 7$ nAChR PAM activity of PNU120596 was also observed with the structurally distinct PAM SB-206553.

It has been suggested that PAMs like PNU120596 which produce profound effects on the kinetics of $\alpha 7$ nAChRs are unlikely to become useful as clinical therapeutic agents (Ng et al., 2007). The reasoning behind this suggestion is that the elimination of desensitization by such type II PAMs may produce excessive opening of $\alpha 7$ nAChRs leading to cell death through massively enhanced Ca^{2+} entry (Orrenius et al., 2003). Of course, any such actions will ultimately be dose-dependent. When Ng et al. (2007) compared the cytotoxicity of PNU120596 and a type I PAM, CCMI (also known as Compound 6), they saw significant cell death with the former but not the latter compound. These toxicity assays were, however, performed at room temperature and our work here shows that pharmacological actions of PNU120596 are much greater at room temperature and become substantially attenuated nearer physiological temperature. Notably, another more recent study with PNU120596 revealed no toxic effects of 24 h of PNU120596 treatment on cultured cortical neurons or PC12 cells, although both cell types were clearly shown to express functional $\alpha 7$ nAChRs (Hu et al., 2009). These toxicity studies, unlike those of Ng et al. (2007), were performed at physiological temperatures.

Our recordings also demonstrated that the strong rectification of the I–V relationship that typifies $\alpha 7$ nAChR-mediated currents was considerably reduced in the presence of the PAM. Thus, it seems likely that the presence of the PAM inhibits whatever process generates inward rectification in $\alpha 7$ nAChRs. To our knowledge, however, the molecular basis of the rectification properties of

$\alpha 7$ nAChRs is not as well understood as it is for other nicotinic receptors (Haghighiand and Cooper, 1998, 2000).

The loss of strong rectification in the maintained presence of PNU120596 meant it was possible to measure response deactivation kinetics at positive potentials. The combination of two facets of $\alpha 7$ nAChR pharmacology means that such measurements are very difficult to make in the absence of a type II PAM. The first of these is that the strong inward rectification properties seen in the absence of a PAM mean responses at positive potentials are by definition small. Secondly, low agonist concentrations are best for measuring deactivation, because they elicit slower and thus less prior desensitization; but such concentration only elicit small currents. In the presence of PNU120596 it was clear that the rate of deactivation became two to three times faster as the membrane potential was depolarized. Deactivation of many ligand-gated channels reflects agonist unbinding kinetics. Thus our observations may mean ACh unbinding may be more rapid at more positive membrane potentials. The direction of this change suggests that voltage-dependent changes to agonist occupancy are very unlikely to be the cause of the loss of rectification in the presence of PNU120596. In future, it would be informative to examine the details of the voltage-dependence of the concentration-dependence of $\alpha 7$ nAChR activation, i.e., measuring EC₅₀ at different membrane potentials.

REFERENCES

- Arendash, G. W., Sanberg, P. R., and Sengstock, G. J. (1995a). Nicotine enhances the learning and memory of aged rats. *Pharmacol. Biochem. Behav.* 52, 517–523.
- Arendash, G. W., Sengstock, G. J., Sanberg, P. R., and Kem, W. R. (1995b). Improved learning and memory in aged rats with chronic administration of the nicotinic receptor agonist GTS-21. *Brain Res.* 674, 252–259.
- Barrantes, F. J. (2004). Structural basis for lipid modulation of nicotinic acetylcholine receptor function. *Brain Res. Brain Res. Rev.* 47, 71–95.
- Barrantes, F. J. (2007). Cholesterol effects on nicotinic acetylcholine receptor. *J. Neurochem.* 103(Suppl. 1), 72–80.
- Bertrand, D., and Gopalakrishnan, M. (2007). Allosteric modulation of nicotinic acetylcholine receptors. *Biochem. Pharmacol.* 74, 1155–1163.
- Bruses, J. L., Chauvet, N., and Rutishauser, U. (2001). Membrane lipid rafts are necessary for the maintenance of the (alpha)7 nicotinic acetylcholine receptor in somatic spines of ciliary neurons. *J. Neurosci.* 21, 504–512.
- Dunlop, J., Lock, T., Jow, B., Sitzia, F., Grauer, S., Jow, F., Kramer, A., Bowlby, M., Randall, A., Kowal, D., Gilbert, A., Comery, T., Laroque, J., Soloveva, V., Brown, J., and Roncarati, R. (2009). Old and new pharmacology: positive allosteric modulation of the alpha7 nicotinic acetylcholine receptor by the 5-HT2B/C receptor antagonist SB-206553. *J. Pharmacol. Exp. Ther.* 328, 766–776.
- Freedman, R., Leonard, S., Gault, J. M., Hopkins, J., Cloninger, C. R., Kaufmann, C. A., Tsuang, M. T., Farone, S. V., Malaspina, D., Svra-kic, D. M., Sanders, A., and Gejman, P. (2001a). Linkage disequilibrium for schizophrenia at the chromosome 15q13-14 locus of the alpha7-nicotinic acetylcholine receptor subunit gene (CHRNA7). *Am. J. Med. Genet.* 105, 20–22.
- Freedman, R., Leonard, S., Olincy, A., Kaufmann, C. A., Malaspina, D., Cloninger, C. R., Svra-kic, D., Faraone, S. V., and Tsuang, M. T. (2001b). Evidence for the multigenic inheritance of schizophrenia. *Am. J. Med. Genet.* 105, 794–800.
- Gotti, C., Moretti, M., Bohr, I., Ziabreva, I., Vailati, S., Longhi, R., Riganti, L., Gaimarri, A., McKeith, I. G., Perry, R. H., Aarsland, D., Larsen, J. P., Sher, E., Beattie, R., Clementi, F., and Court, J. A. (2006). Selective nicotinic acetylcholine receptor subunit deficits identified in Alzheimer's disease, Parkinson's disease and dementia with Lewy bodies by immunoprecipitation. *Neurobiol. Dis.* 23, 481–489.
- Gronlien, J. H., Hakerud, M., Ween, H., Thorin-Hagene, K., Briggs, C. A., Gopalakrishnan, M., and Malysz, J. (2007). Distinct profiles of alpha7 nAChR positive allosteric modulation revealed by structurally diverse chemotypes. *Mol. Pharmacol.* 72, 715–724.
- Haghighiand, A. P., and Cooper, E. (1998). Neuronal nicotinic acetylcholine receptors are blocked by intracellular spermine in a voltage-dependent manner. *J. Neurosci.* 18, 4050–4062.
- Haghighiand, A. P., and Cooper, E. (2000). A molecular link between inward rectification and calcium permeability of neuronal nicotinic acetylcholine alpha3beta4 and alpha4beta2 receptors. *J. Neurosci.* 20, 529–541.
- Hajos, M., Hurst, R. S., Hoffmann, W. E., Krause, M., Wall, T. M., Higdon, N. R., and Groppi, V. E. (2005). The selective alpha7 nicotinic acetylcholine receptor agonist PNU-282987 [N-[(3R)-1-Azabicyclo [2.2.2]oct-3-yl]-4-chlorobenzamide hydrochloride] enhances GABAergic synaptic activity in brain slices and restores auditory gating deficits in anesthetized rats. *J. Pharmacol. Exp. Ther.* 312, 1213–1222.
- Hajos, M., and Rogers, B. N. (2010). Targeting alpha7 nicotinic acetylcholine receptors in the treatment of schizophrenia. *Curr. Pharm. Des.* 16, 538–554.
- Haydar, S. N., and Dunlop, J. (2010). Neuronal nicotinic acetylcholine receptors – targets for the development of drugs to treat cognitive impairment associated with schizophrenia and Alzheimer's disease. *Curr. Top. Med. Chem.* 10, 144–152.
- Hellstrom-Lindahl, E., Court, J., Keverne, J., Svedberg, M., Lee, M., Marutle, A., Thomas, A., Perry, E., Bednar, I., and Nordberg, A. (2004). Nicotine reduces A beta in the brain and cerebral vessels of APPsw mice. *Eur. J. Neurosci.* 19, 2703–2710.
- Hu, M., Gopalakrishnan, M., and Li, J. (2009). Positive allosteric modulation of alpha7 neuronal nicotinic acetylcholine receptors: lack of cytotoxicity in PC12 cells and rat primary cortical neurons. *Br. J. Pharmacol.* 158, 1857–1864.
- Hu, M., Schurdak, M. E., Puttfarcken, P. S., El Kouhen, R., Gopalakrishnan, M., and Li, J. (2007). High content screen microscopy analysis of A beta 1-42-induced neurite outgrowth reduction in rat primary cortical neurons: neuroprotective effects of alpha 7 neuronal nicotinic acetylcholine receptor ligands. *Brain Res.* 1151, 227–235.

- Hurst, R. S., Hajos, M., Raggenbass, M., Wall, T. M., Higdon, N. R., Lawson, J. A., Rutherford-Root, K. L., Berkenpas, M. B., Hoffmann, W. E., Piotrowski, D. W., Groppi, V. E., Allaman, G., Ogier, R., Bertrand, S., Bertrand, D., and Arneric, S. P. (2005). A novel positive allosteric modulator of the $\alpha 7$ neuronal nicotinic acetylcholine receptor: in vitro and in vivo characterization. *J. Neurosci.* 25, 4396–4405.
- Kellner, R. R., Baier, C. J., Willig, K. I., Hell, S. W., and Barrantes, F. J. (2007). Nanoscale organization of nicotinic acetylcholine receptors revealed by stimulated emission depletion microscopy. *Neuroscience* 144, 135–143.
- Kihara, T., Shimohama, S., Sawada, H., Honda, K., Nakamizo, T., Shibasaki, H., Kume, T., and Akaiki, A. (2001). Alpha 7 nicotinic receptor transduces signals to phosphatidylinositol 3-kinase to block A beta amyloid-induced neurotoxicity. *J. Biol. Chem.* 276, 13541–13546.
- Leiser, S. C., Bowlby, M. R., Comery, T. A., and Dunlop, J. (2009). A cog in cognition: how the $\alpha 7$ nicotinic acetylcholine receptor is geared towards improving cognitive deficits. *Pharmacol. Ther.* 122, 302–311.
- Leonard, S., Gault, J., Hopkins, J., Logel, J., Vianzon, R., Short, M., Drebing, C., Berger, R., Venn, D., Sirota, P., Zerbe, G., Olincy, A., Ross, R. G., Adler, L. E., and Freedman, R. (2002). Association of promoter variants in the $\alpha 7$ nicotinic acetylcholine receptor subunit gene with an inhibitory deficit found in schizophrenia. *Arch. Gen. Psychiatry* 59, 1085–1096.
- Levin, E. D., Bettegowda, C., Blosser, J., and Gordon, J. (1999). AR-R17779, and $\alpha 7$ nicotinic agonist, improves learning and memory in rats. *Behav. Pharmacol.* 10, 675–680.
- Lindstrom, J. (1996). Neuronal nicotinic acetylcholine receptors. *Ion Channels* 4, 377–450.
- Ng, H. J., Whittemore, E. R., Tran, M. B., Hogenkamp, D. J., Broide, R. S., Johnstone, T. B., Zheng, L., Stevens, K. E., and Gee, K. W. (2007). Nootropic $\alpha 7$ nicotinic receptor allosteric modulator derived from GABAA receptor modulators. *Proc. Natl. Acad. Sci. U.S.A.* 104, 8059–8064.
- Olincy, A., Harris, J. G., Johnson, L. L., Pender, V., Kongs, S., Allensworth, D., Ellis, J., Zerbe, G. O., Leonard, S., Stevens, K. E., Stevens, J. O., Martin, L., Adler, L. E., Soti, F., Kem, W. R., and Freedman, R. (2006). Proof-of-concept trial of an $\alpha 7$ nicotinic agonist in schizophrenia. *Arch. Gen. Psychiatry* 63, 630–638.
- Orrenius, S., Zhivotovsky, B., and Nicotera, P. (2003). Regulation of cell death: the calcium-apoptosis link. *Nat. Rev. Mol. Cell Biol.* 4, 552–565.
- Roncarati, R., Scali, C., Comery, T. A., Grauer, S. M., Aschmi, S., Bothmann, H., Jow, B., Kowal, D., Gianfriddo, M., Kelley, C., Zanelli, U., Ghiron, C., Haydar, S., Dunlop, J., and Terstapen, G. C. (2009). Procognitive and neuroprotective activity of a novel $\alpha 7$ nicotinic acetylcholine receptor agonist for treatment of neurodegenerative and cognitive disorders. *J. Pharmacol. Exp. Ther.* 329, 459–468.
- Simosky, J. K., Stevens, K. E., Kem, W. R., and Freedman, R. (2001). Intragastric DMXB-A, an $\alpha 7$ nicotinic agonist, improves deficient sensory inhibition in DBA/2 mice. *Biol. Psychiatry* 50, 493–500.
- Stevens, K. E., Kem, W. R., Mahnir, V. M., and Freedman, R. (1998). Selective $\alpha 7$ -nicotinic agonists normalize inhibition of auditory response in DBA mice. *Psychopharmacology (Berl.)* 136, 320–327.
- Thomsen, M. S., Hansen, H. H., Timmerman, D. B., and Mikkelsen, J. D. (2010). Cognitive improvement by activation of $\alpha 7$ nicotinic acetylcholine receptors: from animal models to human pathophysiology. *Curr. Pharm. Des.* 16, 323–343.
- Timmermann, D. B., Gronlien, J. H., Kohlhaas, K. L., Nielsen, E. O., Dam, E., Jorgensen, T. D., Ahling, P. K., Peters, D., Holst, D., Chrsitensen, J. K., Malysz, J., Briggs, C. A., Gopalakrishnan, M., and Olsen, G. M. (2007). An allosteric modulator of the $\alpha 7$ nicotinic acetylcholine receptor possessing cognition-enhancing properties in vivo. *J. Pharmacol. Exp. Ther.* 323, 294–307.
- Williams, D. K., Wang, J., and Papke, R. L. (2011). Investigation of the molecular mechanism of the $\alpha 7$ nicotinic acetylcholine receptor positive allosteric modulator PNU-120596 provides evidence for two distinct desensitized states. *Mol. Pharmacol.* 80, 1013–1032.
- Young, G. T., Zwart, R., Walker, A. S., Sher, E., and Millar, N. S. (2008). Potentiation of $\alpha 7$ nicotinic acetylcholine receptors via an allosteric transmembrane site. *Proc. Natl. Acad. Sci. U.S.A.* 105, 14686–14691.

Conflict of Interest Statement: The authors declare that the research was conducted in the absence of any commercial or financial relationships that could be construed as a potential conflict of interest.

Received: 09 July 2011; accepted: 30 November 2011; published online: 27 December 2011.

Citation: Sitzia F, Brown JT, Randall AD and Dunlop J (2011) Voltage- and temperature-dependent allosteric modulation of $\alpha 7$ nicotinic receptors by PNU120596. *Front. Pharmacol.* 2:81. doi: 10.3389/fphar.2011.00081

This article was submitted to *Frontiers in Pharmacology of Ion Channels and Channelopathies*, a specialty of *Frontiers in Pharmacology*.

Copyright © 2011 Sitzia, Brown, Randall and Dunlop. This is an open-access article distributed under the terms of the Creative Commons Attribution Non Commercial License, which permits non-commercial use, distribution, and reproduction in other forums, provided the original authors and source are credited.